

LOAN DOCUMENT

PHOTOGRAPH THIS SHEET

DITC ACCESSION NUMBER

LEVEL

INVENTORY

WL-YR-97-4075

DOCUMENT IDENTIFICATION

Apr 97

DISTRIBUTION STATEMENT A

Approved for public release;
Distribution Unlimited

DISTRIBUTION STATEMENT

DISTRIBUTION STAMP

DRG QUALITY INSTRUMENTS

19970703 056

DATE RECEIVED IN DTIC

REGISTERED OR CERTIFIED NUMBER

PHOTOGRAPH THIS SHEET AND RETURN TO DTIC-FDAC

WL-TR-97-4075

**PROCEEDINGS OF THE ANNUAL
MECHANICS OF COMPOSITES
REVIEW (11TH)**



Sponsored by:

**Air Force Wright Aeronautical Laboratories
Materials Laboratory**

APRIL 1997

FINAL REPORT FOR PERIOD 22-24 OCTOBER 1985

Approved for public release; distribution unlimited

**MATERIALS DIRECTORATE
WRIGHT LABORATORY
AIR FORCE MATERIEL COMMAND
WRIGHT-PATTERSON AFB OH 45433-7734**

REPORT DOCUMENTATION PAGE

Form Approved
OMB No. 0704-0188

Public reporting burden for this collection of information is estimated to average 1 hour per response, including the time for reviewing instructions, searching existing data sources, gathering and maintaining the data needed, and completing and reviewing the collection of information. Send comments regarding this burden estimate or any other aspect of this collection of information, including suggestions for reducing this burden, to Washington Headquarters Services, Directorate for Information Operations and Reports, 1215 Jefferson Davis Highway, Suite 1204, Arlington, VA 22202-4302, and to the Office of Management and Budget, Paperwork Reduction Project (0704-0188), Washington, DC 20503.

1. AGENCY USE ONLY (Leave blank)	2. REPORT DATE	3. REPORT TYPE AND DATES COVERED	
	April 1997	Final Report 22-24 OCT 1985	
4. TITLE AND SUBTITLE		5. FUNDING NUMBERS	
PROCEEDINGS OF THE ANNUAL MECHANICS OF COMPOSITES REVIEW (11th)			
6. AUTHOR(S)			
7. PERFORMING ORGANIZATION NAME(S) AND ADDRESS(ES)		8. PERFORMING ORGANIZATION REPORT NUMBER	
Air Force Materials Laboratory Nonmetallic Materials Division Wright-Patterson AFB OH 45433			
9. SPONSORING/MONITORING AGENCY NAME(S) AND ADDRESS(ES)		10. SPONSORING/MONITORING AGENCY REPORT NUMBER	
Materials Directorate Wright Laboratory Air Force Materiel Command Wright-Patterson AFB Ohio 45433-7734 POC: Tammy Oaks, WL/MLBM, 937-255-3068		WL-TR-97-4075	
11. SUPPLEMENTARY NOTES			
12a. DISTRIBUTION AVAILABILITY STATEMENT		12b. DISTRIBUTION CODE	
APPROVED FOR PUBLIC RELEASE; DISTRIBUTION IS UNLIMITED			
13. ABSTRACT (Maximum 200 words)			
<p>This report contains the basic unedited vu-graphs of the presentations at the "Mechanics" of Composites Review" sponsored jointly by the Non-metallic Materials Division of the Air Force Materials Laboratory, the Structures Division of the Air Force Flight Dynamics Laboratory and the Directorate of Aerospace Sciences of the Air Force Office of Scientific Research. The presentations cover current in-house and contract programs under the sponsorship of these three organizations.</p>			
14. SUBJECT TERMS		15. NUMBER OF PAGES	
epoxy-matrix composites; composite materials; resin matrix composites; composite bonded joints; fatigue of graphite/epoxy composites; fracture and fatigue of bi-materials		158	
		16. PRICE CODE	
17. SECURITY CLASSIFICATION OF REPORT	18. SECURITY CLASSIFICATION OF THIS PAGE	19. SECURITY CLASSIFICATION OF ABSTRACT	20. LIMITATION OF ABSTRACT
UNCLASSIFIED	UNCLASSIFIED	UNCLASSIFIED	SAR

AGENDA
MECHANICS OF COMPOSITES REVIEW
22-24 OCTOBER 1985

<u>TUESDAY, 22 OCTOBER 1985</u>	<u>PAGE</u>
7:15 A.M. REGISTRATION	
8:15 OPENING REMARKS	
8:30 DETECTION OF FAILURE PROGRESSION IN CROSS-PLY GRAPHITE/EPOXY DURING FATIGUE LOADING THROUGH ACOUSTIC EMISSION: J. AWERBUCH, W. ECKLES, AND E. KATZ, DREXEL UNIVERSITY	1
9:10 MONITORING ACOUSTIC EMISSION IN IMPACT-DAMAGED COMPOSITES: J. AWERBUCH, S. GHAFFARI, AND E. KATZ, DREXEL UNIVERSITY	12
9:50 BREAK	
10:20 PROCESSING THERMOPLASTIC COMPOSITES: G. SPRINGER, STANFORD UNIVERSITY	22
11:00 COMPOSITE CRASH DYNAMICS: H. CARDEN, NASA Langley Research Center, R. Boitnott and K. Jackson, U.S. Army/AVSCOM	26
11:40 LUNCH	
1:00 P.M. DYNAMICS AND AEROELASTICITY OF COMPOSITE STRUCTURES: J. DUGUNDJI AND G-S. CHEN, MASSACHUSETTS INSTITUTE OF TECHNOLOGY	36
1:40 AN ELASTIC STRESS ANALYSIS OF THE DEBOND FRONT IN DCB SPECIMENS: J. CREWS AND K. SHIVAKUMAR, NASA Langley Research Center, AND I. RAJU, ANALYTICAL SERVICES & MATERIALS, INC.	42
2:20 BREAK	
2:50 STATISTICAL LIFE PREDICTION OF COMPOSITE STRUCTURES: D. JONES AND J. YANG, THE GEORGE WASHINGTON UNIVERSITY	48
3:30 ANALYSIS OF DELAMINATION GROWTH FROM MATRIX CRACKS IN LAMINATES SUBJECTED TO BENDING LOADS: G. MURRI, NASA Langley Research Center, AND E. GUYNN, KENTRON INC.	49
4:10 ADJOURN	
5:00 SOCIAL	

AGENDA (CONTINUED)
MECHANICS OF COMPOSITES REVIEW
22-24 OCTOBER 1985

<u>WEDNESDAY, 23 OCTOBER 1985</u>	<u>PAGE</u>
8:30 A.M. ANALYSIS OF PROGRESSIVE MATRIX CRACKING IN COMPOSITE LAMINATES: G. DVORAK, E. WUNG AND K. AHANGAR, RENSSELAER POLYTECHNIC INSTITUTE, AND N. LAWS, UNIVERSITY OF PITTSBURGH	50
9:10 INITIATION OF FREE-EDGE DELAMINATION IN COMPOSITE LAMINATE - PREDICTION AND EXPERIMENT: R. KIM, UNIVERSITY OF DAYTON RESEARCH INSTITUTE, AND S. SONI, ADTECH SYSTEMS RESEARCH INC.	59
9:50 BREAK	
10:20 STRENGTH, DEFLECTIONS AND IMPACT DAMAGE IN ADVANCED COMPOSITE STRUCTURES: P. LAGACE, MASSACHUSETTS INSTITUTE OF TECHNOLOGY	69
11:00 ANALYSIS OF COMPOSITE LAMINATES WITH DELAMINATIONS UNDER COMPRESSION LOADING: H. KAN, NORTHROP CORPORATION	71
11:40 LUNCH	
1:00 P.M. SIMPLE RECTANGULAR ELEMENT FOR ANALYSIS OF LAMINATED COMPOSITE MATERIALS: J. WHITCOMB, NASA LANGLEY RESEARCH CENTER	84
1:40 FORMULATION OF LAMINATED BEAM AND PLATE ELEMENTS FOR A MICRO- COMPUTER: A. CHEN AND T. YANG, PURDUE UNIVERSITY	93
2:20 BREAK	
2:50 APPROXIMATE ANALYSIS OF COMPOSITES WITH DAMAGE: G. SENDECKYJ, FLIGHT DYNAMICS LABORATORY	94
3:30 A METHOD OF LAMINATE DESIGN: I. SUSUKI, MATERIALS LABORATORY	95
4:10 ADJOURN	

AGENDA (CONCLUDED)
MECHANICS OF COMPOSITES REVIEW
22-24 OCTOBER 1985

<u>THURSDAY, 24 OCTOBER 1985</u>		<u>PAGE</u>
8:30 A.M.	MECHANICS OF COMPRESSION FAILURE IN FIBER REINFORCED COMPOSITES: S. WANG, UNIVERSITY OF ILLINOIS	105
9:10	SUPPRESSION OF DELAMINATION IN COMPOSITE LAMINATES SUBJECTED TO IMPACT LOADING: C. SUN, PURDUE UNIVERSITY	106
9:50	BREAK	
10:20	THERMOVISCOELASTIC PROPERTIES OF UNIDIRECTIONAL FIBER COMPOSITES: E. HUMPHREYS AND Z. HASHIN, MATERIALS SCIENCE CORPORATION	114
11:00	COMPOSITE MECHANICS/RELATED ACTIVITIES AT LEWIS RESEARCH CENTER: C. CHAMIS, C. GINTY, AND P. MURTHY, NASA LEWIS RESEARCH CENTER	124
11:40	ADJOURN	
APPENDIX A: PROGRAM LISTINGS		A-1



REVISED AGENDA

MECHANICS OF COMPOSITES REVIEW

22 - 24 OCTOBER 1985

<u>TUESDAY, 22 OCTOBER 1985</u>	<u>PAGE</u>
7:15 a.m. REGISTRATION	
8:15 OPENING REMARKS	
8:30 DETECTION OF FAILURE PROGRESSION IN CROSS-PLY GRAPHITE/EPOXY DURING FATIGUE LOADING THROUGH ACOUSTIC EMISSION: J. Awerbuch, W. Eckles, and E. Katz, Drexel University	1
9:10 MONITORING ACOUSTIC EMISSION IN IMPACT-DAMAGED COMPOSITES: J. Awerbuch, S. Ghaffari, and E. Katz, Drexel University	12
9:50 BREAK	
10:20 PROCESSING THERMOPLASTIC COMPOSITES: G. Springer, Stanford University	22
11:00 COMPOSITE CRASH DYNAMICS: H. Carden, NASA Langley Research Center, R. Boitnott and K. Jackson, U.S. Army/AVSCOM	26
11:40 LUNCH	
1:00 p.m. DYNAMICS AND AEROELASTICITY OF COMPOSITE STRUCTURES: J. Dugundji and G-S. Chen, Massachusetts Institute of Technology	36
1:40 AN ELASTIC STRESS ANALYSIS OF THE DEBOND FRONT IN DCB SPECIMENS: J. Crews and K. Shivakumar, NASA Langley Research Center, and I. Raju, Analytical Services & Materials, Inc.	42
2:20 BREAK	
2:50 A METHOD OF LAMINATE DESIGN: I. Susuki, Materials Laboratory	95
3:30 ANALYSIS OF DELAMINATION GROWTH FROM MATRIX CRACKS IN LAMINATES SUBJECTED TO BENDING LOADS: G. Murri, NASA Langley Research Center, and E. Guynn, Kentron Inc.	49
4:10 ADJOURN	
5:00 SOCIAL	

REVISED AGENDA (CONTINUED)

<u>WEDNESDAY, 23 OCTOBER 1985</u>		<u>PAGE</u>
8:30 a.m.	ANALYSIS OF PROGRESSIVE MATRIX CRACKING IN COMPOSITE LAMINATES: G. Dvorak, E. Wung and K. Ahangar, Rensselaer Polytechnic Institute, and N. Laws, University of Pittsburgh	50
9:10	INITIATION OF FREE-EDGE DELAMINATION IN COMPOSITE LAMINATE - PREDICTION AND EXPERIMENT: R. Kim, University of Dayton Research Institute, and S. Soni, AdTech Systems Research Inc.	59
9:50	BREAK	
10:25	STRENGTH, DEFLECTIONS AND IMPACT DAMAGE IN ADVANCED COMPOSITE STRUCTURES: P. Lagace, Massachusetts Institute of Technology	69
11:05	ANALYSIS OF COMPOSITE LAMINATES WITH DELAMINATIONS UNDER COMPRESSION LOADING: H. Kan, Northrop Corporation	71
11:45	LUNCH	
1:15 p.m.	SIMPLE RECTANGULAR ELEMENT FOR ANALYSIS OF LAMINATED COMPOSITE MATERIALS: J. Whitcomb, NASA Langley Research Center	84
1:55	FORMULATION OF LAMINATED BEAM AND PLATE ELEMENTS FOR A MICRO- COMPUTER: A. Chen and T. Yang, Purdue University	93
2:35	BREAK	
3:10	COMPOSITE MECHANICS/RELATED ACTIVITIES AT LEWIS RESEARCH CENTER: C. Chamis, C. Ginty, and P. Murthy, NASA Lewis Research Center	124
3:50	ADJOURN	
<u>THURSDAY, 24 OCTOBER 1985</u>		
8:30 a.m.	MECHANICS OF COMPRESSION FAILURE IN FIBER REINFORCED COMPOSITES: S. Wang, University of Illinois	105
9:10	SUPPRESSION OF DELAMINATION IN COMPOSITE LAMINATES SUBJECTED TO IMPACT LOADING: C. Sun, Purdue University	106
9:50	BREAK	
10:30	THERMOVISCOELASTIC PROPERTIES OF UNIDIRECTIONAL FIBER COMPOSITES: E. Humphreys and Z. Hashin, Materials Science Corporation	114
11:10	ADJOURN	
	APPENDIX A: PROGRAM LISTINGS	A-1

FOREWORD

THIS REPORT CONTAINS THE ABSTRACTS AND VIEWGRAPHS OF THE PRESENTATIONS AT THE ELEVENTH ANNUAL MECHANICS OF COMPOSITES REVIEW SPONSORED BY THE MATERIALS LABORATORY. EACH WAS PREPARED BY ITS PRESENTER AND IS PUBLISHED HERE UNEDITED. IN ADDITION, A LISTING OF BOTH THE IN-HOUSE AND CONTRACTUAL ACTIVITIES OF EACH PARTICIPATING ORGANIZATION IS INCLUDED.

THE MECHANICS OF COMPOSITES REVIEW IS DESIGNED TO PRESENT PROGRAMS COVERING ACTIVITIES THROUGHOUT THE UNITED STATES AIR FORCE, NAVY, AND NASA. PROGRAMS NOT COVERED IN THE PRESENT REVIEW ARE CANDIDATES FOR PRESENTATION AT FUTURE MECHANICS OF COMPOSITES REVIEWS. THE PRESENTATIONS COVER BOTH IN-HOUSE AND CONTRACT PROGRAMS UNDER THE SPONSORSHIP OF THE PARTICIPATING ORGANIZATIONS.

SINCE THIS IS A REVIEW OF ON-GOING PROGRAMS, MUCH OF THE INFORMATION IN THIS REPORT HAS NOT BEEN PUBLISHED AS YET AND IS SUBJECT TO CHANGE; BUT TIMELY DISSEMINATION OF THE RAPIDLY EXPANDING TECHNOLOGY OF ADVANCED COMPOSITES IS DEEMED HIGHLY DESIRABLE. WORKS IN THE AREA OF MECHANICS OF COMPOSITES HAVE LONG BEEN TYPIFIED BY DISCIPLINED APPROACHES. IT IS HOPED THAT SUCH A HIGH STANDARD OF RIGOR IS REFLECTED IN THE MAJORITY, IF NOT ALL, OF THE PRESENTATIONS IN THIS REPORT.

FEEDBACK AND OPEN CRITIQUE OF THE PRESENTATIONS AND THE REVIEW ITSELF ARE MOST WELCOME AS SUGGESTIONS AND RECOMMENDATIONS FROM ALL PARTICIPANTS WILL BE CONSIDERED IN THE PLANNING OF FUTURE REVIEWS.



GEORGE E. HUSMAN, CHIEF
NONMETALLIC MATERIALS DIVISION
MATERIALS LABORATORY

ACKNOWLEDGEMENT

WE EXPRESS OUR APPRECIATION TO THE AUTHORS FOR THEIR CONTRIBUTIONS AND TO THE POINTS OF CONTACT WITHIN THE ORGANIZATIONS FOR THEIR EFFORTS IN SUPPLYING THE PROGRAM LISTINGS.

DETECTION OF FAILURE PROGRESSION IN CROSS-PLY GRAPHITE/EPOXY
DURING FATIGUE LOADING THROUGH ACOUSTIC EMISSION

Jonathan Awerbuch, William F. Eckles and Eliezer Katz

Department of Mechanical Engineering and Mechanics
Drexel University
Philadelphia, Pennsylvania 19104

ABSTRACT

Monitoring acoustic emission (AE) during fatigue loading appears to offer a practical procedure for detecting fatigue damage and damage growth. This non-destructive tool is particularly attractive because of the simplicity in its use, the acquisition of data in real-time, its potential for monitoring damage initiation, progression and accumulation, for anticipating failure sites, for identifying the different failure mechanisms and determining damage criticality, and for its sensitivity to non-visual damage.

Problems remain to be solved, however: proper interpretation of the voluminous data obtained, the appropriate test methodology to be employed, the correlation between AE results and the actual deformation characteristics and state of damage, identification of the various failure mechanisms and processes, and the distinction between emission generated by damage and that generated by friction.

In this study, AE is monitored in a variety of cross-ply graphite/epoxy laminates of different stacking sequences and containing different ratios of ply thickness. Three loading sequences are applied: monotonic quasi-static loading to failure, quasi-static loading-unloading while incrementally increasing the load to failure, and fatigue loading, all in uniaxial tension. The AE results are compared with a variety of nondestructive (visual, X-radiography, acousto-ultrasonics, and frequency response) and destructive (laminate delving, photomicrography, and scanning electron microscopy) techniques. AE is also monitored with specially designed lay-ups in which the different failure mechanisms can be isolated.

Results indicate that stacking sequence, and to a lesser degree the ratio of ply thicknesses, strongly affects the event intensities. Emphasis is placed on determining the correlation between the AE results and actual failure processes for different laminates. During both quasi-static and fatigue loading, a significant amount of emission is generated by friction, in some cases exceeding that generated by new damage. During fatigue loading, the friction generated emission can be discriminated by the load level at which it occurs and through proper correlation among the AE source intensity variables. Results indicate that matrix failure and fiber breakage result in middle and high range AE source intensities. Due to the rapidity with which matrix cracks and delamination progress, distinction of these processes is more difficult and investigation continues in this direction. Frequency response of the subject laminate is shown to have potential for determining the state of damage. Initiation of transverse cracks, damage accumulation, and the state of transverse crack saturation are clearly distinguished by this method in cross-ply laminates.

CONCLUSIONS

1. Stacking sequence and ply thickness have significant effect on damage initiation and accumulation and on the failure process as detected through acoustic emission.
2. A significant amount of emission is generated by friction among newly created fracture surfaces during both quasi-static and fatigue loading.
3. The friction generated emission can be distinguished from emission generated by new damage through proper correlation among various AE source intensities.
4. Preliminary results indicate that AE source intensities of friction generated emission depend on the type of failure.
5. Monitoring AE during fatigue loading can indicate the cycle number at which damage initiates and progresses and the type of damage.

6. The frequency response of the subject laminate strongly depends on the state of damage. Amplitude reduction and shift in frequency can be qualitatively correlated with state of damage.

**DETECTION OF FAILURE PROGRESSION IN CROSS-PLY
GRAPHITE/EPOXY DURING FATIGUE LOADING
THROUGH ACOUSTIC EMISSION**

Jonathan Awerbuch, William F. Eckles and Eliezer Katz

Department of Mechanical Engineering and Mechanics
Drexel University
Philadelphia, Pennsylvania 19104

Program sponsored by AFWAL/FDL, F33615-84-3204.
George P. Sendeckyj of AFWAL/FIBEC is the program
monitor.

OBJECTIVE

DETERMINE THE VALIDITY OF THE ACOUSTIC EMISSION TECHNIQUE
IN DETECTING DAMAGE INITIATION AND ACCUMULATION AND IN
IDENTIFYING THE FAILURE MECHANISMS AND PROCESSES IN
GRAPHITE/EPOXY LAMINATES DURING FATIGUE LOADING

APPROACH

- IDENTIFY THE APPROPRIATE TESTING, DATA REDUCTION AND DATA ANALYSIS METHODOLOGIES
- PERFORM EXPERIMENTAL PROGRAM WITH A VARIETY OF CROSS-PLY LAMINATES AND DETERMINE THE EFFECT OF STACKING SEQUENCE AND PLY THICKNESS ON ACOUSTIC EMISSION RESULTS
- DETERMINE THE ACOUSTIC EMISSION SOURCE INTENSITIES WHICH BEST IDENTIFY MATRIX CRACKING, DELAMINATION, FIBER BREAKAGE AND FRICTION
- CORRELATE THE ACOUSTIC EMISSION RESULTS WITH OTHER NONDESTRUCTIVE (Visual, X-Radiography, Acusto-Ultrasonics, and Frequency Response) and DESTRUCTIVE (Laminate Dely, Photomicrography, and SEM) TECHNIQUES

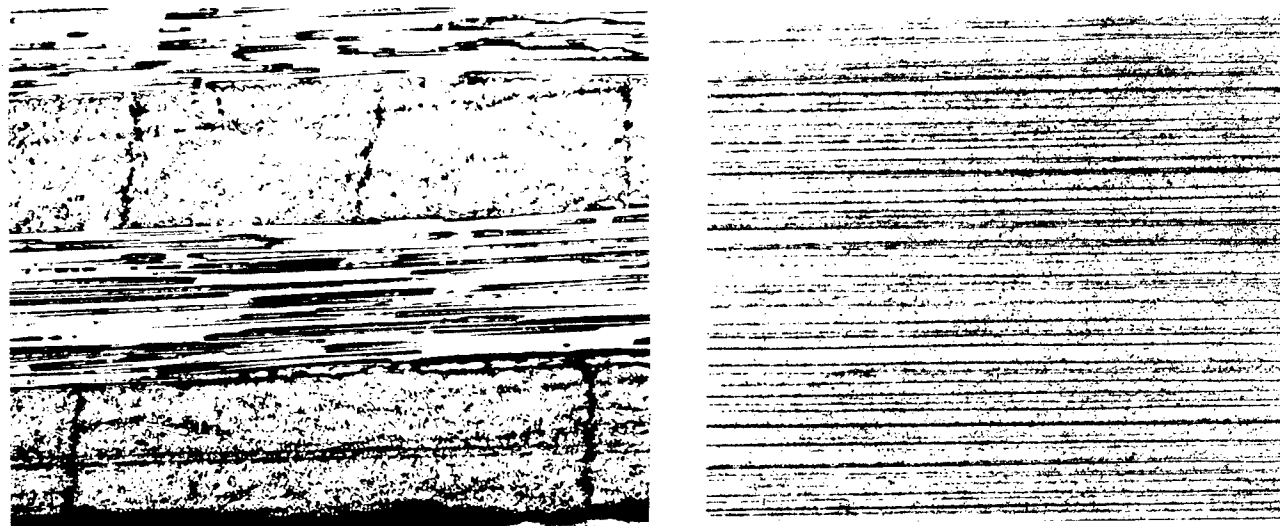


Figure 1. Photomicrograph and X-radiograph of graphite/epoxy [90/0/90]s laminate loaded to 60% of ultimate load. Number of transverse cracks is approximately 3 per mm.

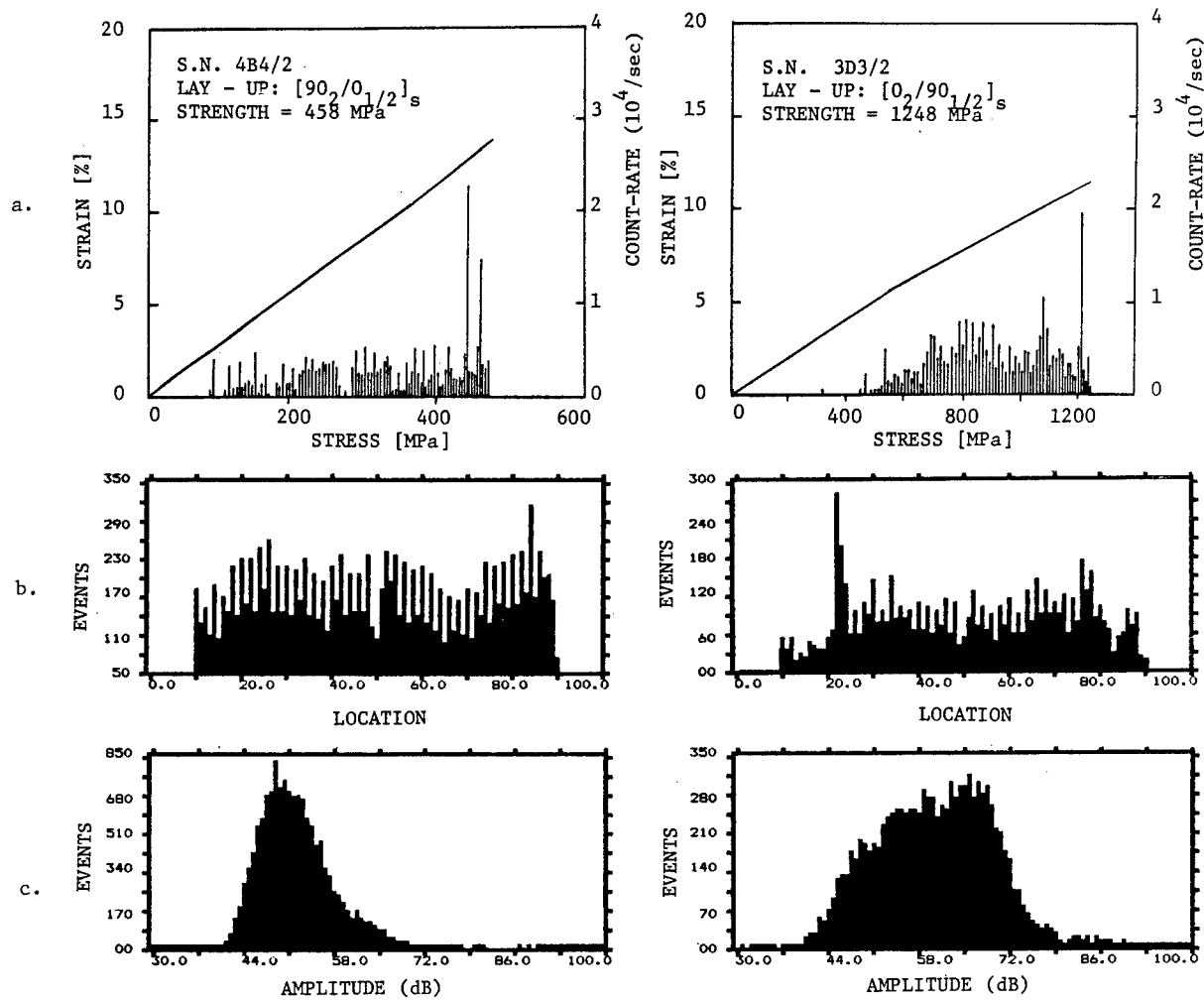


Figure 2. Acoustic emission accumulated during quasi-static tensile loading to failure in two cross-ply graphite/epoxy laminates: a) count-rate and deformation; b) location distribution histograms of events; c) amplitude distribution histograms of events. Results indicate effect of stacking sequence on AE results.

SPEC. NO. 4A8/1 $\sigma_f = 370.1$ MPa
 LAY - UP: $[90_2/0_1/2]_s$ $E^f = 4,381$ EVENTS

SPEC. NO. 3C9/2 $\sigma_f = 1695.6$ MPa
 LAY - UP: $[0_2/90_1/2]_s$ $E^f = 16,561$ EVENTS

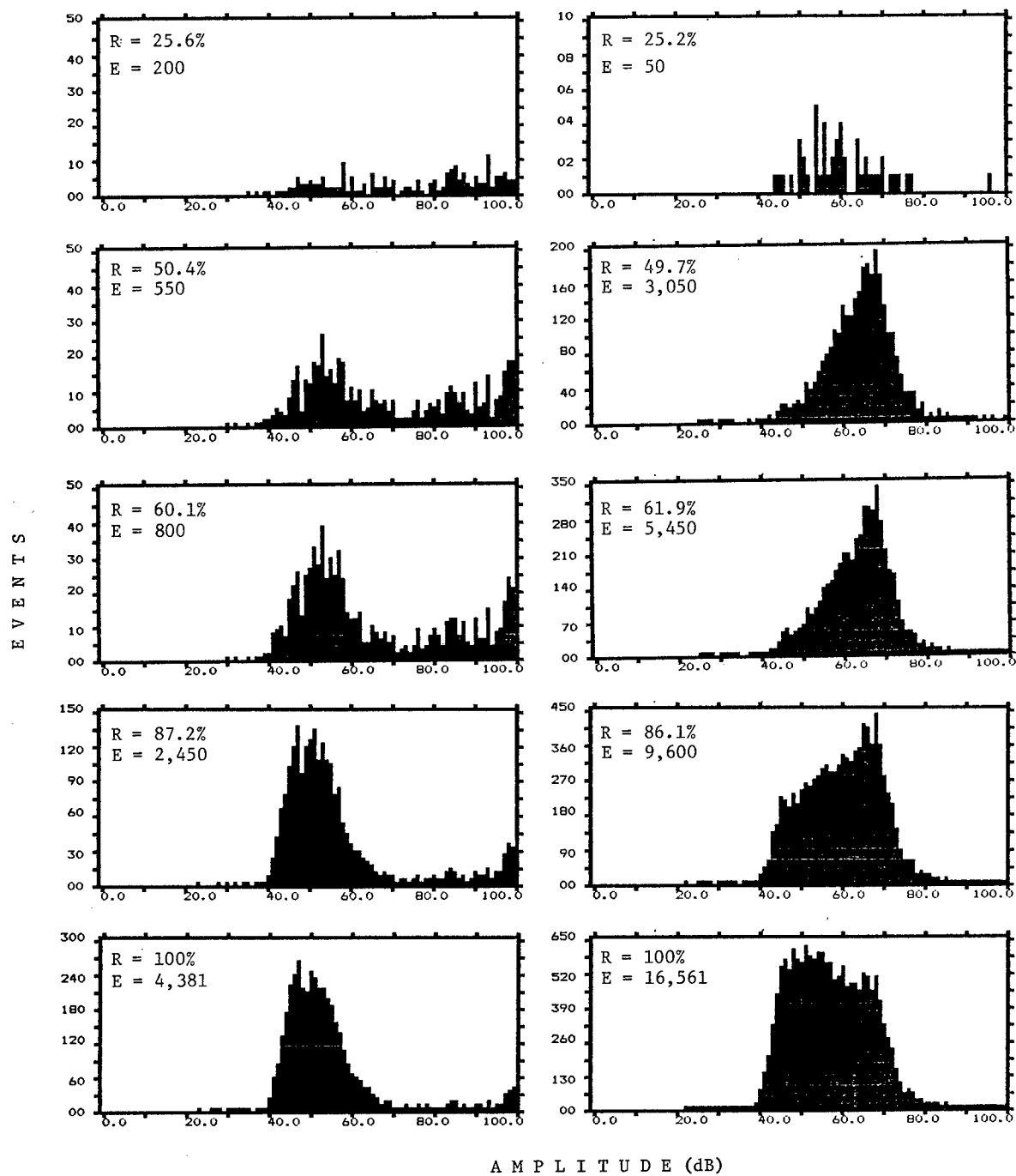


Figure 3. Amplitude distribution histograms of events accumulated at different load levels ($R = \sigma/\sigma_f \times 100\%$) during quasi-static tensile loading to failure for two cross-ply graphite/epoxy laminates. Results indicate effect of stacking sequence on the failure process.

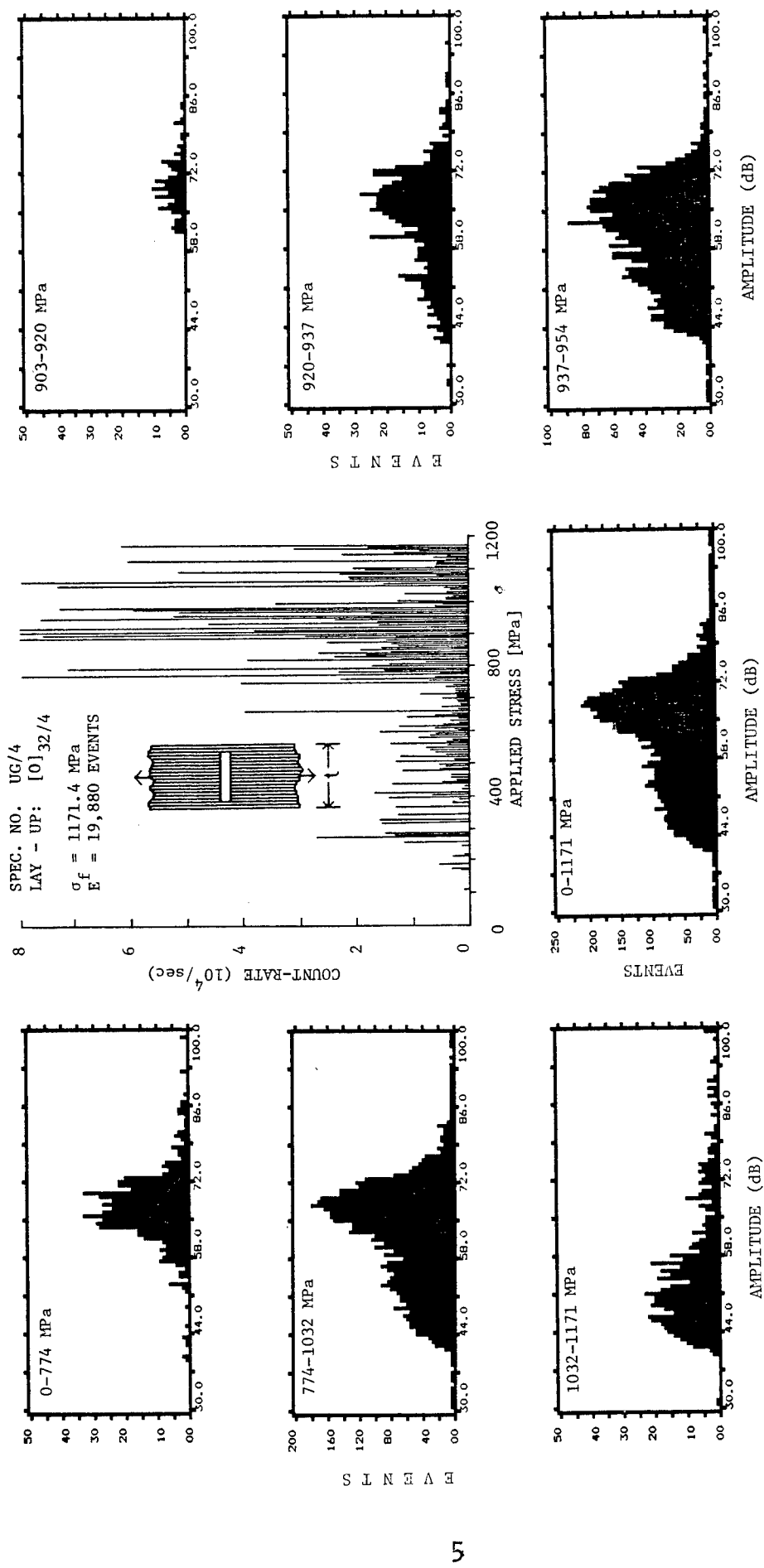


Figure 4. Acoustic emission accumulated during quasi-static tensile loading to failure of unidirectional graphite/epoxy. Inner 28 layers contain an artificial gap at the center of the specimen (inset). Delamination at the tips of the gap and splitting of the outer 4 layers can be correlated with the amplitude distribution histograms of events accumulated at different stages of loading.

SPEC. NO. 5C3/1
LAY - UP: $[0_2/90_2/0]_s$

$\sigma_d = 397.7$ MPa
1 Volt = 159.1 MPa

$N = 0 - 11,500$ Cycles
 $f = 1.0$ Hz $E = 2,301$ EVENTS

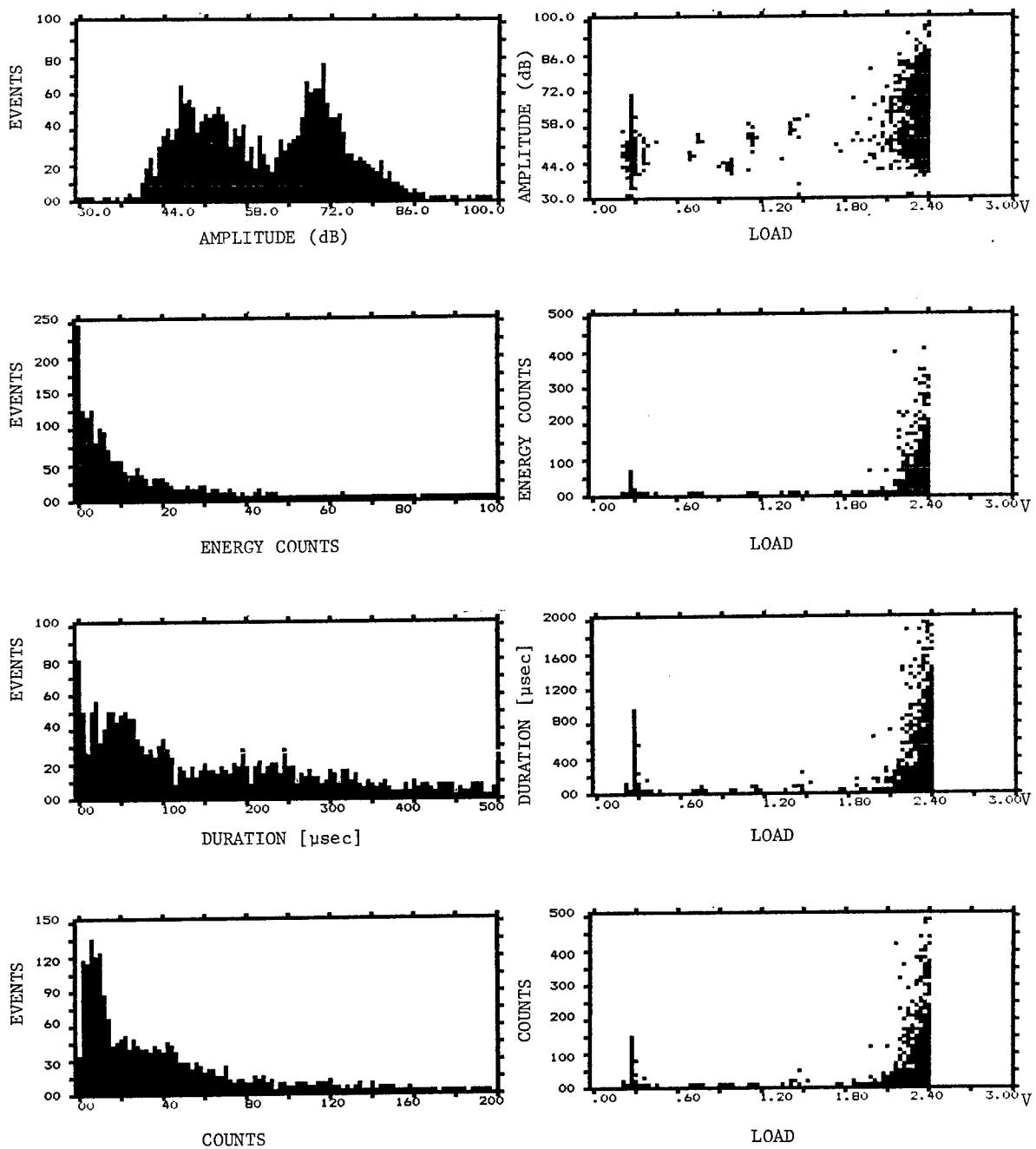


Figure 5. Distribution of AE source intensities for events accumulated during the initial part of fatigue loading ($R = 0.1$) of graphite/epoxy $[0_2/90_2/0]_s$ laminate. Significant emission is generated by friction among newly created fracture surfaces. High source intensities occur only at the upper load range.

SPEC. NO. 5C3/1

$\sigma_d = 397.7$ MPa

$N = 15,400 - 19,475$ Cycles

LAY - UP: $[0_2/90_2/0]_s$

1 Volt = 159.1 MPa

$f = 1.0$ Hz $E = 9,931$ EVENTS

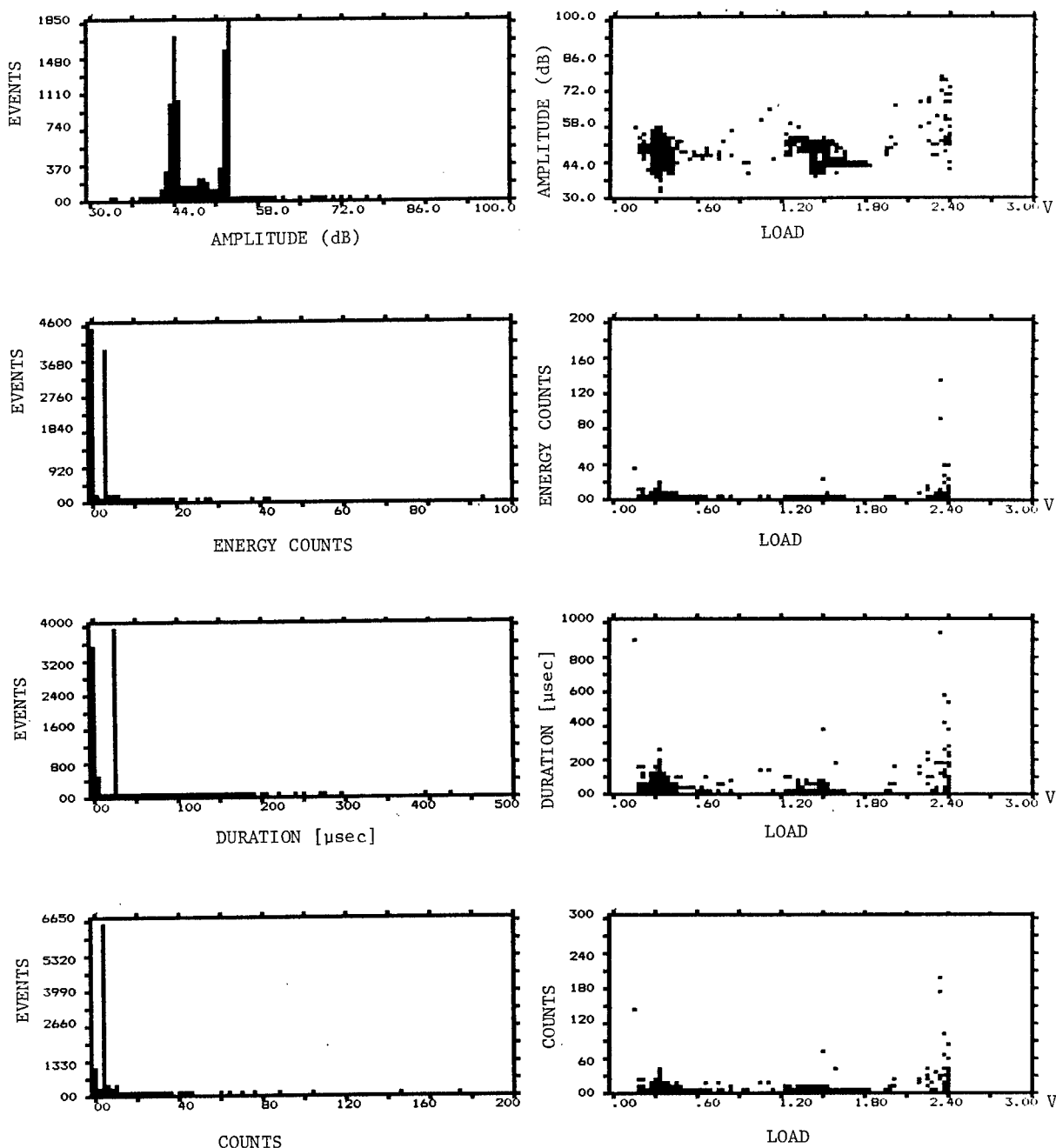


Figure 6. Distribution of AE source intensities, for the same specimen shown in Figure 5, for events accumulated during a different range of cycle numbers. Practically no new damage has occurred and all emission is generated by friction.

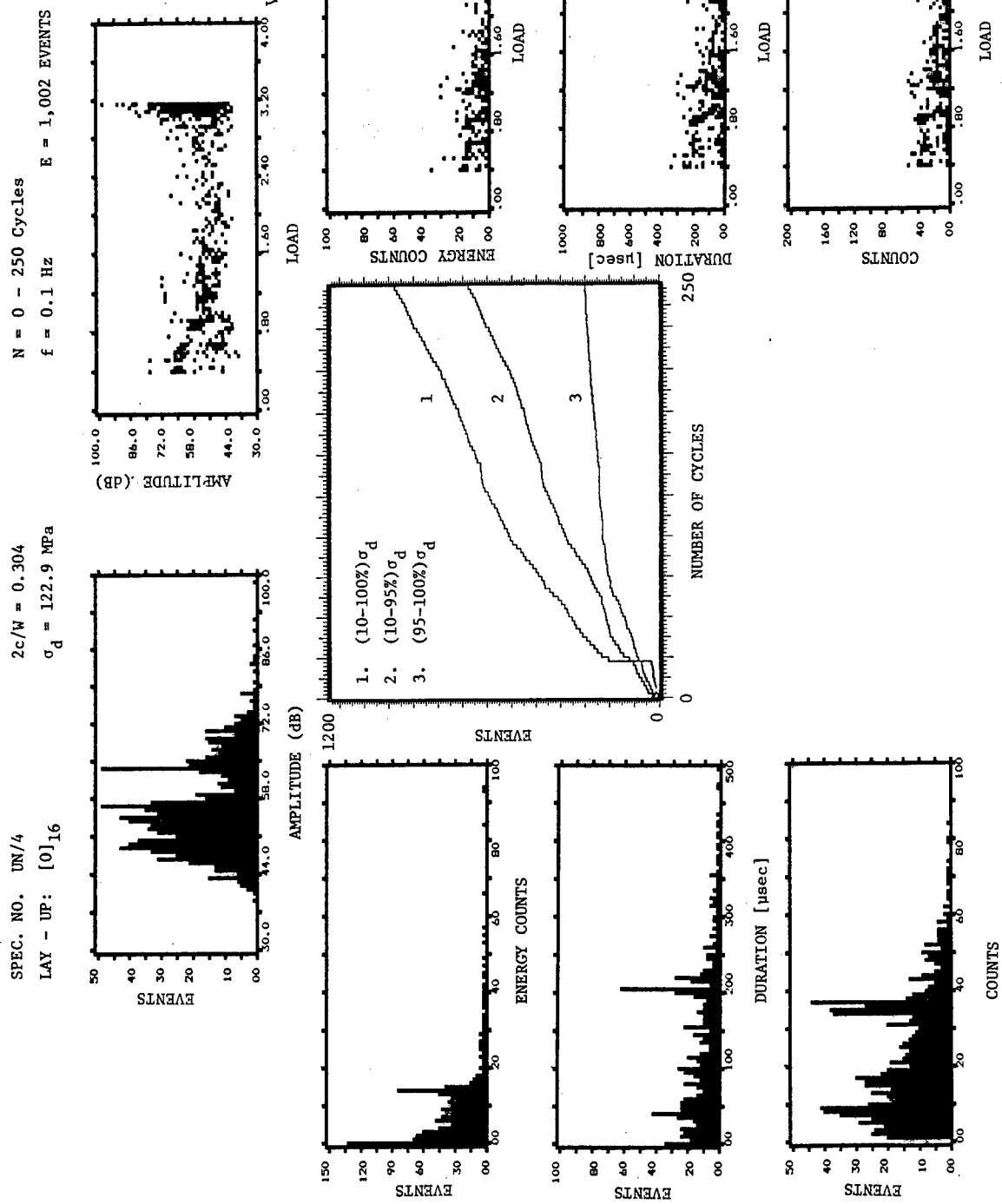


Figure 7. Distribution of AE source intensities for events accumulated during the first 250 cycles of fatigue loading ($R = 0.1$) of double edge notched unidirectional graphite/epoxy. Initially significant emission is due to damage (matrix splitting). With increasing number of cycles most of the emission is due to friction and is generated at the lower range of the applied stress.

1 Volt = 37.2 MPa

SPEC. NO. UN/4
LAY - UP: [0]₁₆

$2c/W = 0.304$
 $\sigma_d = 122.9$ MPa

$N = 15 - 30$ Cycles
 $f = 0.1$ Hz

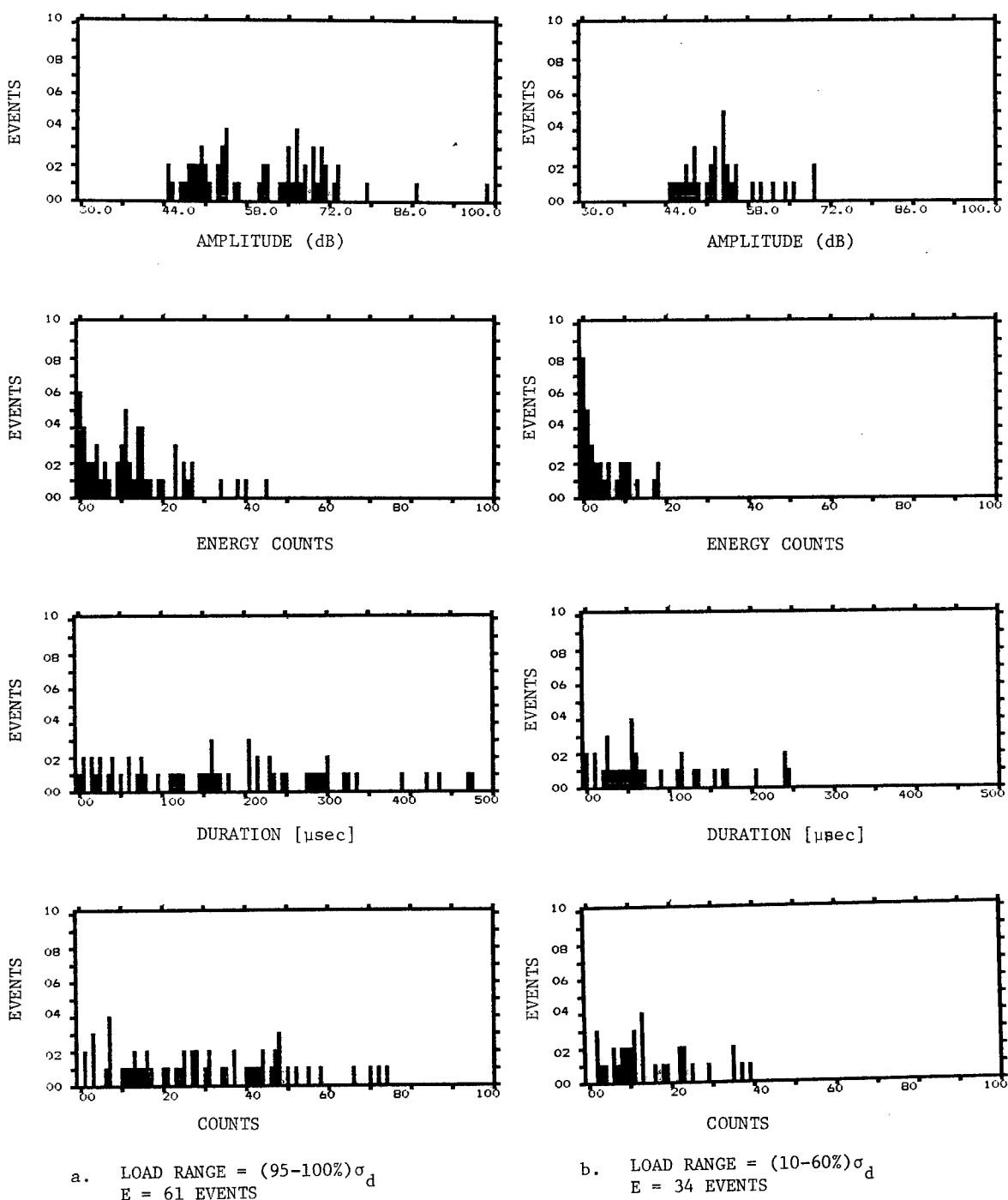


Figure 8. Distribution of AE source intensities for events accumulated during cycle 15 through 30 of the same specimen shown in Figure 7 for a) events generated at the upper part of the load range; b) events generated at the lower part of the load range. Low and middle range AE source intensities are generated by friction and matrix failure, respectively.

SPEC. NO. UN/4
LAY - UP: $[0]_{16}$

$2c/W = 0.304$
 $\sigma_d = 122.9$ MPa

$N = 210 - 250$ Cycles
 $f = 0.1$ Hz

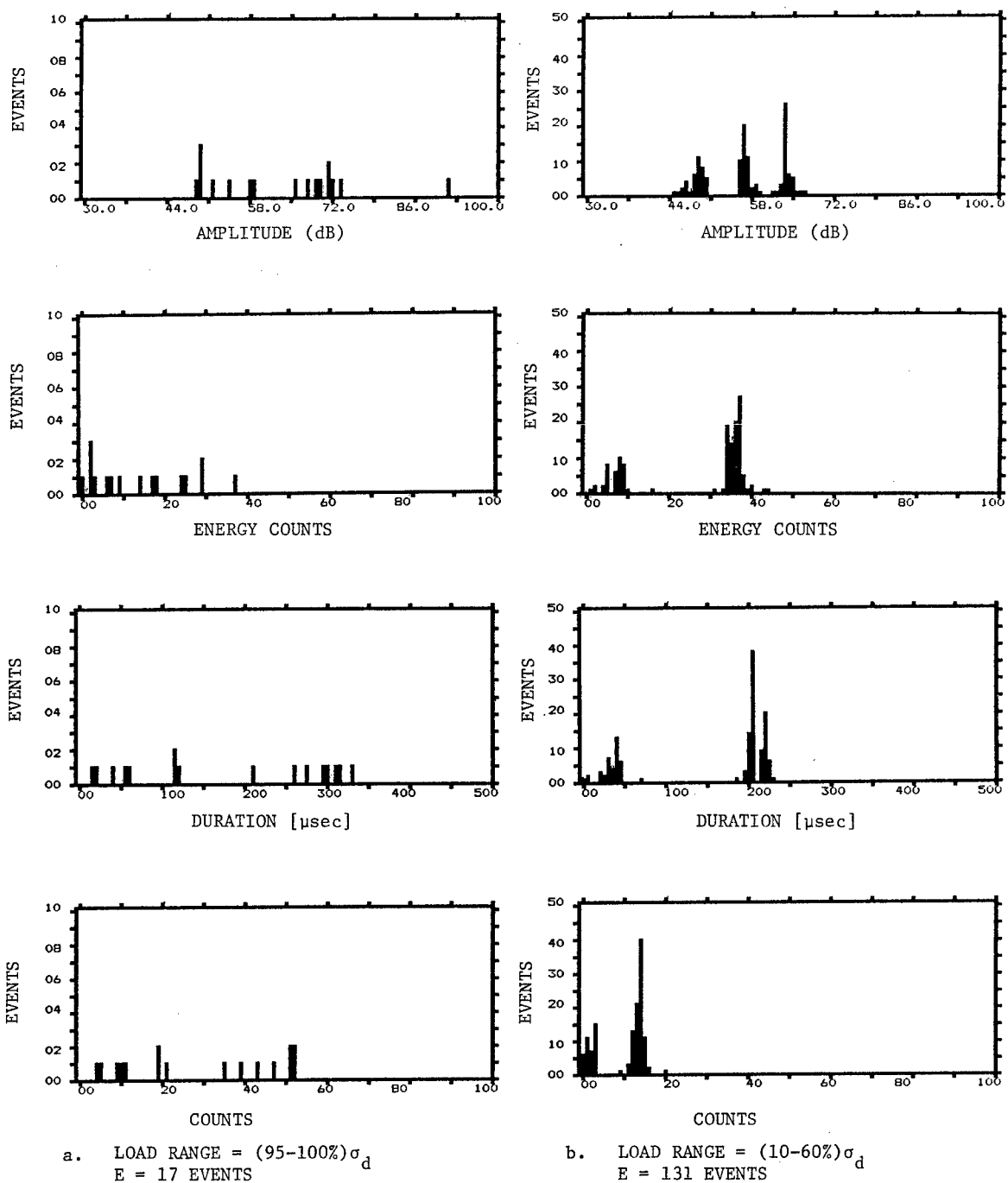


Figure 9. Distribution of AE source intensities for events accumulated during cycle 210 through 250 of the same specimen shown in Figure 7 for a) events generated at the upper part of the load range; b) events generated at the lower part of the load range. Identification of damage through AE may require analysis of several source intensities and load ranges.

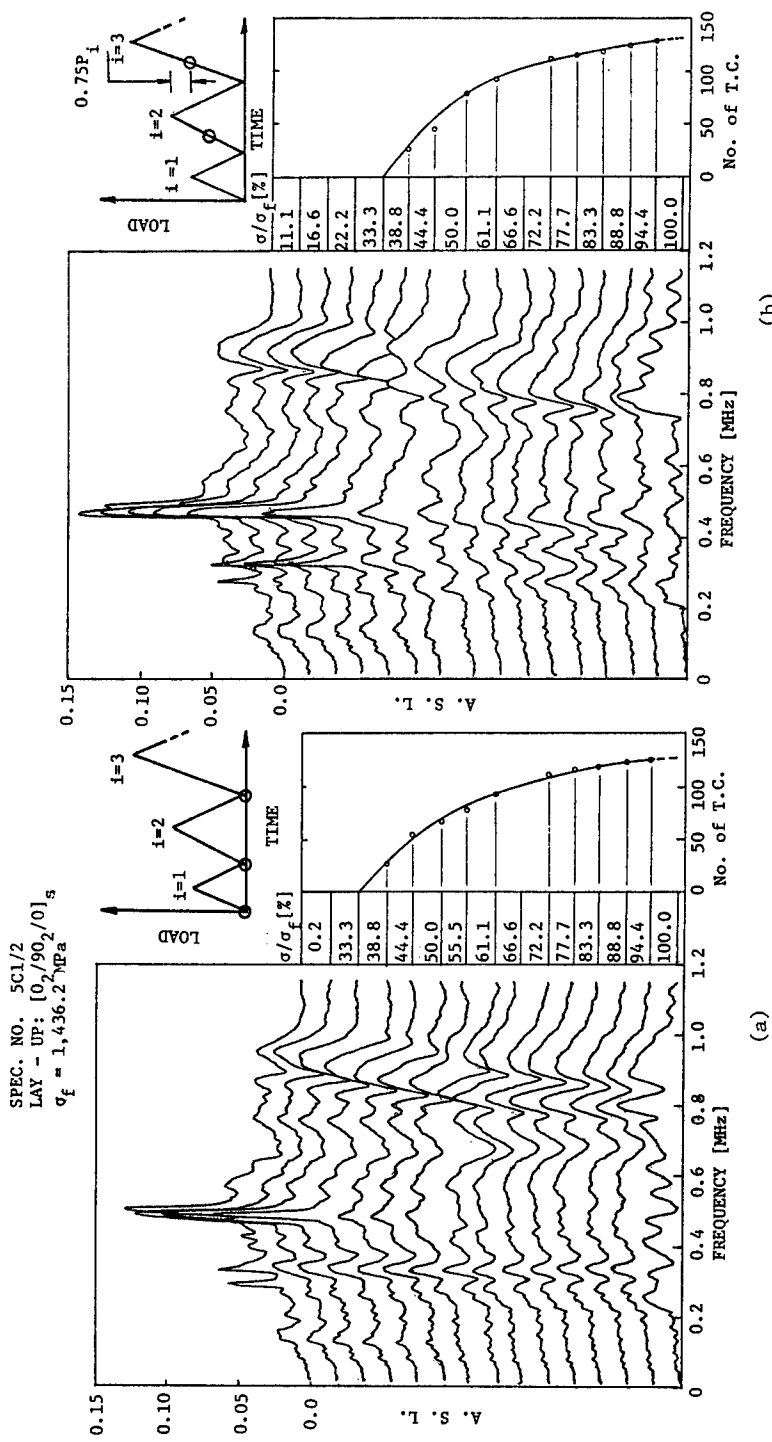


Figure 10. Frequency response versus state of stress, and number of transverse cracks for graphite/epoxy [0₂/90₂/0₁]_s laminate: a) unloaded specimen; b) specimen under 75% of maximum previous load cycle. Amplitude at frequencies of 150 and 470 KHz reduces dramatically with damage initiation. In the frequency range of 0.8 - 1.0 MHz amplitude is constant but a shift in frequency occurs during damage accumulation. Following damage saturation, frequency is unchanged.

MONITORING ACOUSTIC EMISSION IN IMPACT-DAMAGED COMPOSITES

Jonathan Averbuch, Shahrokh Gaffari and Eliezer Katz

Department of Mechanical Engineering and Mechanics
Drexel University
Philadelphia, Pennsylvania 19104

ABSTRACT

The composite laminates now being used in aircraft and aerospace structures are subjected to a variety of impact threats, such as dropped tools during fabrication and handling, or hard objects such as runway stones, ice balls, etc. Research results during the past two decades indicate that such impact damage is frequently non-visual but nevertheless results in significant performance degradation. This sensitivity of composites to non-visual internal damage is of major concern, primarily when these materials are used in primary structures.

Among the conventional nondestructive techniques for detecting and locating non-visual impact damage are ultrasonic C-scan and X-radiography. Monitoring acoustic emission (AE) is a promising NDT procedure in that it can provide information about damage progression and damage criticality in real-time. Consequently, this study focuses on the applicability of the AE technique to impact-damaged composites subjected to external loading.

This research constitutes a comprehensive program to provide a detailed characterization of impact damage in graphite/epoxy laminates subjected to low velocity (20-500 m/sec) impact and to develop the proper procedures for monitoring acoustic emission in impact-damaged laminates. A variety of experimental and analytical techniques are employed in order to determine impact damage criticality, with primary emphasis being placed on the applicability of the acoustic emission technique to detect and locate non-visual impact damage, monitor its progression under external loading, and determine its criticality. Four major areas are addressed in this program: 1. nondestructive detection and evaluation with emphasis on the acoustic emission technique; 2. destructive examination for detailed mapping of the impact-damaged region; 3. failure, fracture, degradation in performance and their modeling; and 4. determination of damage criticality to identify the major causes of degradation in properties and the NDT detection threshold.

The acoustic emission results indicate that artificially induced damage (e.g. circular holes and slits) could be easily detected and located at relatively early stages of loading. Similar results were obtained with laminates containing complete perforation due to impact. However, when non-visual impact damage occurs, with significant delamination, matrix cracking and splitting (as detected through stereo X-radiographs, ultrasonic C-and F-scans, photomicrographs and delplied laminates), detection and location of existing damage during proof loading is more difficult, mainly because of the significant emission generated from throughout the specimen length during the rapid progression and accumulation of the matrix dominated failures. It has been determined, through the analysis of the AE event intensities, that during quasi-static loading significant emission is generated by friction between impact-damaged fracture surfaces in contact with each other. The more severe the damage is, the larger the amount of friction generated emission and the lower the stress level at which it initiates. Only at higher loads is actual damage progression detected through the AE. Consequently, an experimental procedure and AE data analysis methodology have been developed to detect and locate non-visual impact damage during cyclic loading. The results indicate that, based on the friction generated emission, such damage could be easily detected and located with a few load cycles and for dynamic stress levels less than 30% of static ultimate stress. With an increasing number of cycles, damage initiation and progression could be identified as well.

Other NDT techniques and examination procedures developed and applied in this research program include the acousto-ultrasonic (AU) technique and the frequency response of the impact-damaged laminate. The results indicate that both techniques can easily detect the existence of damage and its severity and they qualitatively correlate well with the strength degradation of the subject laminate. From stereo X-radiographs the

depth of the delaminated interfaces and the extent of splitting could be approximately identified, and these results also correlated well with the results obtained with the ultrasonic F-Span and deplying techniques. Other issues addressed in this study include the effects of artificially induced damage (e.g. delamination, broken fibers and notches), oblique impact, laminate thickness and configuration, strength degradation, etc., most of which are discussed in the formal presentation.

CONCLUSIONS

1. Impact damage is largely non-visual, nevertheless nondestructive and destructive examinations reveal significant internal damage in the form of delamination, intraply cracks, matrix splitting in all damaged plies, and fiber breakage. Degree of stiffness and strength degradation depend on laminate configuration.
2. During quasi-static loading in tension, the detection and location of non-visual impact damage through acoustic emission is difficult. Significant emission is generated by friction among the impact-damaged fracture surfaces.
3. However, based on this friction generated emission, during cyclic loading impact damage could be easily detected and located with a few load cycles and at relatively low dynamic stress levels. Damage progression could be easily tracked and failure mechanisms identified.
4. Damage severity could be easily determined through the acousto-ultrasonic technique. All event intensities strongly depend on the level of damage and rapidly attenuate with increasing severity.
5. Similar results are obtained using the frequency response of the subject laminate, which was found to be highly sensitive to impact damage. It seems that the frequency response depends on the details of the impact-damaged region.
6. Good qualitative correlation could be established between the various destructive and nondestructive examination procedures.

MONITORING ACOUSTIC EMISSION IN IMPACT-DAMAGED COMPOSITES

Jonathan Awerbuch, Shahrokh Ghaffari and Eliezer Katz

Department of Mechanical Engineering and Mechanics
Drexel University
Philadelphia, Pennsylvania 19104

Program sponsored by the Office of Naval Research,
N00014-84-K-0460. Yapa Rajapakse is the program
monitor.

OBJECTIVES

- DETERMINE THE APPLICABILITY OF THE ACOUSTIC EMISSION TECHNIQUE TO DETECT AND LOCATE IMPACT DAMAGE IN COMPOSITE LAMINATES, TRACK ITS PROGRESSION, IDENTIFY THE FAILURE MECHANISMS, AND EVALUATE ITS CRITICALITY
- CORRELATE THE ACOUSTIC EMISSION RESULTS WITH THE MOST COMMONLY USED NONDESTRUCTIVE AND DESTRUCTIVE EXAMINATION TECHNIQUES
- CONDUCT A DETAILED CHARACTERIZATION OF THE IMPACT-DAMAGED REGION AND IDENTIFY THE MAJOR MATERIAL VARIABLES AFFECTING ITS SEVERITY

APPROACH

I. DETECTION TECHNIQUES (NON-DESTRUCTIVE)

1. VISUAL
2. X-RADIOPHGRPHS (3-D)
3. ULTRASONICS (C and F- SCANS)
4. ACOUSTO - ULTRASONICS
5. FREQUENCY RESPONSE
6. ACOUSTIC EMISSION
7. C.C.T.V.

II. EXAMINATION TECHNIQUES (DESTRUCTIVE)

1. PHOTOMICROGRAPHY
2. DEPLYING
3. S.E.M. (3-D)

III. FAILURE AND FRACTURE

1. STIFFNESS AND STRENGTH DEGRADATION
2. APPLICATION OF FRACTURE MODELS APPLIED TO COMPOSITES
3. FINITE ELEMENT SIMULATION OF IMPACT DAMAGE

IV. DAMAGE CRITICALITY

1. CORRELATION WITH ARTIFICIALLY INDUCED DAMAGE (Broken Fibers, Inserted delamination, Notches)
2. OBLIQUE IMPACT
3. STACKING SEQUENCE EFFECT(S)
4. LAMINATE CONFIGURATION (EFFECTS)
5. LOADING FUNCTION EFFECT(S)
6. THICKNESS EFFECT(S)

SPEC. NO. 2-B10
LAY - UP: $[0_2/\pm 60/0_2/\pm 60]_s$
Impact Velocity = 58 m/s

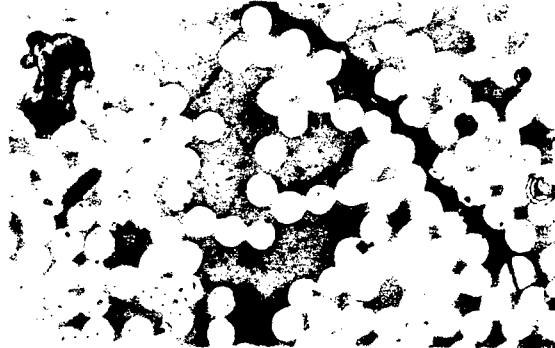


SPEC. NO. AQI-10
LAY - UP: $[0/\pm 45/90]_{2s}$
Impact Velocity = 67 m/s



SPEC. NO. 1-B2
LAY - UP: $[0_2/\pm 60/0_2/\pm 60]_s$
Impact Velocity = 86 m/s

0° and 60° Plies



SPEC. NO. 2-A4
LAY - UP: $[0_2/\pm 60/0_2/\pm 60]_{2s}$
Impact Velocity = 60 m/s

Ply No. 4, -60° Front

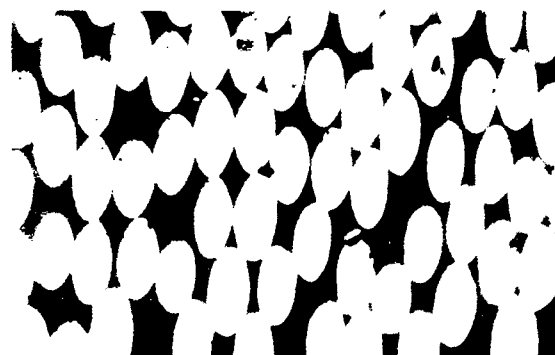


Figure 1. X-radiographs, a C-scan record, photomicrographs and a delplied interface of non-visual impact-damaged graphite/epoxy laminates, all showing significant amount of delamination, intraply matrix cracks and matrix splitting.

SPEC. NO. CQT-21
 $V_1 = 39.6 \text{ m/s}$
 $\sigma_f^1 = 732.6 \text{ MPa}$
 $E_f = 19,863 \text{ EVENTS}$

SPEC. NO. BOT-1
 $V_1 = 135.6 \text{ m/s}$
 $\sigma_f^1 = 292.6 \text{ MPa}$
 $E_f = 2,697 \text{ EVENTS}$

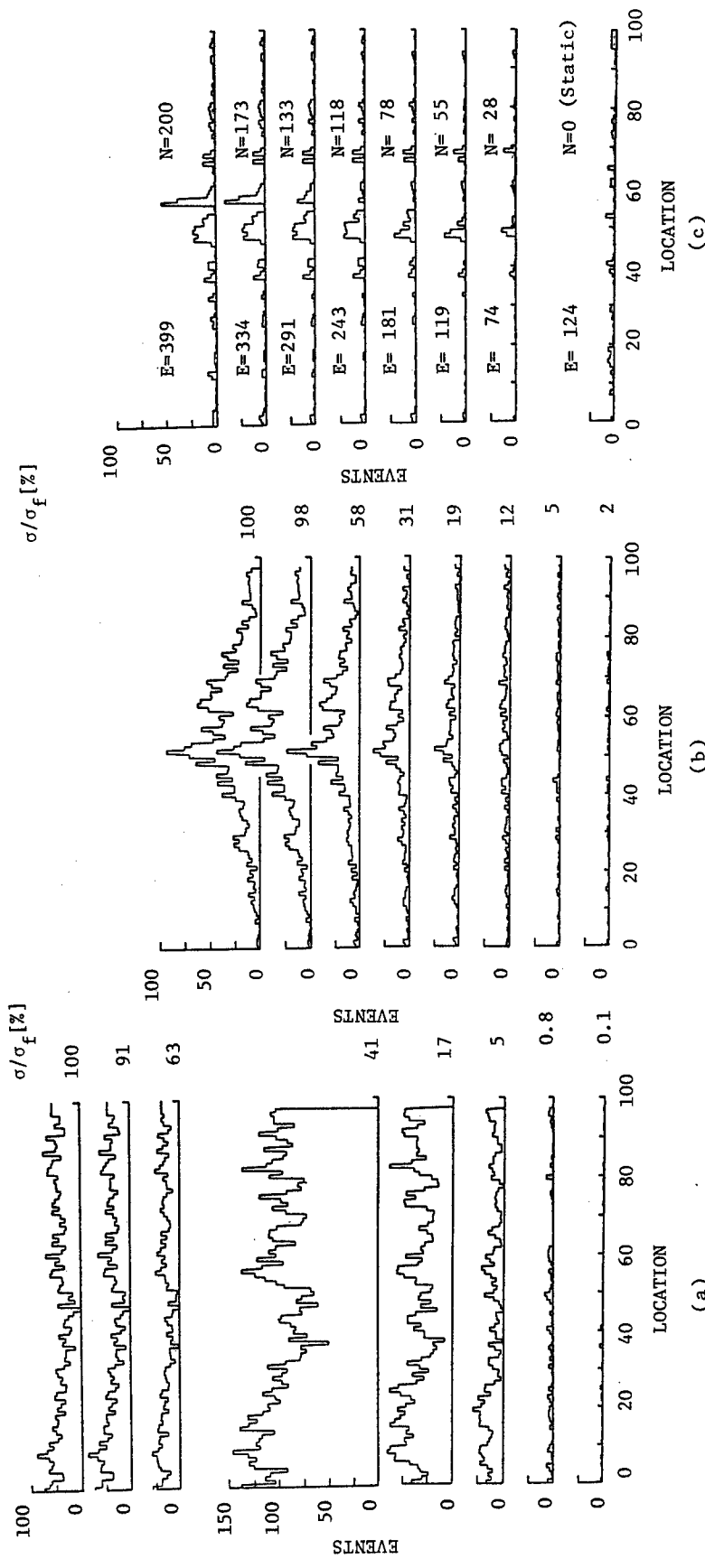


Figure 2. Location distribution histograms of events recorded for impact damaged graphite/epoxy [0/±45/90]2s laminate with: a) non-visual impact damage, recorded during quasi-static loading to failure; b) visual impact damage, recorded during quasi-static loading to failure; and c) non-visual impact damage, recorded during low cycle fatigue loading. Results indicate that impact damage could be easily detected and located during cyclic loading, while during static loading the detection of such damage is more difficult.

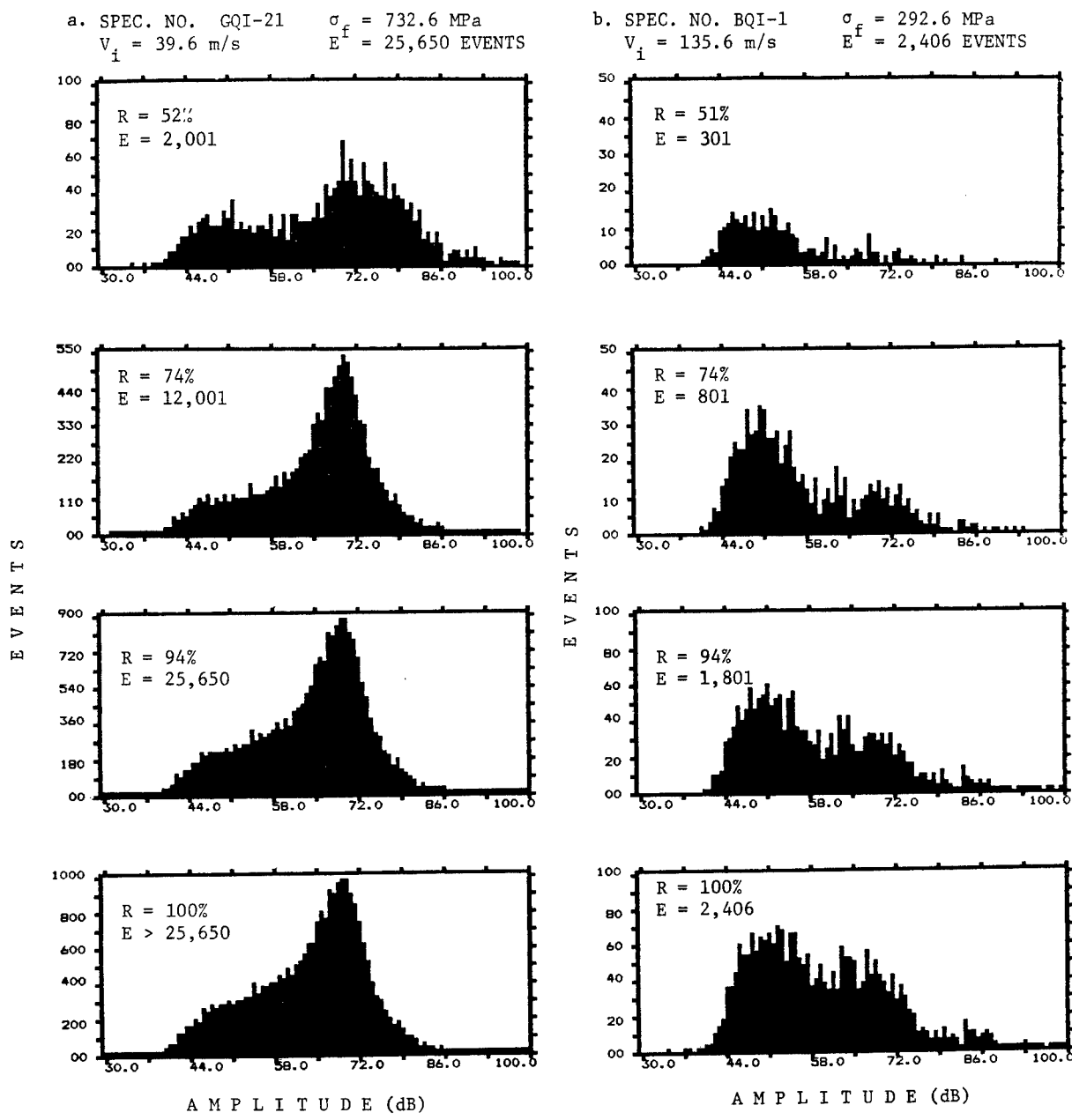


Figure 3. Amplitude distribution histograms of events recorded at different load levels ($R = \sigma/\sigma_f \times 100\%$) during quasi-static loading to failure of graphite/epoxy $[0/\pm 45/90]_2s$ laminates containing: a) non-visual impact damage; and b) visual impact damage. The larger the damage is, the larger the amount of friction generated emission and the higher the relative load level at which damage progresses.

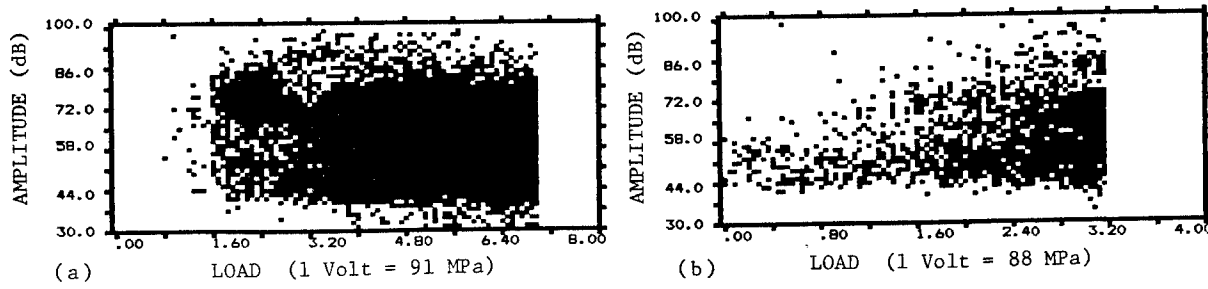


Figure 4. Event amplitudes as a function of applied load recorded during quasi-static loading to failure of the same specimen shown in Figure 3, containing: a) non-visual impact damage; b) visual impact damage. In the case of non-visual impact damage high amplitude events initiate at relatively lower load levels indicating early initiation of damage progression.

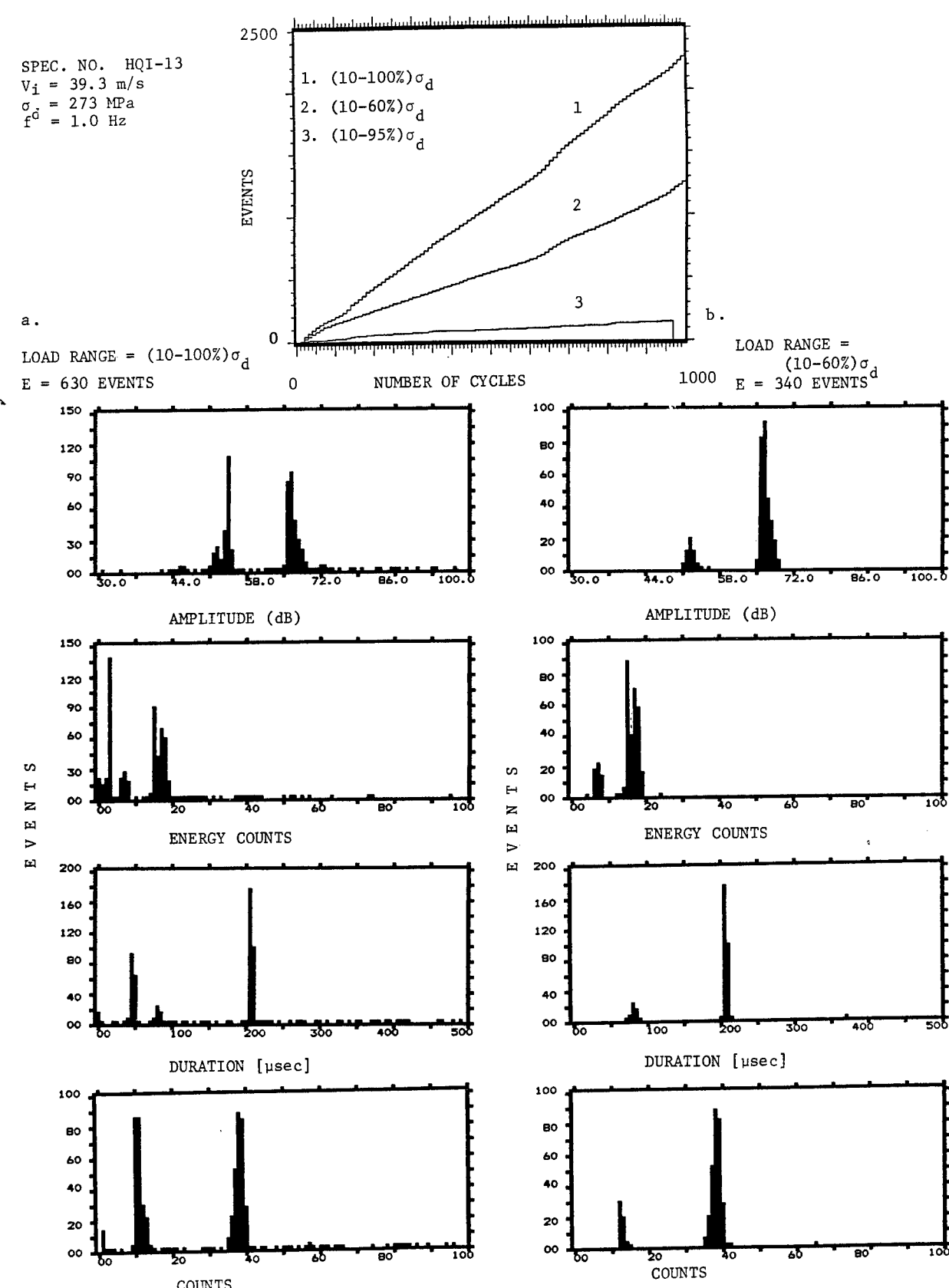


Figure 5. Distribution of acoustic emission source intensities for events accumulated during the initial part of fatigue loading ($R=0.1$) of graphite/epoxy $[0/\pm 45/90]_2s$ laminate: a) events generated through the entire load range; b) events generated at the lower part of the load range. Distinction between emission generated by friction and by actual damage growth may require analysis of several source intensities and load ranges.

SPEC. NO. HQI-13
 $V_i = 39.3$ m/s

$\sigma_d = 273$ MPa
 $f_d = 1.0$ Hz

1 Volt = 45.5 MPa

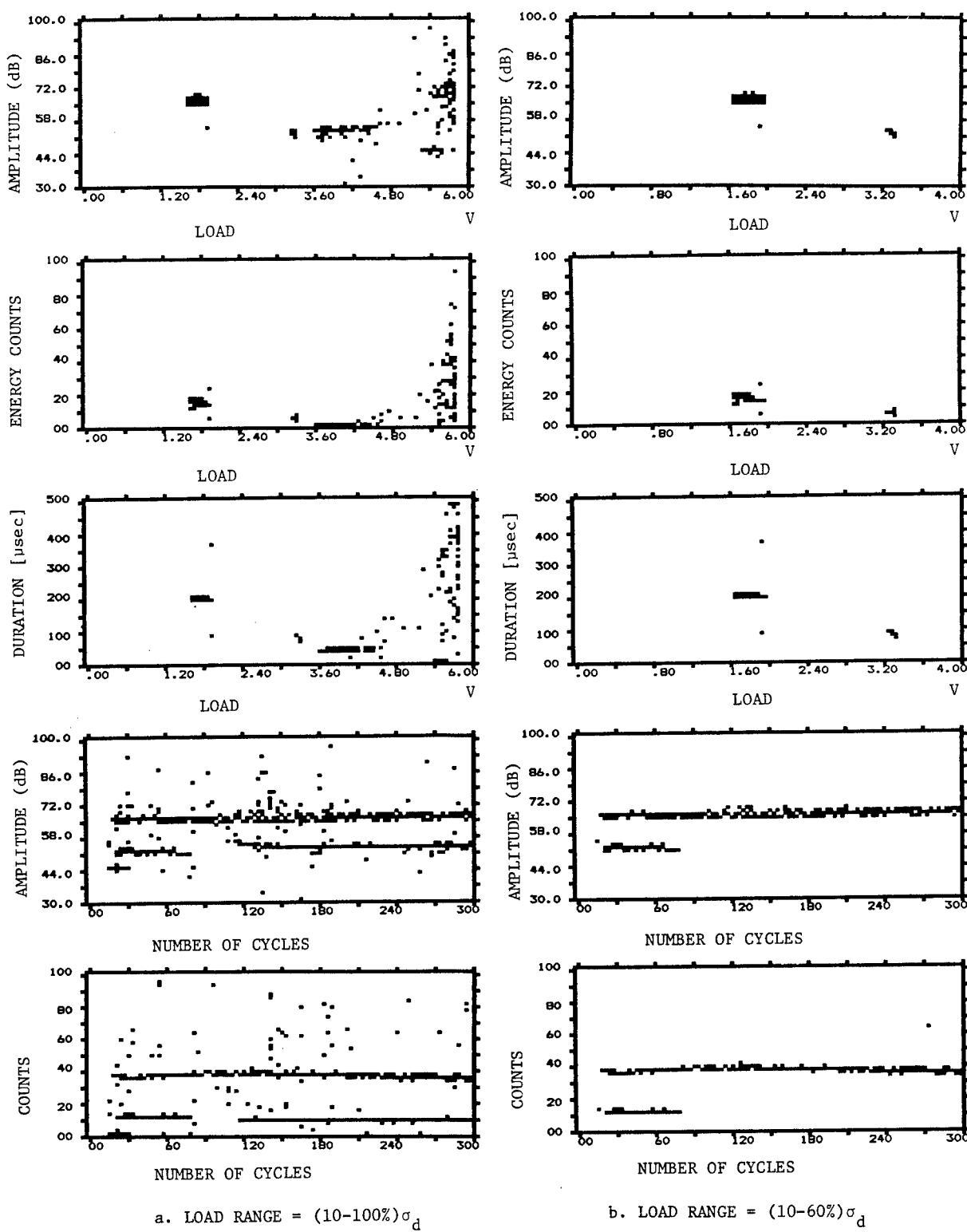


Figure 6. Acoustic emission source intensities as a function of applied dynamic stress and number of cycles during the initial part of fatigue loading of the same specimen shown in Figure 5: a) events generated through the entire load range; b) events generated at the lower part of the load range. High source intensities occur only at the upper part of the load range indicating damage accumulation. At the lower part of the load range all source intensities are of medium and low ranges, all of which are generated by friction. These results were obtained throughout the fatigue loading.

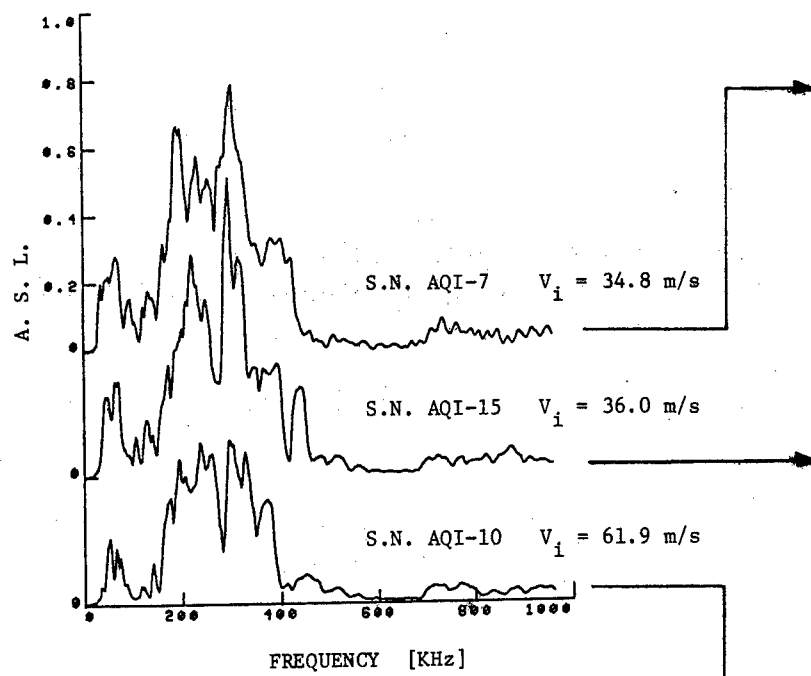


Figure 7. Frequency response of impact-damaged graphite/epoxy $[0/\pm 45/90]_{2s}$ laminate and X-radiographs recorded for three different impact velocities. Results indicate that the frequency response of the subject laminate is sensitive to damage severity.

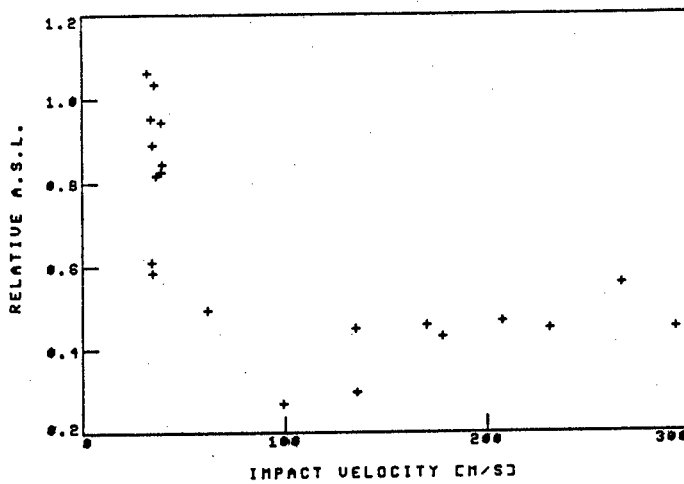


Figure 8. Peak amplitude of average signal level (A.S.L.) of the frequency response (examples of which are shown in Figure 7) measured at 350 KHz versus impact velocity (graphite/epoxy $[0/\pm 45/90]_{2s}$). The peak amplitude is highly sensitive to impact damage.

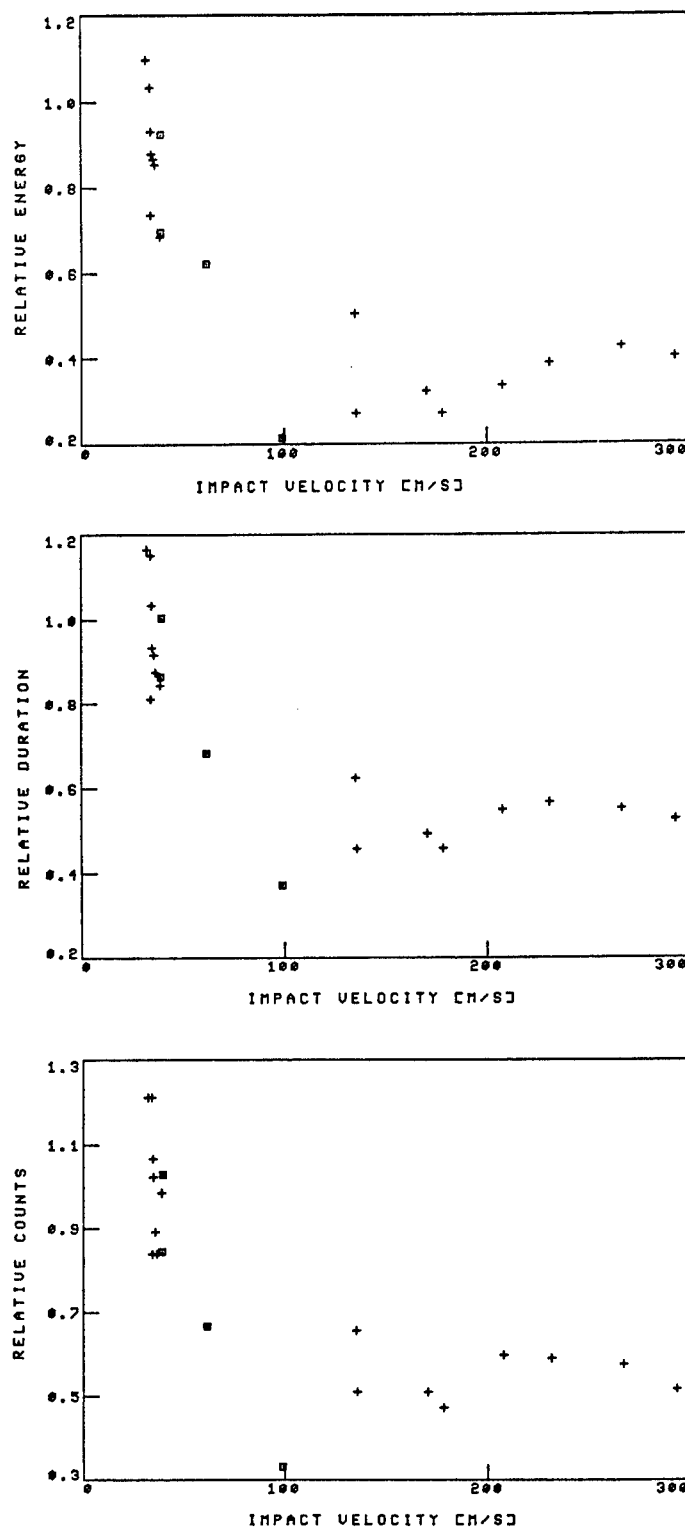


Figure 9. Acousto-ultrasonic (AU) event intensities (counts, duration and energy) versus impact velocity for graphite/epoxy $[0/\pm 45/90]_2s$ laminate. All three AU variables are highly sensitive to state of damage.

PROCESSING THERMOPLASTIC COMPOSITES

George S. Springer

Department of Aeronautics and Astronautics
Stanford University, Stanford, California 94305

Fiber reinforced thermoplastic resin composites are manufactured by heating the composite above the "melting" point of the resin followed by rapid cooling. Pressure is also applied during cooling. The cooling rate determines the crystal structure of the resin. The applied pressure assures the proper resin content and fiber distribution. Hence, both the cooling rate and the applied pressure affect strongly the mechanical properties of the composite. Therefore, the appropriate cooling rates and pressures must be employed to achieve the required mechanical properties.

The objectives of this investigation is to determine the effects of the processing parameters on the mechanical properties, and to establish methods for selecting the proper processing variables (cooling rate, pressure) for each application. To achieve these objectives, a model is being developed which simulates the manufacturing process, and relates the process variables to the thermal, chemical, and mechanical properties. The model consists of two sub-models. The "thermo-chemical" submodel relates the cooling rate to the crystallinity and the mechanical properties of the finished product. The "flow" submodel relates the applied pressure and the resin and fiber distributions.

Thus far, the "thermo-chemical" submodel has been developed. This model provides relationships between the cooling rate and crystallinity, and between the crystallinity and mechanical properties. The model was implemented with a "user-friendly" computer code suitable for generating numerical results for thermoplastic resin composites and, in particular, for PEEK resin composites.

Tests were also performed with PEEK resin. In these tests, first the relationship between the cooling rate and crystallinity was established using differential scanning calorimetry. Second, the tensile, compressive and shear strengths and moduli were measured as functions of the cooling rate. These data, together with the computer code, can be used to determine the optimum cooling rates to be used for PEEK resin composites.

PROCESSING THERMOPLASTIC COMPOSITES

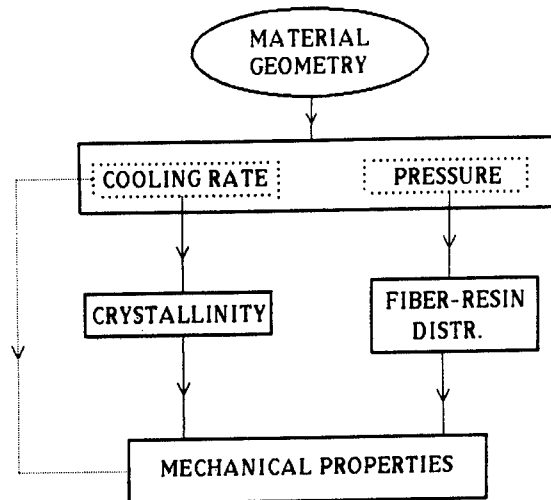
Department of Aeronautics and Astronautics
Stanford University

OBJECTIVE

To establish procedures needed to determine optimum process variables (cooling rate, pressure)

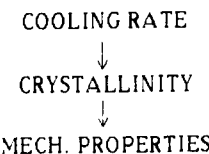
Principal Investigator: George S. Springer

Investigators: J. Burwasser
W. Lee
A. Miller
M. Talbott

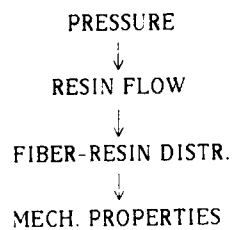


APPROACH

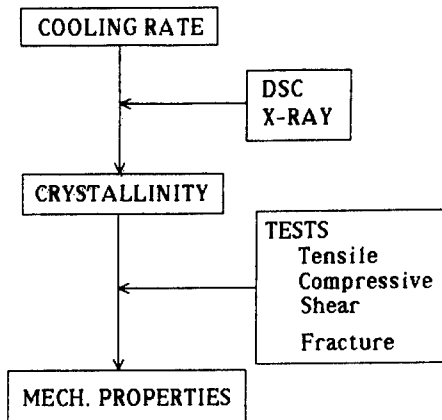
● THERMOCHEMICAL MODEL



○ FLOW MODEL

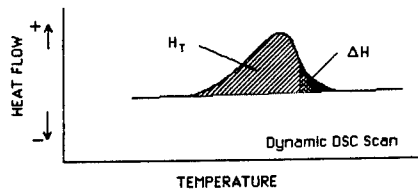


THERMOCHEMICAL MODEL



THERMOCHEMICAL MODEL

- $\log[-\ln(1-c)] = \log \phi - n \log \left(\frac{dT}{dt} \right)$



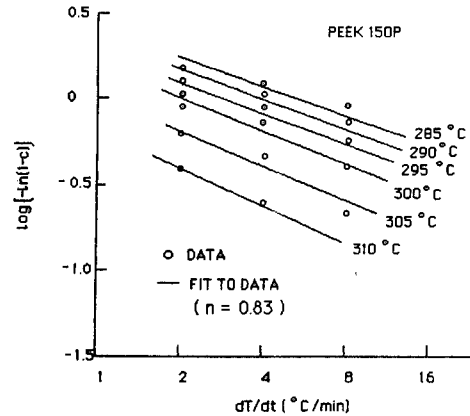
$$c \equiv \frac{\Delta H}{H_T} \quad \text{Relative Crystallinity}$$

$$c_{\text{abs}} \equiv c \cdot q = \frac{\Delta H}{H_{\text{ult}}}$$

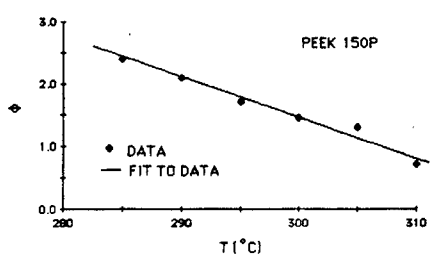
Absolute Crystallinity

$$\log[-\ln(1-c)] = \log \phi - n \log \left(\frac{dT}{dt} \right)$$

$$\phi = -\ln(1-c) \quad \text{when} \quad \frac{dT}{dt} = 1$$

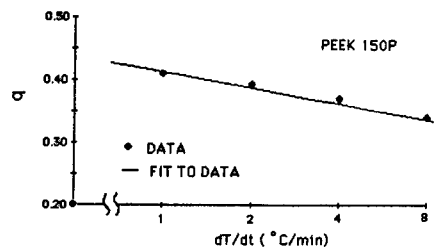


$$\log[-\ln(1-c)] = \log \phi - n \log \left(\frac{dT}{dt} \right)$$



$$\phi = -0.062 T + 20.2$$

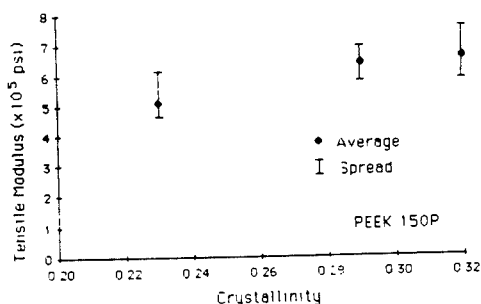
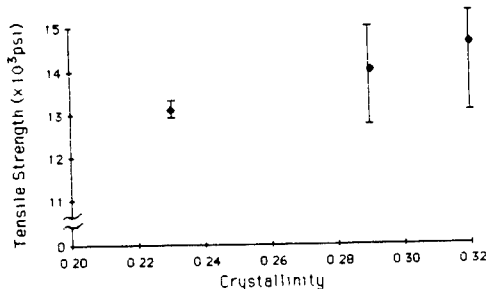
$$q = \frac{H_T}{H_{\text{ult}}}$$



$$q = -0.08 \ln \left(\frac{dT}{dt} \right) + 0.41$$

MECHANICAL PROPERTIES

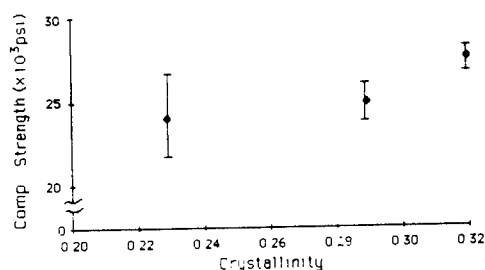
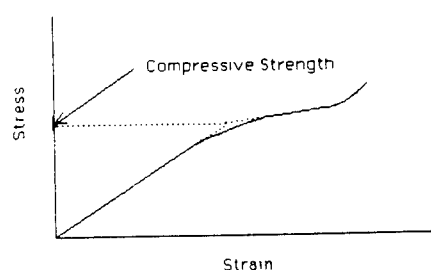
1. Tensile Properties



MECHANICAL PROPERTIES

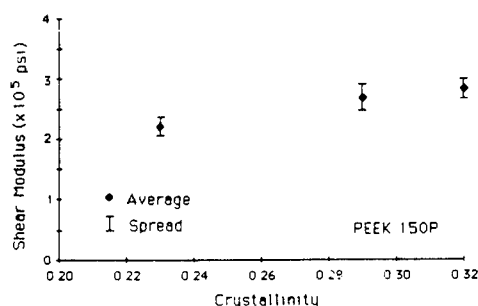
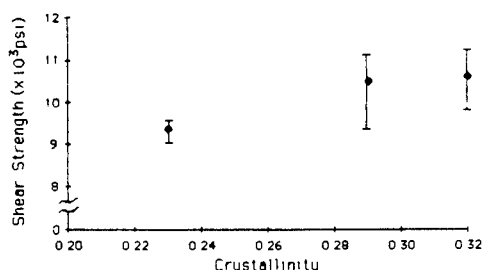
2. Compressive Properties

Definition of Compressive Strength



MECHANICAL PROPERTIES

3. Shear Properties



SUMMARY

PROGRESS TO DATE

- 1) GENERAL PROCEDURE FOR ESTABLISHING PROCESS VARIABLES
- 2) "USER FRIENDLY COMPUTER CODE FOR RELATING COOLING RATE, CRYSTALLINITY AND MECHANICAL PROPERTIES
- 3) TEST METHODS FOR DETERMINING CRYSTALLINITY
- 4) DATA AND EMPIRICAL CORRELATIONS FOR PEEK RESIN
 - CRYSTALLINITY AS A FUNCTION OF COOLING RATE
 - MECHANICAL PROPERTIES AS A FUNCTION OF COOLING RATE

COMPOSITE CRASH DYNAMICS

Huey D. Carden
NASA Langley Research Center
Hampton, VA. 23665

Richard L. Boitnott and Karen E. Jackson
Aerostructures Directorate
U.S. Army Aviation Research and Technology Activities-AVSCOM
NASA Langley Research Center
Hampton, VA. 23665

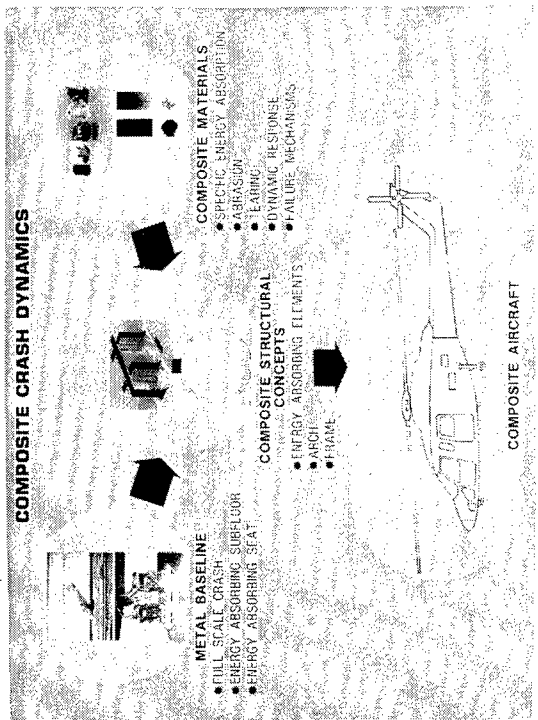
ABSTRACT

There have been many studies of the dynamic behavior of composite materials and structures. However, the majority of these studies have been concerned with the response of laminates to localized impact. Tolerance of the laminate to delamination, fiber breakage, and other forms of damage, and the influence of any damage on the strengths have been the principal concerns of these past studies. In contrast, little has been done to study large deformation transient dynamic response of structural elements as-a-whole, that is global response as opposed to local response. However, with the increasing usage of composite materials for major structural elements in aircraft, more research is needed to understand the response of structural elements to impacts which could simulate hard landings, wheels-up landings, or other short duration but intense loading events that will excite the entire structure, not just a localized region. In general, it is expected that the response of the structural elements to these crash-related loads will involve large deformations and failure. In addition, energy absorption or the lack of it during failure is an important variable if damage to other parts of the structure and possible injury to occupants is to be minimized. Because of these concerns with future structures, work is in progress to study the large deformation response of simple composite structural elements to intense dynamic loadings.

A research program has been formulated to investigate the response characteristics of generic composite components to simulated crash loadings. This program has been arranged to focus on three levels: the laminate level for material properties such as energy absorbing qualities and the behavior of skin materials; the element level focusing on more complex geometry and behavior of beams, frames (rings), arches, and panels; and the substructure level dealing with cylindrical shells, floors, and larger-scale components. Scaling studies will also be included.

The goal of research on the generic components is to provide a data base and understanding of generic composite component behavior subjected to crash loading conditions supported by validated analytical methods. To help achieve this goal, in-house research, contractual efforts, and university grants are included in the program.

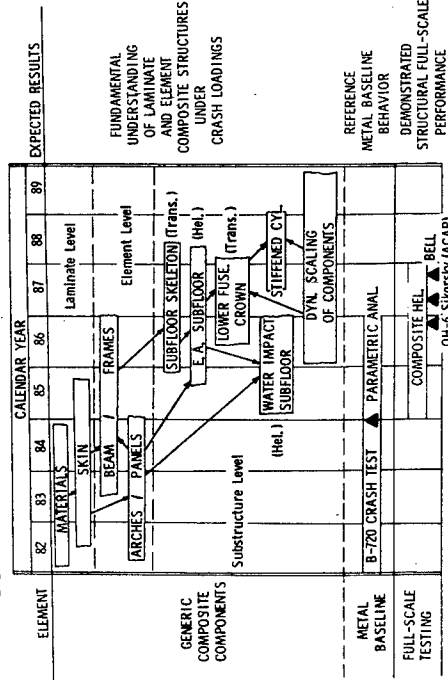
This presentation will summarize results from three of the research areas under the composite crash dynamics program that include: beam impact studies, composite fuselage frame impact studies, and abrasive loadings of skin materials.



COMPOSITE CRASH DYNAMICS

- INTRODUCTION AND BACKGROUND
- COMPOSITE IMPACT DYNAMICS PROGRAM
- EXPERIMENTAL RESULTS
 - Composite Frames
 - Beam Impact
 - Abrasion
- ADDITIONAL RESEARCH EFFORTS
- CONCLUDING COMMENTS

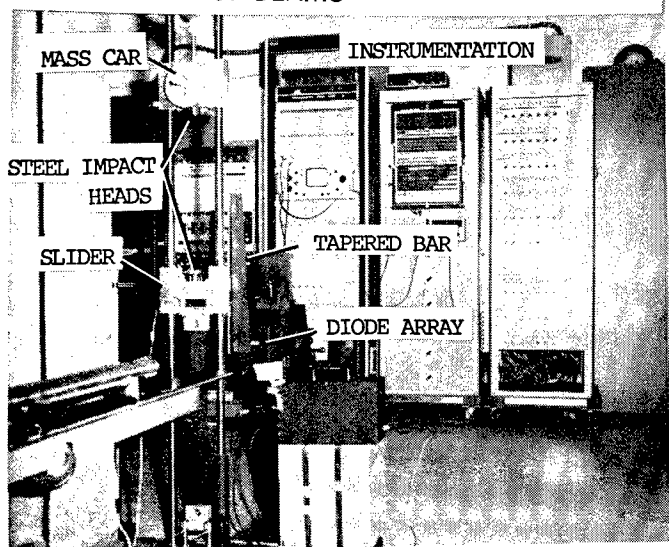
RESPONSE OF GENERIC COMPOSITE COMPONENTS TO CRASH LOADINGS



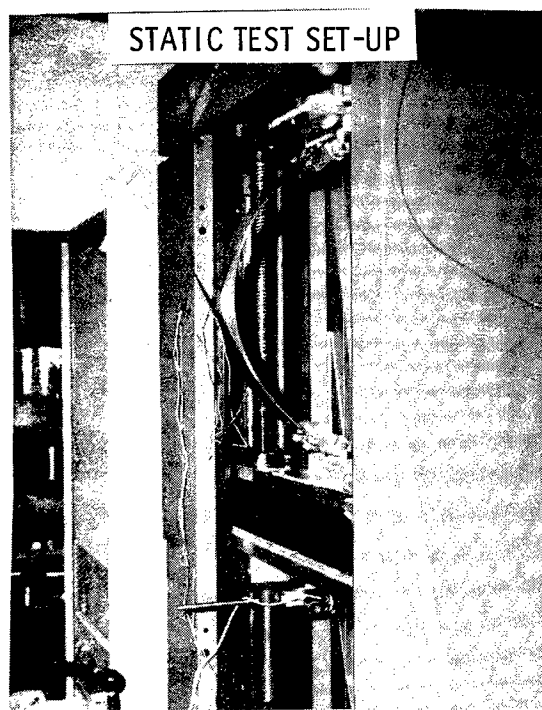
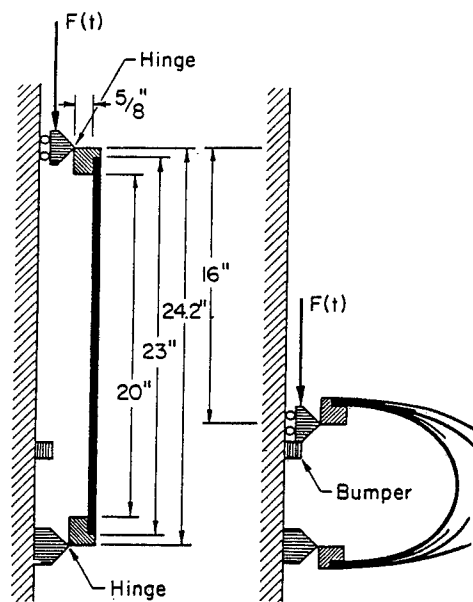
COMPOSITE CRASH DYNAMICS PROGRAM GOALS

- LAMINATE LEVEL**
 - Improve composite crush and energy absorption capability by developing data base on fundamental behavior of structures made from epoxy and thermoplastic resins
- ELEMENT LEVEL**
 - Assess the local and global behavior of various composite structural elements under crash loadings
 - Determine governing parameters that permit scaling of composite structural behavior under dynamic loadings
- SUBSTRUCTURE LEVEL**
 - Evaluate performance of substructures assembled from various basic composite structural elements
 - Assess effects of liquid versus solid terrain on impact behavior
- METAL BASELINE**
 - Include metal structural components as reference baseline for assessing composite behavior under impact loadings
- FULL-SCALE TESTING**
 - Demonstrate structural performance of composite full-scale aircraft under crash loadings

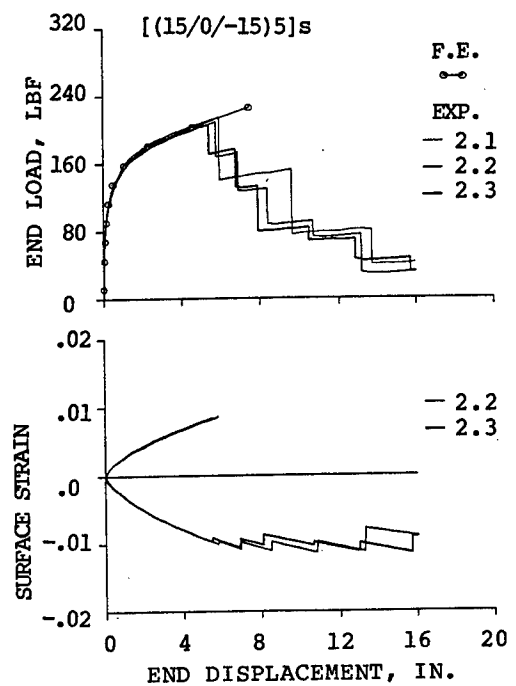
APPARATUS FOR DYNAMIC TESTS
OF BEAMS



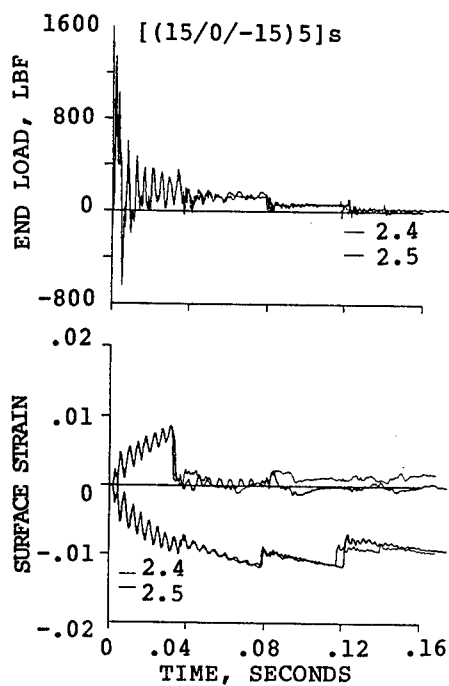
BEAM LOADING CONFIGURATION



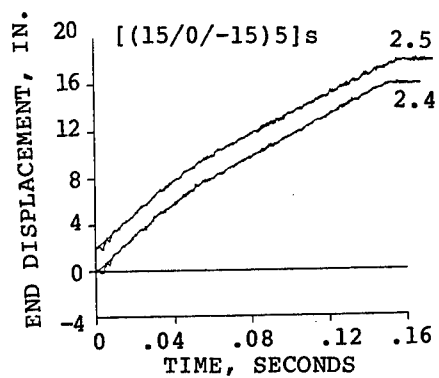
BEAM STATIC END LOAD AND STRAIN
DISPLACEMENT



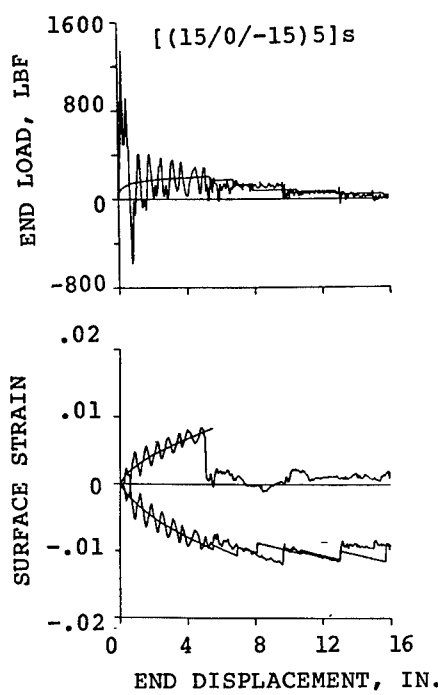
BEAM DYNAMIC END LOAD AND STRAIN HISTORY



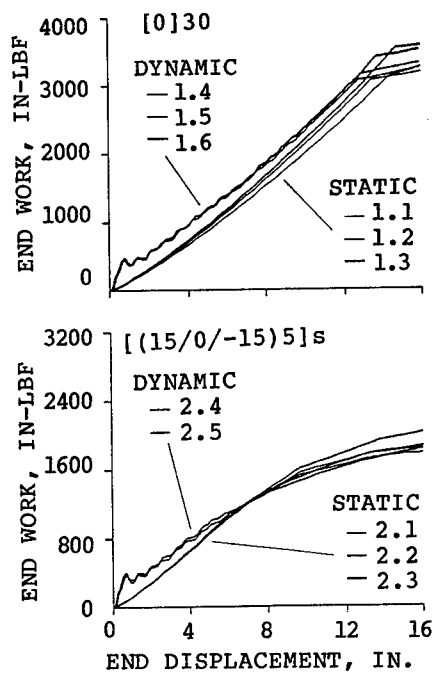
BEAM END DISPLACEMENT

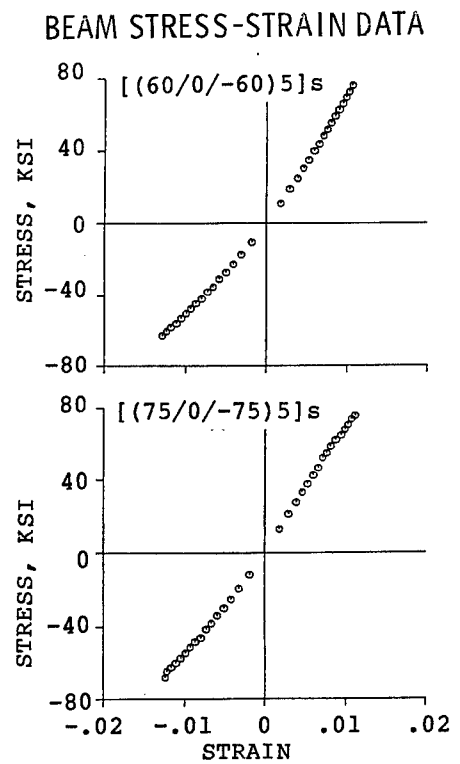
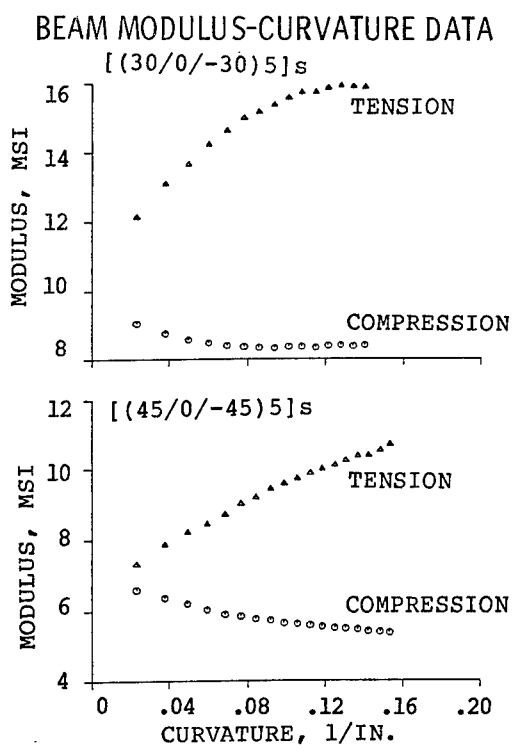


STATIC AND DYNAMIC LOAD AND STRAIN

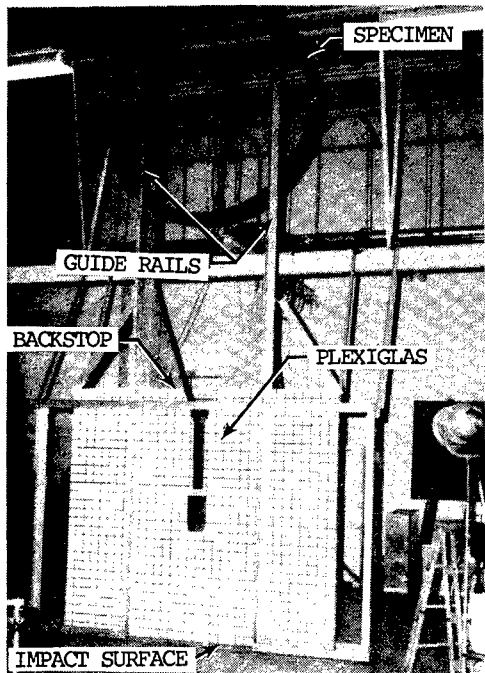


BEAM END WORK

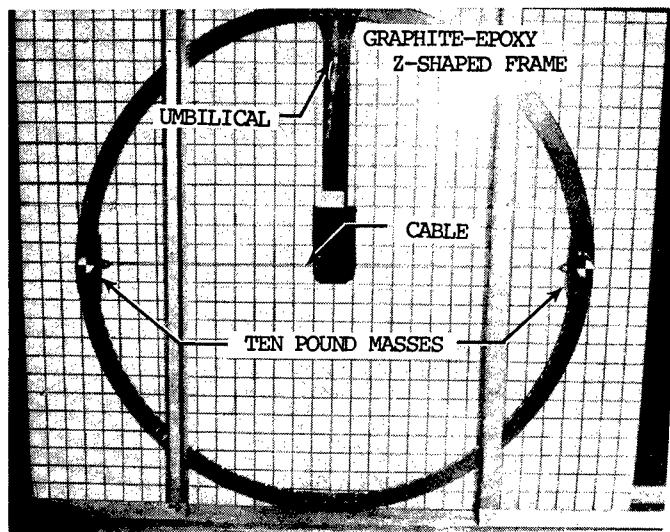


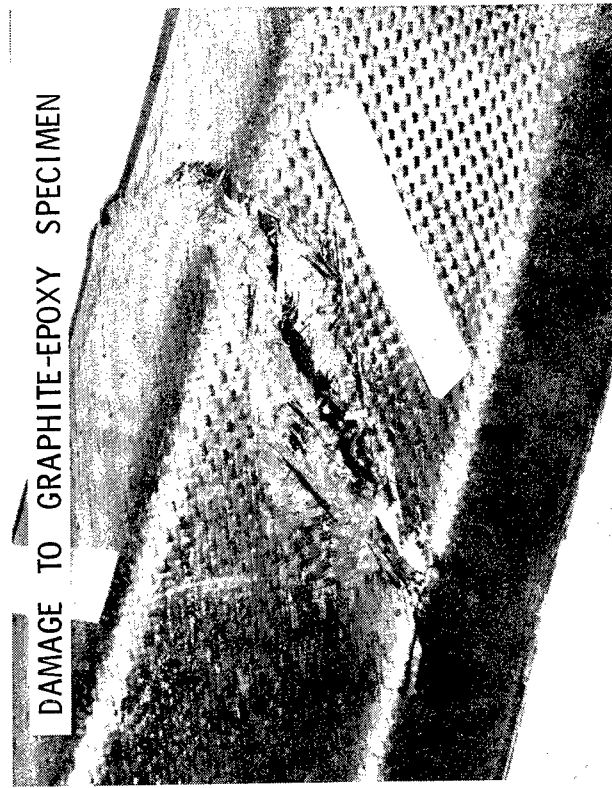
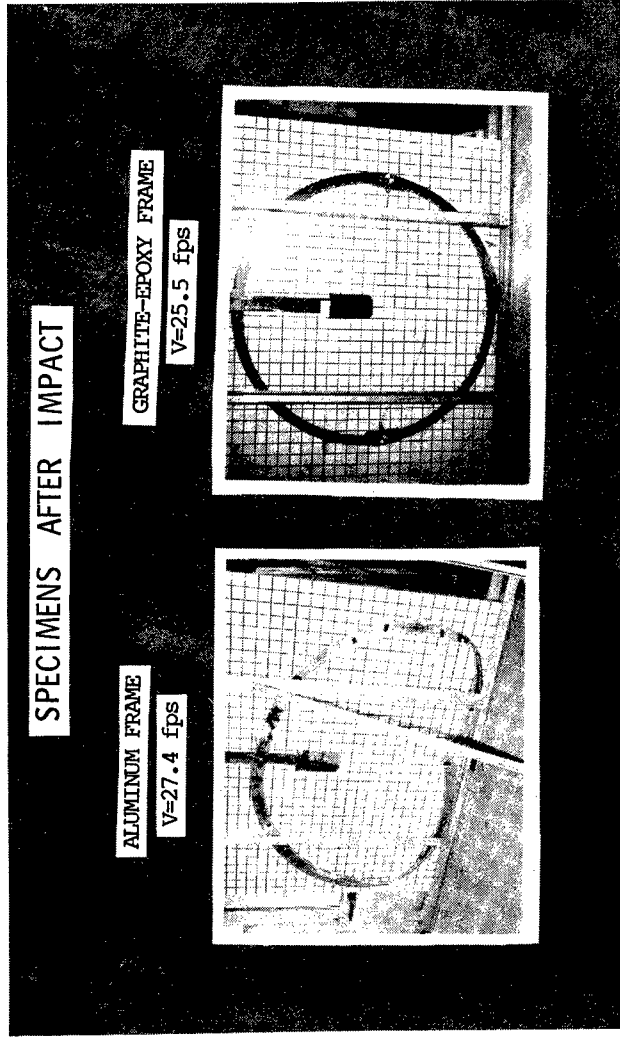


SPECIMEN IN DROP TOWER

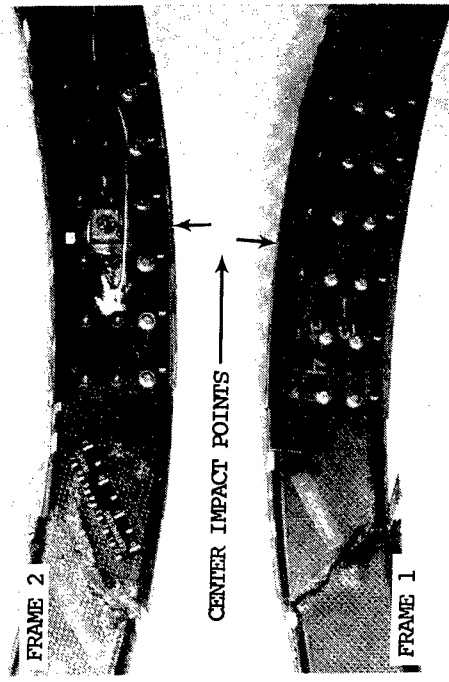


TEST SPECIMEN IN IMPACT POSITION

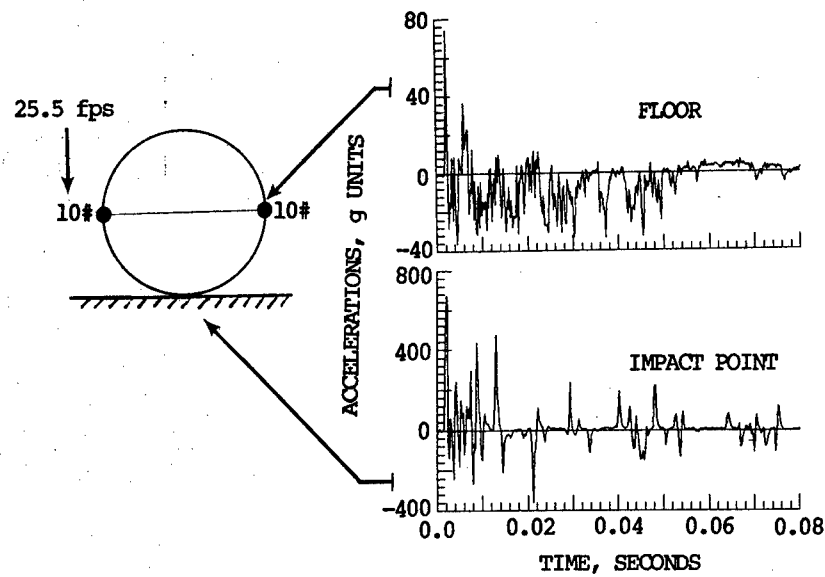




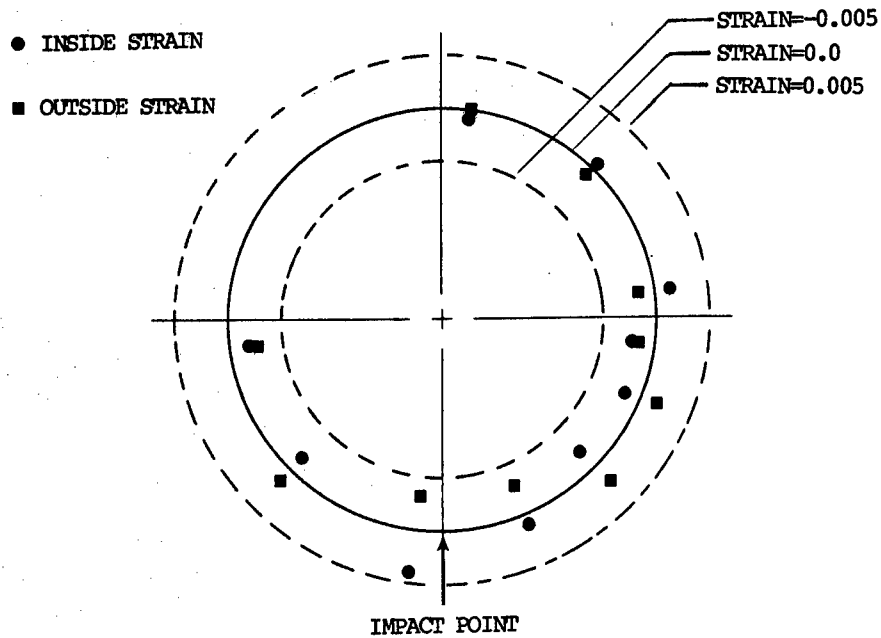
SPECIMEN FAILURE REPEATABILITY



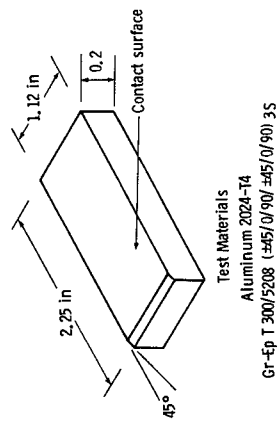
VERTICAL ACCELERATIONS



CIRCUMFERENTIAL STRAIN DISTRIBUTION

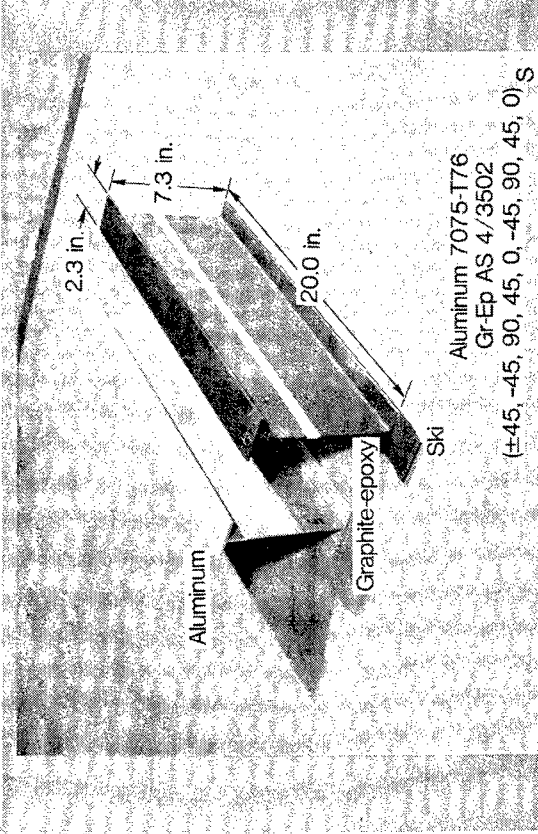


TYPICAL SKIN COUPON ABRASION TEST SPECIMEN



Test Materials
Aluminum 2024-T4
Gr-Ep T 300/5208 (+45/0/90/-45/0/90) 35

TYPICAL ALUMINUM AND GR-EP STIFFENED SKIN SPECIMENS

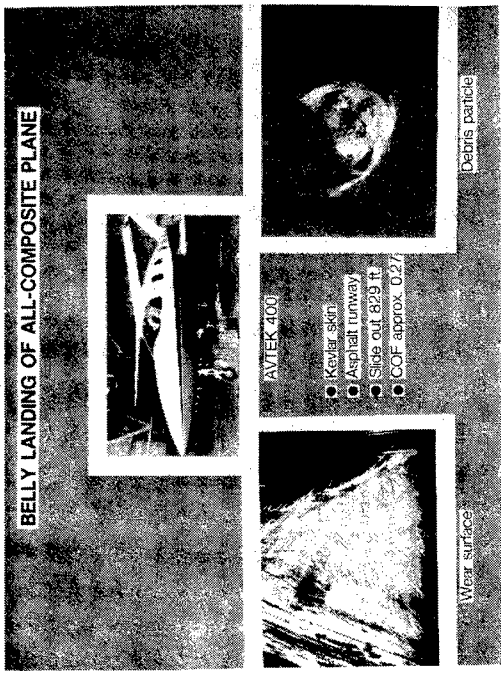


Aluminum 7075-T76
Gr-Ep AS 4/3502
(±45, 90, 45, 0, -45, 90, 45, 0) S

STIFFENED PANEL TEST SPECIMEN

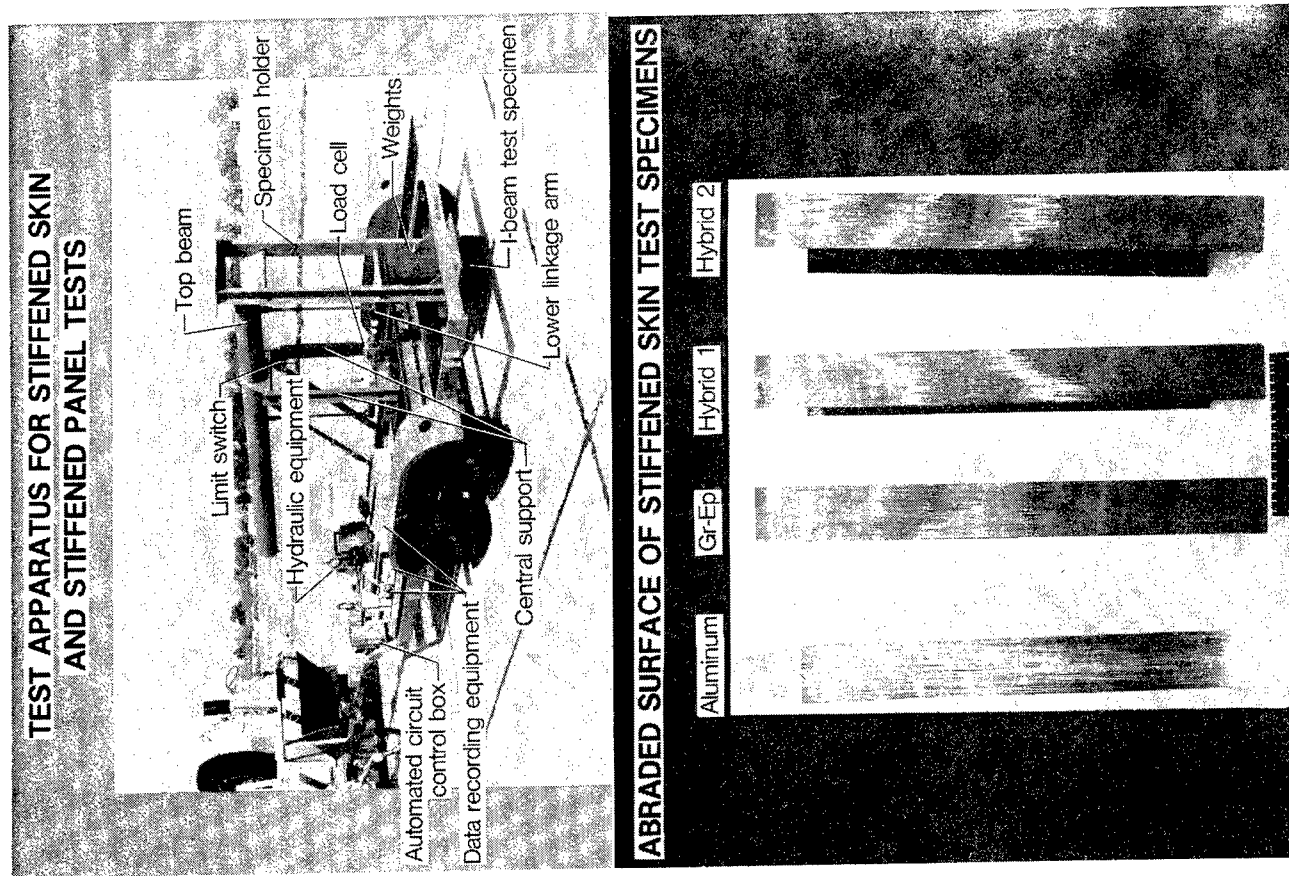


Gr-Ep AS4/3502
(±45, 90, 45, 0, -45, 90, 45, 0) S

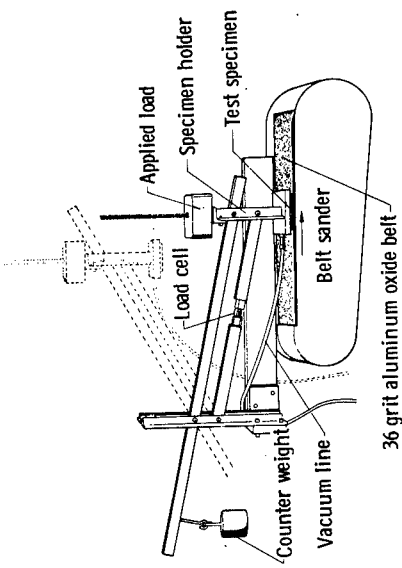


BELLY LANDING OF ALL-COMPOSITE PLANE

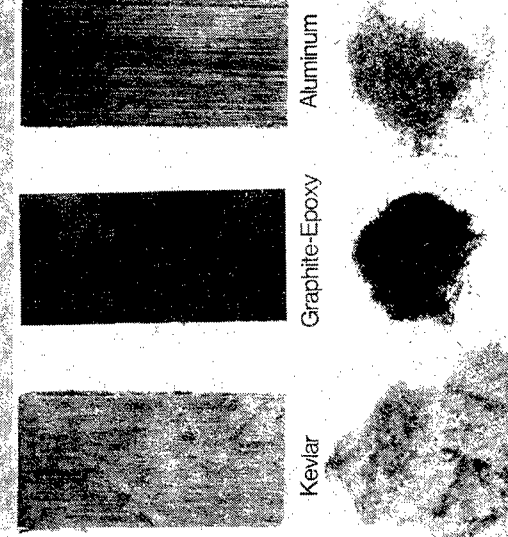
**TEST APPARATUS FOR STIFFENED SKIN
AND STIFFENED PANEL TESTS**



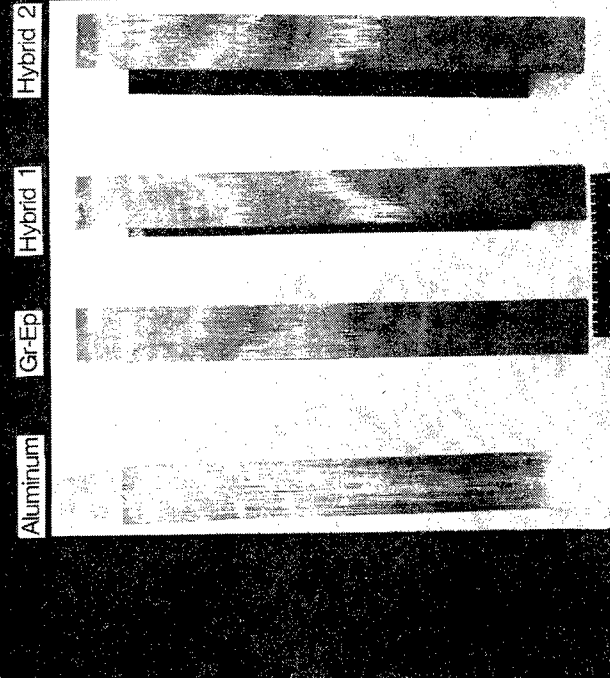
SCHEMATIC OF SKIN COUPON TEST APPARATUS



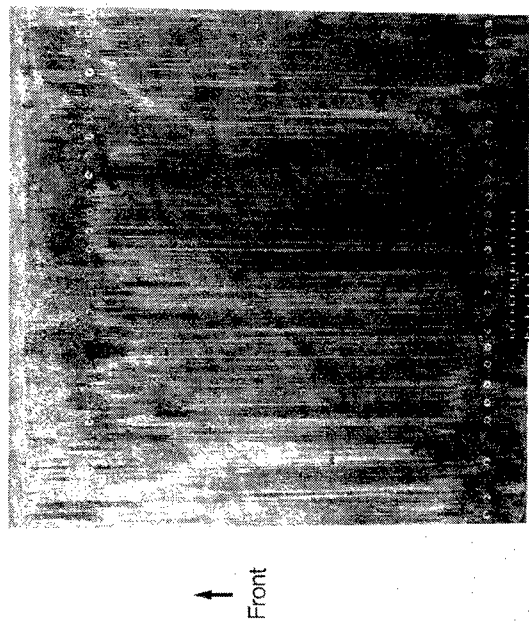
WEAR SURFACES OF TYPICAL SKIN COUPON SPECIMENS



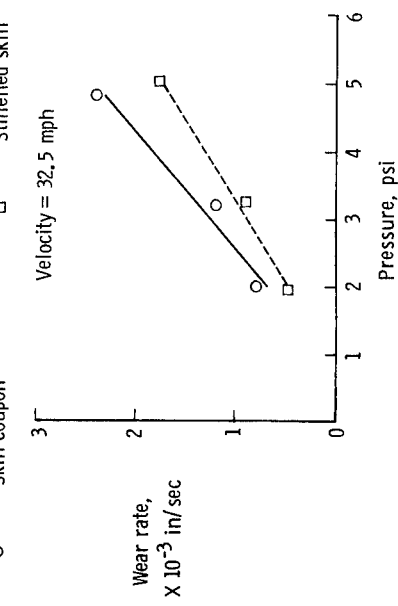
ABRATED SURFACE OF STIFFENED SKIN TEST SPECIMENS



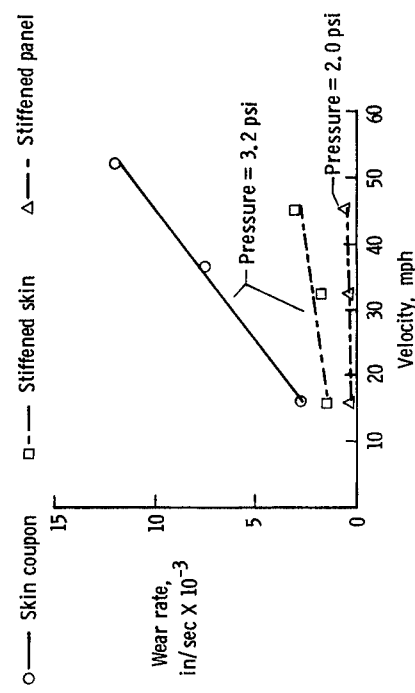
TYPICAL WEAR SURFACE OF GR-EP STIFFENED PANEL



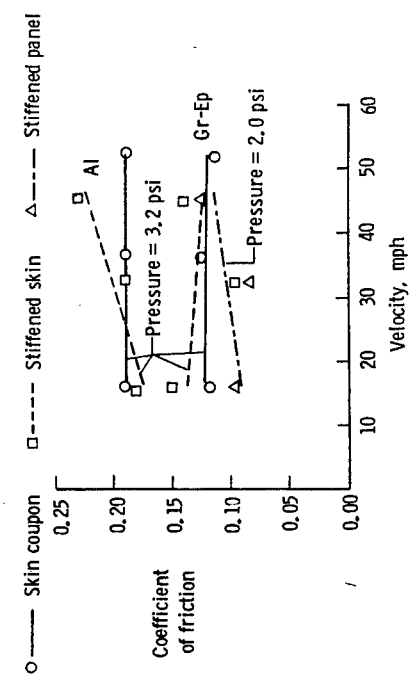
WEAR RATE VERSUS PRESSURE FOR ALUMINUM SKINS



WEAR RATE VERSUS VELOCITY FOR GR-EP SKINS



COEFFICIENT OF FRICTION VERSUS VELOCITY



DYNAMICS AND AEROELASTICITY OF COMPOSITE STRUCTURES

John Dugundji

Gun-Shing Chen

Technology Laboratory for Advanced Composites
Department of Aeronautics and Astronautics
Massachusetts Institute of Technology
Cambridge, Massachusetts 02139

ABSTRACT

In previous investigations at M.I.T., the aeroelastic flutter and divergence behavior of a series of unswept and forward swept, graphite/epoxy cantilever wings were investigated in a small, low-speed wind tunnel. The wings were six-ply graphite/epoxy plates and had strong bending-twisting coupling (D_{16} terms). By adjusting the bending-torsion coupling, the divergence tendency of the forward swept, cantilever wings could be eliminated and the flutter speed raised considerably. See Refs. 1 and 2.

Presently, an investigation is being made into the effects of rigid body aircraft modes on the aeroelastic behavior of forward swept wings. It has recently been pointed out in Refs. 3 and 4, that for forward swept wings, the rigid body modes may possibly couple with the wing bending mode to cause a new low frequency "body-freedom-flutter." Accordingly, a complete, two-sided 30° forward swept wing aircraft model was constructed and mounted with low friction bearings in both pitching and translation, inside the M.I.T. low speed acoustic wind tunnel. The wind tunnel had a 1.5 x 2.3 m (5 x 7 ft.) test section and could reach velocities of 30 m/s. Four different ply layup wings could be interchanged on the model, namely [0₂/90]_s, [+152/0]_s, [+302/0]_s and [-152/0]_s. These wing surfaces were the same ones used in the previous cantilever tests (Refs. 1 and 2), and thus the present tests complemented the previous cantilever tests and isolated the effects of rigid body motions.

The wind tunnel tests included measurement of the static lift and moment characteristics (done at low speeds) and the dynamic stability, flutter, and divergence testing at higher speeds. For all free flying tests, the model was set to a low trim angle of attack, and aircraft vertical height. Also, TV movies were taken. Body-freedom-flutter was encountered for some configurations as well as torsional stall flutter, bending stall flutter, and dynamic instability. Examples are given of various flutter and dynamic instabilities encountered. These experimental tests, along with the previous cantilever wing tests and with corresponding analytical analyses, should provide insight into the actual aeroelastic behavior of forward swept wing aircraft in free flight.

REFERENCES

1. Hollowell, S.J., and Dugundji, J., "Aeroelastic Flutter and Divergence of Stiffness Coupled, Graphite/Epoxy Cantilevered Plates," J. Aircraft, Vol. 21, No. 1, January 1984, pp. 69-76.
2. Landsberger, B., and Dugundji, J., "Experimental Aeroelastic Behavior of Straight and Forward Swept Graphite/Epoxy Wings," J. Aircraft, Vol. 22, No. 8, August 1985, pp. 679-686.
3. Weisshaar, T.A., Zeiler, T.A., Hertz, T.J., and Shirk, M.J., "Flutter of Forward Swept Wings, Analyses and Tests," Proceedings of the 23rd AIAA/ASME/ASCE/AHS Structures, Structural Dynamics, and Materials Conference, New Orleans, Louisiana, May, 1982, AIAA Paper 82-0646.
4. Chipman, R., Rauch, F., Rimer, M., Muniz, B., and Ricketts, R.H., "Transonic Tests of a Forward Swept Wing Configuration Exhibiting Body Freedom Flutter," Proceedings of the 26th AIAA/ASME/ASCE/AHS Structures, Structural Dynamics, and Materials Conference, Orlando, Florida, April 15-17, 1985, AIAA Paper 85-0689.

DYNAMICS AND AEROELASTICITY OF
COMPOSITE STRUCTURES

John Dugundji
Gun-Shing Chen

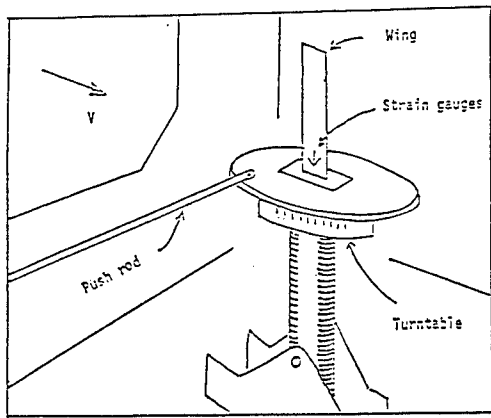
Technology Laboratory for Advanced Composites
Department of Aeronautics and Astronautics
Massachusetts Institute of Technology
Cambridge, Massachusetts 02139

OBJECTIVES

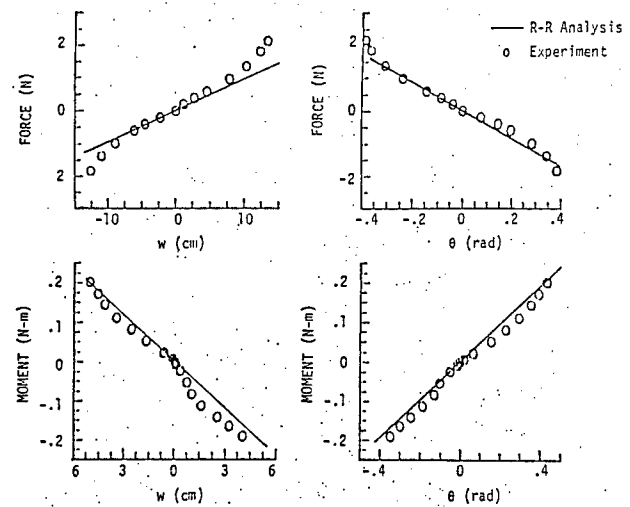
- Investigate the effects of rigid body aircraft modes on the flutter and divergence of forward swept, graphite/epoxy wings
- Explore nonlinear effects of large angle of attack and stall flutter
- Obtain insight into actual aeroelastic behavior of forward swept, aeroelastically tailored aircraft in free flight

APPROACH

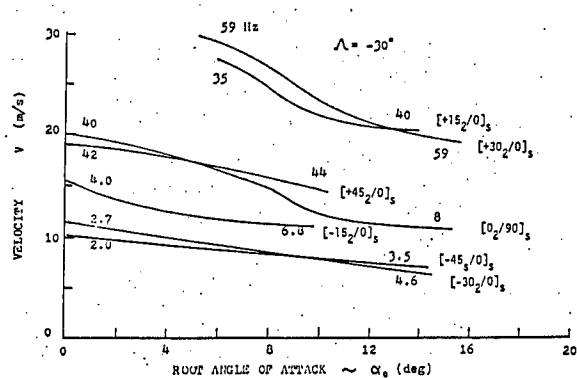
- Build complete, two-sided 30° forward swept wing aircraft model with rigid pitch and rigid translation capability
- Obtain experimental data on model in low speed wind tunnel, and compare with corresponding cantilever wing tests
- Perform analytical flutter and divergence calculations including effects of rigid body modes



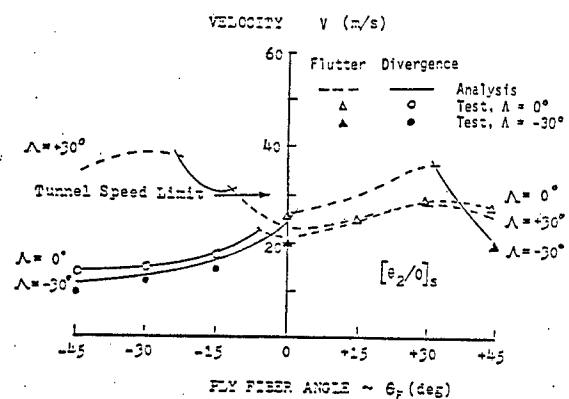
Test Set-Up in Tunnel (Cantilever Wing)



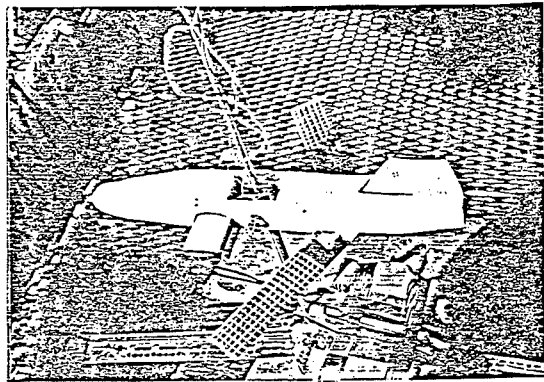
Structural Deflections of $[+30/0]_s$ Wing



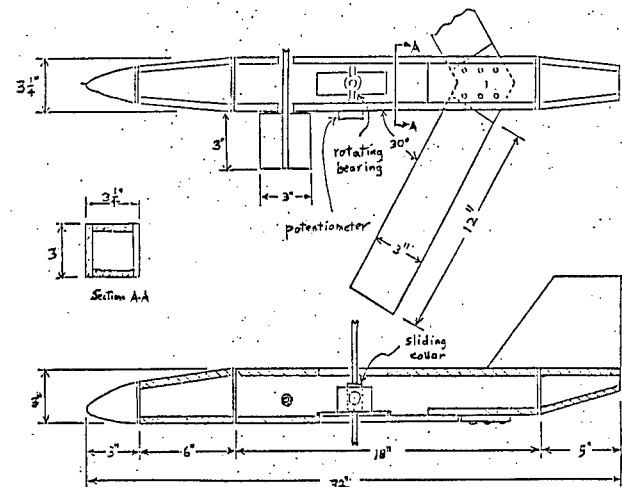
Experimental Flutter and Divergence Boundaries, $\Lambda = -30^\circ$
(Cantilever Wing)



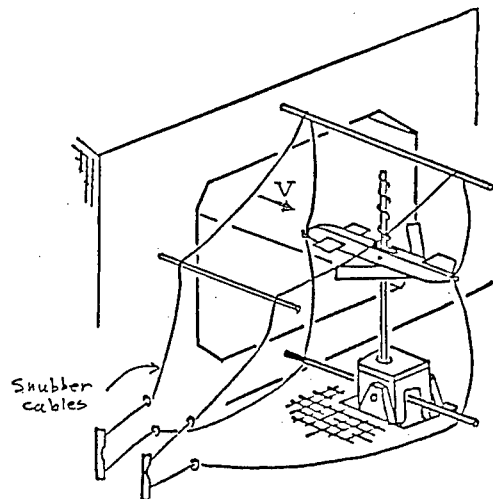
Flutter and Divergence at Low Root Analyses, ξ_0
(Cantilever Wing)



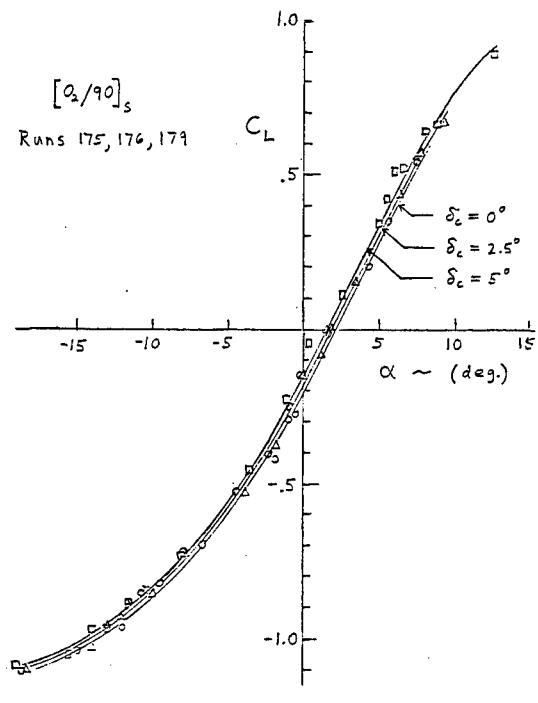
Forward Swept Wing Model

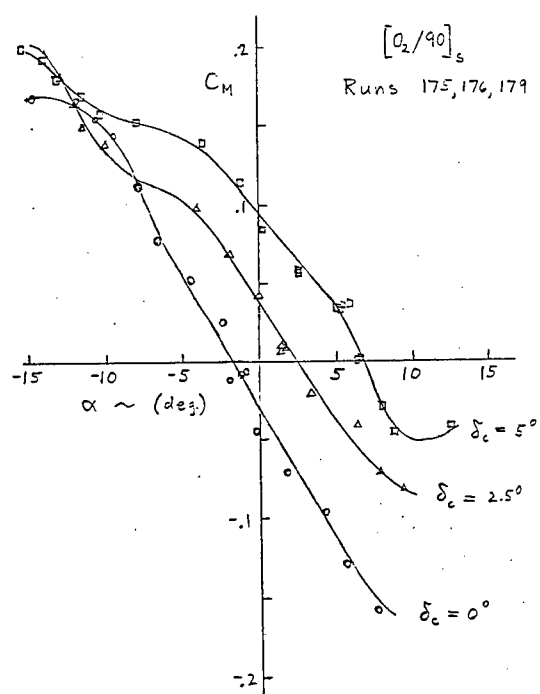


Forward Swept Wing Model

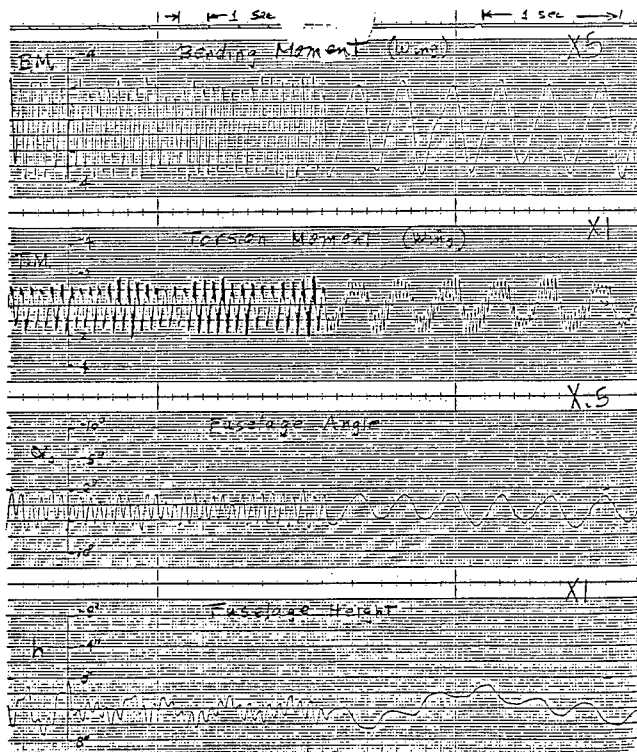


M.I.T. Acoustic Tunnel Test Set-Up

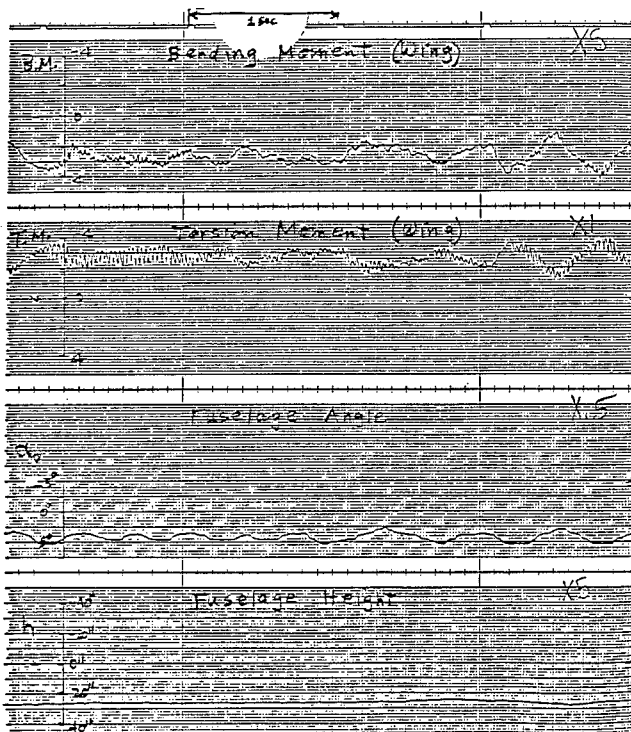




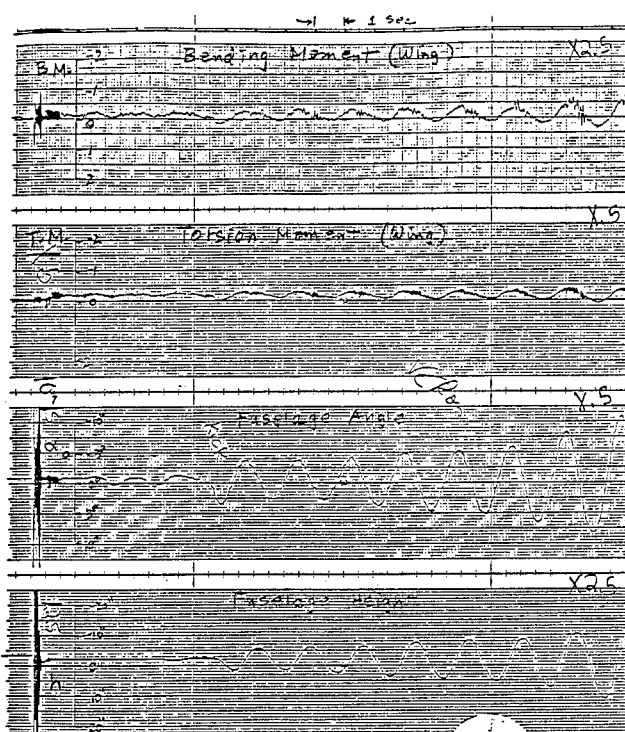
Static Moment Curves



Flutter Record, Run #180, $[O_2/90]_s$, $\delta_c = 2.5^\circ$, $V = 20$ m/s



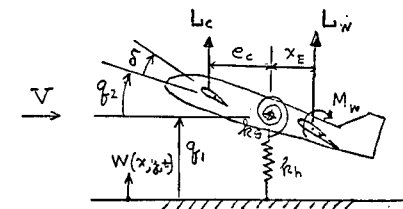
Torsional Stall Flutter, Run #198, $[15_2/0]_s$, $\delta_c = 2.5^\circ$, $V = 28 \text{ m/s}$



Dynamic Instability, Run #185, $[O_2/90]_s$, $\delta_C = 0^\circ$, $V = 10$ m/s

Theoretical Analysis

Equations of Motion



$$W(x, y, t) = \sum_{i=1}^7 Y_i(x, y) q_i(t)$$

q_1 = Rigid Transl.

q_2 = Rigid Pitch

q_3 = 1st Cantil Bend

q_4 = 2nd " "

q_5 = 1st Torsion

q_6 = 2nd "

q_7 = 1st Chordwise

$$\tilde{M} \ddot{q} + \tilde{K} q = \tilde{Q}_{\text{Aero}}$$

$$\text{Vibrations: } q_i = q_i^0 e^{i\omega t}$$

$$[-\omega^2 \tilde{M} + \tilde{K}] q = 0 \rightarrow \text{Solve } W, q$$

$$\text{Flutter: } q_i = q_i^0 e^{pt}$$

$$\left[p^2 \tilde{M} + \tilde{K} - \frac{1}{2} \rho V^2 S \left(B_2 p^2 + B_1 p + B_0 + G_1 \frac{p}{p+q} \right) \right] q = 0$$

$$\rightarrow \text{Solve } p, q$$

$$\text{Divergence: } q_i = q_i^0$$

$$\left[\tilde{K} - \frac{1}{2} \rho V^2 S B_0 \right] q = 0 \rightarrow \text{Solve } V, q$$

$$T = \frac{1}{2} \iint m \dot{w}^2 dx dy = \frac{1}{2} \sum_i \sum_j M_{ij} \dot{q}_i \dot{q}_j$$

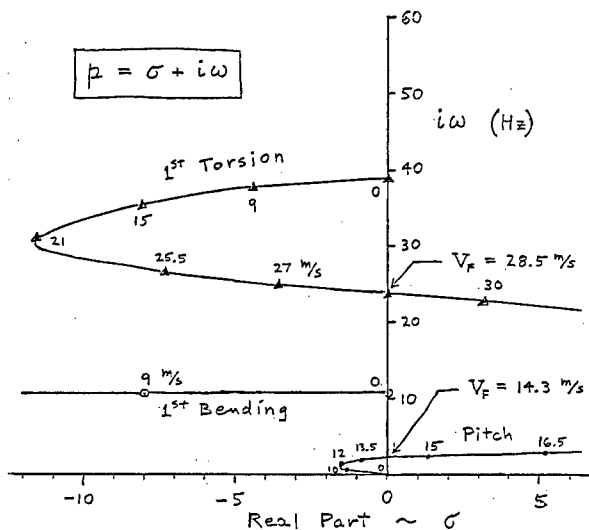
$$U = \frac{1}{2} \iint \left\{ D_{11} w_{xx}^2 + \dots \right\} dx dy + \frac{1}{2} k_1 q_1^2 + \frac{1}{2} k_2 q_2^2$$

$$= \frac{1}{2} \sum_i \sum_j K_{ij} q_i q_j$$

$$\delta W = \sum_i Q_i \delta q_i$$

CURRENT STATUS

- Currently, analyzing results of model wind tunnel tests
- Observed body-freedom-flutter, torsional stall flutter, dynamic instability, nonlinear phenomena
- Currently, performing analytical flutter and divergence analyses to assess experimental results, compare with cantilever results, and assess extent of nonlinear phenomena



Theoretical Stability Plot, [0_{2/90}]S

AN ELASTIC STRESS ANALYSIS OF THE DEBOND
FRONT IN DCB SPECIMENS

J. H. Crews, Jr.
K. N. Shivakumar*
I. S. Raju*

NASA Langley Research Center
Hampton, Virginia 23665-5225

ABSTRACT

Double cantilever beam (DCB) specimens are widely used to measure mode I fracture toughness of adhesive debonding and composite delamination. Various combinations of adherend materials and specimen dimensions are currently being used for these DCB specimens. These specimen parameters can influence the stress distribution ahead of the debond front (ref. 1) and, therefore, should also be expected to influence fracture toughness. This can be especially important for tough resins. Whereas brittle resins fail under the influence of very localized stresses that are characterized by the debond front stress-intensity factor, tough resins may yield extensively ahead of the debond front before fracturing. The stresses ahead of the debond govern the extent of yielding and the corresponding plastic energy dissipation that provides fracture toughness. The objective of the present study was to evaluate several parameters that may influence the peel stress distribution ahead of the debond front.

Aluminum and graphite/epoxy DCB specimens were studied using finite-element analyses. The parameters that were varied included adherend and adhesive thicknesses as well as adherend longitudinal and transverse (thickness-direction) stiffnesses. Results were plotted as σ_y (peel) stress distributions ahead of the debond front.

Neither the adherend thickness nor the longitudinal stiffness had much influence on the peel stress distributions, despite their strong influence on the stress intensity factors. In contrast, both adherend transverse stiffness and adhesive thickness had a noticeable influence on the stress distributions, but did not affect stress intensity factors. Plastic zone sizes were estimated for a wide range of adhesive thicknesses and were found to have a peak value within this range. This trend agrees qualitatively with the well known dependence that DCB fracture toughness has on adhesive thickness.

REFERENCES

1. S. S. Wang, J. F. Mandell, and F. J. McGarry, "An Analysis of the Crack Tip Stress Field in DCB Adhesive Fracture Specimens," International Journal of Fracture, Vol. 14, no. 1, February 1978.

*Analytical Services & Materials, Inc.

AN ELASTIC STRESS ANALYSIS OF THE DEBOND
FRONT IN DCB SPECIMENS

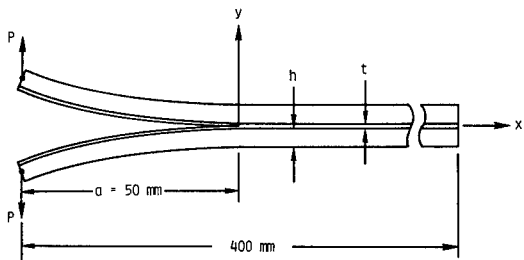
OBJECTIVE

J. H. CREWS, JR.
K. N. SHIVAKUMAR*
I. S. RAJU*

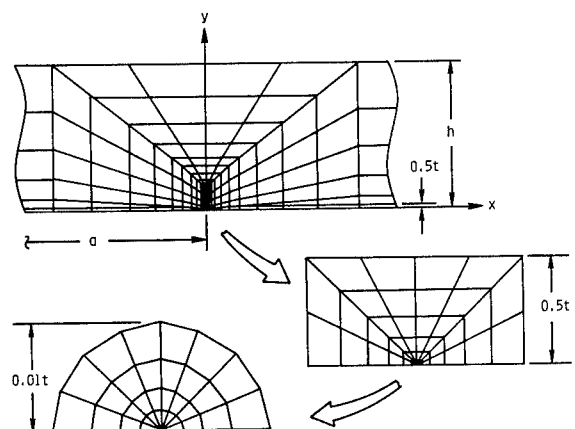
TO EVALUATE DCB SPECIMEN PARAMETERS THAT INFLUENCE
STRESSES AHEAD OF DEBOND FRONT

NASA Langley Research Center, Hampton, VA
*ANALYTICAL SERVICES AND MATERIALS, INC., HAMPTON, VA

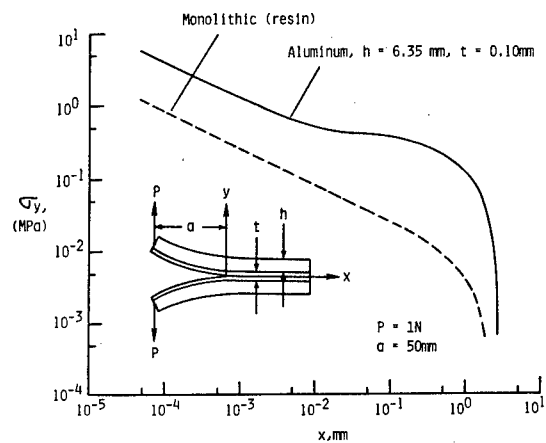
DCB SPECIMEN CONFIGURATION AND LOADING



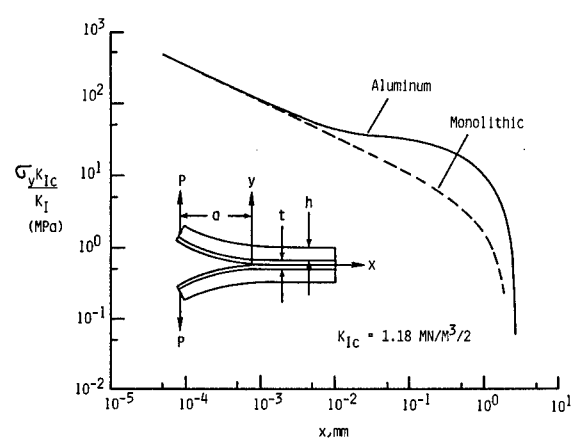
FINITE ELEMENT MODEL



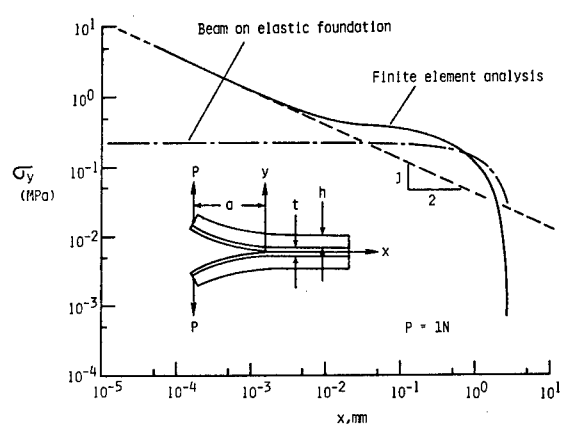
STRESS DISTRIBUTION AHEAD OF DELAMINATION



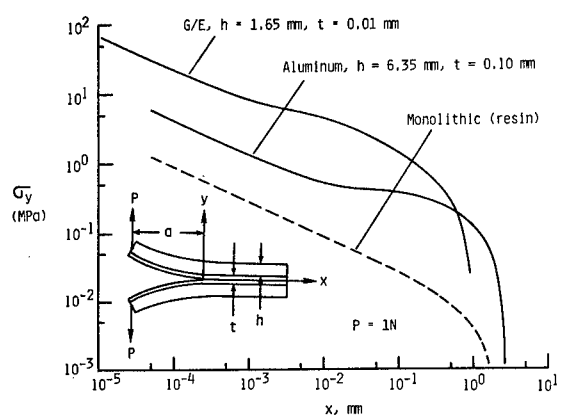
COMPARISON OF STRESS DISTRIBUTIONS



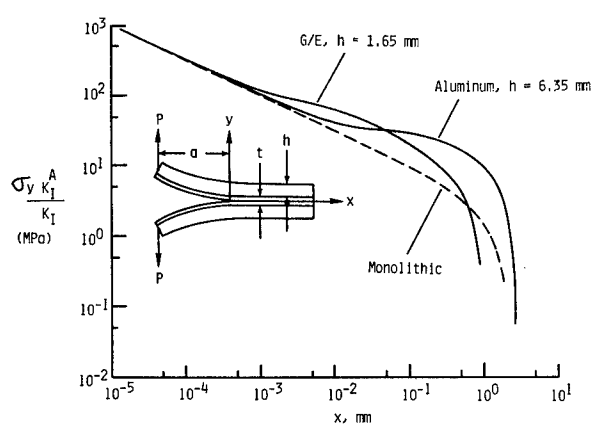
ANALYSIS OF STRESS DISTRIBUTION FOR ALUMINUM DCB



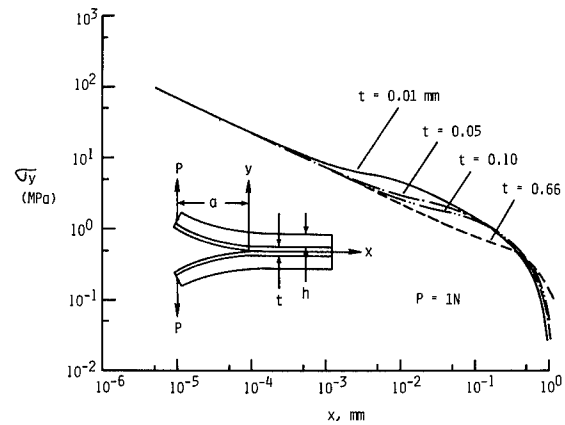
COMPARISON OF ALUMINUM AND G/E DCB SPECIMENS



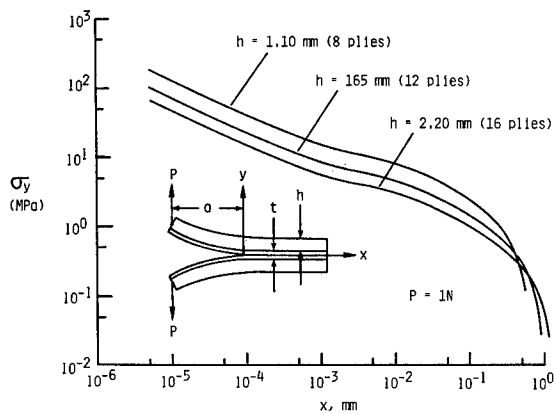
COMPARISON OF ALUMINUM AND G/E DCB SPECIMENS



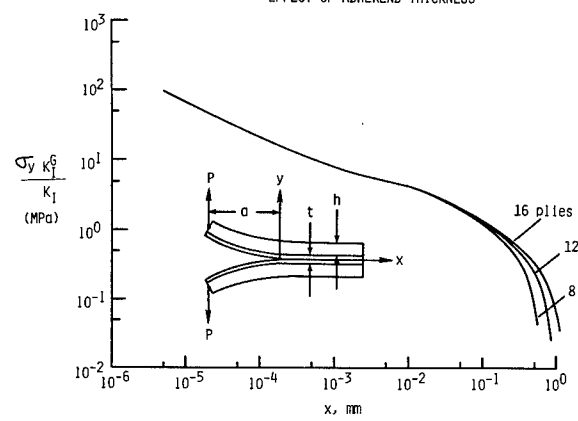
EFFECT OF ADHESIVE THICKNESS



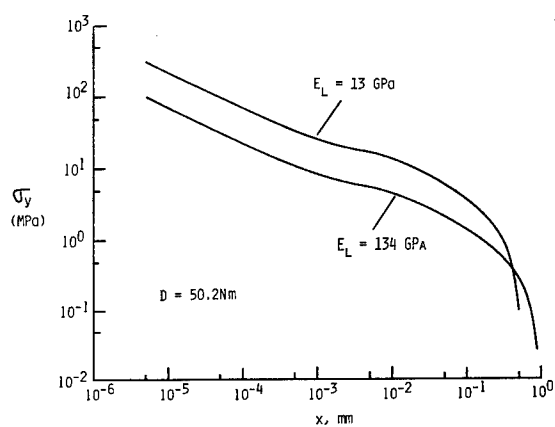
EFFECT OF ADHEREND THICKNESS



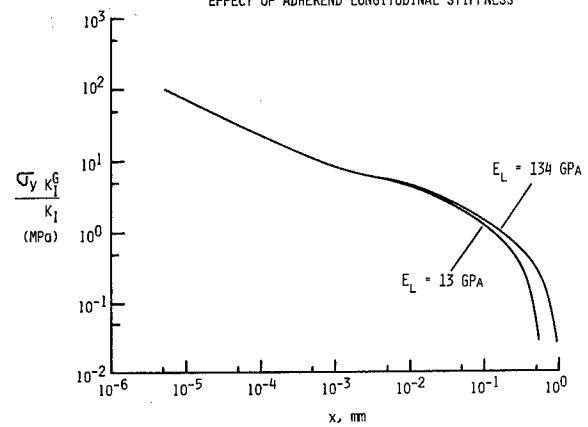
EFFECT OF ADHEREND THICKNESS



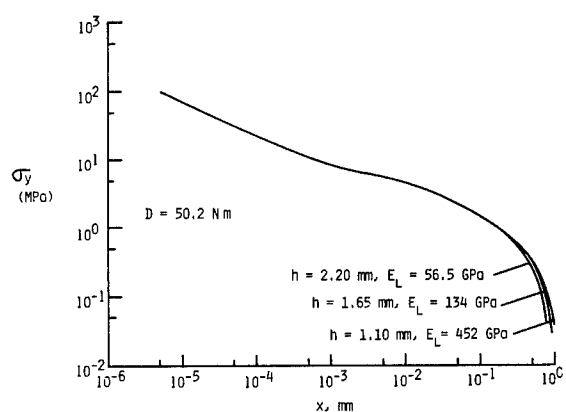
EFFECT OF ADHEREND LONGITUDINAL STIFFNESS



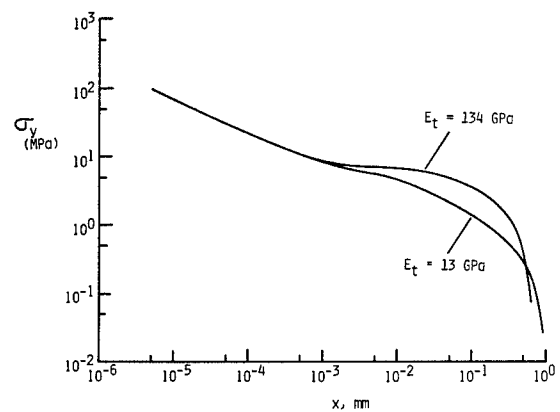
EFFECT OF ADHEREND LONGITUDINAL STIFFNESS



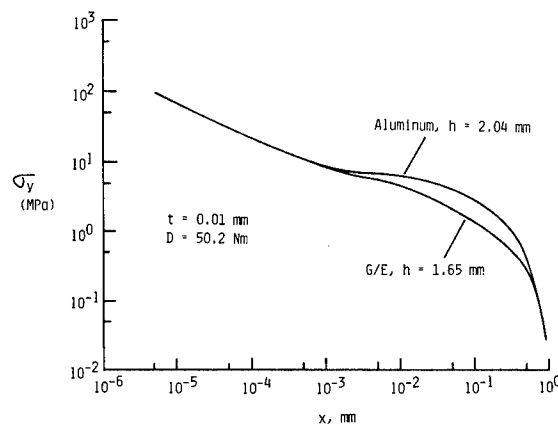
COMPARISON FOR CONSTANT BENDING STIFFNESS



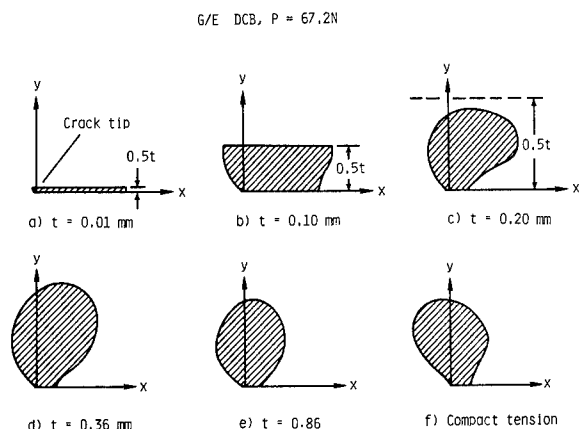
EFFECT OF ADHEREND TRANSVERSE STIFFNESS



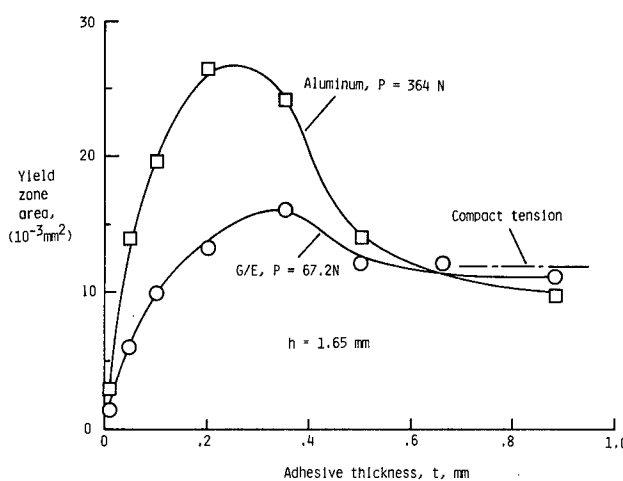
ALUMINUM AND G/E DCB SPECIMENS WITH SAME D



YIELD ZONE SHAPES AND SIZES



YIELD ZONE SIZES



SUMMARY

- o ADHESIVE σ_y (PEEL) STRESSES WERE HIGHER THAN THOSE FOR MONOLITHIC CASE.
- o ADHEREND FLEXURAL STIFFNESS HAD LITTLE EFFECT ON σ_y DISTRIBUTION.
- o ADHEREND TRANSVERSE STIFFNESS (IN THICKNESS DIRECTION) HAD SIGNIFICANT EFFECT ON σ_y DISTRIBUTION
- o PLASTIC ZONE SIZE VARIED WITH ADHESIVE THICKNESS AND HAD A PEAK VALUE.

STATISTICAL LIFE PREDICTION OF COMPOSITE STRUCTURES

D. Jones and J. Yang

The George Washington University

Material not received in time for publication.

ANALYSIS OF DELAMINATION GROWTH FROM MATRIX CRACKS
IN LAMINATES SUBJECTED TO BENDING LOADS

Gretchen Bostaph Murri
E. Gail Guynn*
National Aeronautics and Space Administration
Langley Research Center
Hampton, Virginia 23665-5225

ABSTRACT

Delamination is the most commonly observed damage mode in composite laminates. In thin plates under low-velocity impact from point loads, matrix cracks will form first in the laminate plies, and delaminations will then grow from these matrix cracks where they terminate at ply interfaces. In this study, delamination growth from matrix cracks in laminates subjected to bending loads was evaluated. Using laminate plate theory, simple equations were derived which relate the strain energy release rate associated with the delamination growth to the applied load and laminate stiffness properties. Several bending problems and boundary conditions were considered. In order to isolate the matrix crack and model the problem 2-dimensionally, different layups of graphite-epoxy (5208/T300) laminates were modeled and tested. All tested layups were symmetric and had 90° plies on the outside. For such a laminate under a bending load, matrix cracks will form parallel to the fibers, through the 90° plies, on the tension surface of the laminate. Delaminations then form and grow in the interface between the inmost cracked 90° ply and the adjacent ply. To simulate pure bending, specimens were loaded across their width by pins which were free to rotate on ball bearings, in a 4-point bending apparatus. A three-point bend test was performed in the same type apparatus by supporting the specimen on two pins and loading it at the midspan. To simulate the deformations in laminates subjected to low-velocity impact, specimens were clamped at the ends and loaded across their width at the midspan. For all configurations, the laminates were loaded until delamination was first observed. The delamination loads predicted by the analysis correlated well with the measured delamination loads for the different layups and boundary conditions.

*PRC Kentron, Inc., Hampton, Virginia

ANALYSIS OF PROGRESSIVE MATRIX CRACKING IN COMPOSITE LAMINATES

George J. Dvorak
Rensselaer Polytechnic Institute
Troy, NY 12180

Norman Laws
University of Pittsburgh
Pittsburgh, PA 15260

Edward Wung and Kaveh Ahangar
Rensselaer Polytechnic Institute
Troy, NY 12180

Sponsored by the Air Force Office of Scientific Research

ABSTRACT

The mechanics of transverse cracking in an elastic fibrous composite ply is explored, first for low crack density, and then during progressive cracking under increasing load. Cracks are assumed to initiate from a nucleus created by coalescence of localized fiber debonding and matrix cracking. Conditions for onset of unstable cracking are evaluated with regard to interaction of cracks with adjacent plies of different elastic properties. Interfacial damage is considered as well. It is found that crack propagation may take place in two directions on planes which are parallel to the fiber and perpendicular to the midplane of the ply, and that the actual propagation direction and ply strength depend on ply thickness.

Thin plies are defined by the requirement that the crack nucleus extends across the entire ply thickness before onset of unstable crack propagation. Of course, plies with preexisting through-the-thickness cracks caused by other damage modes, such as impact, should also be regarded as thin plies regardless of their actual thickness. Strength of thin plies is found to be controlled by onset of crack propagation in the fiber direction; these longitudinal cracks are called type L cracks. The strain energy release rate $G(L)$ for these cracks is derived. This leads to expressions which relate ply strength to ply thickness and toughness $G_c(L)$. Both simple and mixed loading modes are considered. Only two strain states, normal tension and longitudinal shear affect ply failure. Transverse shear seems to be neutralized by interlocking asperities created on the crack surface as the crack finds its way between closely spaced fibers.

Thick plies are defined by the condition that the width of a crack nucleus of critical size is much smaller than ply thickness. Thus there is no interaction between the nucleus and adjacent plies. The energy release rates for the nucleus are derived. In addition to $G(L)$ for type L cracks, we also evaluate $G(T)$ that corresponds to type T cracks which propagate in the transverse direction, perpendicular to the fiber axis, across the thickness of the ply. It is found that $G(T) = 2G(L)$, i.e., there is a strong preference for the crack nucleus to propagate first as type T crack across ply thickness, and then change direction and continue as type L crack across the entire loaded area of the ply. It is recognized that the two different crack directions involve different values of ply toughness, G_c , and that $G_c(L) < G_c(T)$. However, experimental evidence appears to indicate that $G_c(T) < 2G_c(L)$, hence the strength of thick plies is controlled by type T cracking, in the same way as strength of thin plies is controlled by type L cracking. Expressions for thick ply strength are obtained in terms of critical size of crack nucleus and ply toughness $G_c(T)$. Since the nucleus size is not usually known, one cannot predict the strength of thick plies. However, it is possible to show that this strength does not depend on ply thickness for a given history of loading to failure.

These results for thin and thick plies compare well with experimentally measured dependence of ply strength on ply thickness. One of the conclusions that can be drawn from these results is that strength of all plies should be evaluated from thin ply formulae, to guard against strength reduction in thick plies which may be caused by preexisting cracks.

In the second part of the presentation, we analyse progressive cracking in a ply under increasing applied strain. This process is essentially a continuous repetition of first ply failure, but both formation of the initial crack nuclei, and energy release rates $G(L)$ and $G(T)$ for unstable cracks are influenced by interaction between the new crack and the cracks which are already present. This type of crack interaction is analyzed by several methods; the self-consistent method, as well as elasticity solutions for a row of parallel cracks are employed. It is found that very similar crack interaction effects are predicted by these different approaches. Of particular interest is the evaluation of $G(L)$ and $G(T)$ of a crack which is about to form in a ply that already contains a certain density of similar cracks. Also, the strain in the ligaments between existing cracks is evaluated.

REFERENCES

1. G.J. Dvorak, N. Laws and M. Hejazi, "Analysis of Progressive Matrix Cracking in Composite Laminates. I. Thermoelastic Properties of a Ply with Cracks," Journal of Composite Materials, Vol. 19, May 1985, pp. 216-234.
2. G.J. Dvorak and N. Laws, "Analysis of Progressive Matrix Cracking in Composite Laminates. II. First Ply Failure," to be published.

PRINCIPAL OBJECTIVES AND RESULTS

PRINCIPAL OBJECTIVES AND RESULTS - CONT.

1. MECHANICS OF FIRST PLY FAILURE
 - 0 CRACK NUCLEATION
 - 0 STRENGTH OF THIN PLIES
 - Energy release rate for longitudinal (type L) slit crack
 - Dependence of ply strength on ply thickness
 - 0 STRENGTH OF THICK PLIES
 - Energy release rates for initial flaws as transverse (type T) cracks
 - Type T and type L cracks
 - Dependence of ply strength on flaw size
 - 0 PLIES OF INTERMEDIATE THICKNESS
 - Interaction of flaws and ply cracks with adjacent plies
 - 0 COMPARISON WITH EXPERIMENTAL DATA
 - E-Glass/Epoxy
 - T300/934
2. PROGRESSIVE CRACKING OF A PLY
 - 0 REPETITIVE FAILURES IN A PLY UNDER INCREASING STRAIN
 - 0 EVALUATION OF STIFFNESS CHANGES IN CRACKED PLY
 - Self consistent estimates
 - Row of parallel cracks solutions,
 - 0 EVALUATION OF ENERGY RELEASE RATES FOR INTERACTING SLIT CRACKS IN A CRACKED PLY
 - 0 EVALUATION OF LIGAMENT STRAINS BETWEEN INTERACTING CRACKS
 - 0 COMPARISON WITH EXPERIMENTS
 - Apparent threshold toughness of cracking ply
 - Critical ligament strain as a criterion for progressive cracking
 - 0 CONCLUSIONS
- 0 STRENGTH OF THIN AND DAMAGED PLIES IS CONTROLLED BY LONGITUDINAL (type L) CRACKS
- 0 STRENGTH OF THICK PLIES IS CONTROLLED BY TRANSVERSE (type T) CRACKS WHICH ARE AUTOMATICALLY FOLLOWED BY LONGITUDINAL (type L) CRACKS.

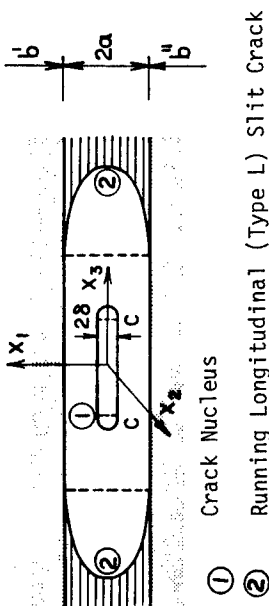
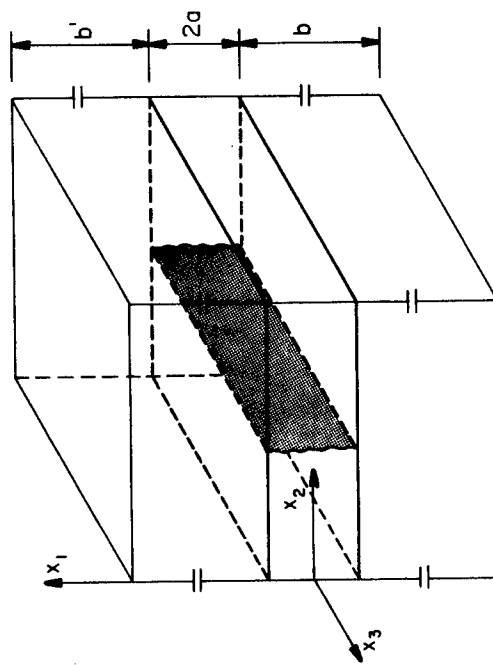


Figure 2. Fiber debonding and coalescence of debonds create a nucleus.

53

- Subcritical growth under applied strain $\bar{\varepsilon}$
- $\delta = \delta(\bar{\varepsilon}(t))$ for $\delta \leq \delta_c$

At $\delta = \delta_c$, nucleus becomes unstable and may propagate

- in transverse direction x_1 as type T crack
- in longitudinal direction x_3 as type L crack

Figure 1. Slit crack in a uniformly strained composite ply. Fibers and cracks are aligned with x_3 axis. Uniform strain imposed by adjacent parts b, b' of the plate. At first ply failure, crack is isolated and does not interact with other cracks.

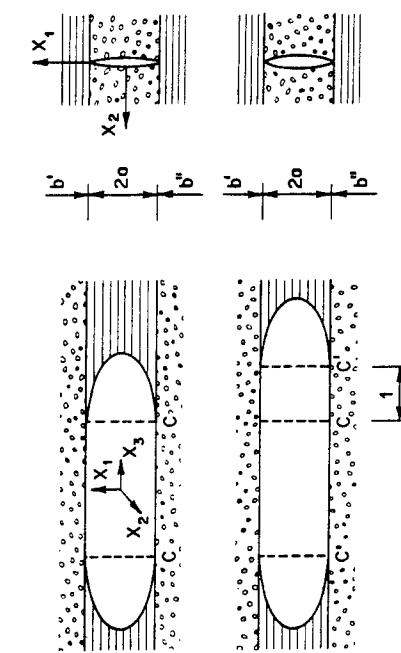


Figure 3. Unit extension of a slit crack

Definition of "thin" ply: $2\delta = 2a$ for $\delta \leq \delta_c$
 Energy release rate for longitudinal (type L) slit crack:

$$G(L) = W_a / 2a$$

W_a - interaction energy of a unit length
 crack of width 2a

$$G(L) = \frac{1}{4} \pi a [\xi_1 \Lambda_{22}^0 \bar{\sigma}_{22}^2 + \xi_{II} \Lambda_{44}^0 \bar{\sigma}_{23}^2 + \xi_{III} \Lambda_{66}^0 \bar{\sigma}_{12}^2]$$

$$\Lambda_{22}^0 = \Lambda_{66}^0 = 2\left(\frac{1}{E_T} - \frac{v_L^2}{E_L}\right), \quad \Lambda_{44}^0 = 1/G_L$$

In the presence of interface damage: $\xi_i = 1$.

- Evaluation of ply strength under simple loading conditions:

$$(\bar{\sigma}_{22})_{cr} = [4G_{IC}(L)/(\pi \xi_1 \Lambda_{22}^0 a)]^{1/2} \quad \text{at } \bar{\sigma}_{23} = 0,$$

$$(\bar{\sigma}_{23})_{cr} = [4G_{IIC}(L)/(\pi \xi_{II} \Lambda_{44}^0 a)]^{1/2} \quad \text{at } \bar{\sigma}_{22} = 0.$$

$G_{IC}(L)$, $G_{IIC}(L)$ are ply toughness values for type L cracks.

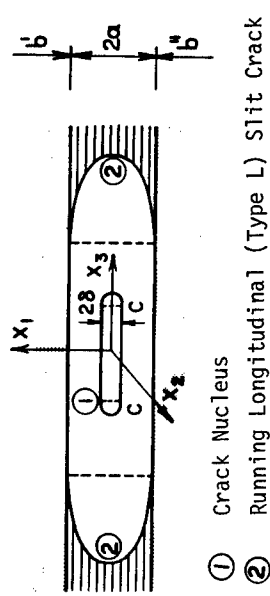
For combined loading $\bar{\sigma}_{23} = q \bar{\sigma}_{22}$ use a mixed mode failure criterion.

Example: Hahn (1983):

$$(1-q)\left(\frac{G_I}{G_{IC}}\right)^{\frac{1}{2}} + q\left(\frac{G_I}{G_{IC}}\right) + \left(\frac{G_{II}}{G_{IIC}}\right) \geq 1,$$

$q = G_{IC}/G_{IIC} \approx 0.1$ for epoxy matrices.

∴ Strength of thin or damaged plies is related only to onset of unstable longitudinal (type L) cracking



Relations between critical width of crack nucleus

$$\delta_{Ic}(L) = 2\gamma_I \delta_{Ic}(\tau)$$

$$\delta_{IIC}(L) = 2\gamma_{II} \delta_{IIC}(\tau).$$

Experimental data suggest:

$$2\gamma_I > 1, \quad 2\gamma_{II} > 1$$

Definition of "thick" ply: $2\delta \ll 2a$ for $\delta \leq \delta_c$.

Energy release rates:

$$G(\tau) = \frac{1}{2} \pi \delta [\Lambda_{22}^0 \tilde{\sigma}^2 + \Lambda_{44}^0 \tilde{\sigma}_{23}^2 + \Lambda_{66}^0 \tilde{\sigma}_{12}^2], \quad \text{for } \delta \ll a.$$

$$G(L) = \frac{1}{4} \pi \delta [\Lambda_{22}^0 \tilde{\sigma}^2 + \Lambda_{44}^0 \tilde{\sigma}_{23}^2 + \Lambda_{66}^0 \tilde{\sigma}_{12}^2], \quad \text{for } \delta \ll a.$$

$$G(\tau) = 2G(L)$$

Ply toughness:

$$G_{Ic}(L) = \gamma_I G_{Ic}(\tau)$$

$$G_{IIC}(L) = \gamma_{II} G_{IIC}(\tau)$$

∴ First ply failure of thick plies starts as a result of transverse (type τ) cracking, followed by longitudinal (type L) cracking.

Ply strength:

$$\text{For } \tilde{\sigma}_{23} = 0, \tilde{\sigma}_{22} \neq 0, \text{ the strength is given by} \\ (\tilde{\sigma}_{22})_{cr} = [2G_{Ic}(\tau)/(\pi \Lambda_{22}^0 \delta_{Ic}(\tau))]^{\frac{1}{2}}$$

$$\text{For } \tilde{\sigma}_{22} = 0, \tilde{\sigma}_{23} \neq 0, \text{ the strength is given by} \\ (\tilde{\sigma}_{23})_{cr} = [2G_{IIC}(\tau)/(\pi \Lambda_{44}^0 \delta_{IIC}(\tau))]^{\frac{1}{2}}$$

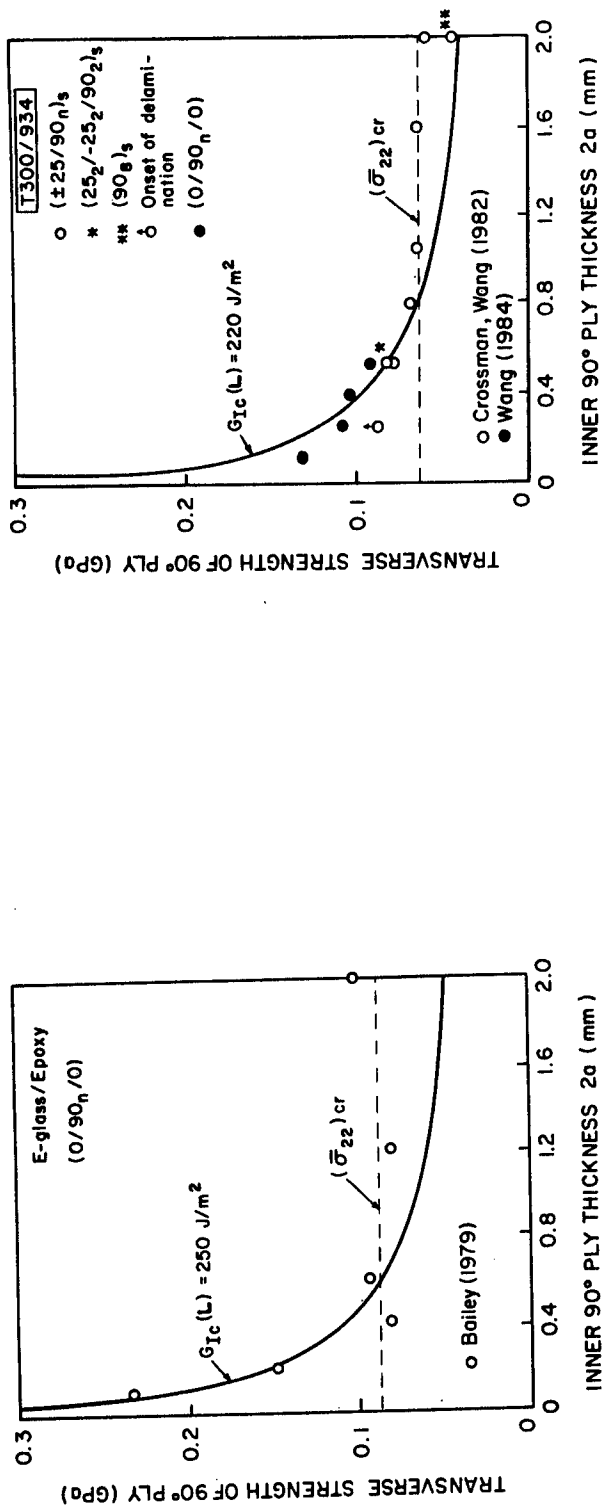
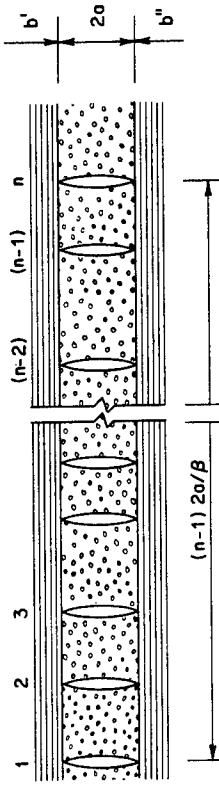


Figure 5. Comparison of theoretical results with experimental data.

Figure 4. Comparison of theoretical results with experimental data.

PART 2: PROGRESSIVE CRACKING OF A PLY

Definition of Crack Density Parameter β :



Crack spacing:

$$n = \# \text{ of cracks/mm}$$

$$n = \beta/2a,$$

STIFFNESS CHANGES CAUSED BY CRACKS:

Self-Consistent Estimates

$$\text{Ply properties: } \bar{\sigma} = L \bar{\varepsilon} - \theta \bar{\delta}, \bar{\varepsilon} = M \bar{\sigma} + \theta \bar{m}$$

$$\text{Stiffness: } L = L_0 - \frac{1}{4} \pi \beta L_0 \Lambda L$$

$$\bar{\delta} = (1 - \frac{1}{4} \pi \beta \Lambda L) \bar{\delta}_0$$

Compliance:

$$\bar{M} = M_0 + \frac{1}{4} \pi \beta \Lambda$$

$$\bar{m} = \bar{m}_0$$

INTERACTION ENERGY FOR ROW OF PARALLEL CRACKS

Self-Consistent Estimate

Ply under small constant strain $\bar{\varepsilon} = \text{const.}$

Strain energy in RVE of volume V

$$U_0 = \frac{1}{2} \bar{\varepsilon}^T L_0 \bar{\varepsilon} \cdot V \quad \text{at } \beta = 0$$

$$U = \frac{1}{2} \bar{\varepsilon}^T L(\beta) \bar{\varepsilon} \cdot V \quad \text{at } \beta \neq 0$$

Number of cracks in RVE: $N = \beta V / 4a^2$

Interaction Energy of a Single Crack

$$W = (U_0 - U) / N = \frac{2a^2}{\beta} \bar{\varepsilon}^T (L_0 - L(\beta)) \bar{\varepsilon}$$

Energy Release Rate of Type L Crack

$$\text{at } \beta \neq 0: G(L) = W/2a = \frac{a}{\beta} \bar{\varepsilon}^T (L_0 - L(\beta)) \bar{\varepsilon},$$

$$\text{at } \beta = 0: G^0(L) = W_0/2a = \frac{1}{4} \pi a [\Lambda_{22}^0 \bar{\sigma}_{22}^2 + \Lambda_{44}^0 \bar{\sigma}_{23}^2 + \Lambda_{66}^0 \bar{\sigma}_{12}^2]$$

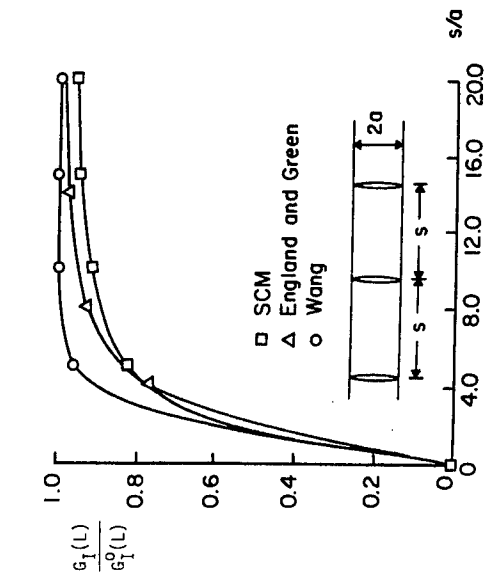


Figure 6. Comparison of Different Evaluations of $G(L)$ Reduction Caused by Crack Interaction. $s/a = 2/\beta$.

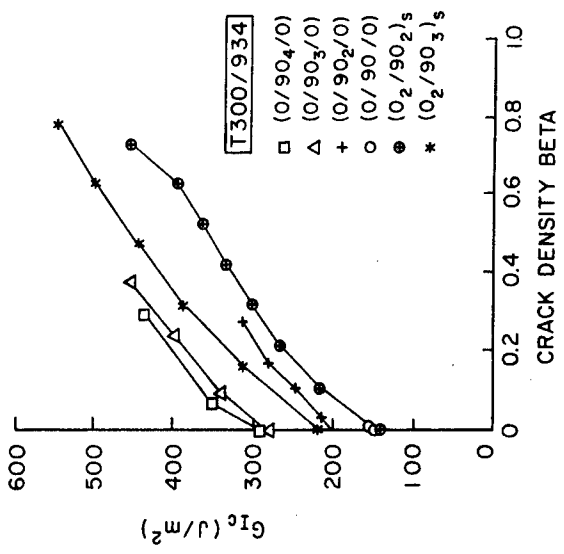


Figure 7. Apparent Ply Toughness $G_{1c}(L)$ as a Function of Crack Density β .

INITIATION OF FREE-EDGE DELAMINATION IN
COMPOSITE LAMINATE - PREDICTION AND EXPERIMENT

Ran Y. Kim

University of Dayton
Research Institute
Dayton, Ohio 45469

and

Som R. Soni

AdTech Systems Research Inc.
211 N. Broad Street
Fairborn, Ohio 45324

ABSTRACT

Delamination along the straight free edge of composite laminates under an inplane uniaxial load has been observed since the early 1970's. The growth of this delamination under load often results in a reduction of strength and stiffness of the laminate. Since then a large number of papers have reported on the free-edge problem in composite laminates, indicating that free-edge delamination is attributed to the existence of interlaminar stresses which are highly localized in the neighborhood of free edge under an inplane loading. As a result of this analytical work [1,2], the nature of interlaminar stresses with regard to magnitude and sign of each interlaminar stress component is reasonably well understood. In spite of the existence of the analytical models that provide interlaminar stress distributions in the free-edge region, no successful prediction method for the onset of delamination was reported.

In the present work an effort has been made to adequately predict the onset of delamination using stress analysis in conjunction with a failure theory.

The first phase of this work was to determine the interlaminar normal stress (σ_z) experimentally. Strain in the thickness direction was measured at the free edge by employing a miniature strain gage, and σ_z is calculated using three-dimensional constitutive relations in conjunction with axial and transverse strain [3]. The experimental results compare very well with the analytical results calculated from the global-local model developed by Pagano and Soni [4].

The second phase of this work was to develop a methodology to adequately predict the onset of delamination due to either interlaminar normal stress [5] or shear stress alone [6]. The global-local laminate variational model has been used to calculate the interlaminar stresses, and the average stress components over one layer from the free edge are assumed to be the effective stress level acting at the free edge. The predicted values in most cases are fairly well compared with the experimental results for a variety of laminates, and the predicted interface of delamination is the same as the experimentally observed one. The quadratic failure theory [7] has been utilized to improve the prediction capability in the case where both normal and shear stress components are significant [8].

REFERENCES

1. N. J. Pagano and R. B. Pipes, "Some Observations on the Interlaminar Strength of Composite Laminates," *Int. J. Mech. Sci.*, Vol. 15, 1973, pp 679-688.
2. N. J. Pagano, "Stress Field in Composite Laminates," *Int. J. Solid Structures*, Vol. 14, 1978, pp 385-400.
3. R. Y. Kim and S. R. Soni, "Initiation of Delamination of Composite Laminates," *Proceedings of the 1982 SEM Spring Conference on Experimental Mechanics*, Honolulu, Hawaii, May 1982.
4. N. J. Pagano and S. R. Soni, "Global-Local Laminate Variational Model," *Int. J. Solids and Structures*, Vol. 19, No. 3, 1983.

5. R. Y. Kim and S. R. Soni, "Experimental and Analytical Studies on the Onset of Delamination in Laminated Composites," *J. of Composite Materials*, Vol. 18, January 1984.
6. S. R. Soni and R. Y. Kim, "Delamination of Composite Laminates Stimulated by Interlaminar Shear," presented at the 7th Symposium on Composite Materials: Testing and Design, Philadelphia, PA, April 1984.
7. S. W. Tsai and E. M. Wu, "A General Theory of Strength for Anisotropic Materials," *J. Composite Materials*, Vol. 5, January 1971.
8. S. R. Soni and R. Y. Kim, "Mixed Mode Free-Edge Delamination of Composite Laminates," presented at the 19th Midwestern Mechanics Conference, Ohio State University, Columbus, Ohio, September 1985.

INITIATION OF FREE-EDGE DELAMINATION IN COMPOSITE LAMINATE - PREDICTION AND EXPERIMENT

RAN Y. KIM

UNIVERSITY OF DAYTON RESEARCH INSTITUTE, DAYTON, OHIO

SOM R. SONI

ADTECH SYSTEMS RESEARCH INC., FAIRBORN, OHIO

SUPPORTED BY AFWAL MATERIALS LABORATORY

OBJECTIVE

TO DEVELOP A METHODOLOGY FOR PREDICTING THE FREE-EDGE DELAMINATION THRESHOLD STRESS AND LOCATION IN COMPOSITE LAMINATES UNDER APPLIED UNIAXIAL LOAD

APPROACH

CALCULATE INTERLAMINAR STRESS COMPONENTS AT FREE EDGE BY GLOBAL-LOCAL MODEL

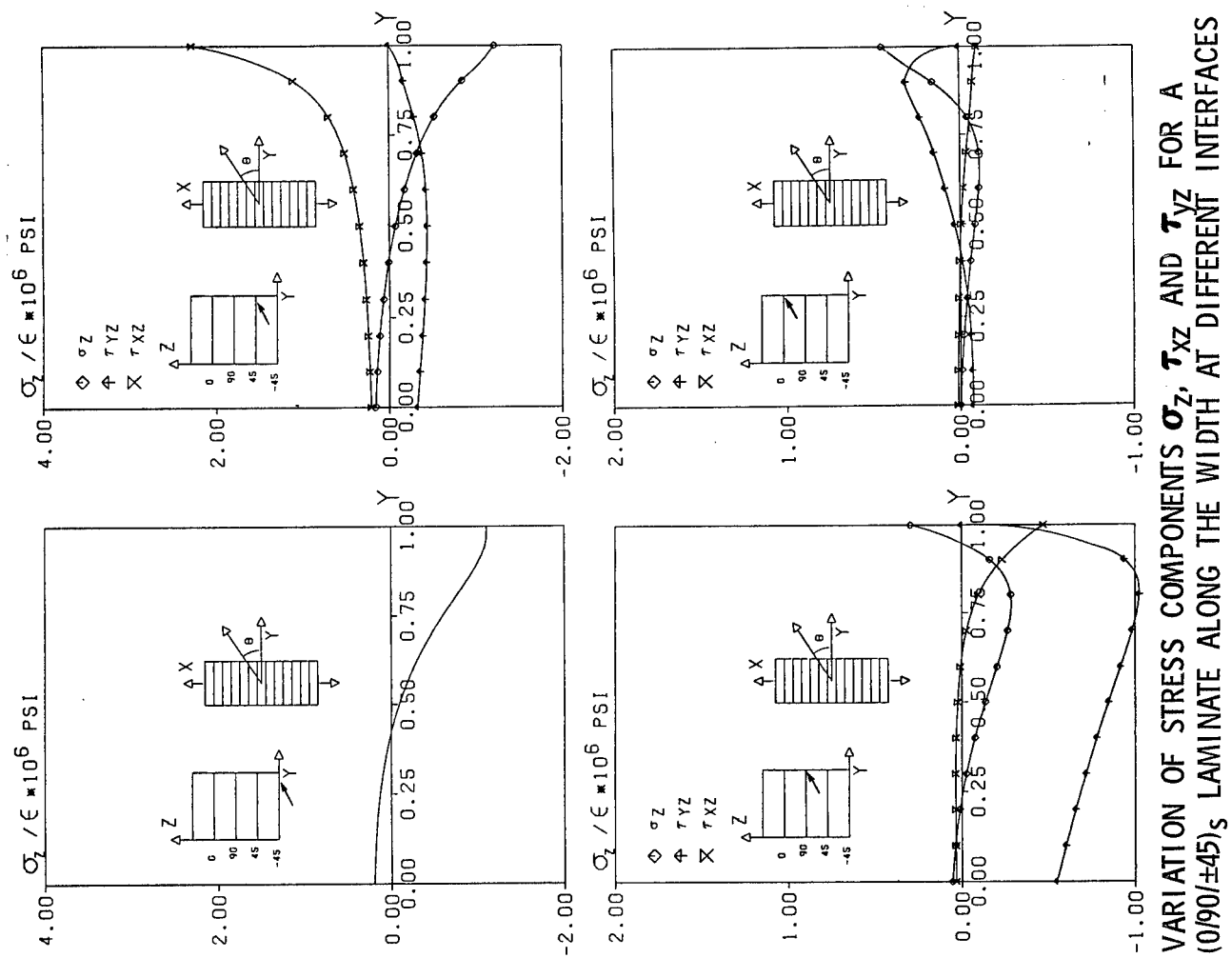
OBSERVE DELAMINATION EXPERIMENTALLY

DETERMINE σ_z

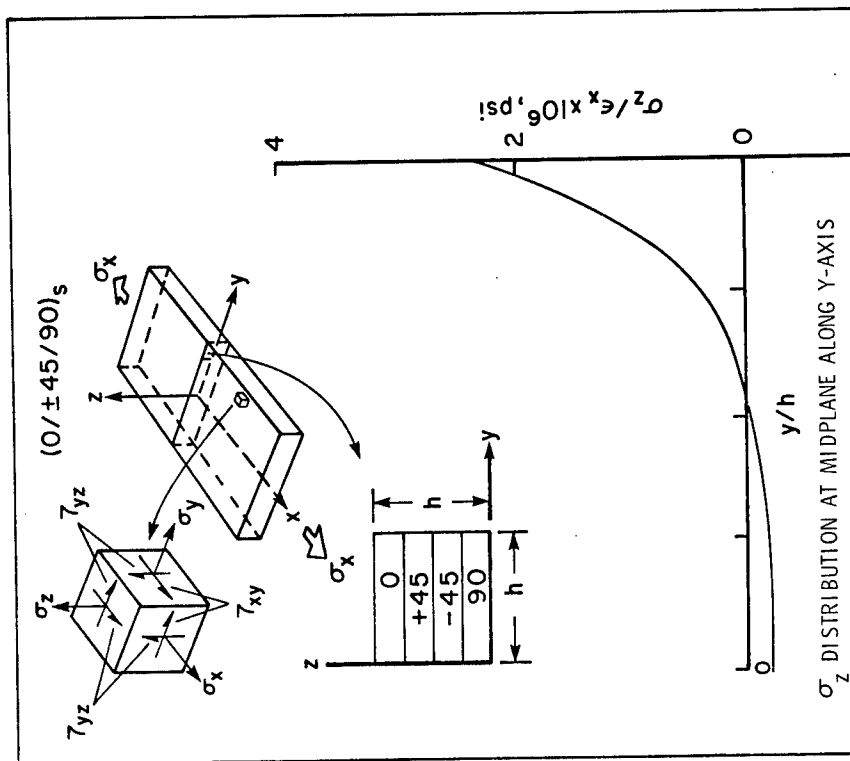
DETECT ONSET OF DELAMINATION

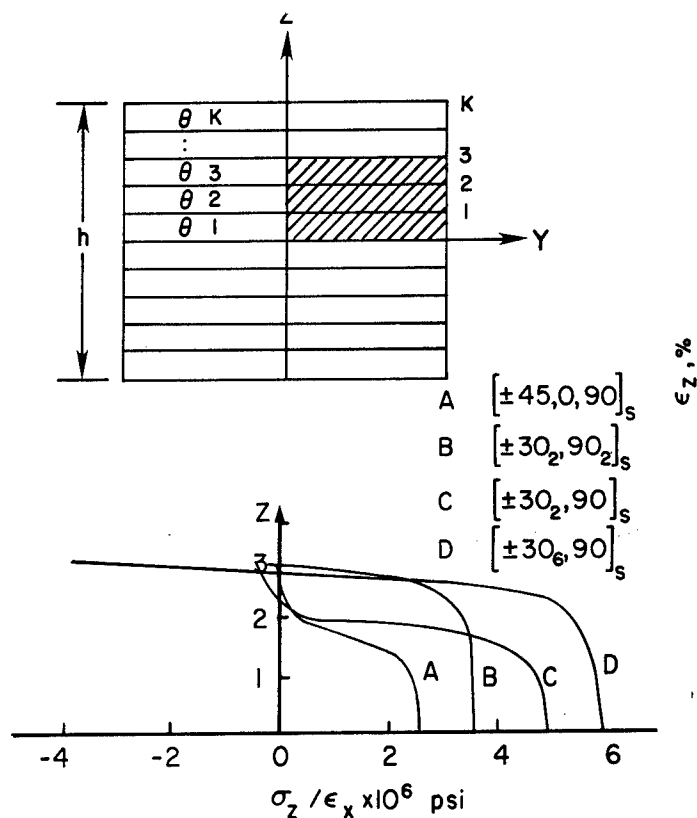
EXAMINE THE FRACTURED SURFACE

EMPLOY AVERAGE STRESS FAILURE THEORY

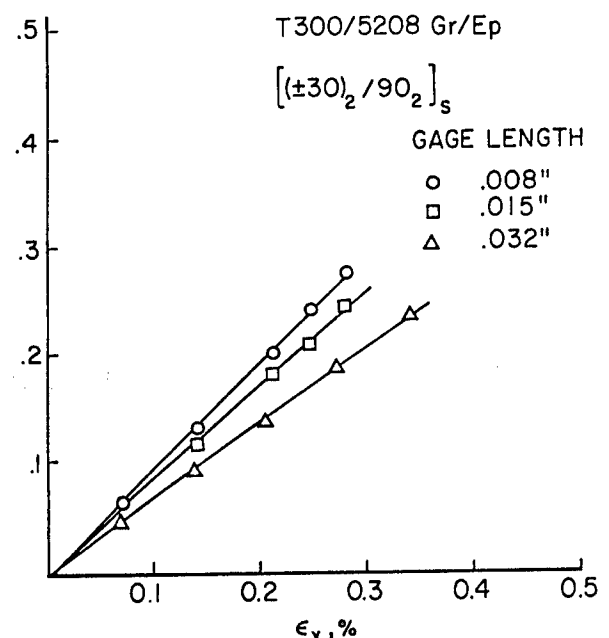


VARIATION OF STRESS COMPONENTS σ_z , τ_{xz} AND τ_{yz} FOR A $(0/90/\pm 45)_S$ LAMINATE ALONG THE WIDTH AT DIFFERENT INTERFACES

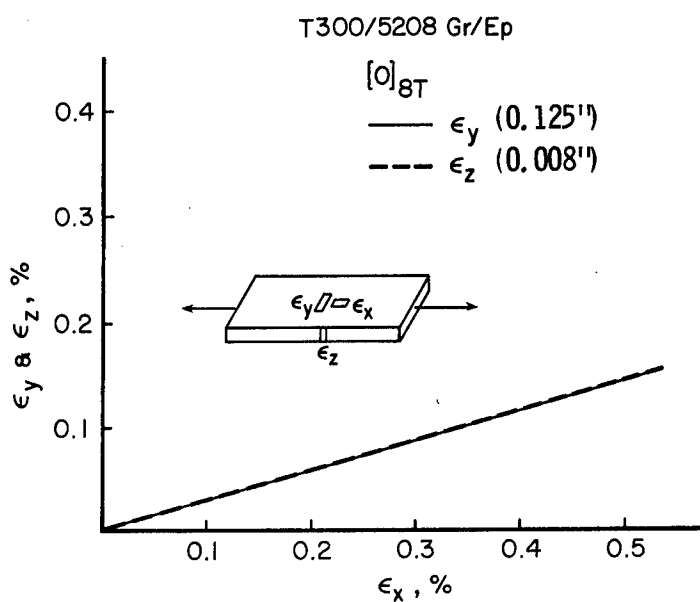




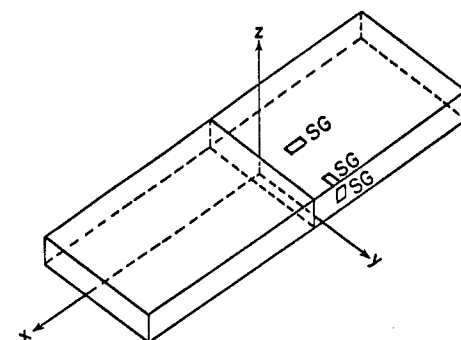
VARIATION OF σ_z AT THE FREE EDGE
OBTAINED FROM ANALYSIS



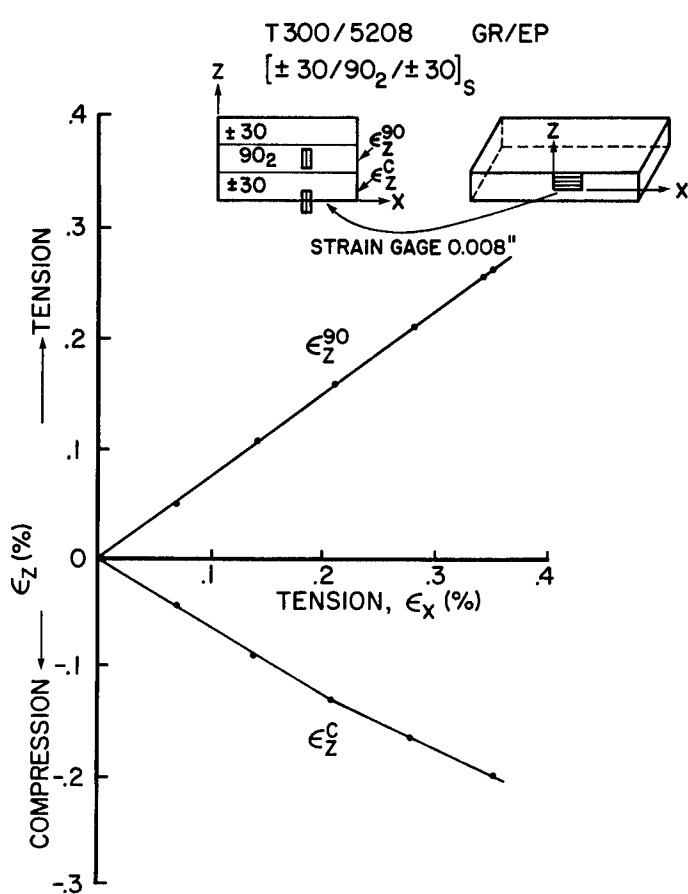
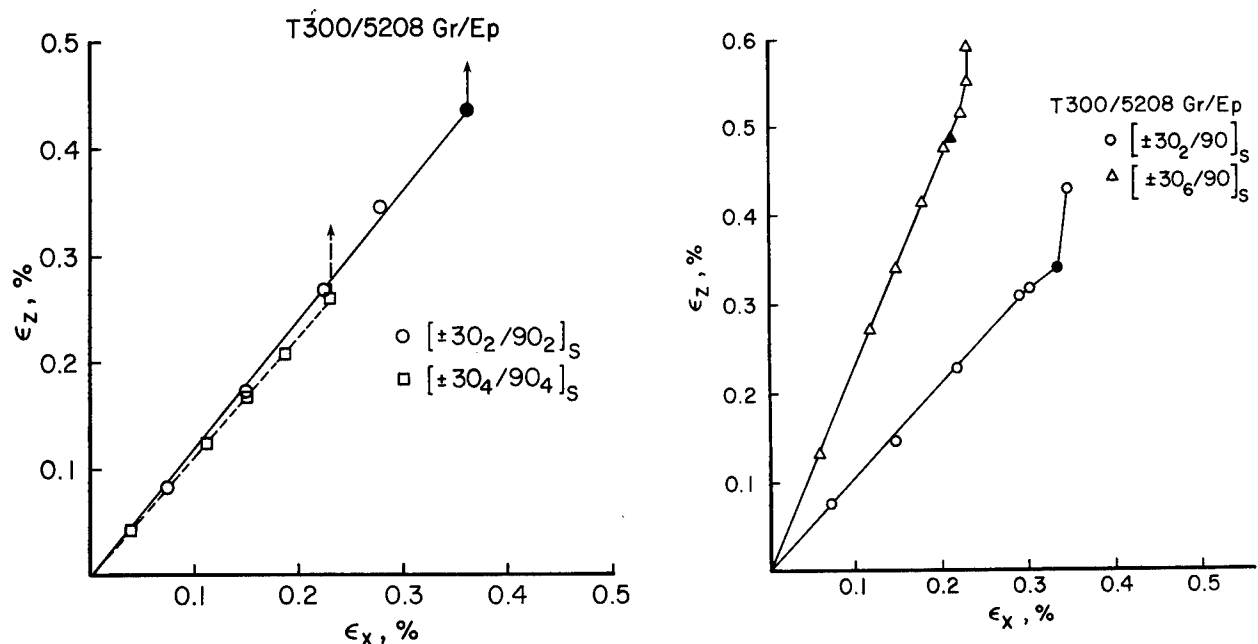
EFFECT OF STRAIN GAGE SIZE ON THE
MEASUREMENT OF ϵ_z



TRANSVERSE STRAIN VS. AXIAL STRAIN



LOCATION OF STRAIN GAGES MOUNTED
ON SPECIMEN



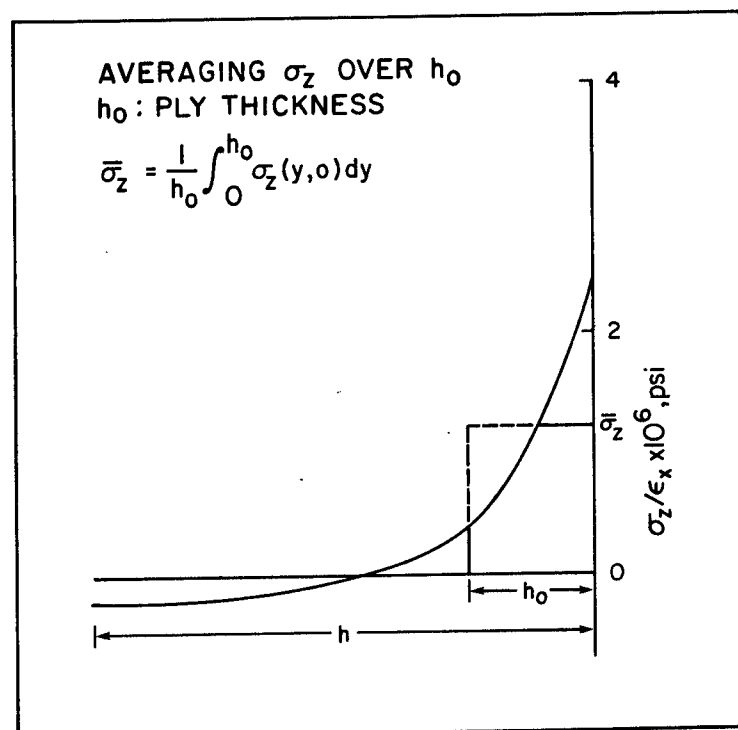
TRANSVERSE STRAIN (Z-DIRECTION) VS. AXIAL STRAIN

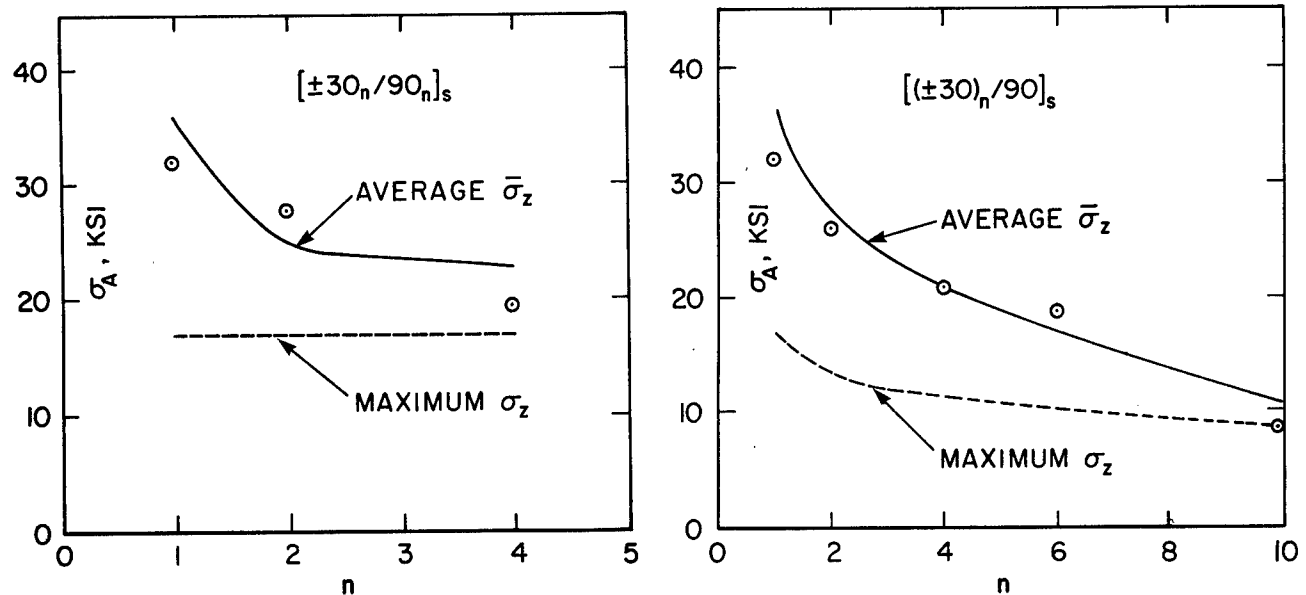
σ_z AT MIDPLANE OF LAMINATE FOR APPLIED AXIAL STRAIN OF 0.1%
T300/5208 Gr/Ep

LAMINATE	** σ_z , psi		NO. OF SPECIMENS
	*ANALYSIS	EXPERIMENT	
$[\pm 30_2/90_2]_s$	3,120	2,870	3
$[\pm 30_4/90_4]_s$	3,120	3,060	3
$[(\pm 30)_2/90]_s$	4,320	3,110	2
$[(\pm 30)_4/90]_s$	4,600	4,360	2
$[(\pm 30)_6/90]_s$	4,800	4,640	3

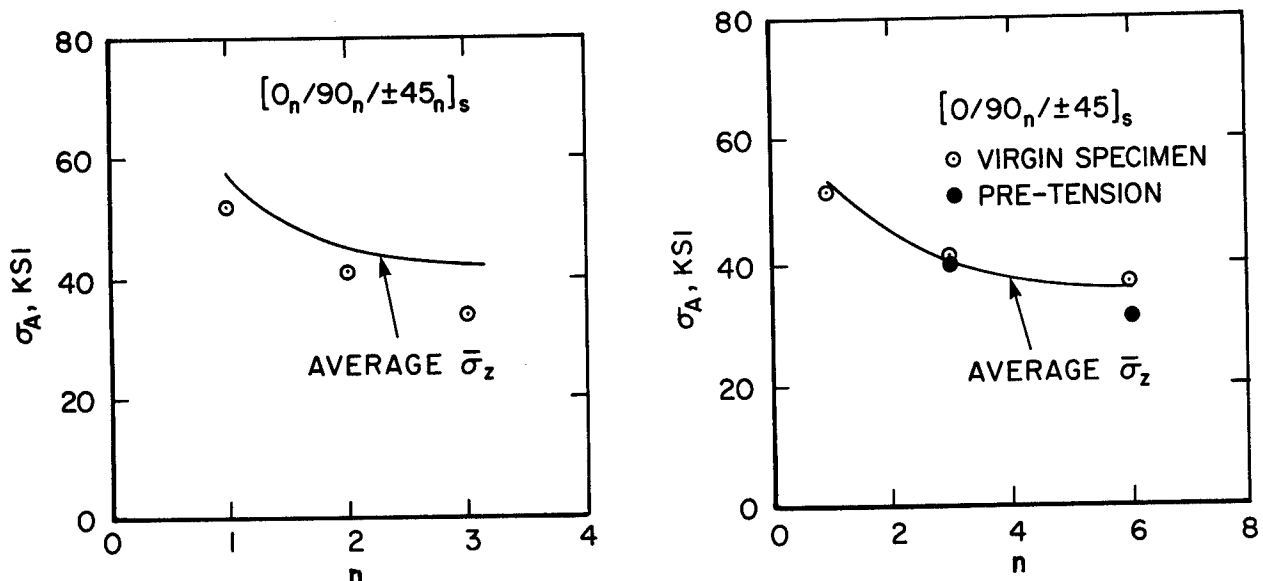
*WITHOUT PRESENCE OF CURING RESIDUAL STRESS

$$** \sigma_z = c_{iz} e_i$$





UNDER APPLIED UNIAXIAL TENSION



UNDER APPLIED UNIAXIAL COMPRESSION

COMPARISON OF EXPERIMENT AND PREDICTION FOR
ONSET OF DELAMINATION: T300/5208 Gr/Ep

STRESS AND STRENGTH ANALYSIS AT DELAMINATION

T300/5208 Gr/Ep

LAMINATE	APPLIED ϵ_1 %	$\bar{\sigma}_z$	APPLIED σ_1 (ksi)
($\pm 45/0/90$) _s	.52	7.9	40.5
(0/ $\pm 45/90$) _s	.66	8.1	51.4
(0 ₂ / $\pm 45/90$ ₂) _s	.54	9.0	42.1
(0/ $\pm 15/90$) _s	.68	7.6	96.0
(0/ $\pm 30/90$) _s	.55	9.2	59.6
($\pm 30/90$) _s	.39	8.4	30.4
(± 30 ₂ / 90) _s	.33	9.0	28.2
(± 30 ₄ / 90) _s	.26	8.7	22.4
(± 30 ₆ / 90) _s	.22	7.7	18.7
($\pm 30/\pm 60$) _s	.61	8.4	34.68
(± 30 ₂ / ± 60 ₂) _s	.53	8.9	29.75
(± 30 ₂ / 90 ₂) _s	.36	9.2	27.7
(± 30 ₄ / 90 ₄) _s	.25	7.7	19.46
(0 ₃ / $\pm 45/90$ ₃) _s	.35	7.0	27.33
(0/ $\pm 45/90$ ₃) _s	.67	9.6	40.61
(0/ $\pm 45/90$ ₆) _s	.54	5.6	24.66
(0/90/ ± 45) _s	-.66	6.6	-51.76
(0/90 ₃ / ± 45) _s	-.68	8.3	-40.67
(0/90 ₆ / ± 45) _s	-.78	9.4	-35.37

NEGATIVE SIGN DENOTES COMPRESSION
AVERAGE OF 4 TO 10 SPECIMENS FOR EACH LAMINATE

ANALYTICAL AND EXPERIMENTAL RESULTS ON ONSET OF DELAMINATION

LAMINATE	TYPE OF LOADING	AVG STRESS, KSI FOR $\epsilon_x = 0.1\%$			ϵ_x AT ONSET OF DELAMINATION, %		OBSERVED INTERFACE DELAMINATED
		$\bar{\sigma}_z$	$\bar{\tau}_{xz}$	INTERFACE	PREDICTION	EXPERIMENT	
PURE GRAPHITE (± 30 ₂ c/ 90 ₂ c) _s	TEN COMP	2.3 ≈ 0	0 3.0	MP +30/-30	0.33 0.42	0.37 0.45	MP & -30/90 30/-30
HYBRID I (± 30 ₂ c/ 90 ₂ c) _s	TEN COMP	1.88 ≈ 0	0 2.80	MP +30/-30	0.51 0.45	0.46 0.50	MP & -30/90 30/-30
HYBRID II (± 30 ₂ s/ 90 ₂ c) _s	TEN COMP	0.88 ≈ 0	0 1.32	MP +30/-30	0.85 1.18	0.76 1.26	MP & -30/90 30/-30
PURE GRAPHITE (0 ₂ / ± 15 ₂) _s	COMP	0.08	4.00	+15/-15	0.31	0.45	15/-15
HYBRID I (0 ₂ c/ ± 15 ₂ s) _s	TEN COMP	-0.03 0.03	1.18 1.18	+15/-15 +15/-15	1.31 1.31	1.38 1.14	15/-15 15/-15
HYBRID II (0 ₂ s/ ± 15 ₂ c) _s	TEN COMP	-0.28 0.28	3.4 3.4	+15/-15 +15/-15	0.37 0.37	0.67 0.50	15/-15 & 0/15 15/-15

C: T300/934C Gr/Ep

S: S-2/934C GI/Ep

MP: Midplane

QUADRATIC POLYNOMIAL FAILURE CRITERION

$$F_{zz} \bar{\sigma}_z^2 + F_{xz} \bar{\tau}_{xz}^2 + F_z \bar{\sigma}_z = 1$$

$$F_{zz} = \frac{1}{zz}, \quad F_{xz} = \frac{1}{S_{xz}^2}, \quad F_z = \frac{1}{z} - \frac{1}{z'}$$

$$R = \frac{\sigma_{\text{allowed}}}{\sigma_{\text{applied}}}$$

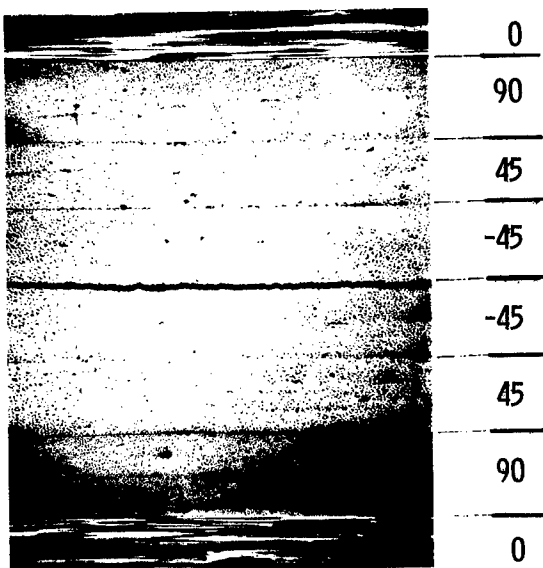
$$aR^2 + bR + C = 0$$

$$R = \frac{-b \pm \sqrt{b^2 - 4ac}}{2a}$$

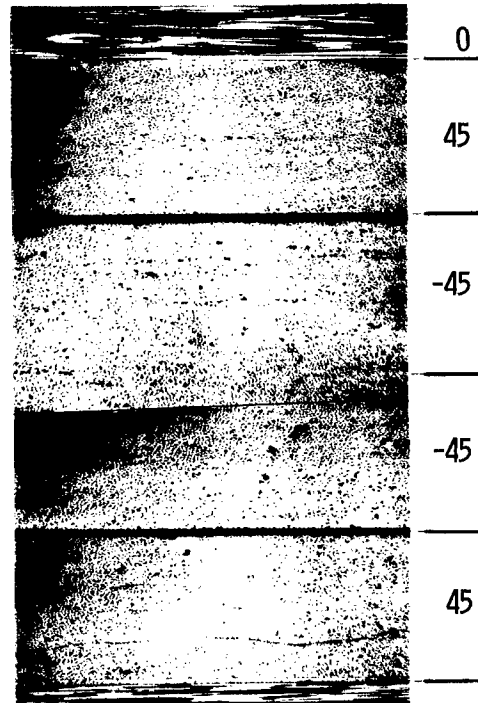
STRENGTH RATIO R AT ONSET OF DELAMINATION
USING QUADRATIC FAILURE CRITERION

Laminate	E_{11} (MSI)	σ_{Del} (KSI)	ϵ_{Del} (%)	$\bar{\sigma}_z$ (KSI)	$\bar{\tau}_{xz}$ (KSI)	R
(90 ₄ / ± 15 ₄) _s	12.2	41.6	0.34	2.72	-16.25	.73
(90 ₄ / ± 30 ₄) _s	7.7	20.8	0.27	4.13	-10.77	.93
(90 ₄ / ± 45 ₄) _s	3.7	13.7	0.37	4.77	-7.44	1.1
(0 ₄ / ± 15 ₄) _s	17.7	61.8	0.35	0.74	17.54	0.75
(0 ₄ / ± 30 ₄) _s	11.7	41.5	0.35	1.54	12.95	0.96
(0 ₄ / ± 45 ₄) _s	8.4	66.4	0.79	1.82	-11.85	1.0
(± 15 ₄) _s	16.3	56.3	0.35	-1.14	-17.2	0.78
(± 30 ₄) _s	6.8	27.9	0.41	0.21	-14.4	0.93
(0 ₂ /90 ₂ / ± 45 ₂) _s	7.8	43.9	0.56	5.9	-8.85	0.90
(TENSION)						
(0 ₄ / ± 15 ₄) _s	17.7	100.9	.57	-1.2	-28.57	.48
(0 ₄ / ± 30 ₄) _s	11.7	99.5	.85	-3.74	-31.45	.46

T300/934C Gr/Ep



[0₂/90₂/ ± 45]_s



[0₄/ ± 45]_s

DELAMINATION UNDER APPLIED COMPRESSION



MIDPLANE
 $[0_2/90_2/\pm45_2]_s$

DELAMINATION DUE TO σ_z UNDER
APPLIED COMPRESSION



+30/-30 INTERFACE
 $[\pm30_2s/90_2c]_s$

DELAMINATION DUE TO τ_{xz} UNDER
APPLIED COMPRESSION

CONCLUSIONS

THE EXPERIMENTALLY DETERMINED σ_z CORRELATES CLOSELY WITH THE ANALYTICAL RESULT.

THE PREDICTED ONSET OF DELAMINATION LOADS EMPLOYING AVERAGE STRESS FAILURE CRITERIA ARE CLOSE TO THE OBSERVED VALUES WHERE SINGLE PREDOMINANT INTERLAMINAR STRESS COMPONENT EXISTS.

QUADRATIC FAILURE CRITERION PREDICTS STRENGTH RATIOS CLOSE TO OBSERVED ONES FOR A NUMBER OF LAMINATES.

THE MODE AND LOCATION OF DELAMINATION IN COMPOSITE LAMINATES ARE PREDICTED ACCURATELY. THE PREDICTED MODES OF DELAMINATION DUE TO σ_z OR τ_{xz} CAN BE CLEARLY IDENTIFIED BY SEM.

FURTHER WORK IS REQUIRED TO INVESTIGATE THE EFFECT OF ORIENTATION ON INTERLAMINAR SHEAR STRENGTH.

STRENGTH, DEFLECTIONS AND IMPACT DAMAGE IN ADVANCED COMPOSITE STRUCTURES

Paul A. Lagace

TECHNOLOGY LABORATORY FOR ADVANCED COMPOSITES
Department of Aeronautics and Astronautics
Massachusetts Institute of Technology
Cambridge, MA 02139

ABSTRACT

The plans for and the progress on two three-year contractual efforts concerning composite materials will be presented. Although the two major work areas are related, they will be treated, for the purpose of presentation, separately. The first area involves the "Strength and Deflections of Advanced Composite Sandwich Structures". The second area is entitled "The Sensitivity of Kevlar/Epoxy and Graphite/Epoxy Structures to Damage from Fragment Impact".

Sandwich construction has been used in the aerospace industry for a number of years. The current effort seeks to investigate such construction for application to high efficiency, ultralight aircraft. This involves the investigation of sandwich structures with relatively thin graphite/epoxy face sheets. Due to this construction, a number of failure modes must be considered: ply or sublamine buckling, skin debonding, core failure, plate buckling, and facesheet fracture. This three-year program has thrusts in three principal areas: the development of analytical tools necessary to predict the strength and deflection of graphite/epoxy sandwich structures; experimentation on sandwich plates to determine their buckling and deflection characteristics to compare with the analysis; and experimentation on sandwich plates to determine their strength properties.

The work during the last nine months has centered on the development of the analytical methodology. The analysis is based on a Rayleigh-Ritz type discretization of the displacement fields and uses direct minimization of the potential energy. All eighteen terms in the A, B, and D matrices are taken into account so that anisotropic plates can be analyzed. Mindlin plate theory is used to incorporate the effects of transverse shear and the effect of initial imperfections can also be evaluated as the program uses Marguerre's shallow shells theory. The loading on the plate can be longitudinal compression, transverse compression, shear, or any combination thereof. The program solves the general buckling/postbuckling problem via an optimal search and a typical plate takes about 20 seconds of CPU time on a VAX 11/782 computer for analysis. Typical results are presented and, where available, agree well with other reported analytical results.

An experimental program has also been devised. The purpose of the program is to investigate the effects of various core materials on the deflections and, ultimately, strength behavior. The experimental technique is discussed and preliminary results presented which correlate well with the analysis for these configurations.

The response of composite laminates to impact is an important consideration in assessing the damage tolerance of a composite structure. Composites are sensitive to impact due to their tendency to delaminate. Furthermore, this damage often goes undetected although it may cause considerable strength reduction in the composite part. The effort in this three-year program is directed toward first establishing the basic response of composites to impact via generic specimens (i.e. coupon type), analysis of the impact event, and the response of the composite to the damage induced by impact. Once the basic mechanisms are established and better understood, the work will progress to structures typically used in aircraft such as stiffened panels, pressurized cylinders (which model fuselages) and the like.

The analysis of the impact event has been broken down into parts. The treatment involves either analysis or experimentally determined data for the contact law and a plate solution for the overall parameters in order to model the local contact problem of a static indentor. This is used with a plate solution to determine the dynamic response on the plate to the impact event. These two analyses yield the stress and strain fields which are then used in conjunction with failure criteria to determine the damage caused by the impact. A modified Bessel function approach is used to solve the axisymmetric contact problem. The analytical solution shows excellent correlation with experimental data presented in the literature. The dynamic problem is solved via a Rayleigh-Ritz formulation and includes shear deformation. The technique is currently being implemented.

An extensive experimental program is underway as well. An impact gun has been setup along with monitoring equipment and this will be discussed. A number of graphite/epoxy coupons have been impacted and then sectioned to characterize the damage. Typical damage modes will be shown. Some tests to failure have also been conducted on impacted specimens and these preliminary results will also be discussed. Additionally, work has been accomplished on modelling damage due to impact via delaminations implanted via teflon inserts. A number of other authors have looked at the compressive response of graphite/epoxy with implanted delaminations. In this investigation, the initial work has been conducted under tension in order to separate out the basic effect the delamination has on the fracture of the material from the structural effect the delamination induces due to local ply/sublamine buckling. The preliminary results, which will be presented, indicate that a delamination located at the midplane of a six-ply laminate is benign in that no strength and little stiffness changes are noted. However, the cases where delaminations are implanted at every ply interface, which is more typical of the damage in an impacted specimen, show strength reductions of 30% for a 30 mm circular delamination in a 70 mm wide specimen.

In addition to the results attained to date, the next steps in the research will be outlined in each case.

ANALYSIS OF COMPOSITE LAMINATES
WITH DELAMINATIONS UNDER COMPRESSION
LOADING

HAN-PIN KAN

NORTHROP CORPORATION
AIRCRAFT DIVISION
HAWTHORNE, CALIFORNIA 90250

ABSTRACT

Delaminations in composite structures are of great concern to aircraft designers and analysts. This is because of the possible local buckling and growth of the delaminations when such a structure is subjected to in-service loading. An extensive technology assessment conducted under Reference 1 has identified that impact damage and delamination are the most critical damage modes that degrade structural strength and fatigue life. Unlike metallic structures, where the material defects propagate under tensile loading, delaminations in composite laminates usually do not propagate under tension. However, under compressive static and fatigue loading, local buckling of the delaminated region may occur below the compression strength of the laminate. The local buckling of the delaminated region provides a means of releasing strain energy and thus making energy available for the delamination to grow. To design composite structures for damage tolerance, analytical methods are needed to predict the initial buckling, to compute the strain-energy-release rate and to determine the mode of failure of the structure.

In the present paper, an analytical method to determine the initial buckling of the delaminated region and to compute the strain-energy-release rate is presented and the interaction of laminate failure mode is discussed. Three types of delaminations, namely, through-the-width, circular and elliptical delaminations are considered. The influence of delamination size and depth on the initial buckling and strain-energy-release rate is investigated.

The initial buckling analysis is based on the energy method employing the Rayleigh-Ritz method. The delaminated laminate is modelled as a homogeneous, elastic, orthotropic plate. The plate is separated into two layers in the delaminated region. The strain energy expression is taken from Reference 2. Out-of-plane displacement functions, satisfying the boundary conditions, are assumed for different delamination types. The initial buckling load is determined by performing the necessary integrations and variations to minimize the total potential energy of the system. Results of the analysis show that the initial buckling load depends on the delamination size, shape, depth and the laminate stacking reference.

As the applied compression load exceeds the initial buckling load of a laminate with a delamination, strain energy will be released for delamination growth. The total strain-energy-release rate, G , is computed. The value of G is obtained under a constant load and according to the usual definition that G is the energy required to create a unit new free surface in the system.

The two layers of a composite laminate separated by a delamination behave as a single undamaged laminate when the applied load is below the initial buckling load; hence the strain energy release rate $G = 0$ in the prebuckling range. Beyond initial buckling, the value of G depends on the initial buckling load which is a function of the delamination size, shape and depth. The results indicate that the value of G , under a constant compression loading, is very sensitive to delamination size, when the delamination is slightly larger than the critical size corresponding to the applied load. As the delamination becomes large as compared to the critical size, the value of G approaches a constant.

The initial buckling of the delaminated region in a laminate with delamination usually does not cause failure of the laminate. The static compression strength of a composite structure with delaminations depends on the initial buckling strength, the material compression strength and interlaminar toughness, and the structural geometries. The mode of failure may be gross compression, local or global buckling or catastrophic delamination growth. A failure prediction technique is developed which takes into consideration of the failure mode interactions. In this technique, the failure strength for different failure mode is plotted as a function of the delamination size. The laminate

failure strength is then given by the minimum strength among all the failure modes. By doing this, the failure is divided into three or more regions depending on the delamination size.

REFERENCES

1. McCarty, J. E. et al, "Damage Tolerance of Composites," AFWAL Contract No. F33615-82-C-3213, Interim Report No. 1-4, March 1983-September 1984.
2. Lekhniskii, S. G., Anisotropic Plates, Gordon and Breach, New York, 1968.

ACKNOWLEDGEMENT

The work reported here was preformed under Northrop's Independent Research and Development Program in support of AFWAL Contract No. F33615-82-C-3213, "Damage Tolerance of Composites."

ANALYSIS OF COMPOSITE LAMINATES WITH DELAMINATIONS UNDER COMPRESSION LOADING

HAN-PIN KAN

**NORTHROP CORPORATION
AIRCRAFT DIVISION
HAWTHORNE, CALIFORNIA 90250**

OBJECTIVE

**TO PREDICT RESIDUAL STRENGTH AND FAILURE MODE
OF COMPOSITE LAMINATES WITH DELAMINATIONS
UNDER COMPRESSION LOADING**

APPROACH

- DETERMINE INITIAL BUCKLING OF DELAMINATED REGION
- COMPUTE STRAIN-ENERGY-RELEASE RATE FOR
DELAMINATION GROWTH
- CONSIDER FAILURE MODE FOR STRENGTH PREDICTION

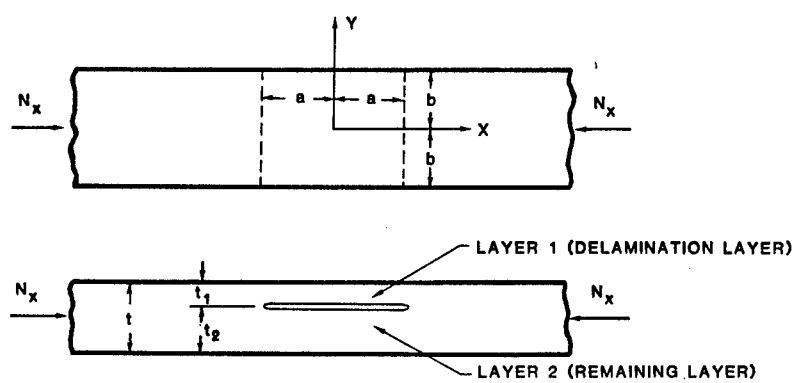
ANALYSIS FEATURES

- SINGLE DELAMINATION
- ANY DELAMINATION SIZE, SHAPE, AND DEPTH
- BOUNDARY VARIATION OF STRAIN-ENERGY-RELEASE RATE INCLUDED
- MULTIPLE FAILURE MODES FOR STRENGTH PREDICTION

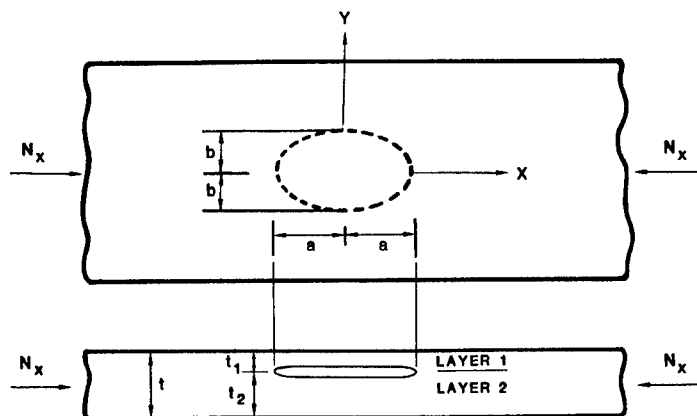
BUCKLING ANALYSIS

- DELAMINATED LAMINATE MODELED AS TWO SEPARATED LAYERS OF HOMOGENEOUS, ELASTIC, ORTHOTROPIC PLATES
- ENERGY FORMULATION EMPLOYED
- INITIAL BUCKLING STRENGTH OF THE WEAKER LAYER IS OBTAINED USING RAYLEIGH-RITZ METHOD
- INITIAL BUCKLING LOAD DEPENDS ON THE DELAMINATION SHAPE, SIZE, LOCATION, AND THE LAMINATE STACKING SEQUENCE

THROUGH-THE-WIDTH DELAMINATION



LAMINATE WITH AN ELLIPTICAL DELAMINATION



DISPLACEMENT FUNCTIONS

THROUGH-THE-WIDTH DELAMINATION

$$w = w(x) = Ae^{\alpha x} + Be^{-\alpha x} + C \sin \alpha x + D \cos \alpha x$$

ELLIPTICAL DELAMINATION

$$w = w(x, y) = \frac{A}{a^4 b^4} (a^2 b^2 - b^2 x^2 - a^2 y^2)^2$$

INITIAL BUCKLING LOADS

THROUGH-THE-WIDTH DELAMINATION

$$N_{CRI} = k \left(\frac{\pi}{a} \right)^2 \cdot D_{11}, \quad k = 1.0306$$

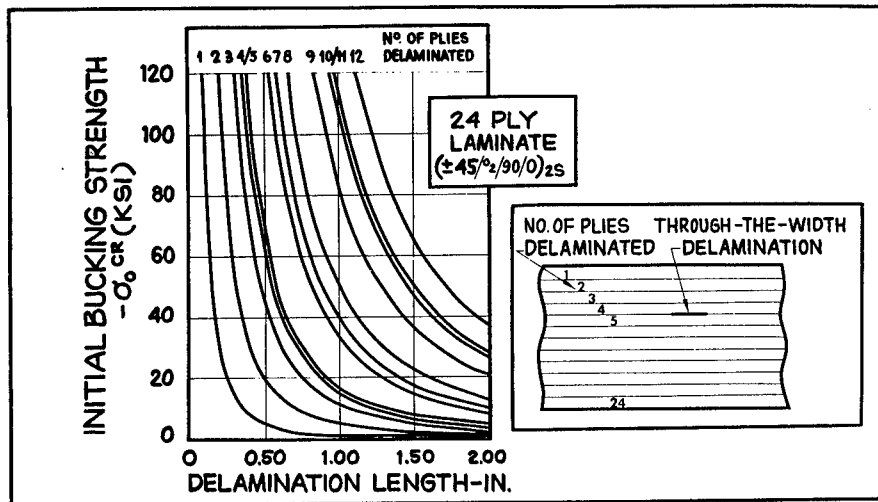
for lowest buckling mode

ELLIPTICAL DELAMINATION

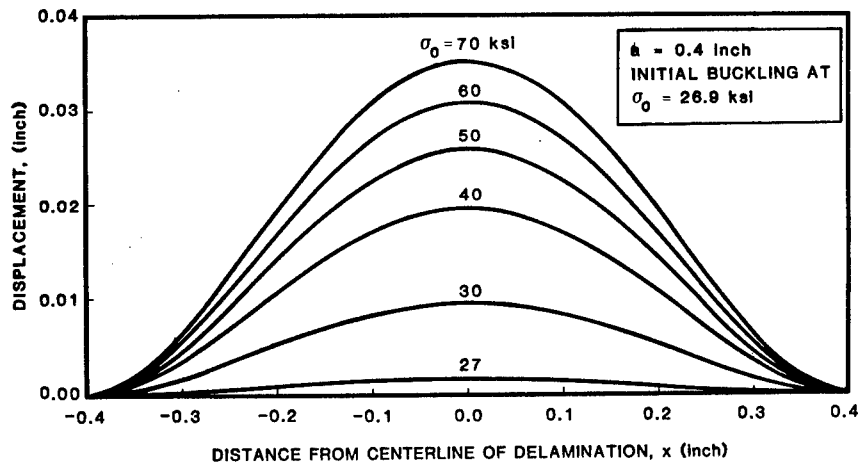
$$N_{CRI} = \frac{3}{a^2} [4D_{11} + \frac{8}{3} \left(\frac{a}{b} \right)^2 D_{12} + 4 \left(\frac{a}{b} \right)^4 D_{22} + \frac{16}{3} \left(\frac{a}{b} \right)^2 D_{66}]$$

D_{ij} ARE PLATE RIGIDITIES OF THE DELAMINATION LAYER

INITIAL BUCKLING STRENGTH



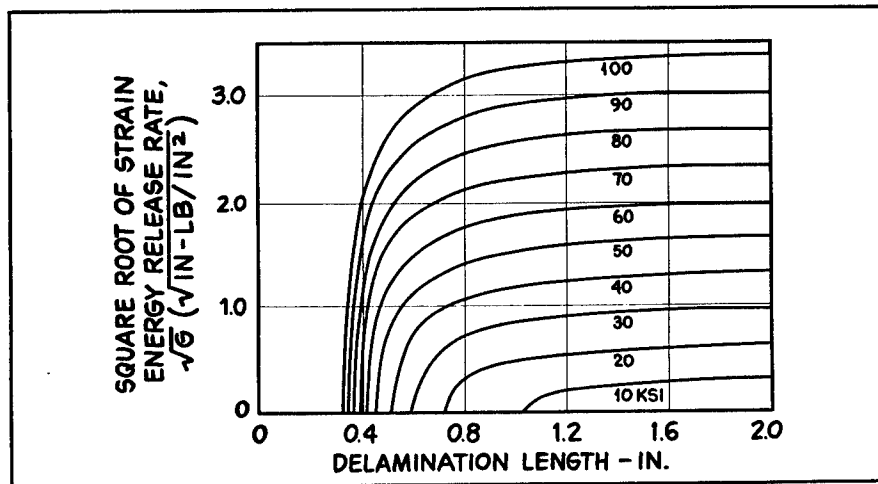
DISPLACEMENT PROFILE OF THE DELAMINATED LAYER



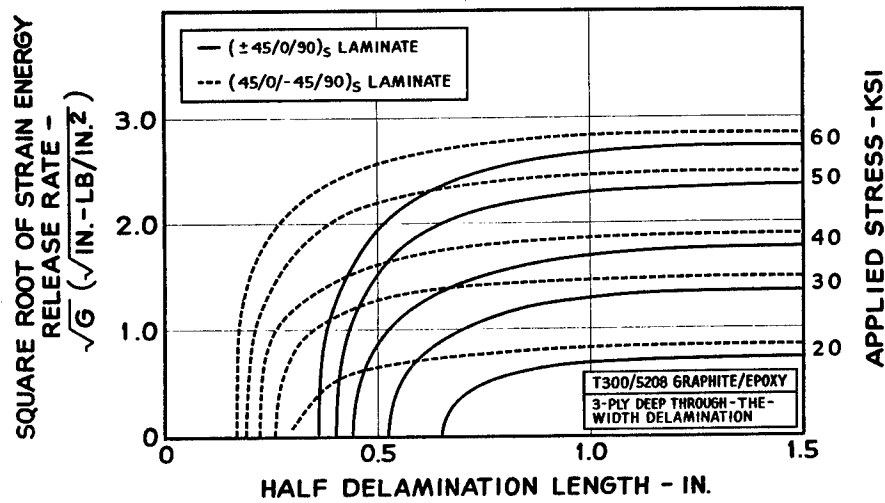
STRAIN-ENERGY RELEASE RATE ANALYSIS

- ASSUME NO ENERGY RELEASED AT APPLIED LOAD LEVEL BELOW INITIAL BUCKLING STRENGTH OF THE DELAMINATED LAYER
- OVERALL STRAIN-ENERGY-RELEASED-RATE IS DETERMINED UNDER CONSTANT LOAD CONDITION
- STRAIN-ENERGY-RELEASE-RATE
$$G = \frac{\partial (W-U)}{\partial a}$$
- G IS A FUNCTION OF DELAMINATION SHAPE, SIZE, LOCATION, AND THE INITIAL BUCKLING LOAD
- FOR CIRCULAR AND ELLIPTICAL DELAMINATIONS, G ALSO VARIES AROUND THE DELAMINATION FRONT

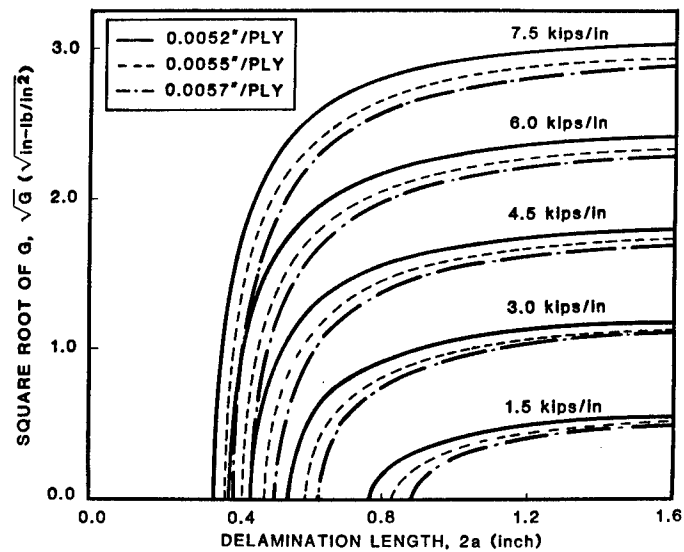
STRAIN-ENERGY RELEASE RATE 16-PLY LAMINATE 3-PLY-DEEP DELAMINATION



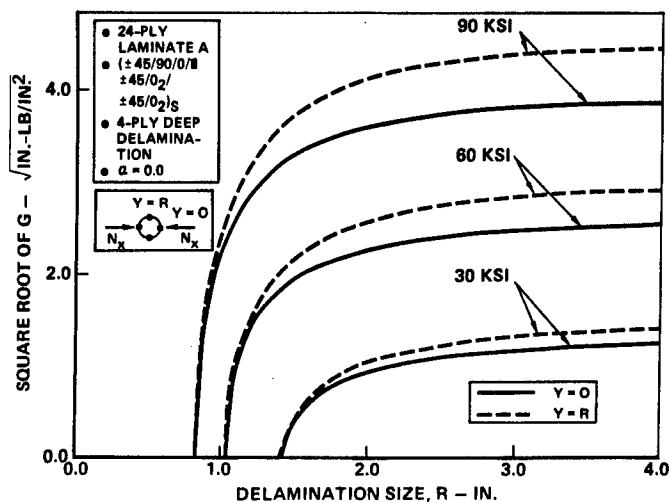
EFFECTS OF STACKING SEQUENCE ON STRAIN ENERGY RELEASE RATE



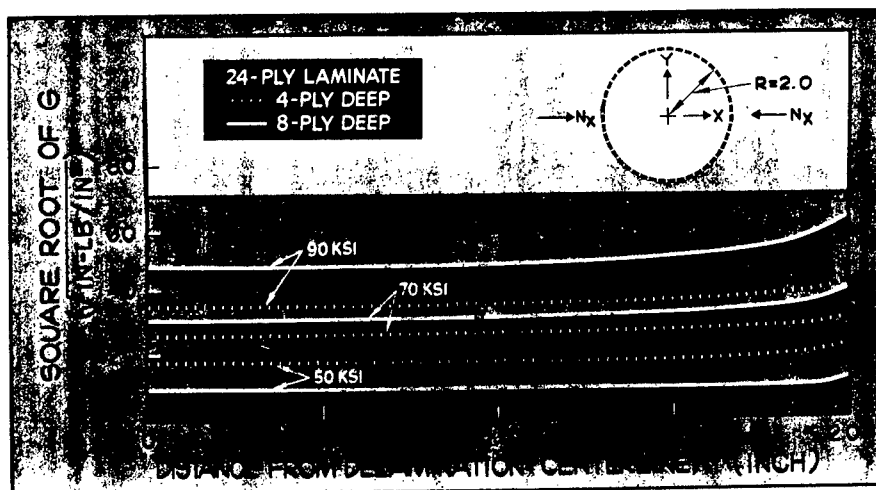
EFFECTS OF PLY THICKNESS ON STRAIN-ENERGY-RELEASE RATE



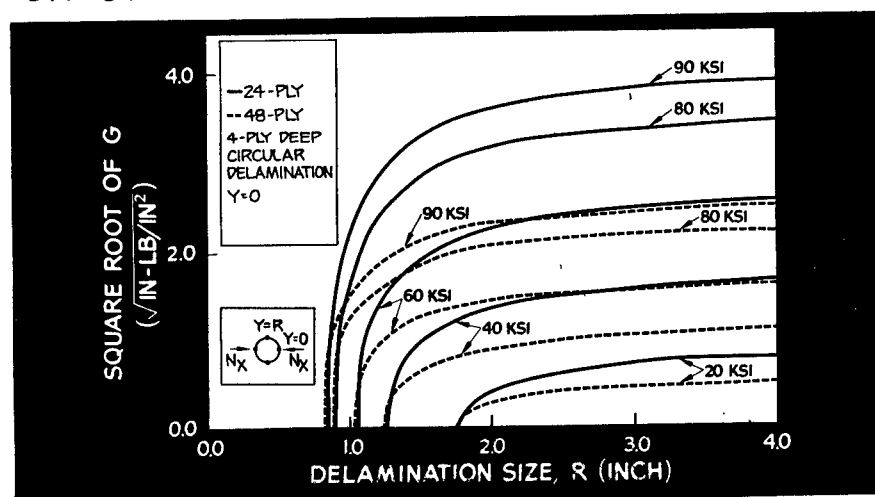
STRAIN-ENERGY-RELEASE RATE CIRCULAR DELAMINATION



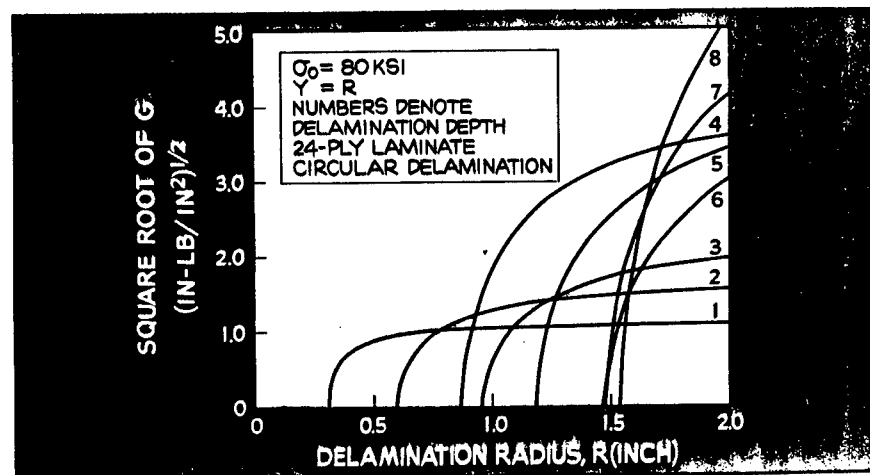
PERIPHERAL VARIATION OF STRAIN-ENERGY-RELEASE-RATE CIRCULAR DELAMINATION



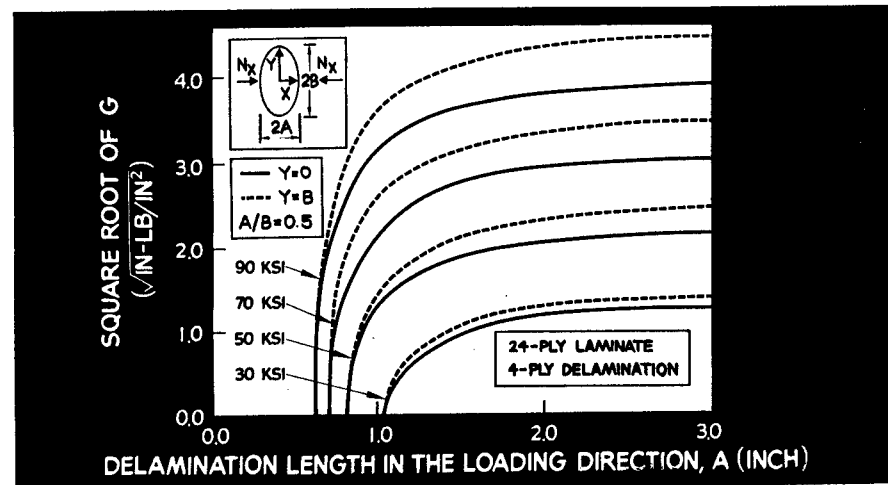
EFFECTS OF LAMINATE THICKNESS ON STRAIN-ENERGY-RELEASE-RATE



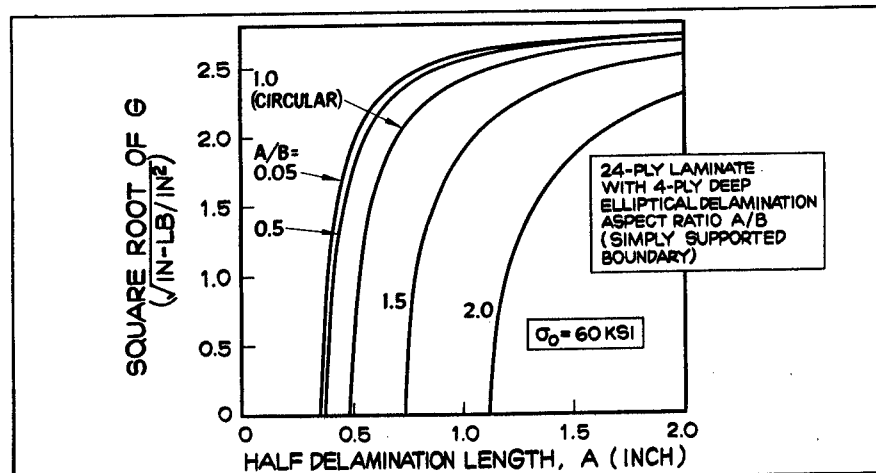
EFFECTS OF DELAMINATION DEPTH ON STRAIN-ENERGY-RELEASE-RATE



STRAIN-ENERGY-RELEASE-RATE ELLIPTICAL DELAMINATION



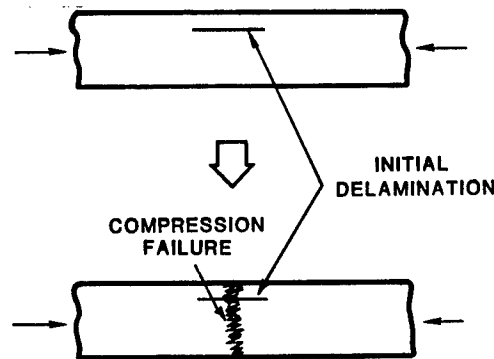
EFFECT OF ELLIPTICAL ASPECT RATIO ON THE STRAIN-ENERGY-RELEASE-RATE



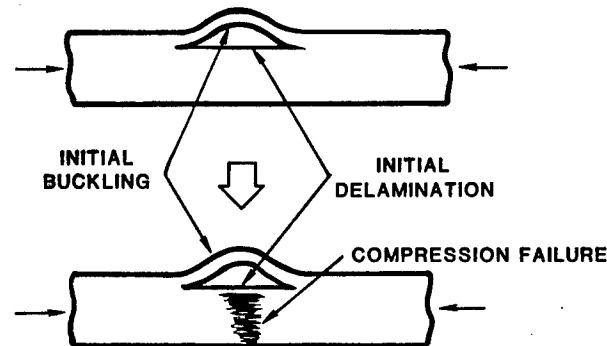
STATIC FAILURE MODES FOR LAMINATE WITH DELAMINATIONS

MODE	DESCRIPTION
1	GROSS COMPRESSION FAILURE
2	INITIAL BUCKLING OF THE DELAMINATION FOLLOWED BY COMPRESSION FAILURE OF THE REMAINING LAYER
3	GLOBAL BUCKLING
4	INITIAL BUCKLING OF THE DELAMINATION FOLLOWED BY GLOBAL BUCKLING OF THE LAMINATE GLOBAL
5	LOCAL BUCKLING INITIAL BUCKLING OF THE DELAMINATION FOLLOWED BY LOCAL BUCKLING OF THE REMAINING LAYER
6	DELAMINATION GROWTH INITIAL BUCKLING OF THE DELAMINATION FOLLOWED BY DELAMINATION GROWTH AND EVENTUALLY FAILED BY MODE 2, 4 OR 5

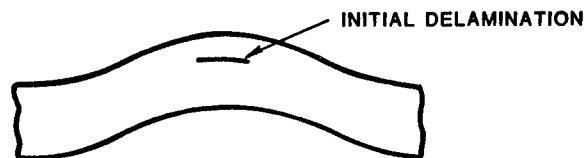
GROSS COMPRESSION FAILURE **(FAILURE MODE 1)**



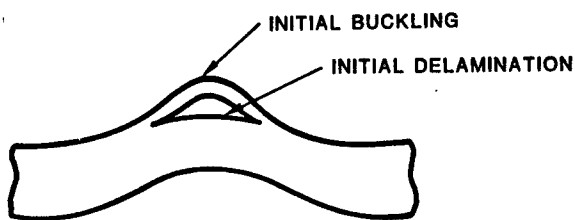
INITIAL BUCKLING OF THE DELAMINATION **FOLLOWED BY COMPRESSION FAILURE** **(FAILURE MODE 2)**



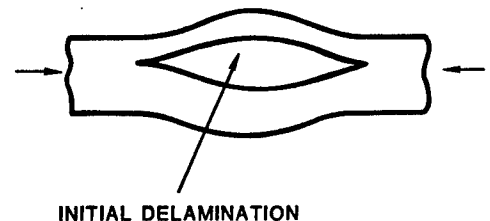
GLOBAL BUCKLING **(FAILURE MODE 3)**



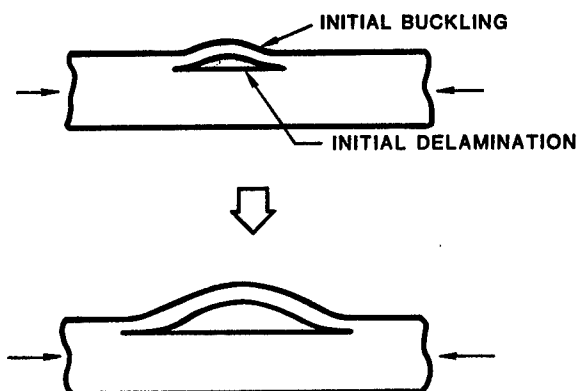
INITIAL BUCKLING OF THE DELAMINATION
FOLLOWED BY GLOBAL BUCKLING
(FAILURE MODE 4)



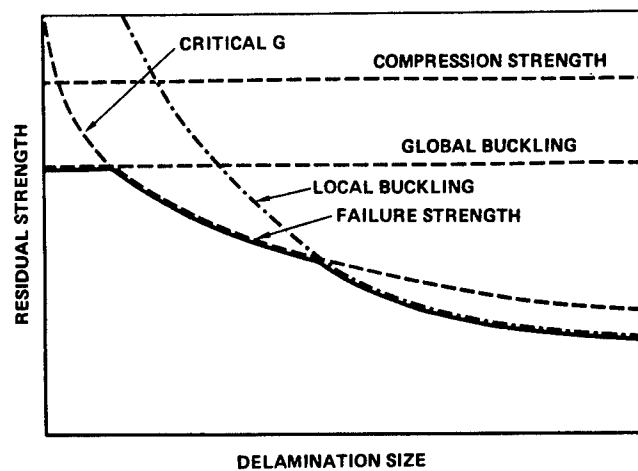
LOCAL BUCKLING
(FAILURE MODE 5)



INITIAL BUCKLING OF THE DELAMINATION
FOLLOWED BY DELAMINATION GROWTH
(FAILURE MODE 6)



FAILURE MODE INTERACTION



SUMMARY

- AN ANALYTICAL PROCEDURE HAS BEEN DEVELOPED FOR STATIC COMPRESSION STRENGTH PREDICTION OF COMPOSITE LAMINATES WITH DELAMINATIONS
- THE INFLUENCE OF DELAMINATION CONFIGURATION ON THE FAILURE STRENGTH AND FAILURE MODE HAS BEEN INVESTIGATED
- THE INFLUENCE OF LAMINATE THICKNESS, PLY THICKNESS AND STACKING SEQUENCE ON STRAIN-ENERGY-RELEASE RATE HAS BEEN EXAMINED

SIMPLE RECTANGULAR ELEMENT FOR
ANALYSIS OF LAMINATED COMPOSITE MATERIALS

John D. Whitcomb

National Aeronautics and Space Administration
Langley Research Center
Hampton, Virginia 23665-5225

ABSTRACT

The development of an appropriate finite element mesh is a key step in successful finite element analysis. For homogeneous materials the mesh refinement is dictated by geometrical considerations. The shape of a structure should be faithfully modeled. Also, extra mesh refinement is required in regions with strong strain gradients caused by holes, cracks, or boundary conditions. For laminated materials the analyst must also account for the different material properties of the various laminae. These ideas are illustrated by the laminated composite beam shown in the first figure. Geometrical considerations require very few elements except close to the points where load is applied, where strain gradients are large. But since standard finite elements cannot account for stacking sequence effects, such elements should not span across lamina boundaries. Hence, because of the laminated character of the material, the mesh should be highly refined even where the strain gradients are small.

The expense of modeling each lamina individually rapidly becomes intolerable as the number of laminae increases. Reference 1 presents an approximate technique to reduce costs. Laminate theory is used to obtain effective extensional moduli for a group of laminae. Then the group of laminae, rather than the individual lamina, are modeled using finite elements. This approach ignores stacking sequence effects within the lamina group. Therefore, the flexural and flexural-extension coupling properties of the lamina group cannot be faithfully modeled. Reference 2 presents a hybrid analysis for thick laminates. In this analysis (which is not a finite element analysis) the laminate is divided into global and local regions. The terms global and local refer to the detail with which the individual lamina is modeled; the local region is modeled with much greater detail than the global region. Conceptually, this is similar to using a finite element model with smaller- or higher-order elements in one region than in another. However, the analysis in reference 2 does not offer the inherent flexibility of the finite element method for modeling complicated geometries and for performing convergence checks. The objective of this paper is to introduce a new type of two-dimensional (i.e., plane stress or plane strain) finite element for analysis of laminated composites.

The element is a four-node, bilinear, rectangular element. An ordinary bilinear rectangle performs poorly in modeling bending-type deformation. The performance can be improved by using reduced numerical integration or substitute shape functions (ref. 3). Because of the multiple laminae within the element, numerical integration is not appropriate. Therefore, substitute shape functions are used to improve the performance. Explicit integration of the element stiffness matrix in terms of generalized displacements minimizes the algebraic effort required to account for the various laminae within a single element.

After describing the theoretical aspects of the element, results from analyses of several simple configurations are discussed.

REFERENCES

1. Wang, A. S. D.; and Crossman, F. W.: Calculation of Edge Stresses in Multi-Layer Laminates by Sub-Structuring. *Journal of Composite Materials*, vol. 12, Jan. 1978, pp. 76-83.

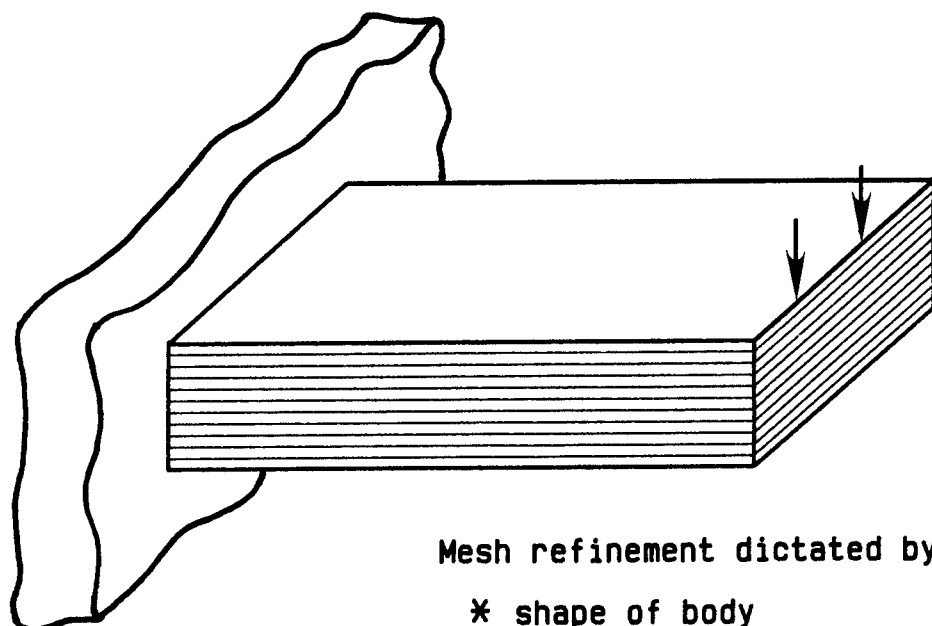
REFERENCES (CONTINUED)

2. Pagano, N. J.; and Soni, S. R.: Global-Local Laminate Variational Model. International Journal for Solids and Structures, vol. 19, no. 3, 1983, pp. 207-228.
3. Zienkiewicz, O. C.: The Finite Element Method in Engineering Science, 3rd Ed., McGraw-Hill, New York, pp. 276-284.

SIMPLE RECTANGULAR ELEMENT FOR ANALYSIS OF LAMINATED COMPOSITE MATERIALS

John D. Whitcomb
NASA Langley Research Center

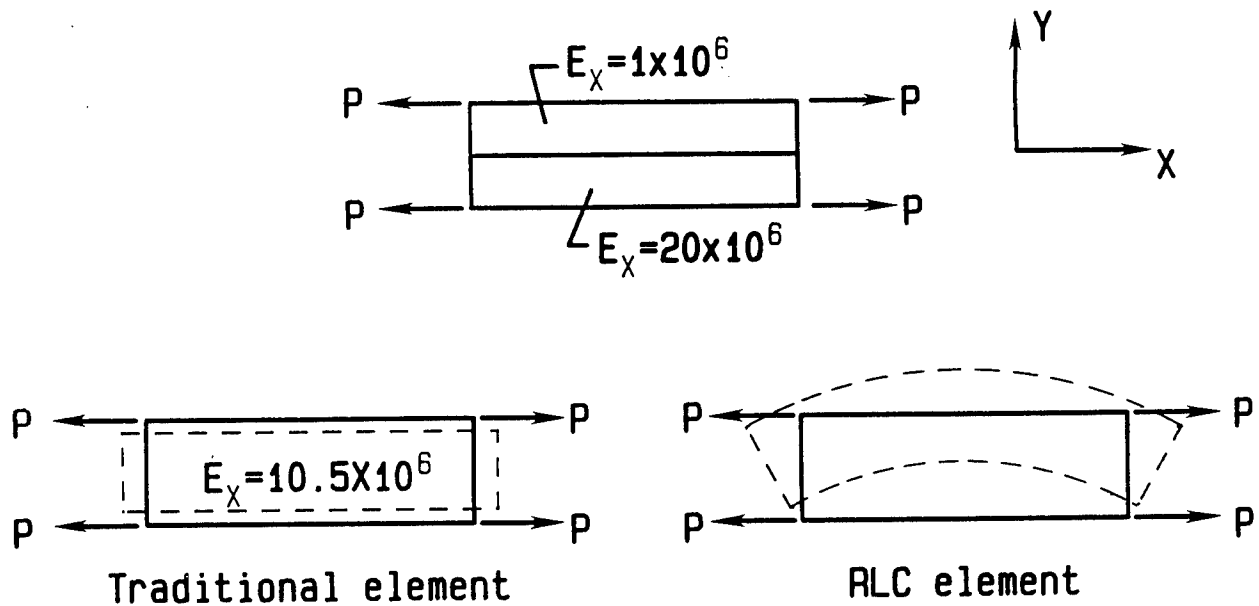
ANALYSIS OF THICK LAMINATES



Mesh refinement dictated by:

- * shape of body
- * strain gradients
- * material property discontinuities

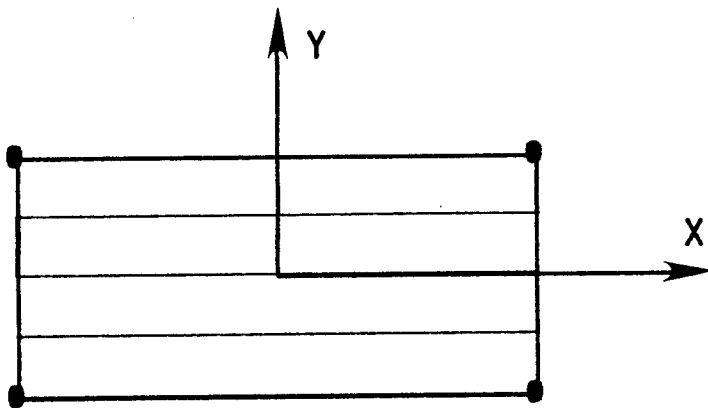
COMPARISON OF TRADITIONAL AND RLC ELEMENT



RECTANGULAR LAMINATED COMPOSITE ELEMENT

- * Plane stress/plane strain
- * Includes stacking sequence effects
 - * Extensional and shear stiffness
 - * Flexural stiffness
 - * Extension-flexure coupling
- * Technique valid for 3-D element

ELEMENT CONFIGURATION



- * Four node rectangle
- * Lamina interfaces parallel to X-axis

STIFFNESS MATRIX

$$K_{mn} = t \int C_{ij} \frac{\partial \epsilon_i}{\partial \Delta_m} \frac{\partial \epsilon_j}{\partial \Delta_n} dA$$

NORMAL STRAINS:

$$u = a + bx + cy + dxy$$

$$v = \bar{a} + \bar{b}x + \bar{c}y + \bar{d}xy$$



$$\epsilon_x = \frac{\partial u}{\partial x} = b + dy$$

$$\epsilon_y = \frac{\partial u}{\partial y} = \bar{c} + \bar{d}x$$

SHEAR STRAIN:

$$u = e + fx + gy$$

$$v = \bar{e} + \bar{f}x + \bar{g}y$$



$$\epsilon_{xy} = \frac{\partial u}{\partial y} + \frac{\partial v}{\partial x} = g + \bar{f} = h$$

STIFFNESS COEFFICIENTS

$$\begin{bmatrix} K_{11} & K_{12} & K_{13} & 0 & 0 \\ K_{21} & K_{22} & K_{23} & 0 & 0 \\ K_{31} & K_{32} & K_{33} & 0 & 0 \\ \text{SYM} & & & K_{44} & 0 \\ & & & & K_{55} \end{bmatrix}$$

$$A_{11} = \sum C_{11}^i (y_{i+1} - y_i)$$

$$A_{12} = \sum C_{12}^i (y_{i+1} - y_i)$$

$$A_{22} = \sum C_{22}^i (y_{i+1} - y_i)$$

$$A_{33} = \sum C_{33}^i (y_{i+1} - y_i)$$

$$B_{11} = 1/2 \sum C_{11}^i (y_{i+1}^2 - y_i^2)$$

$$B_{12} = 1/2 \sum C_{12}^i (y_{i+1}^2 - y_i^2)$$

$$D_{11} = 1/3 \sum C_{11}^i (y_{i+1}^3 - y_i^3)$$

$$K_{11} = 2 l_x t A_{11}$$

$$K_{12} = 2 l_x t B_{11}$$

$$K_{13} = 2 l_x t A_{12}$$

$$K_{22} = 2 l_x t D_{11}$$

$$K_{23} = 2 l_x t B_{12}$$

$$K_{33} = 2 l_x t A_{22}$$

$$K_{44} = 2/3 l_x^3 t A_{22}$$

$$K_{55} = 2 l_x t A_{33}$$

TRANSFORMATION TO NODAL DISPLACEMENTS

GENERALIZED DISPLACEMENTS: $[K] [\Delta] = [F]$

NODAL DISPLACEMENTS: $[\bar{K}] [\delta] = \bar{F}$

WHERE $[\bar{K}] = [T]^T [K] [T]$
 $\bar{F} = [T]^T [F]$

TRANSFORMATION MATRIX: $[\Delta] = [T] [\delta]$

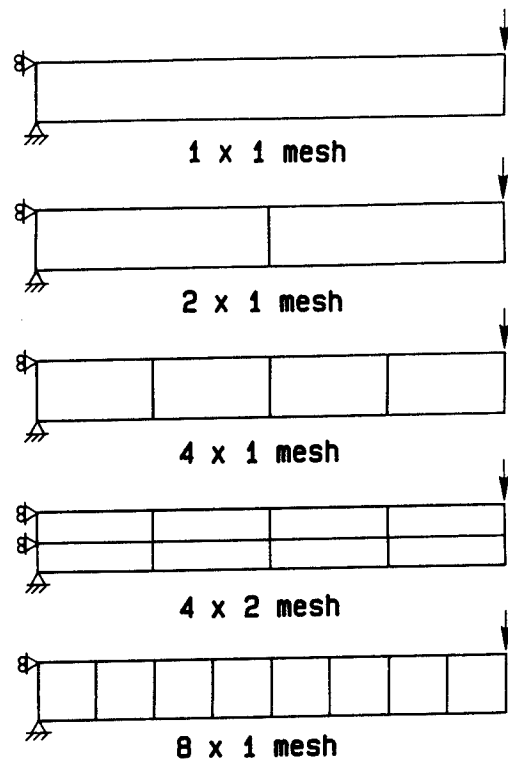
$$\text{BUT } [\Delta] = \begin{bmatrix} \Delta_{\text{NORMAL}} \\ \Delta_{\text{SHEAR}} \end{bmatrix}$$



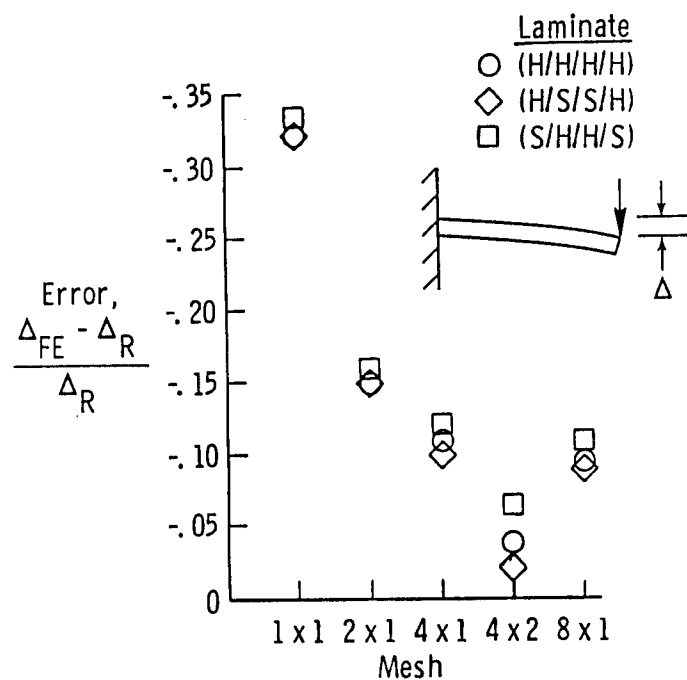
$$[T] = \begin{bmatrix} T_{\text{NORMAL}} \\ T_{\text{SHEAR}} \end{bmatrix}$$

EXAMPLE PROBLEMS

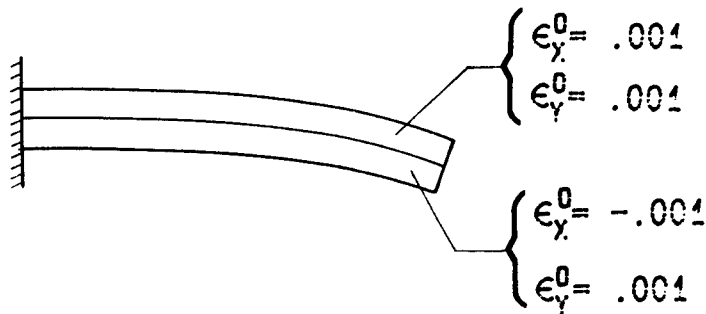
- * MECHANICAL LOAD
- * THERMAL LOAD
- * ISOTROPIC
- * DIFFERENT MODULI OR EXPANSION COEFFICIENTS



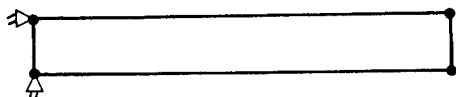
CANTILEVERED BEAM WITH TIP LOAD



UNSYMMETRIC CANTILEVERED BEAM WITH THERMAL LOAD

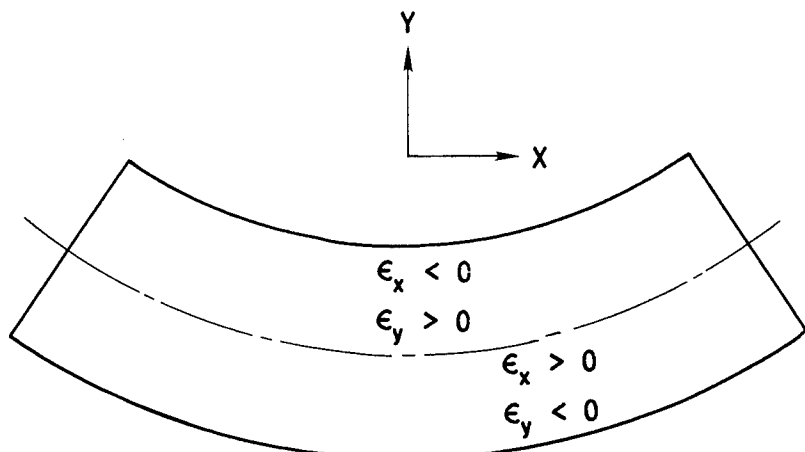


FINITE ELEMENT MODEL



ERROR IN CALCULATED TIP DISPLACEMENT < .1%

BEAM UNDER PURE BENDING



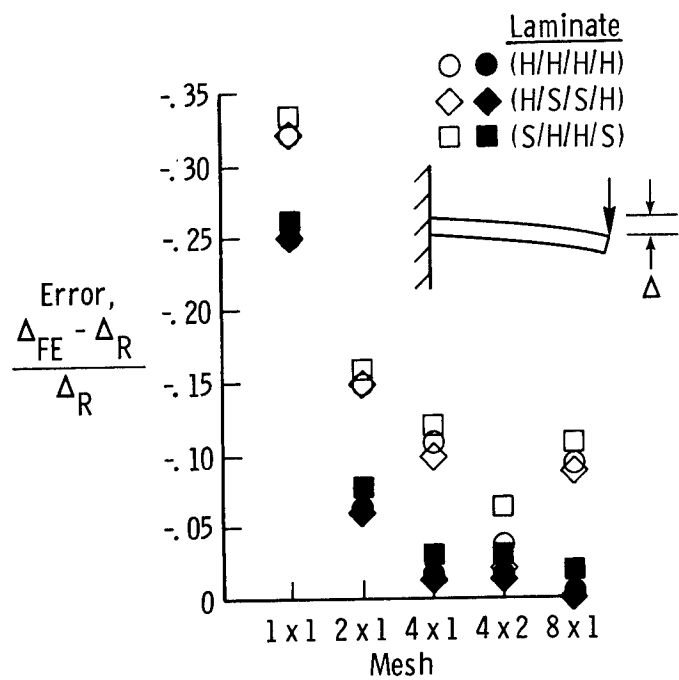
ASSUMED:

$$\begin{aligned}\epsilon_x &= b + dy \\ \epsilon_y &= \bar{c} + \bar{d}x \quad (\text{CONSTANT}) \\ \epsilon_{xy} &= h \quad (\text{ZERO})\end{aligned}$$

THEORETICAL:

$$\begin{aligned}\epsilon_x &= b + dy \\ \epsilon_y &= -\nu(b + dy) \\ \epsilon_{xy} &= \text{ZERO}\end{aligned}$$

CANTILEVERED BEAM WITH TIP LOAD



SUMMARY

- * Need new element to analyse thick laminates
- * Developed Rectangular Laminated Composite element which accounts for stacking sequence effects
- * Performed well in initial tests

FORMULATION OF LAMINATED BEAM AND PLATE ELEMENTS FOR A MICROCOMPUTER

A. Chen and T. Yang

Purdue University

Material not received in time for publication.

See B-1

APPROXIMATE ANALYSIS OF COMPOSITES WITH DAMAGE

G. Sendeckyj

Flight Dynamics Laboratory

Material not received in time for publication.

A Method of Laminate Design

Ippei Susuki

Japan National Aerospace Laboratory

1880 Jindaiji-machi, Chofu, Tokyo 182, Japan

presently

Air Force Wright Aeronautical Laboratories/MLBM

Wright-Patterson Air Force Base, Ohio 45433

abstract

The objective of this research is to develop a design method to translate the strength characteristics of unidirectional composites to that of a multi-directional laminate with maximum strength. Composite laminates have the advantage that their mechanical properties can be tailored through fiber orientations, ply thickness ratios, and stacking sequences. This capability gives a designer an additional degree of flexibility to obtain the desired stiffness or strength.

This work is limited to laminates which are symmetric, and consist of plies with 0, 90, 45, and -45 degree fiber orientations. A method is developed to find the optimal combination of these four ply groups to obtain the maximum strength for a given set of in-plane loadings. The classical laminated plate theory is used in analyzing the stress and strain of each ply. The laminate strength is determined by the first ply failure envelope based on the quadratic failure criterion.

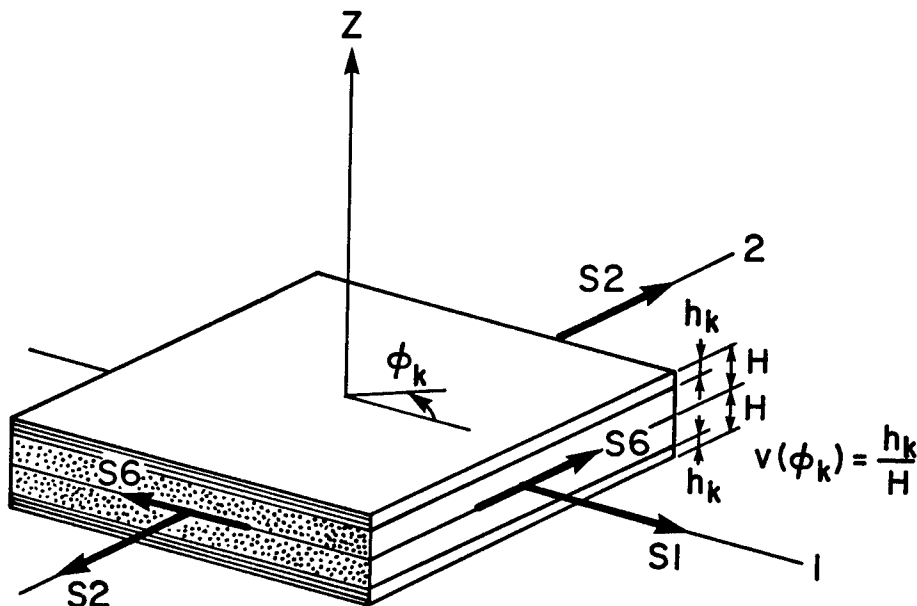
Numerical results using T300/5208 graphite/epoxy composite include:

1. the strength of optimized laminate is about six times as high as that of quasi-isotropic one,
2. the principal stress design is not always the best,
3. theoretical and fractinal ply ratios must be rounded off for practical laminates. The effects of the unit ply thickness and the absolute values of applied loads will be illustrated.
4. the penalty of using balanced laminates under non principal loads (with shears) are also discussed.

User friendly programs on PRIME(by FORTRAN) or EPSON QX-10(by BASIC) for this work are available to interested users upon request.

COORDINATE SYSTEM AND NOTATION OF MULTIDIRECTIONAL LAMINATE

S₁, S₂, S₆: LAMINATE STRESSES
 (SHOWN ARE POSITIVE)
 ϕ_k : PLY ANGLE OF k-TH PLY GROUP
 $v(\phi_k)$: PLY THICKNESS RATIO OF
 k-TH PLY GROUP
H : ONE-HALF OF THE TOTAL THICKNESS
 h_k : ONE-HALF OF k-TH PLY GROUP THICKNESS



$$k = 1, 2, 3, \dots$$

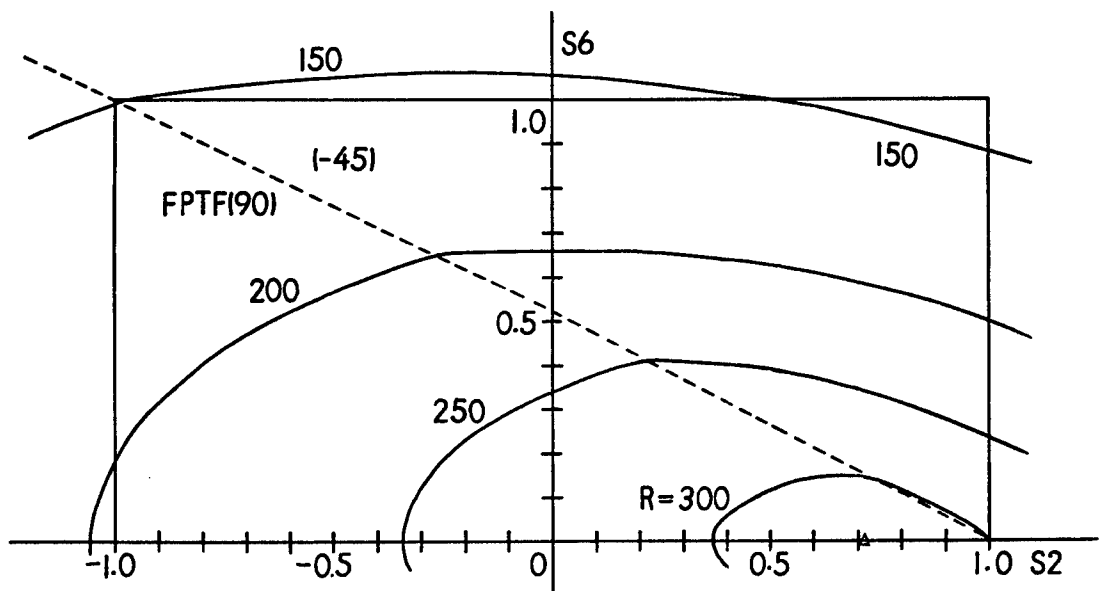
ALUMINUM AND Gr/Ep ELASTIC PROPERTIES

MATERIAL	DENSITY [kg/m ³]	E _x [GPa]	E _y [GPa]	ν_x	E _s [GPa]
Gr/Ep (T300/5208)	1600	181	10.3	0.28	7.17
ALUMINUM (2024-T3)	2771	72	72	0.30	27.7

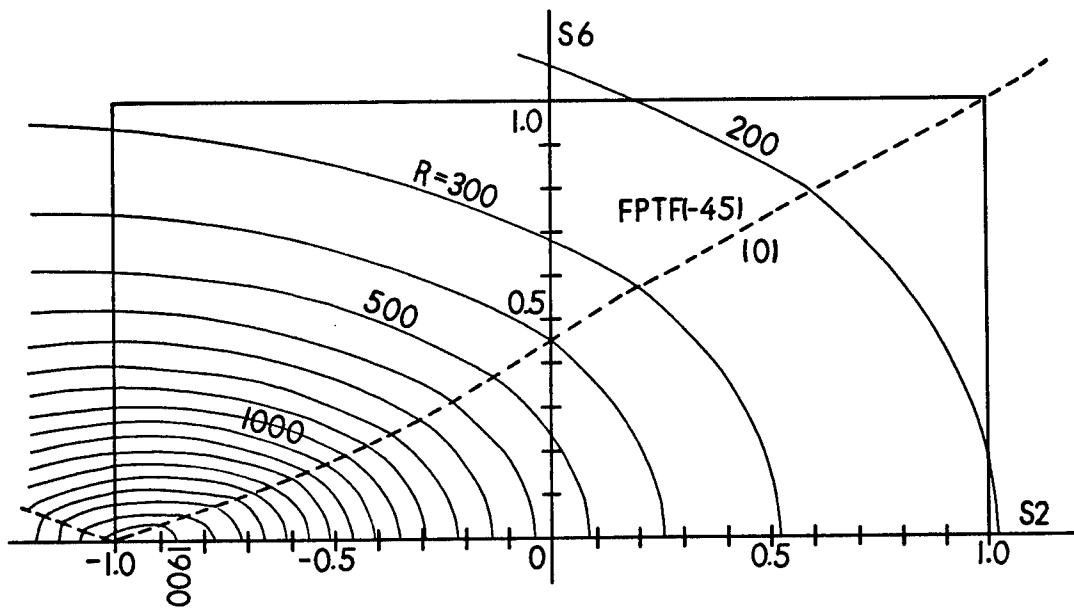
STRENGTH PROPERTIES

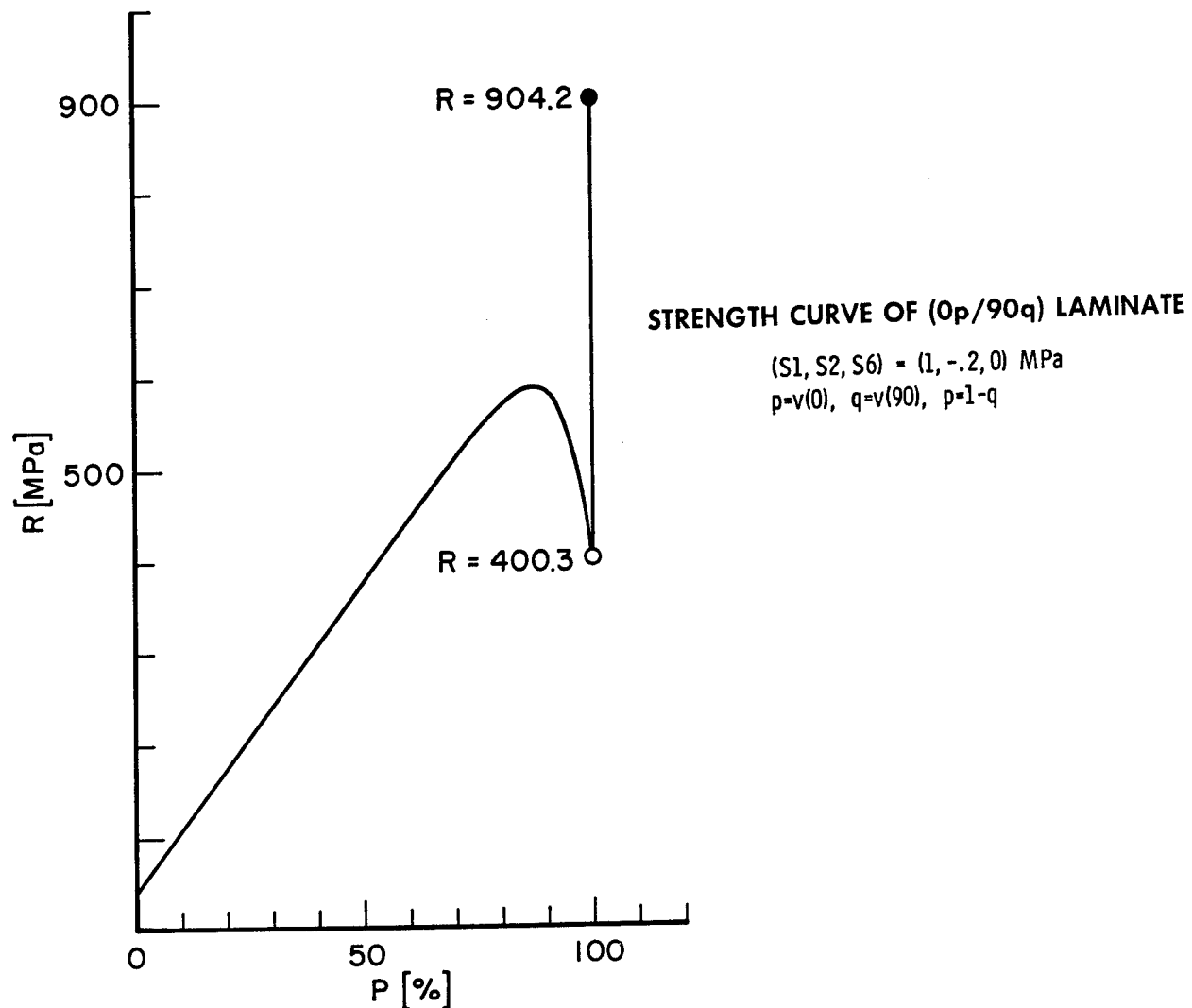
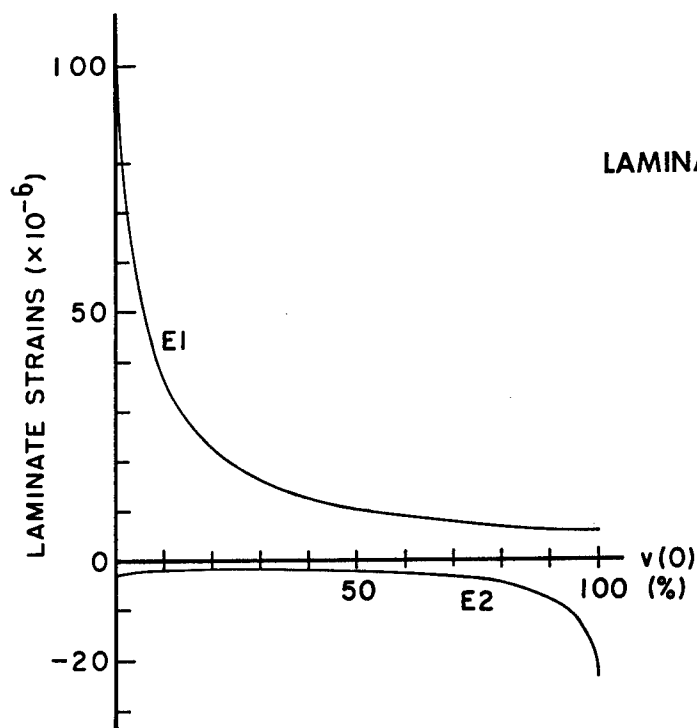
	LONG TENS	LONG COMP	TRANS TENS	TRANS COMP	SHEAR [MPa]
Gr/Ep (T300/5208)	1500	1500	40	246	68
ALUMINUM (2024-T3)	345	345	345	345	199

STRENGTH SURFACE OF
A QUASI-ISOTROPIC LAMINATE IN REGION T ($S_1=1$ MPa)

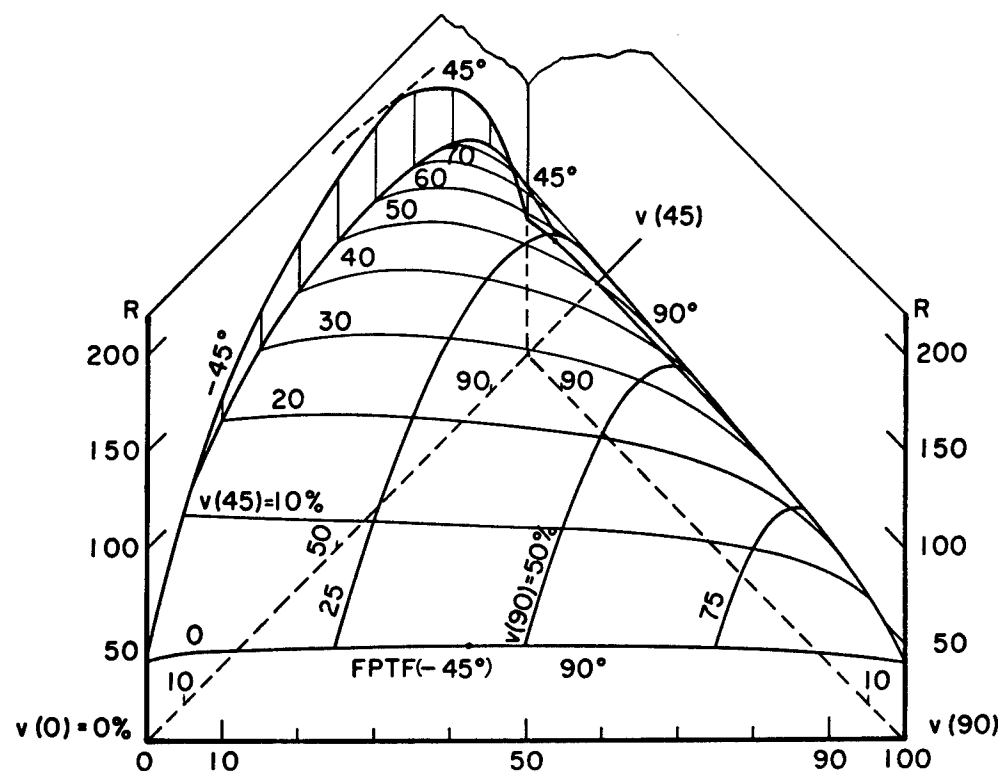


STRENGTH SURFACE OF
A QUASI-ISOTROPIC LAMINATE REGION C ($S_1=-1$ MPa)

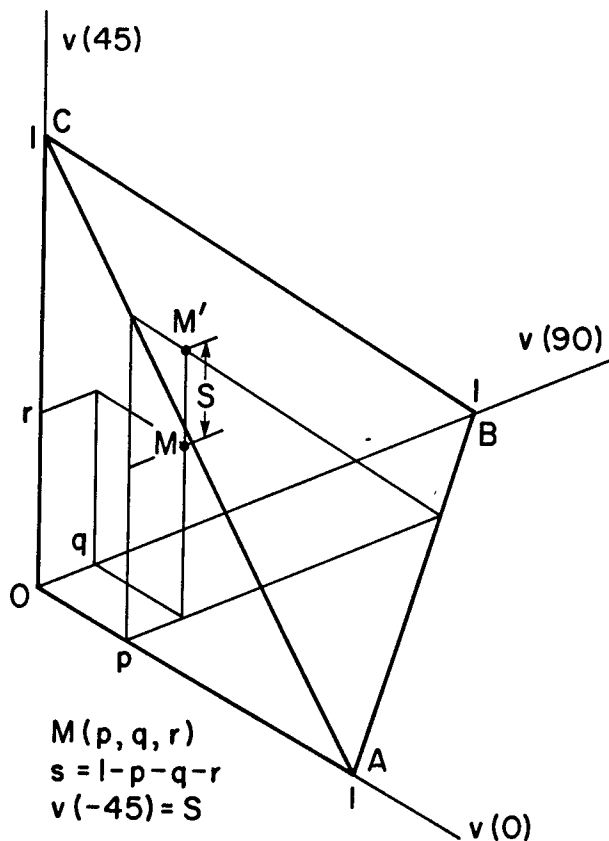




STRENGTH SURFACE OF
 (90q/45r/-45s) LAMINATE UNDER $(S_1, S_2, S_6) = (1, 5, .3)$ MPa



TETRAHEDRON, SCHEMATIC EXPRESSION OF CONSTRAINT ON (0p/90q/45r/-45s) LAMINATE ANALYSIS

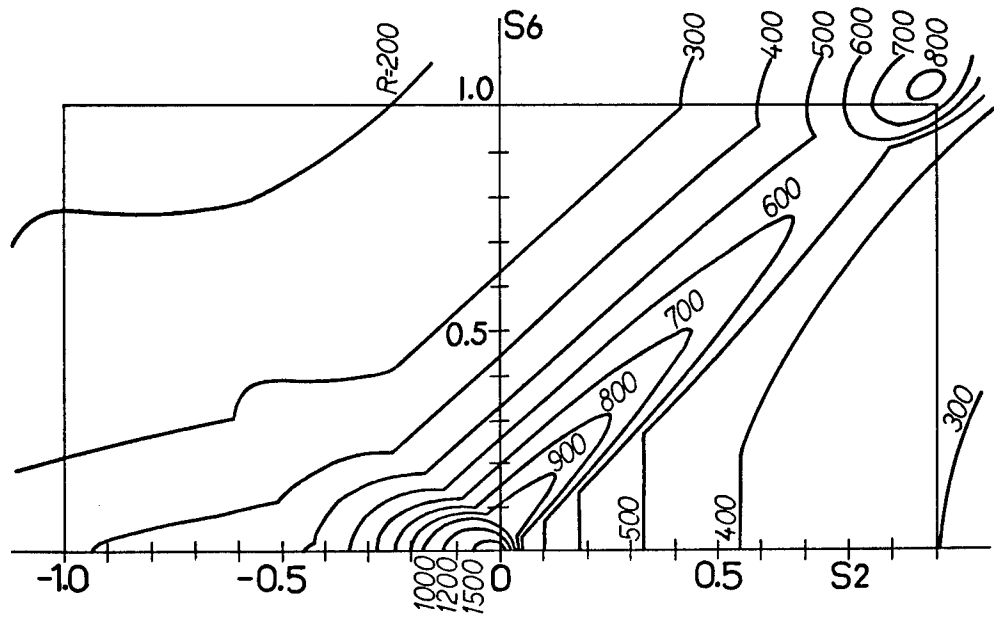


SUBREGION IN TETRAHEDRON CONSTRAINT

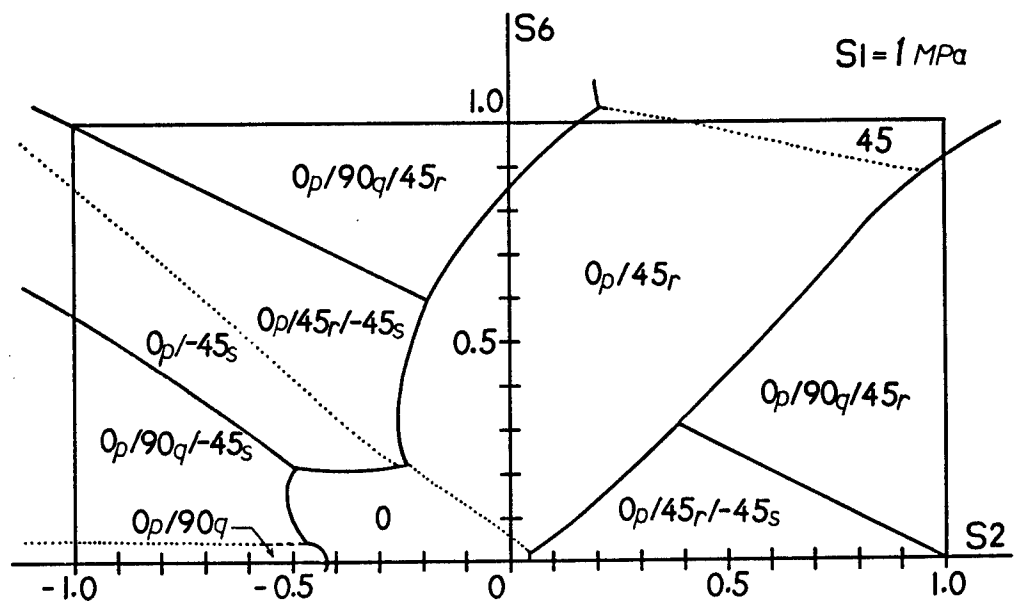
NO.	SUBREGION	PLY THICKNESS RATIO				LAMINATE
		v(0) p	v(90) g	v(45) r	v(-45) s	
0	VERTEX	A	I	0	0	0
1		B	0	I	0	0
2		C	0	0	I	0
3		O	0	0	0	I
4	EDGE	AB	I-x	x	0	0
5		AC	I-x	0	x	0
6		OA	I-x	0	0	x
7		BC	0	I-x	x	0
8		OB	0	I-x	0	x
9		OC	0	0	I-x	x
10		OBC	0	I-x-y	x	y
11	SURFACE	OPC	I-x-y	0	x	y
12		OAB	I-x-y	x	0	y
13		ABC	I-x-y	x	y	0
14	BODY	O-ABC	I-x-y-z	x	y	z
						[0 _p /90 _q /45 _r /-45 _s]

$$0 < x, y, z < 1$$

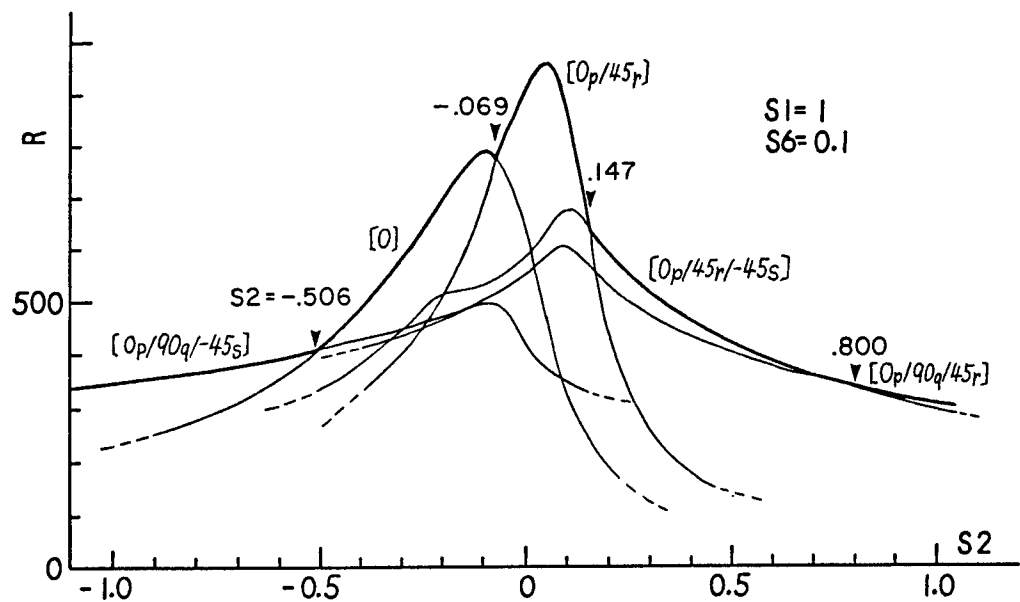
STRENGTH SURFACE OF
OPTIMIZED LAMINATE IN REGION T ($S_1=1$ MPa)



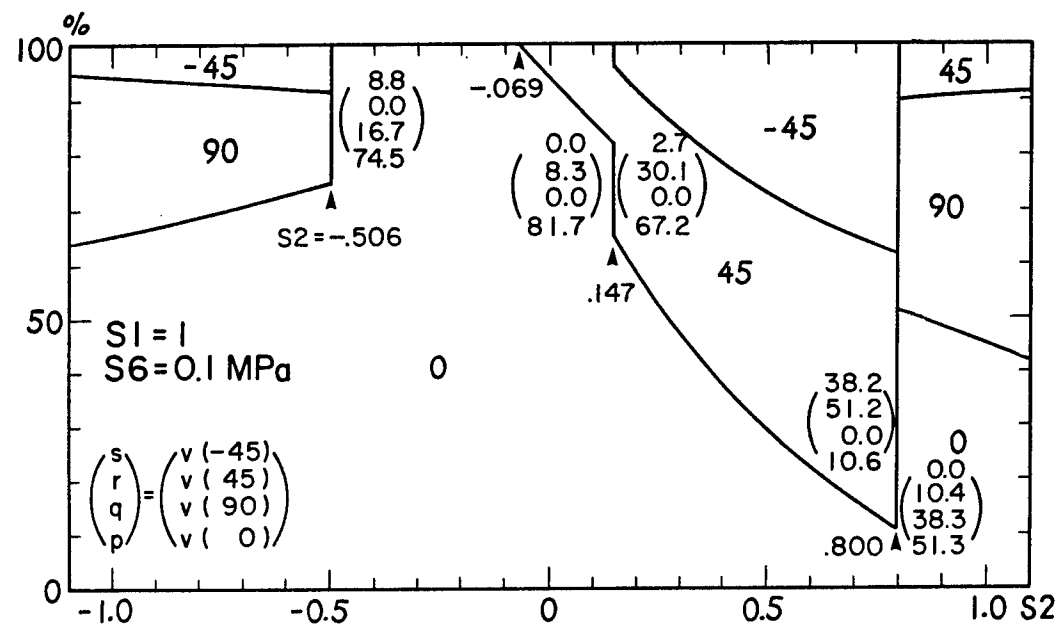
PLY GROUPS OF OPTIMIZED LAMINATE IN REGION T ($S_1=1$ MPa)



**STRENGTH VARIATION IN
OPTIMIZED LAMINATE AT $S_6=1$ MPa IN REGION T**



PLY THICKNESS RATIOS OF OPTIMIZED LAMINATE AT $S_6=1$ MPa IN T



Uniaxial Compression

			N1 N2 N6 (MN/m) :			-1.000	0.000	0.000
			Material :T300/5208 Graphite/Epoxy with f=-0.5					
No.	NTPY	H(mm)	NHPY	C	0 90 45-45	FPTF	Rmin	R(0)R(90)R(45)R(-45)
1	6	0.75	3	(3 0 0 0)	0	1.125	1.125 0.000 0.000 0.000
2	6	0.75	3	(2 1 0 0)	0	1.060	1.060 2.186 0.000 0.000
3	8	1.00	4	(3 1 0 0)	0	1.552	1.552 3.220 0.000 0.000
4	8	1.00	4	(4 0 0 0)	0	1.500	1.500 0.000 0.000 0.000
5	8	1.00	4	(2 2 0 0)	0	1.108	1.108 2.269 0.000 0.000
6	10	1.25	5	(4 1 0 0)	0	2.031	2.031 4.238 0.000 0.000
7	10	1.25	5	(5 0 0 0)	0	1.875	1.875 0.000 0.000 0.000
8	10	1.25	5	(3 2 0 0)	0	1.618	1.618 3.326 0.000 0.000
9	10	1.25	5	(3 1 0 1)	0	1.339	1.339 2.680 0.000 1.871
10	10	1.25	5	(3 1 1 0)	0	1.339	1.339 2.680 1.871 0.000

next:31

* N1(MN/m)=-10

Uni-axial Compression

			N1 N2 N6 (MN/m) :			-10.000	0.000	0.000
			Material :T300/5208 Graphite/Epoxy with f=-0.5					
No.	NTPY	H(mm)	NHPY	C	0 90 45-45	FPTF	Rmin	R(0)R(90)R(45)R(-45)
1	48	6.00	24	(22 2 0 0)	0	1.032	1.032 2.210 0.000 0.000
2	48	6.00	24	(21 3 0 0)	0	1.023	1.023 2.164 0.000 0.000
3	48	6.00	24	(23 1 0 0)	0	1.008	1.008 2.207 0.000 0.000
4	50	6.25	25	(23 2 0 0)	0	1.074	1.074 2.304 0.000 0.000
5	50	6.25	25	(22 3 0 0)	0	1.068	1.068 2.262 0.000 0.000
6	50	6.25	25	(24 1 0 0)	0	1.048	1.048 2.296 0.000 0.000
7	50	6.25	25	(21 4 0 0)	0	1.046	1.046 2.196 0.000 0.000
8	50	6.25	25	(20 5 0 0)	0	1.015	1.015 2.119 0.000 0.000
9	52	6.50	26	(24 2 0 0)	0	1.117	1.117 2.398 0.000 0.000
10	52	6.50	26	(23 3 0 0)	0	1.113	1.113 2.359 0.000 0.000

next:

Biaxial Tension

			N1 N2 N6 (MN/m) :			2.000	0.400	0.000
			Material :T300/5208 Graphite/Epoxy with f=-0.5					
No.	NTPY	H(mm)	NHPY	C	0 90 45-45	FPTF	Rmin	R(0)R(90)R(45)R(-45)
1	28	3.50	14	(8 0 3 3)	45	1.025	1.339 0.000 1.025 1.025
2	30	3.75	15	(9 0 3 3)	45	1.101	1.382 0.000 1.101 1.101
3	30	3.75	15	(8 0 3 4)	-45	1.039	1.465 0.000 1.111 1.039
4	30	3.75	15	(8 0 4 3)	45	1.039	1.465 0.000 1.039 1.111
5	30	3.75	15	(7 0 4 4)	45	1.024	1.523 0.000 1.024 1.024
6	30	3.75	15	(10 0 2 3)	-45	1.005	1.191 0.000 1.115 1.005
7	30	3.75	15	(10 0 3 2)	45	1.005	1.191 0.000 1.005 1.115
8	30	3.75	15	(11 0 2 2)	-45	1.002	1.045 0.000 1.002 1.002
9	32	4.00	16	(10 0 3 3)	45	1.171	1.417 0.000 1.171 1.171
10	32	4.00	16	(8 0 4 4)	45	1.127	1.615 0.000 1.127 1.127
11	32	4.00	16	(9 0 3 4)	-45	1.121	1.522 0.000 1.201 1.121
12	32	4.00	16	(9 0 4 3)	45	1.121	1.522 0.000 1.121 1.201
13	32	4.00	16	(11 0 3 2)	45	1.054	1.215 0.000 1.054 1.169
14	32	4.00	16	(11 0 2 3)	-45	1.054	1.215 0.000 1.169 1.054
15	32	4.00	16	(8 0 3 5)	-45	1.047	1.546 0.000 1.171 1.047
16	32	4.00	16	(8 0 5 3)	45	1.047	1.546 0.000 1.047 1.171
17	32	4.00	16	(12 0 2 2)	45	1.042	1.065 0.000 1.042 1.042
18	32	4.00	16	(7 0 4 5)	-45	1.031	1.606 0.000 1.077 1.031
19	32	4.00	16	(7 0 5 4)	45	1.031	1.606 0.000 1.031 1.077
20	32	4.00	16	(10 0 2 4)	-45	1.028	1.301 0.000 1.221 1.028
21	32	4.00	16	(10 0 4 2)	45	1.028	1.301 0.000 1.028 1.221
22	32	4.00	16	(11 1 2 2)	90	1.028	1.315 1.028 1.143 1.143
23	32	4.00	16	(12 2 1 1)	90	1.027	1.253 1.027 1.122 1.122
24	32	4.00	16	(13 3 0 0)	90	1.026	1.211 1.026 0.000 0.000
25	32	4.00	16	(13 1 1 1)	90	1.017	1.051 1.017 1.033 1.033
26	32	4.00	16	(14 2 0 0)	90	1.015	1.042 1.015 0.000 0.000

Design w/wo Shear

(1) T300/5208

[1] Stress resultant N1 N2 N6 (MN/m) : 1.000 0.100 0.100
 Material :T300/5208 Graphite/Epoxy with f=-0.5
 No. NTPY H(mm) NHPY [0 90 45-45] FPTF Rmin R(0)R(90)R(45)R(-45)

1	10	1.25	5 (4 0 1 0)	45	1.033	1.243	0.000	1.033	0.000
2	12	1.50	6 (5 0 1 0)	45	1.270	1.387	0.000	1.270	0.000
3	12	1.50	6 (4 0 2 0)	45	1.032	1.574	0.000	1.032	0.000
4	14	1.75	7 (6 0 1 0)	45	1.490	1.503	0.000	1.490	0.000
5	14	1.75	7 (5 0 2 0)	45	1.297	1.863	0.000	1.297	0.000
6	14	1.75	7 (4 0 3 0)	45	1.020	1.672	0.000	1.020	0.000
7	16	2.00	8 (7 0 1 0)	0	1.605	1.605	0.000	1.694	0.000
8	16	2.00	8 (6 0 2 0)	45	1.560	2.106	0.000	1.560	0.000
9	16	2.00	8 (5 0 3 0)	45	1.283	2.033	0.000	1.283	0.000
10	16	2.00	8 (5 0 2 1)	-45	1.165	2.027	0.000	1.432	1.165

[2] Stress resultant N1 N2 N6 (MN/m) : 1.011 0.089 0.000
 Material :T300/5208 Graphite/Epoxy with f=-0.5
 No. NTPY H(mm) NHPY [0 90 45-45] FPTF Rmin R(0)R(90)R(45)R(-45)

1	14	1.75	7 (5 0 1 1)	45	1.208	1.823	0.000	1.208	1.208
2	14	1.75	7 (6 1 0 0)	90	1.006	1.454	1.006	0.000	0.000
3	16	2.00	8 (6 0 1 1)	45	1.406	2.034	0.000	1.406	1.406
4	16	2.00	8 (5 0 1 2)	-45	1.202	2.004	0.000	1.331	1.202
5	16	2.00	8 (5 0 2 1)	45	1.202	2.004	0.000	1.202	1.331
6	16	2.00	8 (7 1 0 0)	90	1.163	1.637	1.163	0.000	0.000
7	16	2.00	8 (4 0 2 2)	45	1.094	1.894	0.000	1.094	1.094
8	16	2.00	8 (6 2 0 0)	90	1.041	1.657	1.041	0.000	0.000
9	16	2.00	8 (6 1 0 1)	90	1.027	1.549	1.027	0.000	1.075
10	16	2.00	8 (6 1 1 0)	90	1.027	1.549	1.027	1.075	0.000

(2) Kevlar49/Epoxy

[10] Stress resultant N1 N2 N6 (MN/m) : 1.000 0.100 0.100
 Material :Kevlar 49/Epoxy Aramid/Epoxy f=-0.5
 No. NTPY H(mm) NHPY [0 90 45-45] FPTF Rmin R(0)R(90)R(45)R(-45)

1	12	1.50	6 (5 0 1 0)	45	1.204	1.460	0.000	1.204	0.000
2	14	1.75	7 (6 0 1 0)	45	1.503	1.510	0.000	1.503	0.000
3	16	2.00	8 (7 0 1 0)	0	1.529	1.529	0.000	1.776	0.000
4	16	2.00	8 (6 0 2 0)	45	1.154	2.279	0.000	1.154	0.000
5	18	2.25	9 (8 0 1 0)	0	1.536	1.536	0.000	2.024	0.000
6	18	2.25	9 (7 0 2 0)	45	1.458	2.516	0.000	1.458	0.000
7	20	2.50	10 (8 0 2 0)	45	1.775	2.697	0.000	1.775	0.000
8	20	2.50	10 (9 0 1 0)	0	1.540	1.540	0.000	2.250	0.000
9	20	2.50	10 (7 0 3 0)	45	1.177	2.810	0.000	1.177	0.000
10	22	2.75	11 (9 0 2 0)	45	2.094	2.828	0.000	2.094	0.000

[11] Stress resultant N1 N2 N6 (MN/m) : 1.011 0.089 0.000
 Material :Kevlar 49/Epoxy Aramid/Epoxy f=-0.5
 No. NTPY H(mm) NHPY [0 90 45-45] FPTF Rmin R(0)R(90)R(45)R(-45)

1	26	3.25	13 (9 0 2 2)	45	1.060	3.551	0.000	1.060	1.060
2	28	3.50	14 (10 0 2 2)	45	1.138	3.847	0.000	1.138	1.138
3	28	3.50	14 (8 0 3 3)	45	1.101	3.193	0.000	1.101	1.101
4	28	3.50	14 (12 0 1 1)	45	1.022	2.468	0.000	1.022	1.022
5	30	3.75	15 (11 0 2 2)	45	1.213	4.096	0.000	1.213	1.213
6	30	3.75	15 (9 0 3 3)	45	1.199	3.620	0.000	1.199	1.199
7	30	3.75	15 (13 0 1 1)	45	1.081	2.479	0.000	1.081	1.081
8	30	3.75	15 (7 0 4 4)	45	1.072	2.694	0.000	1.072	1.073
9	30	3.75	15 (10 0 2 3)	-45	1.058	3.988	0.000	1.397	1.058
10	30	3.75	15 (10 0 3 2)	45	1.058	3.988	0.000	1.058	1.397

MECHANICS OF COMPRESSION FAILURE IN FIBER REINFORCED COMPOSITES

S. Wang

University of Illinois

Material not received in time for publication.

SUPPRESSION OF DELAMINATION IN COMPOSITE LAMINATES SUBJECTED TO IMPACT LOADING

C. T. Sun

School of Aeronautics and Astronautics
Purdue University
West Lafayette, Indiana 47907

ABSTRACT

Two major failure modes are predominant in composite laminates subjected to low velocity impact, i.e., matrix cracks and delamination [1]. Delamination, in particular, may cause a great reduction in compressive strength and, thus, suppression of delamination is highly desirable.

Analysis results indicate that delamination is induced by matrix cracks. Two types of matrix cracks are induced by transverse shear stresses and bending stresses. Bending cracks usually occur in the bottom layer where bending stresses are the greatest, while transverse shear cracks occur more often in the interior layers. Delamination can result from branching of both bending cracks and transverse shear cracks. In thin laminates it is not produced by reflection of waves propagating through the thickness of the laminate.

Two methods of delamination suppression are investigated: adding through-the-thickness reinforcements by stitching, and adding tough adhesive layers along interfaces of the laminate. Experimental results indicate that stitching can reduce the spreading of delamination cracks but cannot prevent initiation of delamination. On the other hand, the use of adhesive layers proves to be quite effective in suppressing delamination.

Thin structural adhesives were placed along the interfaces of a composite laminate subjected to impact loading. The base line specimen was AS4/3501-6 graphite/epoxy [0^o/90^o/0^o] laminate. One group of specimens contained layers of 5 mil thick adhesive film (FM1000 by American Cyanamid) between the 0^o- and 90^o-plies. Impacted beam specimens were sectioned transversely and longitudinally through the impact site and were examined using an optical electron microscope and then photographed. From these photographs, matrix cracks and delamination size were measured. The X-ray technique was also used to map the delamination area.

When compared, the base line laminate and the one with adhesive layers exhibited significant differences in damage mode. For instance, the threshold velocity at which damage (matrix cracking or delamination) occurred, was found to be much lower for the laminate with no adhesives. It was found that a delamination crack could not be initiated in the laminate with adhesives until the impact velocity reached 26 m/sec, while under a 13 m/sec impact, the laminate without adhesives began to suffer delamination.

Transverse shear crack in the upper lamina was also noted to be affected by the presence of adhesive layers. For example, at 15 m/sec transverse shear cracks appeared in the upper lamina in the specimen without adhesives, while no transverse cracks emerged in the upper lamina in the beam with adhesives at velocities below 26 m/sec. There was indication that delamination could be caused by transverse cracks.

The adhesive layers in the laminate appeared to have affected the size of indentation during impact. As a result, the distribution of contact pressure was also affected. Experiments were conducted, and the relations between the contact area and impact velocity for laminates with adhesives and without adhesives were obtained. The results showed that adhesive layers tended to enlarge the contact area and, as a result, spread out the contact pressure. The distribution of the contact pressure was found to significantly affect the transverse shear stress distribution through the thickness. This result was used successfully to interpret the difference in transverse shear crack patterns in the two types of laminates due to impact loading.

The effect of adhesive layers on transverse shear stress distribution was studied by using 2-D finite elements. The results show that the adhesive layer can diffuse shear stress concentration in the top layer (impacted side) resulting in a significant reduction in transverse shear cracks. Effects of adhesive layer locations were also investigated.

ACKNOWLEDGMENT

This work was supported by ONR Contract N00014-84-K-0554.
Dr. Yapa Rajapakse is Technical Monitor.

REFERENCES

1. S. P. Joshi and C. T. Sun, "Impact Induced Fracture in a Laminated Composite," Journal of Composite Materials, Vol. 19, No. 1, 1985, pp. 51-66.

SUPPRESSION OF DELAMINATION IN COMPOSITE LAMINATES SUBJECTED TO IMPACT LOADING

OBJECTIVE

C. T. SUN

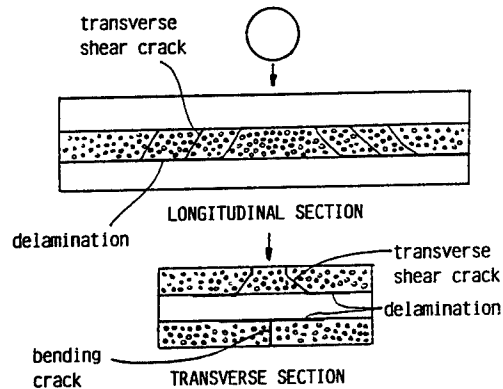
TO INVESTIGATE THE EFFECTIVENESS IN
USING STITCHING AND ADHESIVE LAYERS
FOR SUPPRESSION OF DELAMINATION

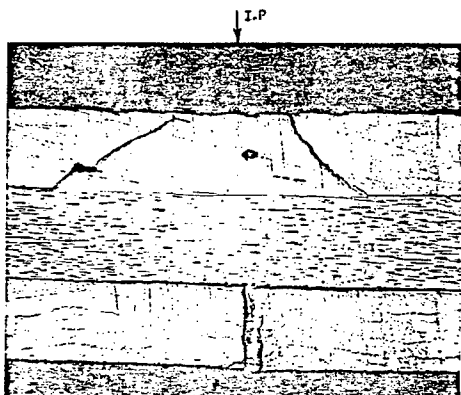
School of Aeronautics and Astronautics
Purdue University
West Lafayette, Indiana 47907

Sponsored by ONR
Technical Monitor: Dr. Y. Rajapakse

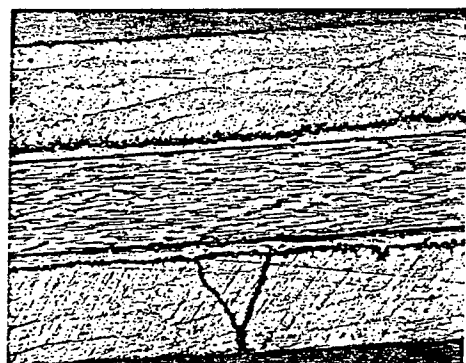
APPROACH

- IMPACT $[0_5/90_5/0_5]$ LAMINATES WITH
STITCHING AND ADHESIVE LAYERS
- DETERMINE CONTACT AREAS
- USE PHOTOMICROGRAPHS TO OBSERVE
IMPACT DAMAGE
- USE 2-D FINITE ELEMENTS TO PERFORM
DYNAMIC STRESS ANALYSIS TO INTERPRET
EXPERIMENTAL RESULTS



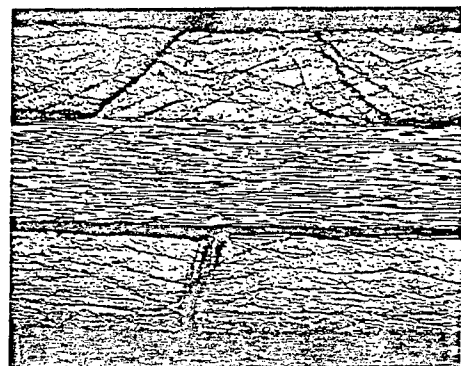


(a) [0₅/90₅/0₅] laminate without adhesives



(b) [0₅/A/90₅/A/0₅]

Transverse cross sections of laminates after impact
of a 1/2" steel ball at velocity 21 m/s



(a) [0₅/90₅/0₅] laminate without adhesives

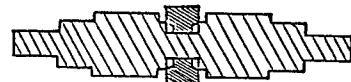


(b) [0₅/A/90₅/A/0₅] laminate with adhesives

Transverse cross sections of laminates after impact
of a 1/2" steel ball at velocity about 26 m/s

○ UPPER INTERFACE DELAMINATION

○ LOWER INTERFACE DELAMINATION

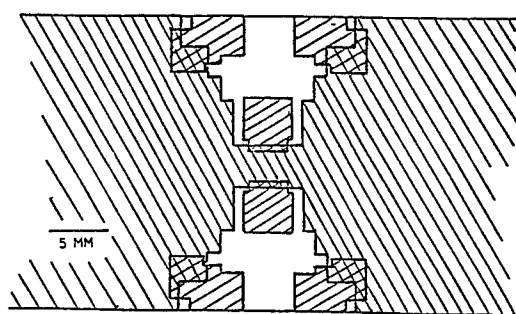


IMPACT VELOCITY 16 m/sec

Delamination zones

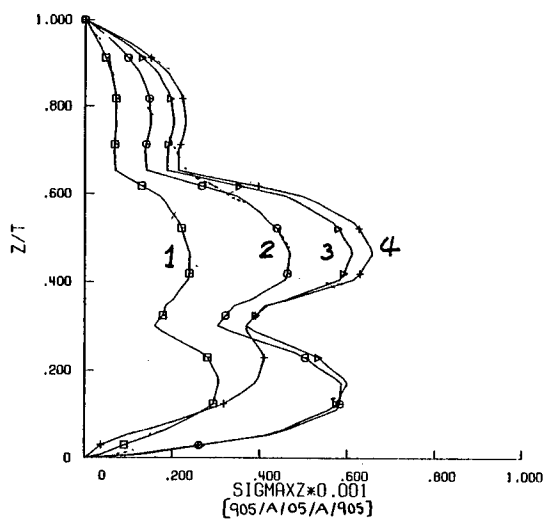
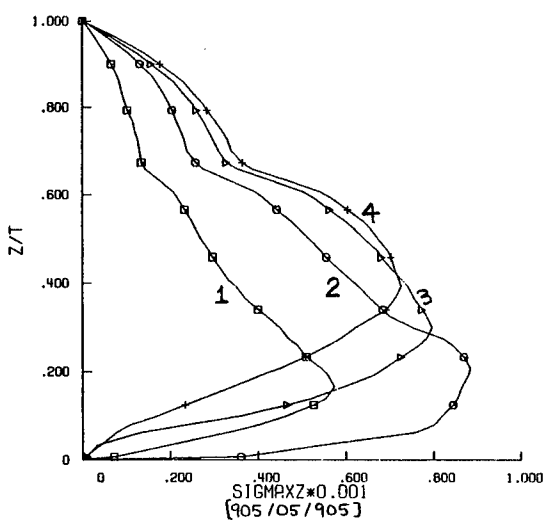
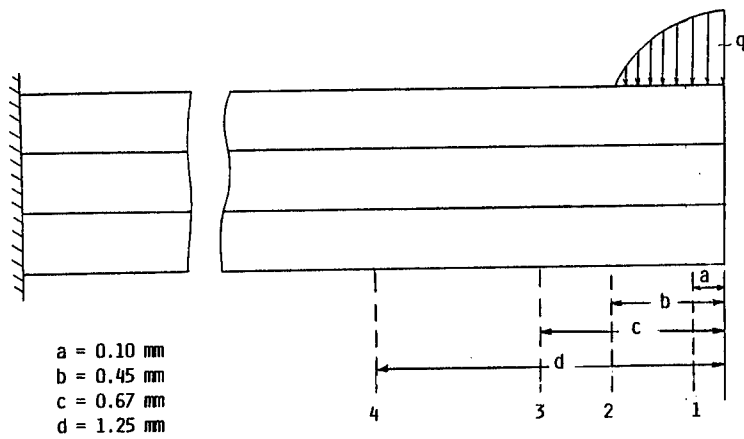
○ UPPER INTERFACE DELAMINATION

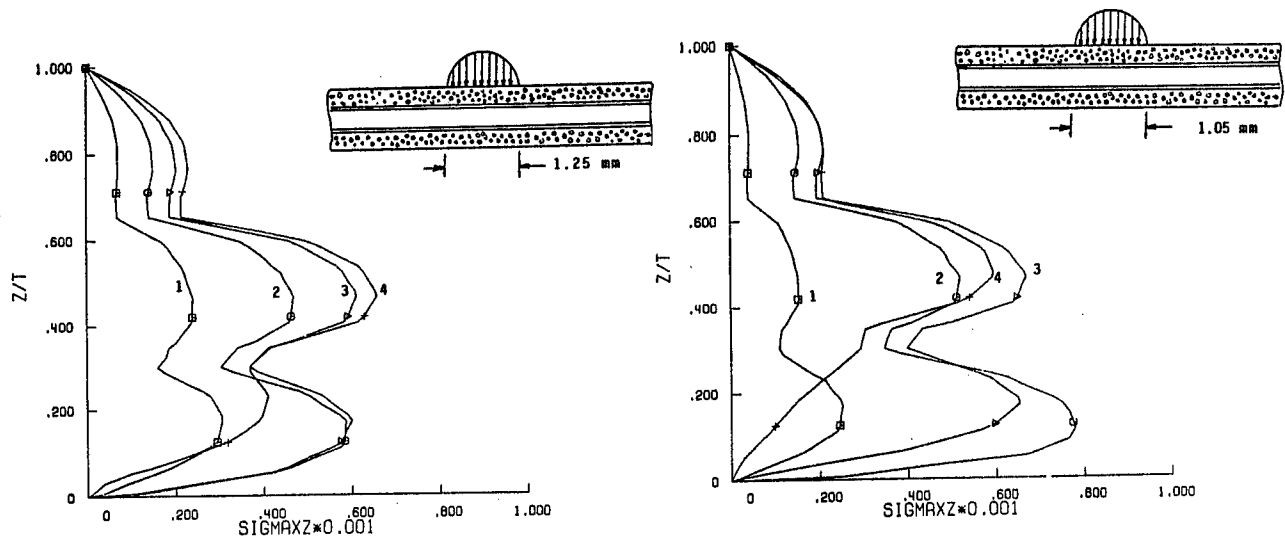
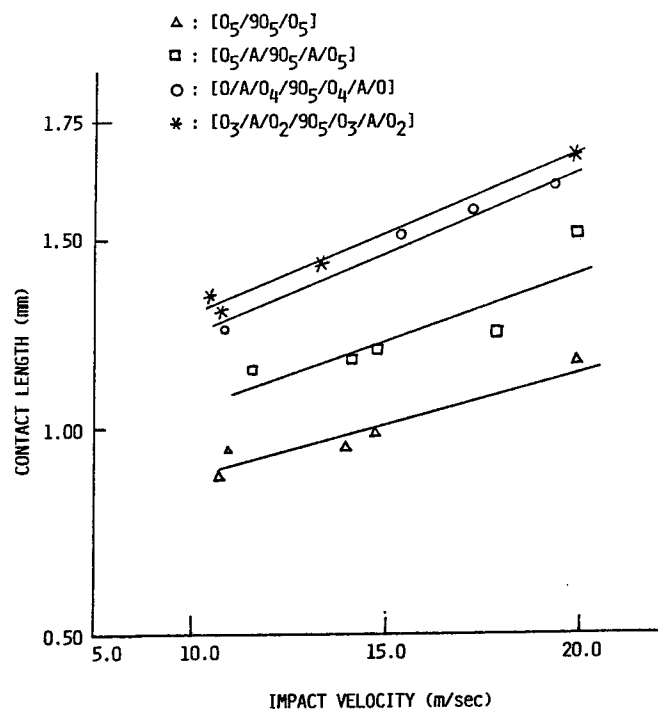
○ LOWER INTERFACE DELAMINATION

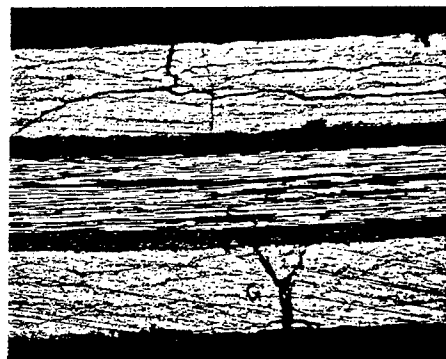


IMPACT VELOCITY 23 m/sec

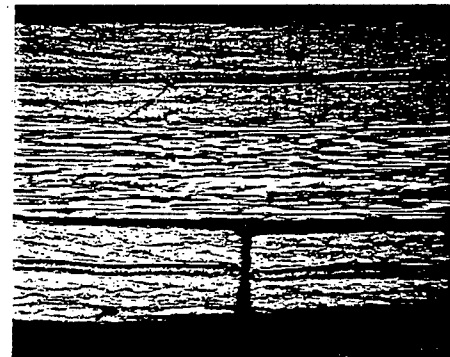
Delamination zones



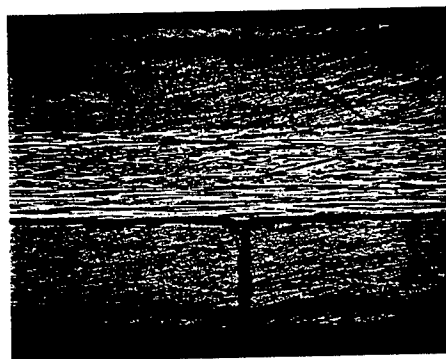




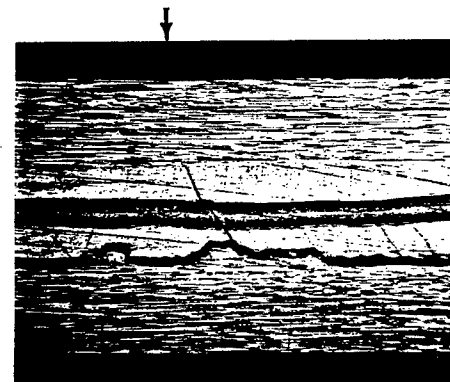
impact velocity 34 m/sec
delamination in 0_5 -layer
fiber breakage



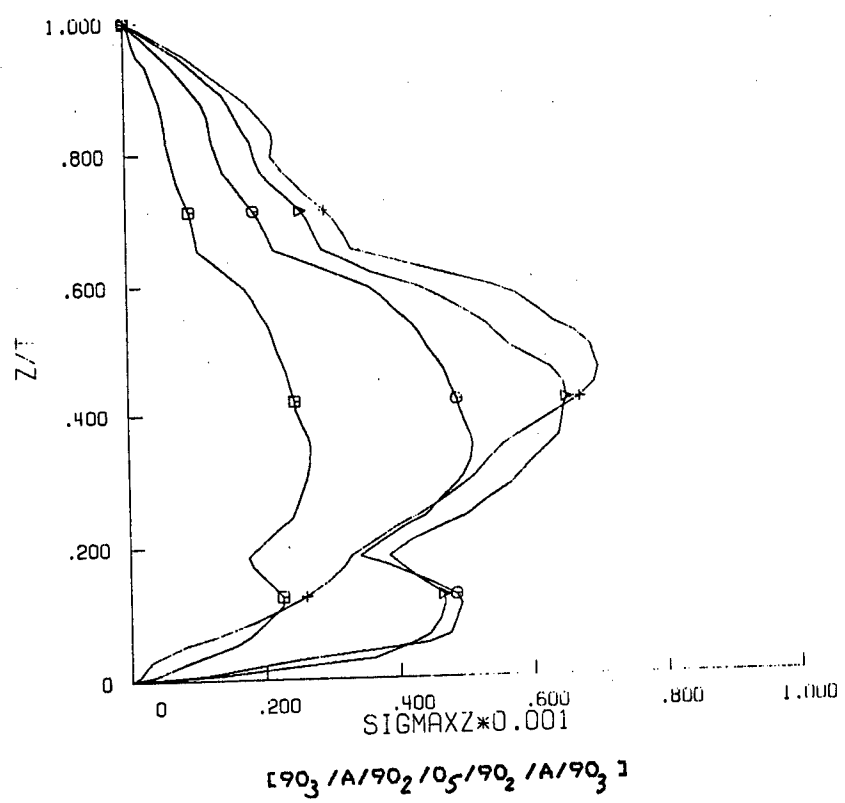
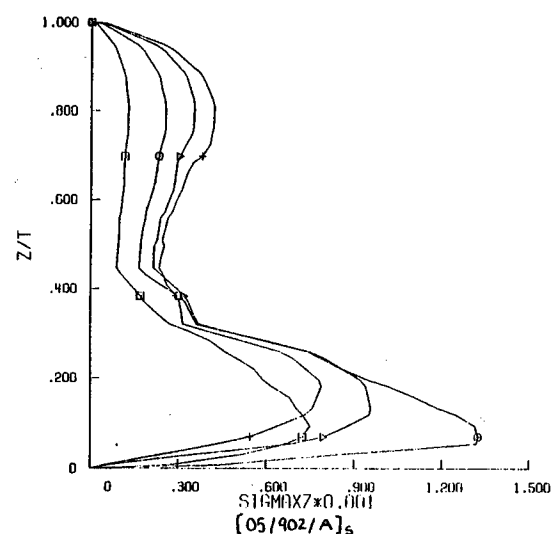
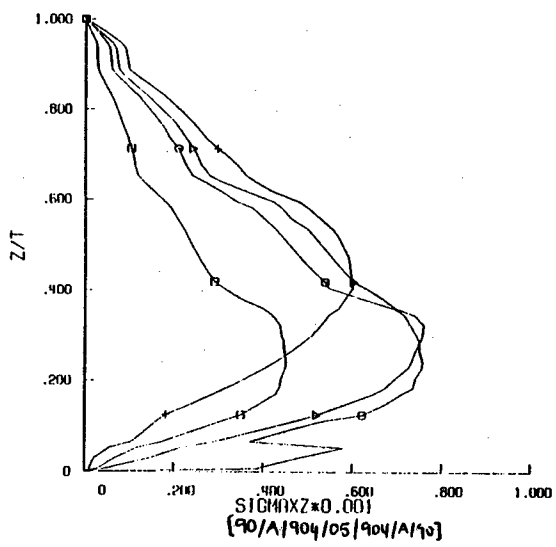
impact velocity 14.6 m/sec
adhesive layers in 0_5 layer

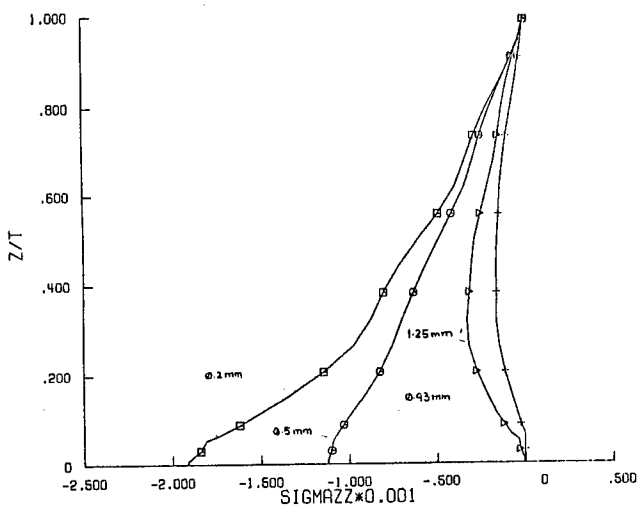


impact velocity 14 m/sec
adhesive layer near top
and bottom surface



impact velocity 14.6 m/sec
adhesive layer at the
middle surface





CONCLUSIONS

- STITCHING CAN REDUCE DELAMINATION SIZE BUT CANNOT SUPPRESS INITIATION.
- ADHESIVE LAYERS WHEN PLACED AT INTERFACES ARE EFFECTIVE IN SUPPRESSING DELAMINATION.
- ADHESIVE LAYERS CAN REDUCE TRANSVERSE SHEAR CRACKS.
- ADHESIVE LAYERS CANNOT STOP BENDING CRACKS.

THERMOVISCOELASTIC PROPERTIES OF UNIDIRECTIONAL FIBER COMPOSITES

Z. Hashin and E. A. Humphreys

Materials Sciences Corporation
Gwynedd Plaza II
Bethlehem Pike
Spring House, Pennsylvania 19477

ABSTRACT

Structural materials in space are subjected to severe thermal cycling as the structure moves between full sunlight and the shadow of the earth. The range of temperatures experienced can be as large as 116°K to 589°K. For polymeric matrix fiber composites this produces creep deformations and relaxation of stress which must be accurately assessed. The purpose of this study is to (a) provide analytical methods to determine the thermoviscoelastic (TVE) properties of graphite/polymer unidirectional fiber composite (UFC), (b) to apply this information to the assessment of composite structural response.

TVE characterization of polymeric matrix materials is not a simple matter and various schemes have been devised in addressing this problem. In this study we have adopted the simplest representation which can adequately characterize the response of a TVE polymer. The representation used retains the temperature dependence of the initial elastic modulus while the time dependent response is governed by a temperature dependent time shift function.

It will be recalled that for isothermal viscoelasticity there is a correspondence principle which directly relates effective viscoelastic and elastic properties for any model of a composite materials [1,2] but no such correspondence exists for a composite with a TVE constituent. It therefore becomes necessary to resort to direct analysis of a model. We have employed two models of a UFC - the composite cylinder assemblage (CCA) model which is suitable for axisymmetric states, including free thermal expansion and for axial shear, and the hexagonal array model for the case of transverse shear. It may be shown that any average stress or strain state can be decomposed into axisymmetric part, transverse shear and axial shear. Thus analysis of these three states provides the general stress-strain response of a UFC.

The advantage of the CCA model is in that the analysis reduces to that of a single composite cylinder. Carrying out such analyses for axisymmetric states and axial shear it was found that in each case the problem was reduced to solution a system of integral equations in the time which is easily done numerically in an incremental fashion. The CCA model is not amenable to transverse shear analysis and therefore this case has been analyzed in terms of the hexagonal array model with TVE finite elements which were specially developed for this study. Note that the CCA and the hexagonal array are both transversely isotropic models as required and that their predictions for elastic constants of UFC are numerically literally identical.

The constitutive relations for UFC developed have to be utilized to study the vibrations of a cantilever beam. With respect to this vibration problem it is important to recognize that a UFC will have small time dependent response when loaded in fiber direction and large time dependence when sheared along the fiber direction (axial shear). Thus, in bending vibrations of a beam which is uniaxially reinforced in the direction of the beam axis the effect of shear is very significant and therefore, we have based the analysis on the Timoshenko beam concept which takes into account shear deformation and rotatory inertia. For this purpose the Timoshenko beam vibration equations have been converted to viscoelasticity in terms of complex moduli (axial Young's modulus and axial shear modulus) of the UFC. These have been evaluated at different temperatures in terms of matrix complex moduli and fiber elastic moduli. We have evaluated the attenuation of free bending vibrations of a cantilever with circular tubular section without and with the shear deformation effect. The results show that shear deformation provides very significant attenuation of vibrations. Indeed it is seen that modes higher than the first are effectively eliminated by the damping.

REFERENCES

1. Z. Hashin, "Viscoelastic Behavior of Heterogeneous Media," *J. Appl. Mech.*, 32, 1965, pp. 157-173.
2. Z. Hashin, "Viscoelastic Fiber Reinforced Materials," *AIAA J.*, 1966, pp. 1411-1417.

OBJECTIVES

- OBTAIN THERMO-VISCOELASTIC CONSTITUTIVE RELATIONS FOR UNIDIRECTIONAL FIBER COMPOSITES
- INVESTIGATE COMPOSITE STRUCTURAL RESPONSE

APPROACH

- MICROMECHANICS MODELLING
- STRUCTURAL MODELLING

THERMO-VISCOELASTIC RESPONSE OF UNIDIRECTIONAL FIBER COMPOSITE

FIBERS - THERMO-ELASTIC ANISOTROPIC GRAPHITE, CARBON

MATRIX - THERMO-VISCOELASTIC POLYMER

INPUT - $\bar{\epsilon}_{ij}(t)$, $\phi(t)$ FIND - $\bar{\sigma}_{ij}(t)$

RELAXATION

INPUT - $\bar{\sigma}_{ij}(t)$, $\phi(t)$ FIND - $\bar{\epsilon}_{ij}(t)$

CREEP

THERMO-ELASTIC DILATATION RESPONSE

$$\sigma_{ij} = \sigma \delta_{ij} + s_{ij}$$

$$\epsilon_{ij} = \epsilon \delta_{ij} + e_{ij}$$

$$\sigma = \frac{1}{3} (\sigma_{11} + \sigma_{22} + \sigma_{33})$$

$$\epsilon = \frac{1}{3} (\epsilon_{11} + \epsilon_{22} + \epsilon_{33})$$

$$\sigma [\phi(t)] = 3K [\phi(t)] \left\{ \epsilon(t) - \alpha [\phi(t)] \phi(t) \right\}$$

THERMO-ELASTIC RELATION

$\phi(t)$ - TIME DEPENDENT TEMPERATURE

THERMO-VISCOELASTICITY

ISOTHERMAL $\phi = \text{CONST}$

$$s_{ij}(t) = 2G(t, \phi) e_{ij}(0) + 2 \int_{0^+}^t G(t-t', \phi) \frac{\partial e_{ij}}{\partial t'} dt'$$

$$e_{ij}(t) = \frac{1}{2}g(t, \phi) s_{ij}(0) + \frac{1}{2} \int_{0^+}^t g(t-t', \phi) \frac{\partial s_{ij}}{\partial t'} dt'$$

$G(t, \phi)$ - SHEAR RELAXATION MODULUS

$g(t, \phi)$ - SHEAR CREEP COMPLIANCE

THERMORHEOLOGICALLY SIMPLE

$$s_{ij}(t) = 2G(\xi) e_{ij}(0) + 2 \int_{0^+}^t G(\xi-\xi') \frac{\partial e_{ij}}{\partial t'} dt'$$

$$e_{ij}(t) = \frac{1}{2}g(\xi) s_{ij}(0) + \frac{1}{2} \int_{0^+}^t g(\xi-\xi') \frac{\partial s_{ij}}{\partial t'} dt'$$

$$\xi(t) = \int_0^t \frac{du}{a[\phi(u)]} \quad \text{REDUCED TIME}$$

a - HORIZONTAL SHIFT FACTOR

$$G(t, \phi_0) = F(\log t)$$

$$G(t, \phi) = F[\log(t/a)]$$

THERMORHEOLOGICALLY COMPLEX

SIMPLEST MODEL

$$G(t, \phi) = G_0(0, \phi_0) + G_1(0, \phi) + G_2(t, \phi)$$

$$s_{ij}(t) = 2 \left\{ G_0(0, \phi_0) e_{ij}(t) + [G_1(0, \phi) + G_2(\xi)] e_{ij}(0) + \int_{0^+}^t [G_1(0, \phi) + G_2(\xi - \xi')] \frac{\partial e_{ij}}{\partial \tau} d\tau \right\}$$

$$e_{ij}(t) = \frac{1}{2} \left\{ g_0(0, \phi_0) s_{ij}(t) + [g_1(0, \phi) + g_2(\xi)] s_{ij}(0) + \int_{0^+}^t [g_1(0, \phi) + g_2(\xi - \xi')] \frac{\partial s_{ij}}{\partial \tau} d\tau \right\}$$

$$s_{ij} = 2 \underline{I} e_{ij}$$

$$e_{ij} = \frac{1}{2} \underline{Y} s_{ij}$$

TRANSVERSELY ISOTROPIC FIBER COMPOSITE

$$[\bar{\sigma}_{ij}] = \begin{bmatrix} \bar{\sigma}_{11} & 0 & 0 \\ 0 & \frac{1}{2}(\bar{\sigma}_{22} + \bar{\sigma}_{33}) & 0 \\ 0 & 0 & \frac{1}{2}(\bar{\sigma}_{22} + \bar{\sigma}_{33}) \end{bmatrix} + \begin{bmatrix} 0 & 0 & 0 \\ 0 & \frac{1}{2}(\bar{\sigma}_{22} - \bar{\sigma}_{33}) & 0 \\ 0 & 0 & -\frac{1}{2}(\bar{\sigma}_{22} - \bar{\sigma}_{33}) \end{bmatrix} + \begin{bmatrix} 0 & \sigma_{12} & \sigma_{13} \\ \bar{\sigma}_{12} & 0 & 0 \\ \bar{\sigma}_{13} & 0 & 0 \end{bmatrix}$$

AXISYMMETRIC

TRANSVERSE SHEAR

AXIAL SHEAR

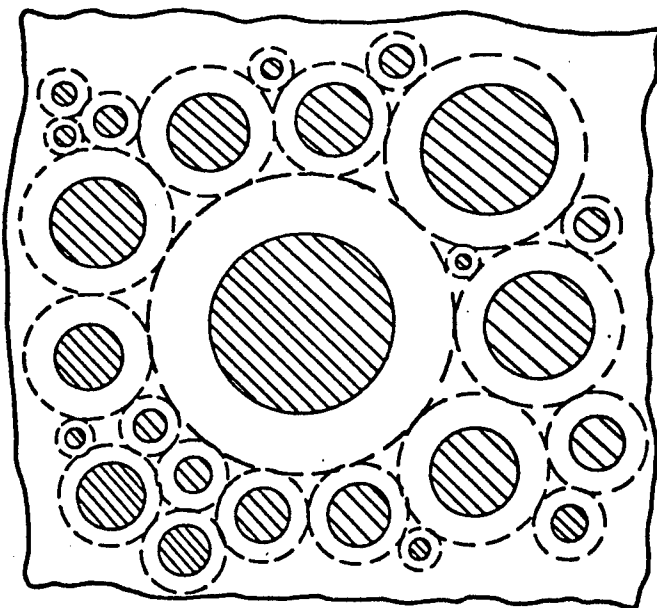
$$[\bar{\epsilon}_{ij}] = \begin{bmatrix} \bar{\epsilon}_{11} & 0 & 0 \\ 0 & \frac{1}{2}(\bar{\epsilon}_{22} + \bar{\epsilon}_{33}) & 0 \\ 0 & 0 & \frac{1}{2}(\bar{\epsilon}_{22} + \bar{\epsilon}_{33}) \end{bmatrix} + \begin{bmatrix} 0 & 0 & 0 \\ 0 & \frac{1}{2}(\bar{\epsilon}_{22} - \bar{\epsilon}_{33}) & 0 \\ 0 & 0 & -\frac{1}{2}(\bar{\epsilon}_{22} - \bar{\epsilon}_{33}) \end{bmatrix} + \begin{bmatrix} 0 & \bar{\epsilon}_{12} & \bar{\epsilon}_{13} \\ \bar{\epsilon}_{12} & 0 & 0 \\ \bar{\epsilon}_{13} & 0 & 0 \end{bmatrix}$$

COMPOSITE CYLINDER
ASSEMBLAGE

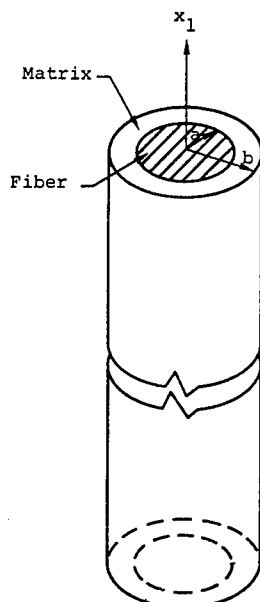
HEXAGONAL
ARRAY

COMPOSITE CYLINDER
ASSEMBLAGE

COMPOSITE CYLINDER ASSEMBLAGE



AXISYMMETRIC



$$u_1 = \epsilon_{11}(t)x_1 \quad \text{or} \quad \bar{\sigma}_{11}(t) \text{ Given}$$

$$u_r(b, t) = \epsilon_T(t)b \quad \text{or} \quad \sigma_{rr}(b, t) = \sigma_T(t)$$

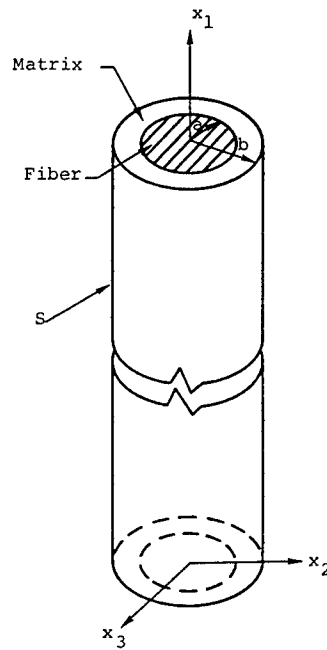
$$\epsilon_T = \frac{1}{2} (\bar{\epsilon}_{22} + \bar{\epsilon}_{33})$$

$$\sigma_T = \frac{1}{2} (\bar{\sigma}_{22} + \bar{\sigma}_{33})$$

$$\phi = \phi(t)$$

FREE THERMAL EXPANSION

$$\bar{\sigma}_{11} = 0 \quad \sigma_{rr}(b, t) = 0$$



AXIAL SHEAR

$$u_1(s, t) = \bar{\epsilon}_{12}(t)x_1 \quad u_2(s, t) = \bar{\epsilon}_{12}(t)x_2 \quad u_3(s, t) = 0$$

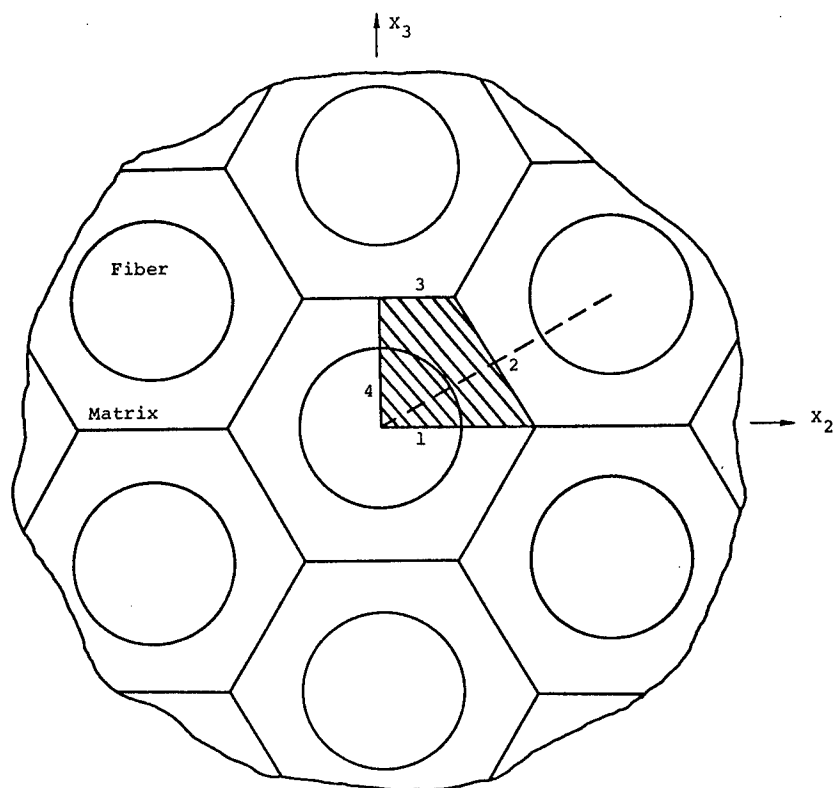
FIND $\bar{\sigma}_{12}(t)$

$$T_1(s, t) = \bar{\sigma}_{12}(t)x_1 \quad T_2(s, t) = \bar{\sigma}_{12}(t)x_2 \quad T_3(s, t) = 0$$

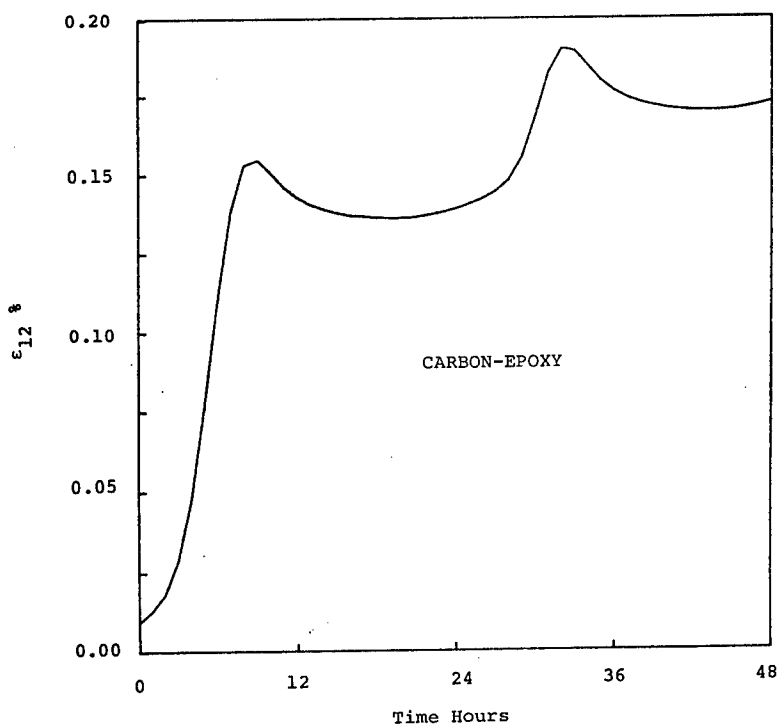
FIND $\bar{\epsilon}_{12}(t)$

$$\left[1 + v_f + v_m G_f \gamma \right] \bar{\sigma}_{12}(t) = 2 \left[v_m \Gamma + (1 + v_f) G_f \right] \bar{\epsilon}_{12}(t)$$

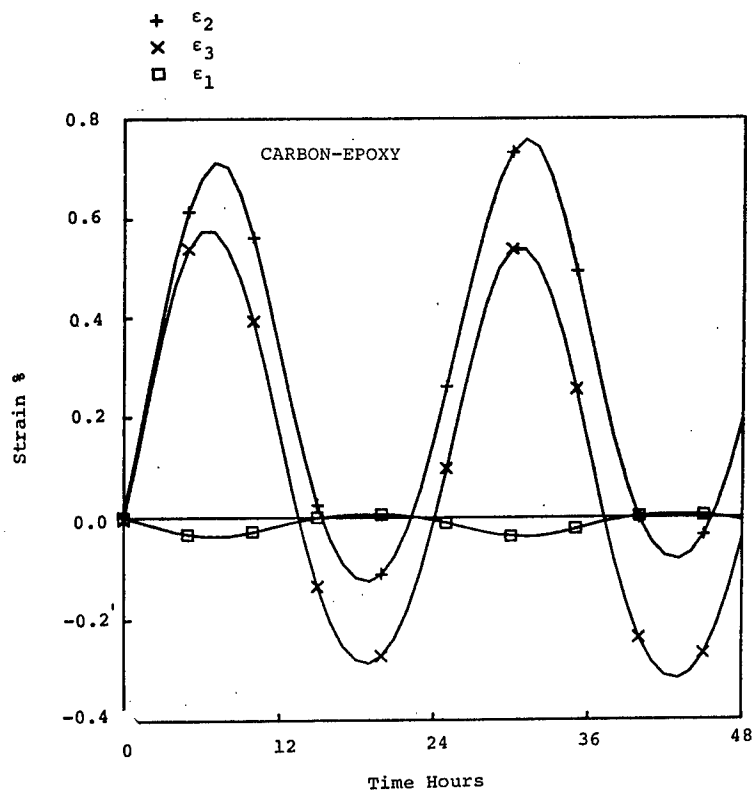
PERIODIC HEXAGONAL ARRAY AND REPEATING ELEMENT



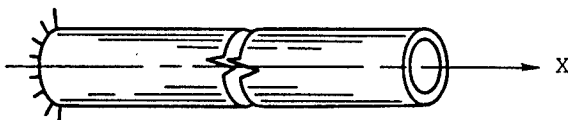
AXIAL SHEAR STRAIN DUE TO 1 MPA STRESS AND CYCLIC TEMPERATURE



STRAIN HISTORY FOR 1 MPa σ_2 STRESS AND CYCLIC TEMPERATURE



ELASTIC BEAM VIBRATIONS



NEGLECT SHEAR DEFORMATION AND ROTATORY INERTIA

$$EI \frac{\partial^4 w}{\partial x^4} + \rho A \frac{\partial^2 w}{\partial t^2} = 0$$

WITH SHEAR DEFORMATION AND ROTATORY INERTIA.

TIMOSHENKO BEAM

$$EI \frac{\partial^4 w}{\partial x^4} + \rho A \frac{\partial^2 w}{\partial t^2} - \rho I \left(1 + \frac{E}{k'G}\right) \frac{\partial^4 w}{\partial x^2 \partial t^2} + \frac{\rho^2 I}{k'G} \frac{\partial^4 w}{\partial t^4} = 0$$

k' - SHEAR COEFFICIENT

VISCOELASTIC VIBRATIONS

$$w(x,t) = w(x) e^{i\tilde{\omega}t}$$

$$E \rightarrow E'(\omega) + i E''(\omega)$$

$$G \rightarrow G'(\omega) + i G''(\omega)$$

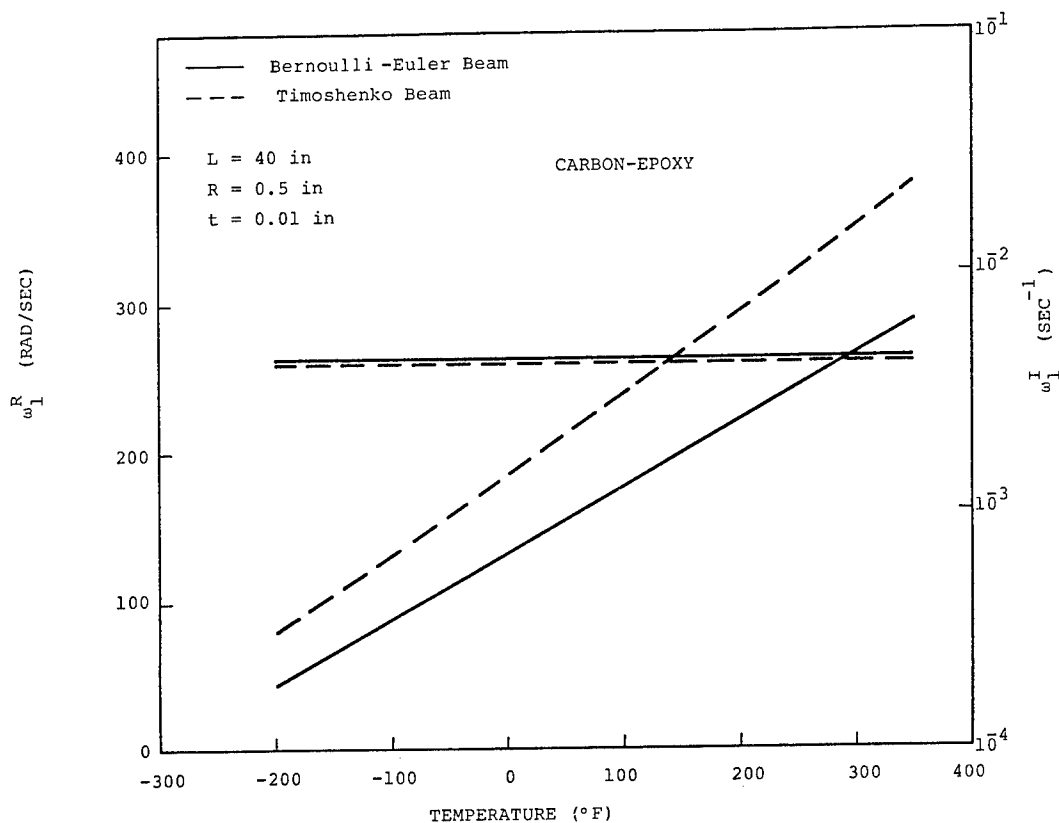
$$\tilde{\omega}_n = \omega'_n + i \omega''_n$$

COMPLEX NATURAL FREQUENCY

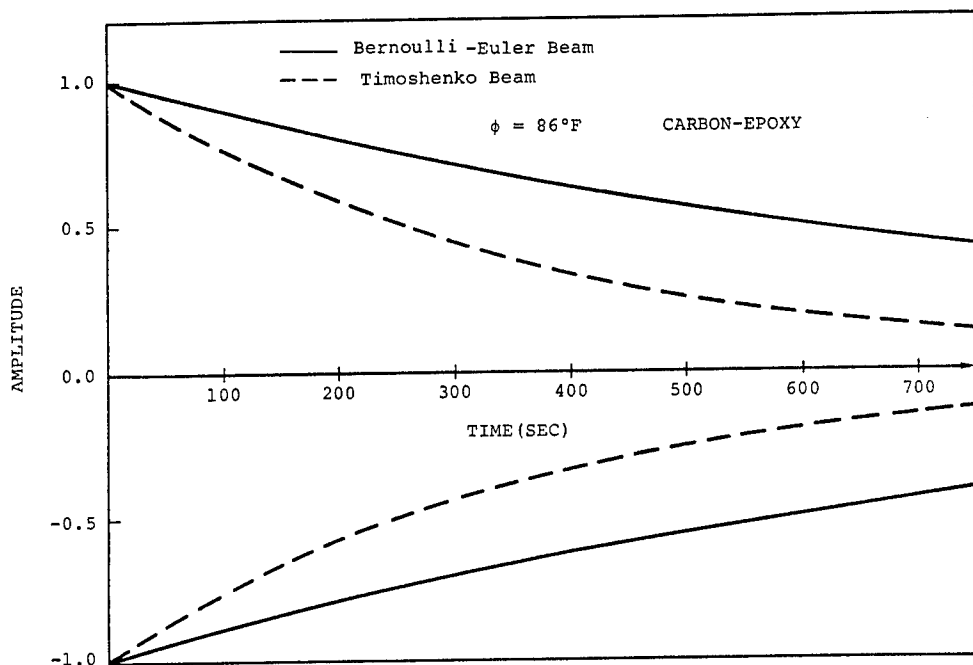
$$w_n(x,t) = w_n(x) e^{i\omega'_n t} e^{-\omega''_n t}$$

Mode
 Sinusoidal
 Attenuation

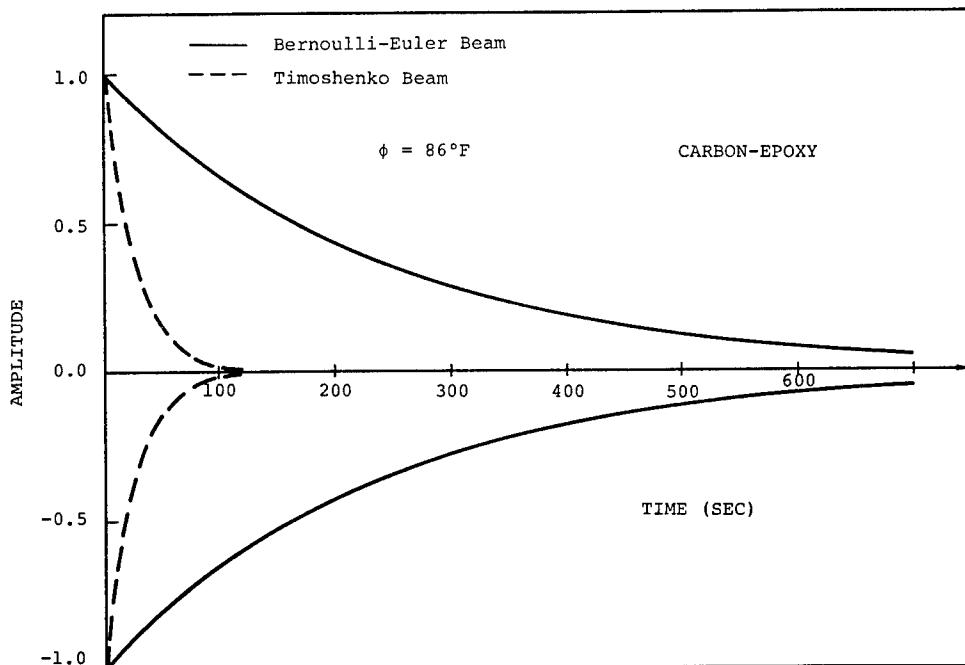
FIRST MODE NATURAL FREQUENCIES, CANTILEVER BEAM



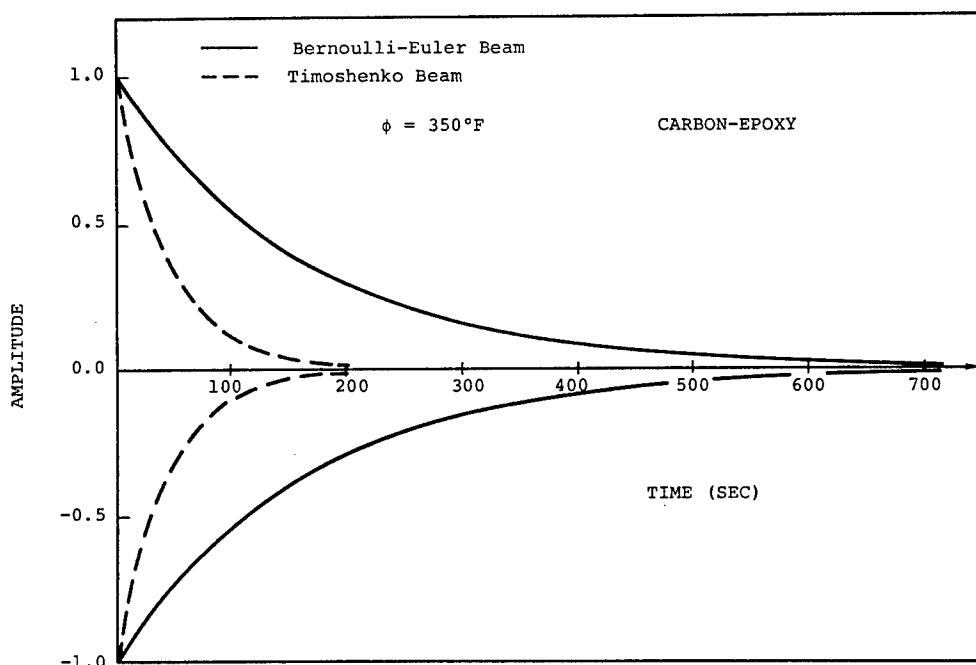
ENVELOPE OF FIRST MODE RESPONSE, CANTILEVER BEAM



ENVELOPE OF SECOND MODE RESPONSE, CANTILEVER BEAM



ENVELOPE OF FIRST MODE RESPONSE, CANTILEVER BEAM



SUMMARY

- TEMPERATURE DEPENDENCE OF INITIAL PROPERTIES SIGNIFICANT
- SECONDARY STRESS DOMINATE BEAM DAMPING
- STRUCTURAL MODELS MUST INCORPORATE SECONDARY STRESSES

COMPOSITE MECHANICS/RELATED ACTIVITIES AT LEWIS RESEARCH CENTER

C. C. CHAMIS, C. A. GINTY, AND P. L. N. MURTHY

NASA LEWIS RESEARCH CENTER
CLEVELAND, OHIO 44135

ABSTRACT

Lewis research activities and progress in composite mechanics and closely related areas are summarized. The research activities summarized include: (1) Composite Mechanics; (2) Computer Programs for Composites; and (3) High Temperature Composites. The research activities focus on: (1) Composite mechanics -- simplified procedures for sizing laminates, substructuring in composite mechanics for free edge stress-field behavior, interlaminar fracture toughness in composites, and progressive fracture in composites; (2) Computer programs for composites -- integrated composite analysis, composite blade structural analysis, composite durability structural analysis, thermoviscoplastic composite behavior, structural tailoring of engine and SSME blades, and structural tailoring of advanced turboprops; and (3) High temperature composites -- test methods development and characterization, composite burner liner and refractory wire reinforced superalloys for SSME turbopump blades.

OBJECTIVE

COMPOSITE MECHANICS/RELATED ACTIVITIES
AT LEWIS RESEARCH CENTER

SUMMARY OF LEWIS RESEARCH ACTIVITIES AND PROGRESS IN:

- o COMPOSITE MECHANICS
- o COMPUTER PROGRAMS FOR COMPOSITES
- o HIGH TEMPERATURE COMPOSITES

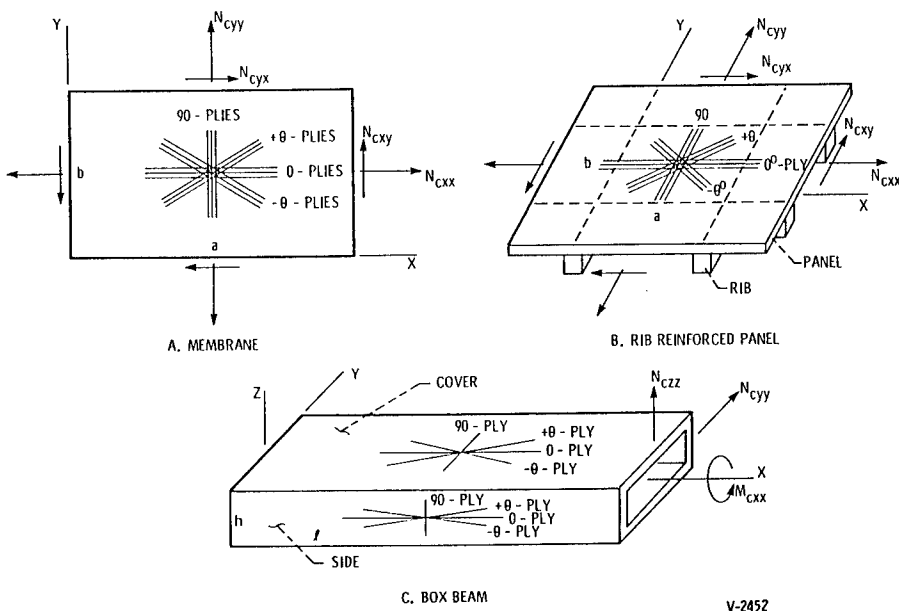
C. C. CHAMIS, C. A. GINTY, AND P. L. N. MURTHY
NASA LEWIS RESEARCH CENTER
CLEVELAND, OHIO 44135

COMPOSITE MECHANICS

ELEVENTH ANNUAL MECHANICS OF COMPOSITES REVIEW
DAYTON, OHIO, OCTOBER 22-24, 1985

- o SIMPLIFIED PROCEDURES FOR SIZING LAMINATES
- o SUBSTRUCTURING IN COMPOSITE MECHANICS: WIDTH, LOADING CONDITION AND ENVIRONMENTAL EFFECTS ON FREE EDGE STRESSES
- o INTERLAMINAR FRACTURE IN COMPOSITES
- o PROGRESSIVE FRACTURE OF COMPOSITES WITH AND WITHOUT DEFECTS

SCHEMATICS OF SELECT COMPOSITE STRUCTURAL COMPONENTS WITH RESPECTIVE GEOMETRY AND TYPICAL LOADINGS



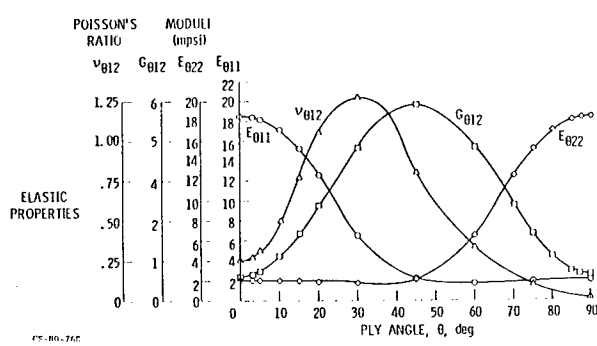
V-2452

LEWIS DEVELOPED DESIGN PROCEDURE

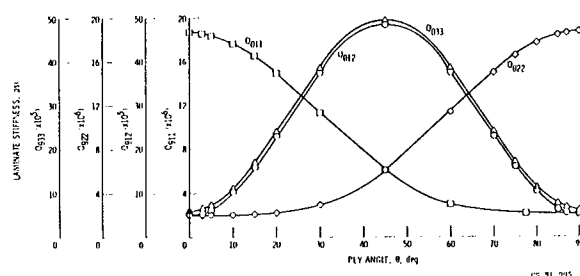
CONSISTS OF:

- TABULATED TYPICAL PROPERTIES OF VARIOUS UNIDIRECTIONAL COMPOSITES
- SUITABLE GRAPHS TO EXPEDITE REPETITIOUS CALCULATIONS
- PLY STRESS INFLUENCE COEFFICIENTS
- EXPLICIT, SIMPLE EQUATIONS FOR HYGROTERMAL EFFECTS AND FATIGUE
- APPROXIMATE, SIMPLE EQUATIONS FOR BUCKLING

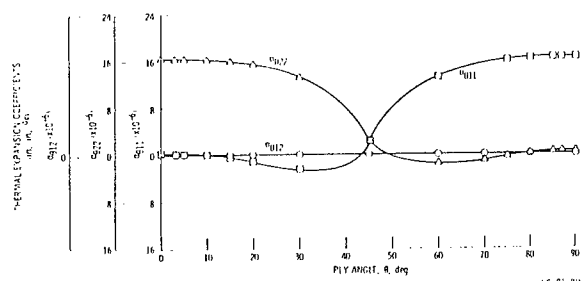
ELASTIC PROPERTIES OF AS-GRAFHTE-FIBER/EPOXY (AS/E) $\pm\theta$ LAMINATES



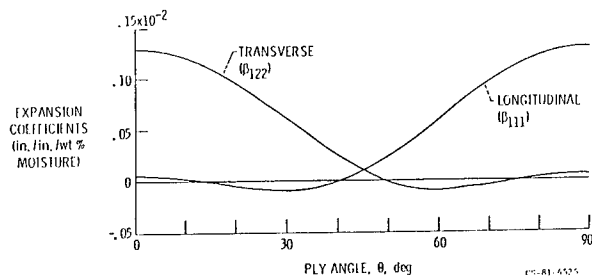
REDUCED STIFFNESSES OF AS GRAPHITE-FIBER/EPOXY (AS/E) $\pm\theta$ LAMINATES



Thermal Expansion Coefficients of AS Graphite-Fiber/Epoxy
(AS/E) $\pm\theta$ LAMINATES

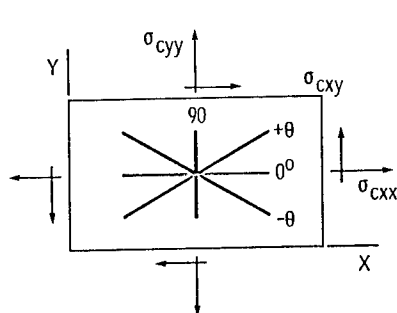


Moisture Expansion Coefficients of AS Graphite-Fiber/Epoxy
(AS/E) $\pm\theta$ LAMINATES

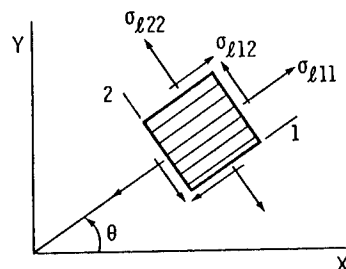


PLY STRESS INFLUENCE COEFFICIENTS (PSIC) - DEFINITION

PSIC (\mathcal{I}) RELATE THE θ PLY MATERIAL AXES STRESSES TO LAMINATE STRUCTURAL AXES STRESSES



LAMINATE STRUCTURAL AXES (X, Y) STRESSES



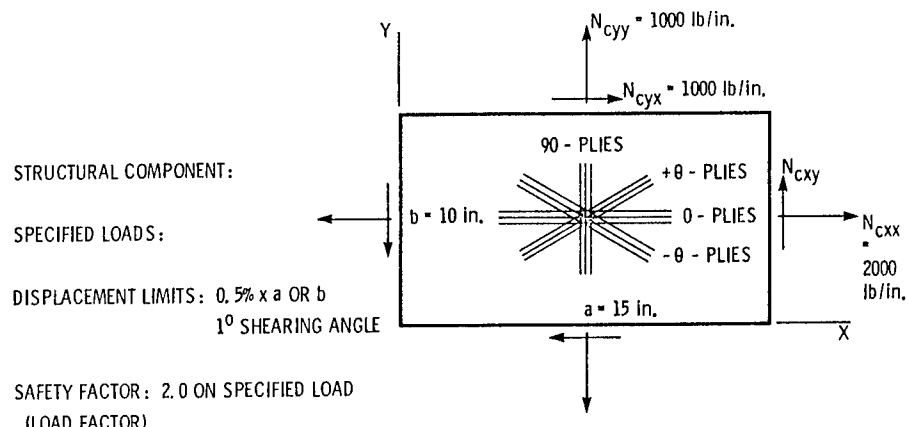
θ PLY MATERIAL AXES (1, 2) STRESSES

$$\sigma_{ll11} = \mathcal{I}_{L/X} \sigma_{cxx} + \mathcal{I}_{L/Y} \sigma_{cyy} + \mathcal{I}_{L/S} \sigma_{cxy}$$

$$\sigma_{ll22} = \mathcal{I}_{T/X} \sigma_{cxx} + \mathcal{I}_{T/Y} \sigma_{cyy} + \mathcal{I}_{T/S} \sigma_{cxy}$$

$$\sigma_{ll12} = \mathcal{I}_{S/X} \sigma_{cxx} + \mathcal{I}_{S/Y} \sigma_{cyy} + \mathcal{I}_{S/S} \sigma_{cxy}$$

SAMPLE DESIGN: COMPOSITE PANEL SUBJECTED TO IN-PLANE COMBINED LOADS



GENERAL LAMINATE DESIGN RESULTS SUMMARY

[LAMINATE CONFIGURATION: $[+45/0/90/0]_{2S}$ AS/E; $t_c = 0.10$ in.]

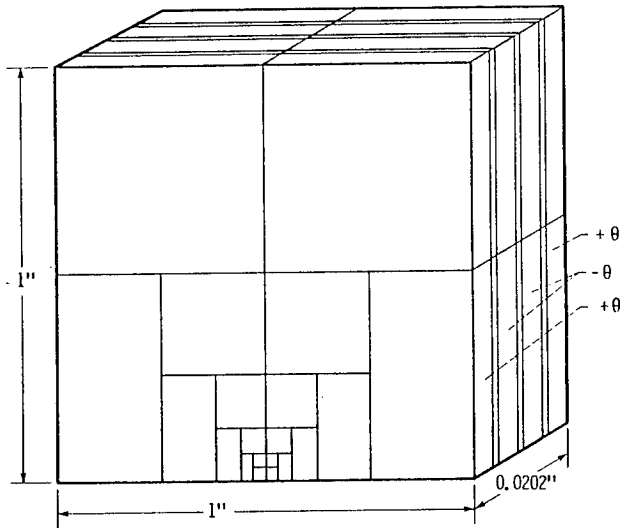
MARGINS OF SAFETY (M. O. S.) FOR:								
DISPLACEMENT		PLY STRESSES			BUCKLING			
TYPE	M. O. S.	PLY	M. O. S.		CASE, ksi			M. O. S.
u/a	0.43	---	$\sigma_{\ell 11}$	$\sigma_{\ell 22}$	$\sigma_{\ell 12}$	$\sigma_{c_{xx}}$	$\sigma_{c_{yy}}$	$\sigma_{c_{xy}}$
v/b	1.94	0	2.77	0.61	1.30	0	0	20
$\Delta\theta$.33	+45	0.79	∞	∞	40	20	20
	----	-45	4.43	^a .27	∞	----	----	----
	----	90	6.00	.12	1.30	----	----	----

^aAT SPECIFIED LOAD (AT DESIGN LOAD M. S. = 0.38).

CD-85-16564

FREE-EDGE SUPERELEMENT

(224 F. E.; 2355 D. O. F.)



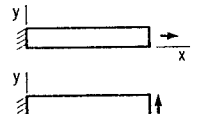
CD-85-15804

CASES STUDIED

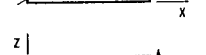
- FREE-EDGE AXIAL STRESS VARIATION VERSUS PLY ANGLE

- WITH/THICKNESS RATIO EFFECTS ON FREE-EDGE STRESSES

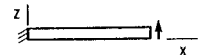
- AXIAL TENSION - REFERENCE



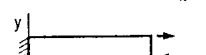
- IN-PLANE SHEAR/BENDING



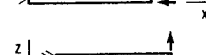
- OUT-OF-PLANE SHEAR/BENDING



- BENDING MOMENT



- TWISTING MOMENT



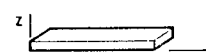
- COMBINED LOADING
(AXIAL TENSION/IN-PLANE SHEAR)



- UNIFORM THERMAL LOAD



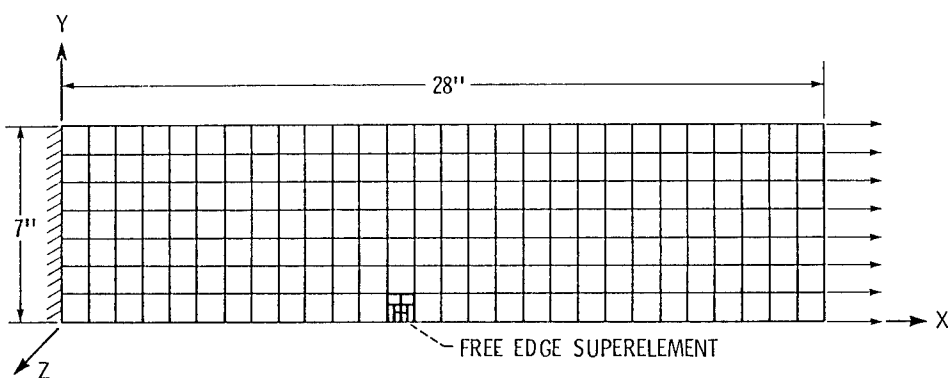
- UNIFORM MOISTURE LOAD



CD-85-15810

FINITE ELEMENT MODEL OF ANGLEPLIED LAMINATE

UNDER UNIFORM EXTENSIONAL STRESS



F. E. STATISTICS

1589 20-NODE SOLID F. E.

224 F. E.'s IN SUPERELEMENT

22683 D. O. F.

PROPERTIES
(AS/EP 0° PLY AND INTERPLY LAYER)

$$\begin{bmatrix} \sigma_{11} \\ \sigma_{22} \\ \sigma_{33} \\ \sigma_{44} \\ \sigma_{55} \\ \sigma_{66} \end{bmatrix} = \begin{bmatrix} G_{11} & G_{12} & G_{13} & G_{14} & G_{15} & G_{16} \\ & G_{22} & G_{23} & G_{24} & G_{25} & G_{26} \\ & & G_{33} & G_{34} & G_{35} & G_{36} \\ & & & G_{44} & G_{45} & G_{46} \\ & & & & G_{55} & G_{56} \\ & & & & & G_{66} \end{bmatrix} \times \begin{bmatrix} \epsilon_{11} \\ \epsilon_{22} \\ \epsilon_{33} \\ \epsilon_{44} \\ \epsilon_{55} \\ \epsilon_{66} \end{bmatrix}$$

$$G_{11} = 19.4 \quad G_{12} = 0.5164 \quad G_{13} = 0.5164 \quad G_{22} = 1.384$$

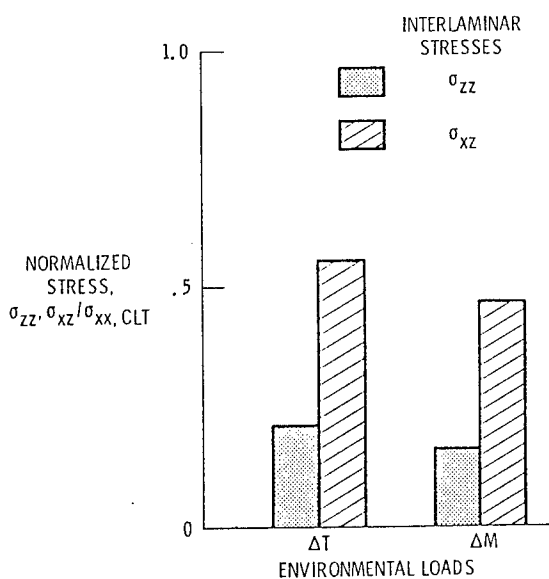
$$G_{23} = 0.4473 \quad G_{33} = 1.483 \quad G_{44} = 0.6667 \quad G_{55} = 0.3974$$

$$G_{66} = 0.6667 \quad E = 0.50; \nu = 0.35$$

(UNITS $\times 10^6$ psi)

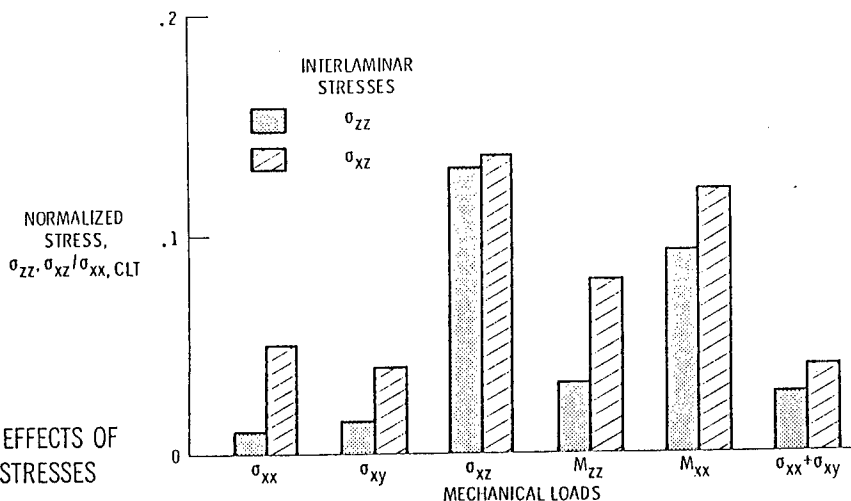
COMPARISON OF FREE-EDGE STRESSES
DUE TO ENVIRONMENTAL LOADS

($\pm 10^0$ AS/E APL AT 0.55 FVR)



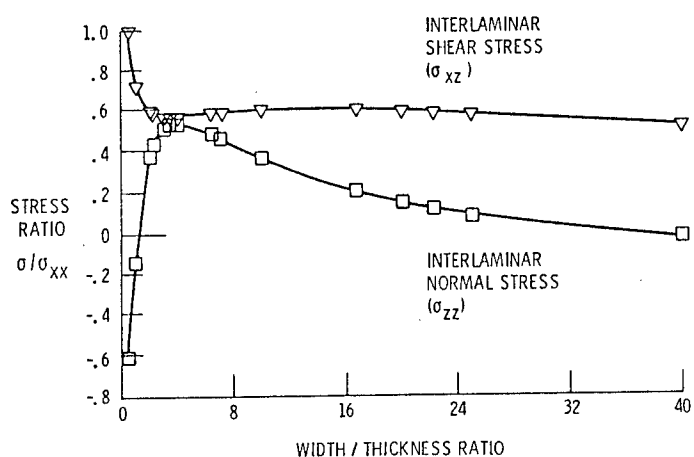
COMPARISON OF FREE-EDGE STRESSES DUE TO MECHANICAL LOADS

($\pm 10^0$ AS/E APL AT 0.55 FVR)

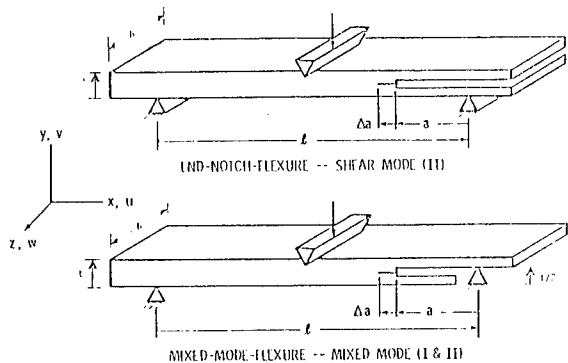


WIDTH TO THICKNESS RATIO EFFECTS OF
INTERLAMINAR FREE-EDGE STRESSES

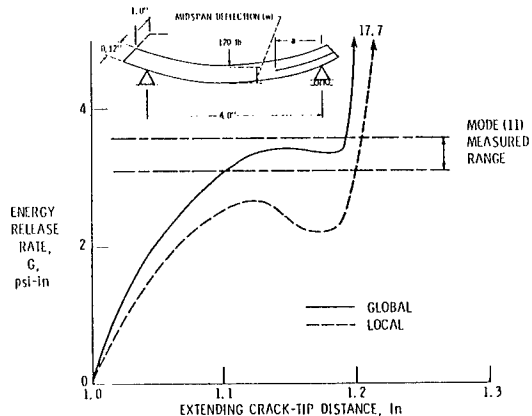
($\pm 45^0$ AS/E APL, 0.55 FVR)



SCHEMATIC OF FLEXURAL TEST FOR INTERLAMINAR FRACTURE MODE TOUGHNESS

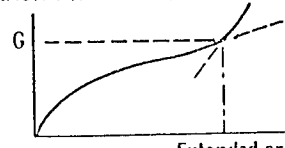


END-NOTCH-FLEXURE ENERGY RELEASE RATE COMPARISONS



GENERAL PROCEDURE FOR PREDICTING COMPOSITE INTERLAMINAR FRACTURE TOUGHNESS USING THE END-NOTCH-FLEXURE (ENF) OR MIXED-MODE-FLEXURE (MMF) METHOD

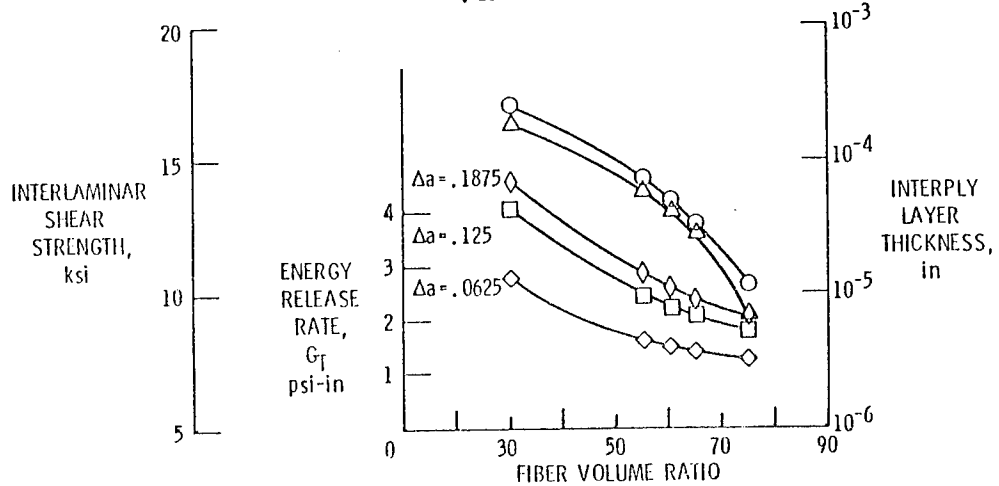
- DETERMINE REQUISITE PROPERTIES AT DESIRED CONDITIONS USING COMPOSITE MICROMECHANICS
- RUN 3-D FINITE ELEMENT ANALYSIS ON ENF (MMF) FOR AN ARBITRARY LOAD
- SCALE LOAD TO MATCH INTERLAMINAR SHEAR STRESS AT ELEMENT NEXT TO CRACK-TIP
- WITH SCALED LOAD EXTEND CRACK AND PLOT STRAIN ENERGY RELEASE RATE VS CRACK LENGTH
- SELECT CRITICAL "G" } AND CRITICAL "a" }
- METHOD HAS VERSATILITY/GENERALITY



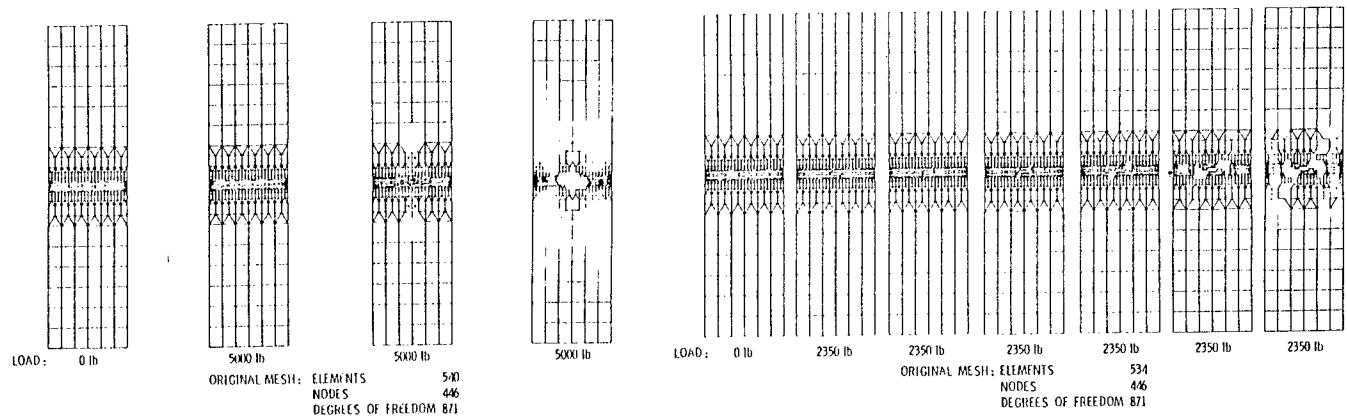
FIBER VOLUME RATIO EFFECT ON INTERLAMINAR FRACTURE TOUGHNESS PARAMETERS

END-NOTCH-FLEXURE (AS/E)

- INTERLAMINAR SHEAR STRENGTH
- △ INTERPLY LAYER THICKNESS
- ◊ MODE II ENERGY RELEASE RATE



CODSTRAN RESULTS

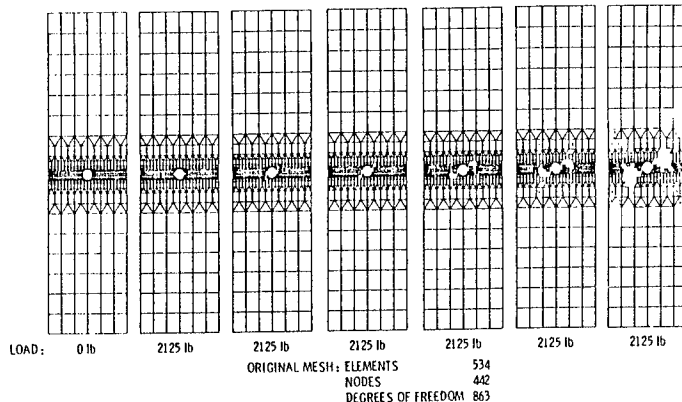


SUCCESSIVE DAMAGE EXTENT AND DEFECT GROWTH

$[\pm 15]_s$ GRAPHITE/EPOXY SOLID LAMINATE

SUCCESSIVE DAMAGE EXTENT AND DEFECT GROWTH

$[\pm 15]_s$ GRAPHITE/EPOXY LAMINATE WITH THROUGH-SLIT



SUCCESSIVE DAMAGE EXTENT AND DEFECT GROWTH

$[\pm 15]_s$ GRAPHITE/EPOXY LAMINATE WITH THROUGH-HOLE

FRACTURE MODES* OF $[\pm 0]_s$ G/E LAMINATES
(PREDICTED BY CODSTRAN)

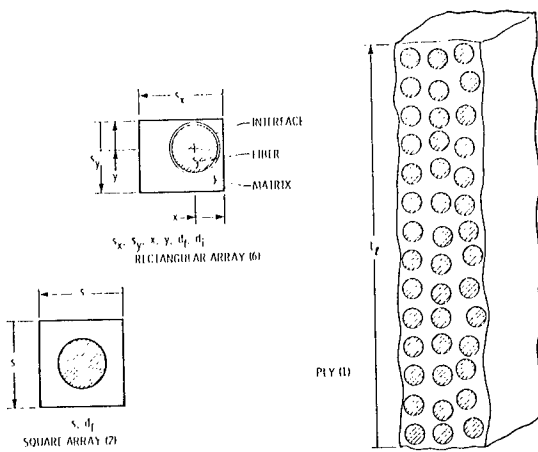
NOTCH TYPE	PLY ORIENTATION; $[\pm 0]_s$; θ IN DEGREES									
	0	3	5	10	15	30	45	60	75	90
UNNOTCHED--SOLID	LT	LT S ¹	LT S ³	LT S ³	I S	S	I S	TT	TT	TT
NOTCHED--THRU SLIT	S ¹ LT	S ¹ LT	S ¹ LT	S	S	I ⁴ S	I ⁴ S	TT S ²	TT	TT
NOTCHED--THRU HOLE	S ¹ LT	S ¹ LT	S ¹ LT	S	S LT	I ⁴ S	I ⁴ S TT	I ⁴ TT	TT	TT

* LT = LONGITUDINAL TENSION
TT = TRANSVERSE TENSION

S = INTRAPLY SHEAR: 1) INITIAL FRACTURE DUE TO INTRAPLY SHEAR IN THE NOTCH TIP ZONE
 2) MINIMAL INTRAPLY SHEARING DURING FRACTURE
 3) SOME INTRAPLY SHEAR OCCURRING NEAR CONSTRAINTS (GRIPS)
 4) DELAMINATIONS OCCUR IN NOTCH TIP ZONE PRIOR TO ANY INTRAPLY DAMAGE

I = INTERPLY DELAMINATION

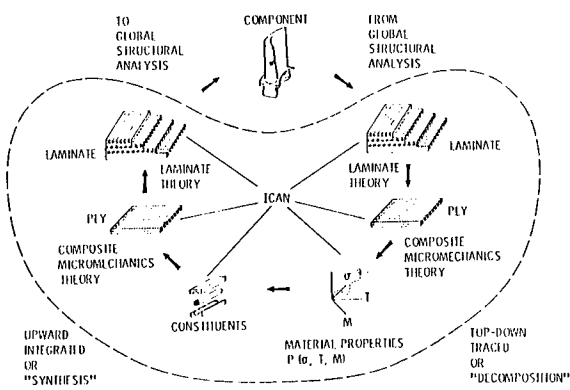
COMPOSITE MICROMECHANICS - SCALE LEVELS



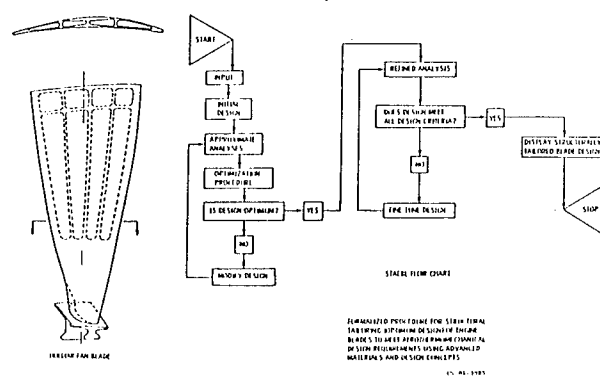
COMPUTER PROGRAMS FOR COMPOSITES

- o ICAN INTEGRATED COMPOSITES ANALYZER - INTERACTIVE
- o COBSTRAN COMPOSITE BLADE STRUCTURAL ANALYSIS - STAND ALONE
- o CODSTRAN COMPOSITE DURABILITY STRUCTURAL ANALYSIS - STAND ALONE
- o N. L. COBSTRAN NONLINEAR COMPOSITE BLADE STRUCTURAL ANALYSIS - STAND ALONE
- o STAEBL STRUCTURAL TAILORING OF ENGINE BLADES - HIGH TEMPERATURE
- o STAT STRUCTURAL TAILORING OF ADVANCED TURBOPROPS

ICAN: INTEGRATED COMPOSITES ANALYZER



STRUCTURAL TAILORING OF ENGINE BLADES (STAEBL)



STRUCTURALLY TAILORED SHROUDLESS BLADES
WITH COMPLEX INTERNAL STRUCTURE

PARAMETER	PERCENT CHANGE FROM REFERENCE DESIGN	
	HOLLOW BLADE WITH COMPOSITE INLAYS	SUPERHYBRID COMPOSITE
BLADE CHORD	-18	-9
BLADE WEIGHT	-52	-37
DIRECT OPERATIONAL COST PLUS INTEREST (DOC +I)		
ENGINE WEIGHT	-0.33	-0.23
ENGINE COST	-0.15	-0.18
MAINTENANCE COST	+0.03	+0.05
TOTAL	-0.45	-0.36

DESIGN REQUIREMENTS SATISFIED:

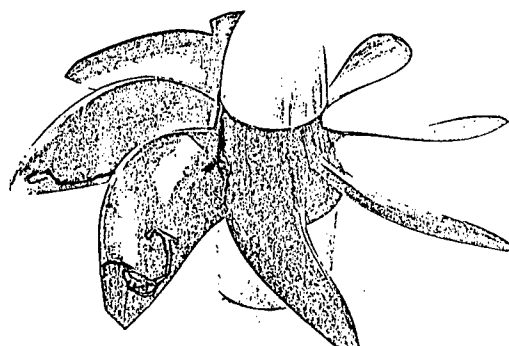
- RESONANCE MARGINS (FIRST, SECOND, THIRD, AND FOURTH MODES)
- FLUTTER-LOG DECREMENT (FIRST, SECOND, AND THIRD MODES)
- BIRD INGESTION (LOCAL AND ROOT STRESSES)
- STEADY-STATE STRESS (THROUGHOUT THE BLADE)

OPTIMUM BLADE DESIGN
EFFECT OF THERMAL AND PRESSURE LOADS

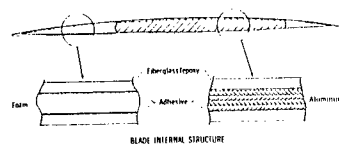
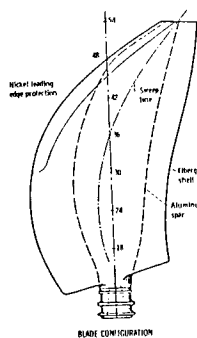
OPTIMUM DESIGN	PRESSURE LOAD ONLY	PRESSURE AND THERMAL LOADS TEMPERATURE - DEPENDENT PROPERTIES
WEIGHT (LBS) PERCENT SPAN THICKNESS (IN) CHORD (IN) THICK/CHORD	9.88 0. 50. 100. .47 .08 .10 3.33 3.66 4.22 .14 .02 .02	9.69 0. 50. 100. .48 .08 .08 3.27 3.60 4.15 .14 .02 .02
CONSTRAINTS RESONANCE MARGINS MODE 1 MODE 2 MODE 3 FLUTTER CONSTRAINT ROOT STRESS	.05 1.55 1.71 .510 .782	.05 1.47 1.67 .520 .813

OPTIMUM BLADE DESIGN
EFFECT OF THERMAL ENVIRONMENT

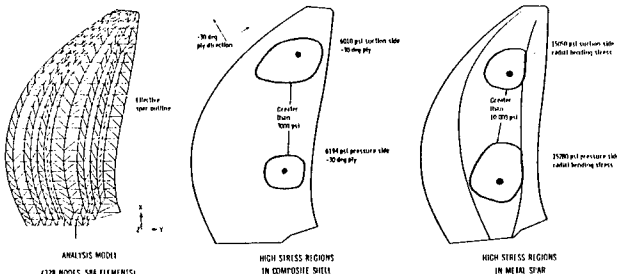
OPTIMUM DESIGN	CONTROL CASE: No.THERMAL LOADS	THERMAL LOADS			THERMAL LOADS TEMPERATURE DEPENDENT PROPERTIES
		TEMPERATURE INDEPENDENT PROPERTIES			
WEIGHT (LBS)	7.95	8.22		8.24	
PERCENT SPAN	0. 50. 100.	0. 50. 100.		0. 50. 100.	
THICKNESS (IN)	.24 .13 .08	.24 .15 .08		.24 .15 .08	
CHORD (IN)	1.70 1.88 2.16	1.68 1.85 2.13		1.69 1.86 2.14	
THICK/CHORD	.14 .07 .04	.14 .08 .04		.14 .08 .04	
CONSTRAINTS RESONANCE MARGINS					
Root 1	.05	.06		.06	
Root 2	1.27	1.28		1.27	
Root 3	1.65	1.67		1.65	
FLUTTER CONSTRAINTS	.988	.999		.999	
ROOT STRESS	.055	.062		.062	



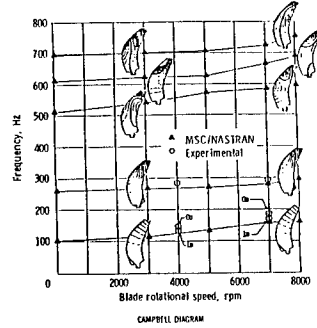
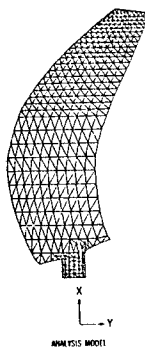
COMPOSITE TURBOPROP BLADE



COMPOSITE TURBOPROP STRESS ANALYSIS

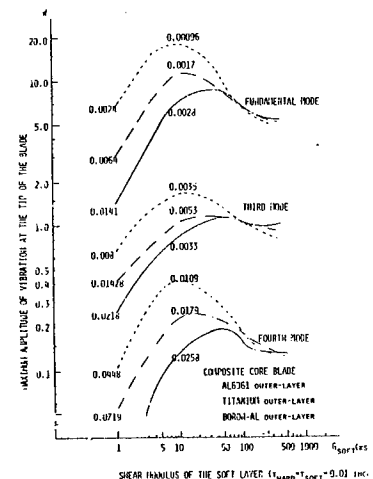


COMPOSITE TURBOPROP VIBRATION ANALYSIS



VIBRATION MODE
COMPOSITE TURBOPROP BLADE

CONSTRAINED LAYER DAMPING OF ADVANCED PROPFANS



ANALYSIS TEST

	BENDING	MEMBRANE BENDING	MEMBRANE BENDING	TRAN. SHEAR
1st BENDING	154	158	147	156
1st EDGE	338	339	334	325
2nd BENDING	373	369	364	371
1st TORSION	585	571	561	536
3rd BENDING	655	650	635	623

NATURAL FREQUENCIES OF SR7A

HIGH TEMPERATURE COMPOSITES

- o TEST METHODS AND CHARACTERIZATION
- o COMPOSITE BURNER LINER
- o FRS FOR SSME TURBOPUMP BLADES

CONCLUSIONS

- o CURRENT LEWIS RESEARCH ACTIVITIES ON COMPOSITE MECHANICS/RELATED AREAS INCLUDE:
 - o COMPOSITE MECHANICS, COMPUTER PROGRAMS FOR COMPOSITES, HIGH TEMPERATURE COMPOSITES AND COMPOSITE ENGINE STRUCTURAL COMPONENTS
 - o RECENT PROGRESS INCLUDES:
 - o SIMPLIFIED DESIGN PROCEDURE FOR GENERAL LAMINATES
 - o WIDTH, LOADING CONDITIONS AND ENVIRONMENTAL EFFECTS ON FREE EDGE STRESSES
 - o INTERLAMINAR FRACTURE IN COMPOSITES
 - o PROGRESSIVE FRACTURE OF COMPOSITES WITH/WITHOUT DEFECTS
 - o CONTINUING DEVELOPMENT OF: ICAN, CODSTRAN, N. L. COBSTRAN, STAEBL, STAT
 - o INITIATION OF RESEARCH IN HIGH TEMPERATURE COMPOSITES
 - o STRUCTURAL TAILORING OF COMPOSITE FAN BLADES, TURBOPROPS, SSME BLADES
 - o THERMOVISCOPLASTIC STRUCTURAL ANALYSIS OF TURBINE BLADES MADE FROM TUNGSTEN-FIBER REINFORCED SUPERALLOYS - DEDICATE ANALYSIS

APPENDIX A: PROGRAM LISTINGS

AIR FORCE WRIGHT AERONAUTICAL LABORATORIES
MATERIALS LABORATORY

INHOUSE

ADVANCED COMPOSITES
WORK UNIT DIRECTIVE (WUD) NUMBER 45
77 April - 85 April

WUD Leader: James M. Whitney
Materials Laboratory
Air Force Wright Aeronautical Laboratories
AFWAL/MLBM
Wright-Patterson AFB, OH 45433-6533
(513) 255-2340 Autovon: 785-2340

Objective: The objective of the current thrust under this work is to develop and demonstrate concepts of damage resistance as applied to fiber reinforced composite laminates. Short term objectives (1-2 yrs) include the following:

- (a) Development of failure mode models with emphasis on delamination and matrix cracking.
- (b) Assess the role of matrix toughness in composite failure processes.
- (c) To develop concepts of interface/interphase strengthening.

CONTRACTS

IMPROVED, DAMAGE RESISTANT COMPOSITE MATERIALS
F33615-84-C-5070
1 Sep 84 - 1 Feb 88

Project Engineer: James M. Whitney
Materials Laboratory
Air Force Wright Aeronautical Laboratories
AFWAL/MLBM
Wright-Patterson AFB, OH 45433-6533
(513) 255-2340 Autovon: 785-2340

Principal Investigator: Ron Servais
University of Dayton Research Institute
300 College Park Avenue
Dayton, OH 45469

Objective: The objective of this program is to investigate from both an experimental and analytical standpoint the potential of new and/or modifications of existing polymeric materials and reinforcement forms for use in advanced composite materials, including processing/mechanical property relationships. Such materials are subsequent candidates for use in advanced aircraft and aerospace structural applications.

3-DIMENSIONAL RESPONSE OF COMPOSITES
F33615-85-C-5034
1 Jun 85 - 1 Dec 87

Project Engineer: Nicholas J. Pagano
Materials Laboratory
Air Force Wright Aeronautical Laboratories
AFWAL/MLBM
Wright-Patterson AFB, OH 45433-6533
(513) 255-6762 Autovon: 785-6762

Principal Investigator: Som R. Soni
Adtech Systems Research Inc.
211 N. Broad Street
Fairborn, OH 45324

Objective: The objective of this program is to develop 3-dimensional analytical models capable of predicting the mechanical response of thick laminated composites and residual stress failure of carbon-carbon composites.

INITIAL IMPACT DAMAGE OF COMPOSITES
F33615-84-C-5096
28 Sep 84 - 15 Sep 86

Project Engineer: James M. Whitney
Materials Laboratory
Air Force Wright Aeronautical Laboratories
AFWAL/MLBM
Wright-Patterson AFB, OH 45433-6533
(513) 255-2340 Autovon: 785-2340

Principal Investigator: Jonathan Goering
Materials Sciences Corporation
Gwynedd Plaza II
Bethlehem Pike
Springhouse, PA 19477

Objective: The objective of this program is to develop an analytical model for predicting damage initiation in laminated fiber reinforced composites subjected to low velocity impact.

FUNDAMENTAL MATRIX STIFFNESS FORMULATIONS FOR LAMINATE STRUCTURES
F33615-83-C-5076
1 Jun 83 - 31 Mar 86

Project Engineer: Steven L. Donaldson
Materials Laboratory
Air Force Wright Aeronautical Laboratories
AFWAL/MLBM
Wright-Patterson AFB, OH 45433-6533
(513) 255-3068 Autovon: 785-3068

Principal Investigator: Henry T. Yang
School of Aeronautical & Astronautical Engineering
Purdue University
West Lafayette, IN 47907
(317) 494-5117

Objective: This program will develop the mathematical formulation of the stiffness and mass matrices of laminated plates and beams, to ultimately obtain the stress fields, the vibrational, and the buckling response of structural laminates. A through-the-thickness calculation shall be made of individual ply stresses and strength ratios. The elements will be formulated in such a way that they can be simply implemented on micro and minicomputers.

FAILURE ANALYSIS FOR COMPOSITE STRUCTURE MATERIALS
F33615-84-C-5010
Jun 84 - Nov 86

Project Engineer: Frank Fechek
Materials Laboratory
Air Force Wright Aeronautical Laboratories
AFWAL/MLSE
Wright-Patterson AFB, OH 45433-6533
(513) 255-7483 Autovon: 785-7483

Principal Investigator: Brian Smith
The Boeing Company
P.O. Box 3707
Mail Stop 73-43
Seattle, WA 98124

Objective: The objectives of this program are: a) to verify the capability of state-of-the-art analysis techniques and procedures to produce useful data toward the understanding of the cause of composite failures, beginning with the failed part and, b) to organize this information into a compendium defining a failure logic network which will assist the failure analyst in sequentially selecting the appropriate tests, techniques, and procedures to be applied when conducting a failure analysis of a composite structure.

CURING PROCESS OF COMPOSITE MATERIALS
F33615-84-C-5049
Sep 84 - 1 Oct 87

Project Engineer: Stephen W. Tsai
Materials Laboratory
Air Force Wright Aeronautical Laboratories
AFWAL/MLBM
Wright-Patterson AFB, OH 45433
(513) 255-3068 Autovon: 785-3068

Principal Investigator: George S. Springer
Dept of Aeronautics and Astronautics
Stanford University
Stanford, CA 94305
(415) 497-4135

Objective: To extend the analytical modeling developed by the Principal Investigator to include the curing thermosetting and thermal plastics as the matrix materials. To provide criteria for automated process controls and optimization.

AIR FORCE OFFICE OF SCIENTIFIC RESEARCH

INHOUSE

NONE

GRANTS AND CONTRACTS

DAMAGE MODELS FOR CONTINUOUS FIBER COMPOSITES
84 February 01 - 87 January 31

Principal Investigator: Dr David H Allen
Department of Aerospace Engineering
Texas A&M University
College Station, TX 77843
(409) 845-7541

Program Manager: Maj David A Glasgow
AFOSR/NA
Bolling AFB DC 20332-6448
(202) 767-4937

Objective: To develop a damage model for predicting strength and stiffness of continuous fiber composite structure subjected to fatigue loading, and to verify this model with experimental results.

DELAMINATION AND TRANSVERSE FRACTURE IN GRAPHITE/EPOXY COMPOSITES
84 February 01 - 86 March 31

Principal Investigator: Dr Walter L Bradley
Department of Mechanical Engineering
Texas A&M University
College Station, TX 77843
(409) 845-1259

Program Manager: Maj David A Glasgow
AFOSR/NA
Bolling AFB DC 20332-6448
(202) 767-4937

Objective: To better define the deformation and fracture physics of delamination and transverse fracture in graphite epoxy composites, and to incorporate more realistic macroscopic measures of the fracture process into linear and nonlinear materials characterization.

DYNAMICS AND AEROELASTICITY OF COMPOSITE STRUCTURES
84 May 01 - 86 June 30

Principal Investigator: Dr John Dugundji
Department of Aeronautics & Astronautics
Massachusetts Institute of Technology
Cambridge, MA 02139
(617) 253-3758

Program Manager: Dr Anthony K Amos
AFOSR/NA
Bolling AFB DC 20332-6448
(202) 767-4937

Objective: To pursue combined experimental and theoretical investigations of aeroelastic tailoring effects on flutter and divergence of aircraft systems.

ANALYTICAL AND EXPERIMENTAL CHARACTERIZATION OF DAMAGE PROCESSES IN COMPOSITE LAMINATES
84 September 30 - 85 September 29

Principal Investigator: Dr George J Dvorak
Department of Civil Engineering
Rensselaer Polytechnic Institute
Troy, NY 12181
(518) 266-6943

Program Manager: Maj David A Glasgow
AFOSR/NA
Bolling AFB DC 20332-6448
(202) 767-4937

Objective: To develop distributed damage analysis applicable to high matrix crack densities, examine damage propagation across and along ply interfaces, model damage growth from intensely damaged regions, and analyze stability and compressive strength of laminated plates containing distributed and/or concentrated damage.

BEHAVIOR OF FIBRE REINFORCED COMPOSITES UNDER DYNAMIC TENSION
84 March 15 - 86 March 14

Principal Investigators: Dr John Harding
Dr C Ruiz
Department of Engineering Science
University of Oxford
Oxford, OX1 3PJ England

Program Manager: Dr Anthony K Amos
AFOSR/NA
Bolling AFB DC 20332-6448
(202) 767-4937

Objective: To characterize the mechanical behavior and failure mechanisms of carbon/epoxy, Kevlar/epoxy, and hybrid composites under tensile impact loading using specially designed split Hopkinson bar equipment.

ANALYSIS OF FATIGUE DAMAGE AND FAILURE IN COMPOSITE MATERIALS
84 September 30 - 87 December 31

Principal Investigator: Dr Zvi Hashin
Dept of Materials Science and Engineering
University of Pennsylvania
Philadelphia, PA 19104
(215) 898-8337

Program Manager: Maj David A Glasgow
AFOSR/NA
Bolling AFB DC 20332-6448
(202) 767-4937

Objective: To evaluate stiffness change in laminates due to distribution of intralaminar and interlaminar cracks by the use of variational methods, and to determine the relationship between the stiffness deterioration and the strength deterioration of cracked laminates.

RESISTANCE CURVE APPROACH TO PREDICTING RESIDUAL STRENGTH OF COMPOSITES
84 August 01 - 86 July 31

Principal Investigator: Dr H P Kan
Northrop Corporation
One Northrop Avenue
Hawthorne, CA 90250
(213) 970-2134

Program Manager: Maj David A Glasgow
AFOSR/NA
Bolling AFB DC 20332-6448
(202) 767-4937

Objective: To experimentally determine the Mode II delamination growth resistance of composite laminates and to develop analytical techniques for application of the R-curve concept to residual strength prediction of composite laminates with delaminations.

ULTRASONIC NDE OF DAMAGE IN CONTINUOUS FIBER COMPOSITES
84 February 01 - 87 January 31

Principal Investigator: Dr Vikram K Kinra
Department of Aerospace Engineering
Texas A&M University
College Station, TX 77843
(409) 845-1667

Program Manager: Maj David A Glasgow
AFOSR/NA
Bolling AFB DC 20332-6448
(202) 767-4937

Objective: To develop, test, and implement ultrasonic nondestructive evaluation techniques to characterize damage states produced in continuous fiber composites by monotonic and fatigue loading.

FRACTURE AND LONGEVITY OF COMPOSITE STRUCTURES
82 January 01 - 85 March 14

Principal Investigator: Dr Paul A Lagace
Department of Aeronautics & Astronautics
Massachusetts Institute of Technology
Cambridge, MA 02139
(617) 253-2426

Program Manager: Maj David A Glasgow
AFOSR/NA
Bolling AFB DC 20332-6448
(202) 767-4937

Objective: To develop theoretical and semi-empirical fracture laws and failure criteria and to correlate them with extensive experimental data generated in the program.

NONLINEAR DYNAMIC RESPONSE OF COMPOSITE ROTOR BLADES
82 September 01 - 86 November 30

Principal Investigators: Dr Ozden Ochoa
Department of Mechanical Engineering
Texas A&M University
College Station, TX 77843
(409) 845-2022

Dr John J Engblom
Department of Mechanical Engineering
Texas A&M University
College Station, TX 77843
(409) 845-2813

Program Manager: Dr Anthony K Amos
AFOSR/NA
Bolling AFB DC 20332
(202) 767-4937

Objective: To develop nonlinear finite element models suitable for predicting the structural dynamic response and resulting damage of composite rotor blades under impact and other transient excitations.

INTERLAMINAR FRACTURE TOUGHNESS IN RESIN MATRIX COMPOSITES
83 January 01 - 87 April 14

Principal Investigator: Dr Lawrence W Rehfield
School of Aerospace Engineering
Georgia Institute of Technology
Atlanta, GA 30332
(404) 894-3067

Program Manager: Maj David A Glasgow
AFOSR/NA
Bolling AFB DC 20332-6448
(202) 767-4937

Objective: To develop a Mode II interlaminar fracture coupon and test that can be used in both tension and compression testing, can be analyzed conveniently so that behavior can be readily interpreted and provides an experimental means for isolating Mode II contributions to fracture.

DAMAGE MODELS FOR DELAMINATION AND TRANSVERSE FRACTURE IN FIBROUS COMPOSITES
84 February 15 - 86 February 14

Principal Investigator: Dr Richard A Schapery
Department of Civil Engineering
Texas A&M University
College Station, TX 77843
(409) 845-7512

Program Manager: Maj David A Glasgow
AFOSR/NA
Bolling AFB DC 20332-6448
(202) 767-4937

Objective: To develop and verify mathematical models of delamination and transverse fracture which account for local (crack tip) and global damage distributions, separating the lay-up dependent fracture energy associated with microcracking from the intrinsic fracture energy of the separation process which occur at the tip of an advancing delamination crack.

EFFECT OF LOCAL MATERIAL IMPERFECTIONS ON BUCKLING OF COMPOSITE STRUCTURAL ELEMENTS
83 June 30 - 85 August 31

Principal Investigator: Dr George J Simitses
Dept of Engineering Science and Mechanics
Georgia Institute of Technology
Atlanta, GA 30332
(404) 894-2770

Program Manager: Dr Anthony K Amos
AFOSR/NA
Bolling AFB DC 20332-6448
(202) 767-4937

Objective: To investigate the effects of localized material, geometric, and process imperfections on the buckling characteristics of composite structural elements, and to incorporate them in analytical prediction methods.

COMPREHENSIVE STUDY ON DAMAGE TOLERANCE PROPERTIES OF NOTCHED COMPOSITE LAMINATES
84 September 30 - 85 September 29

Principal Investigator: Dr Albert S D Wang
Dept of Mechanical Engineering and Mechanics
Drexel University
Philadelphia, PA 19104
(215) 895-2297

Program Manager: Maj David A Glasgow
AFOSR/NA
Bolling AFB DC 20332-6448
(202) 767-4937

Objective: To conduct a comprehensive analysis of the stress fields in notched laminates so as to develop a fundamental understanding of the damage mechanisms near the notch region.

RESIDUAL STRESS INDUCED DAMAGE IN COMPOSITE MATERIALS
84 February 01 - 85 January 31

Principal Investigator: Dr Y Weitsman
Department of Civil Engineering
Texas A&M University
College Station, TX 77843
(409) 845-7512

Program Manager: Maj David A Glasgow
AFOSR/NA
Bolling AFB DC 20332-6448
(202) 767-4937

Objective: To develop and verify methods for predicting damage formation, growth, and arrest due to residual stresses in fiber-reinforced, resin matrix composites.

OFFICE OF NAVAL RESEARCH
ARLINGTON, VA 22217

CONTRACTS

FLAW GROWTH AND FRACTURE OF COMPOSITE MATERIALS
AND ADHESIVE JOINTS
N00014-79-C-0579
July 83 - Nov 87

Project Engineer: Dr. Yapa Rajapakse
OFFICE OF NAVAL RESEARCH
Mechanics Division, Code 432S
Arlington, VA 22217
(202) 696-4306 Autovon 226-4306

Principal Investigator: Prof. S. S. Wang
University of Illinois
Department of Theoretical and Applied Mechanics
Urbana, Illinois 61801
(217) 333-1835

Objective: Analytical and numerical studies will be conducted of flaw growth and Fracture in Fiber Composite Laminates and adhesively bonded structural joints under static and dynamic loading conditions.

DAMAGE ACCUMULATION AND RESIDUAL PROPERTIES OF COMPOSITES
N00014-82-K-0572
July 82 - March 86

Project Engineer: Dr. Yapa Rajapakse
OFFICE OF NAVAL RESEARCH
Mechanics Division, Code 432S
Arlington, VA 22217
(202) 696-4306 Autovon 226-4306

Principal Investigator: Prof. I. M. Daniel
Illinois Institute of Technology
Department of Mechanical Engineering
Chicago, Illinois 60616
(312) 567-3186

Objective: Investigate damage mechanisms and damage accumulation in graphite/epoxy laminates for the development of models for predicting residual stiffness, residual strength, and residual life.

INVESTIGATIONS OF ENVIRONMENTAL EFFECTS AND ENVIRONMENTAL
DAMAGE IN COMPOSITES
N00014-82-K-0562
October 84 - September 87

Project Engineer: Dr. Yapa Rajapakse
OFFICE OF NAVAL RESEARCH
Mechanics Division, Code 423S
Arlington, VA 22217
(202) 696-4306 Autovon 226-4306

Principal Investigator: Prof. Y. Weitsman
Texas A&M University
Department of Civil Engineering
College Station, Texas 77843
(713) 845-7512

Objective: Research will be conducted to study the effects of stress and moisture on the mechanical response of graphite/epoxy composites. Special attention will be given to environmental induced damage growth and its effect on compressive and shear response.

INVESTIGATIONS OF IMPACT DAMAGE IN COMPOSITES
N00014-84-K-0460
June 84 - Jan 88

Project Engineer: Dr. Yapa Rajapakse
OFFICE OF NAVAL RESEARCH
Mechanics Division, Code 423S
Arlington, VA 22217
(202) 696-4306 Autovon 226-4306

Principal Investigator: Prof. J. Awerbuch
Drexel University
Department of Mechanical Engineering and Mechanics
Philadelphia, PA 19104
(215) 895-2291

Objective: Investigations of damage in graphite/epoxy laminates due to normal and oblique impact will be carried out using a variety of experimental techniques. The use of acoustic emission for damage assessment will be explored fully.

SUPPRESSION OF DELAMINATION IN COMPOSITE LAMINATES SUBJECTED
TO IMPACT LOADING
N00014-84-K-0554
July 84 - June 86

Project Engineer: Dr. Yapa Rajapakse
OFFICE OF NAVAL RESEARCH
Mechanics Division, Code 423S
Arlington, VA 22217
(202) 696-4306 Autovon 226-4306

Principal Investigator: Prof. C. T. Sun
Purdue University
West Lafayette, IN 47907
(317) 494-5130

Objective: Research will be performed to investigate and establish quantitative models for delamination growth in composite laminates specifically designed to suppress delamination by the use of 3-D stitching reinforcement and by the introduction of soft adhesive layers.

CONSTRUCTION OF NON-LINEAR MODEL FOR BINARY METAL MATRIX COMPOSITES
N00014-84-K-0468
July 84 - June 86

Project Engineer: Dr. A. S. Kushner
OFFICE OF NAVAL RESEARCH
Mechanics Division, Code 423S
Arlington, VA 22213
(202) 696-4306 Autovon 226-4306

Principal Investigator: Prof. H. Murakami
University of California, San Diego
La Jolla, CA 92093
(619) 452-3821

Objective: Non-linear theory for metal matrix composites will be developed, based on variational principles and multi-variable asymptotic expansion techniques. The theory will account for the effect of fiber breakage, fiber-matrix debonding and slip, matrix plasticity and delamination.

METAL MATRIX COMPOSITE INTERFACES
N00014-84-K-0495
September 84 - August 87

Project Engineer: Dr. A. S. Kushner
OFFICE OF NAVAL RESEARCH
Mechanics Division, Code 423S
Arlington, VA 22213
(202) 692-4306 Autovon 226-4306

Principal Investigator: Prof. A. S. Argon
MIT
Department of Mechanical Engineering
Cambridge, MA 02139
(617) 253-2217

Objective: Research will be conducted to develop the micro-mechanical model of the interface in metal matrix composites which have the features of predictability for the purpose of optimizing existing fiber-matrix systems.

FRACTURE OF FIBROUS COMPOSITES AND LAMINATES
N00014-85-K-0247
March 85 - Apr 87

Project Engineer: Dr. Yapa Rajapakse
OFFICE OF NAVAL RESEARCH
Mechanics Division, Code 423S
Arlington, VA 22217
(202) 696-4306 Autovon 226-4306

Principal Investigator: Prof. G. J. Dvorak
Rensselaer Polytechnic Institute
Department of Civil Engineering
Troy, NY 12181
(518) 266-6363

Objective: Research will be conducted to investigate the fracture behavior of notched metal matrix composites, accounting for plasticity effects.

MECHANICAL PROPERTIES OF COMPOSITES AT ELEVATED
TEMPERATURES
N00014-85-K-0480
July 85 - June 88

Project Engineer: Dr. Yapa Rajapakse
OFFICE OF NAVAL RESEARCH
Mechanics Division, Code 423S
Arlington, VA 22217
(202) 696-4306 Autovon 226-4306

Principal Investigator: Prof. G. S. Springer
Stanford University
Dept. of Aeronautics and Astronautics
Stanford, CA 94305
(415) 497-4135

Objective: Mechanics-based models for changes in mechanical properties and failure characteristics of organic-matrix composites will be established.

PRECISION ULTRASONIC MEASUREMENTS IN COMPOSITE
MATERIALS
N00014-85-K-0595
July 85 - June 87

Project Engineer: Dr. Yapa Rajapakse
OFFICE OF NAVAL RESEARCH
Mechanics Division, Code 423S
Arlington, VA 22217
(202) 696-4306 Autovon 226-4306

Principal Investigator: Prof. W. Sachse
Cornell University
Dept. of Theoretical and Applied Mechanics
Ithaca, NY 14853

Objective: Research will be conducted to establish the capability to distinguish between the different failure modes in composite by the analysis of acoustic emission signals.

NAVAL AIR SYSTEMS COMMAND
WASHINGTON, D.C. 20361

INHOUSE

DEVELOPMENT OF CERTIFICATION METHODOLOGY FOR
COMPOSITE MATERIALS
October 84 - October 87

Principal Investigator: Prof. E. Wu
Naval Post Graduate School
Department of Aeronautics, Code 67WT
Monterey, CA 93943
(408) 646-3459 Autovon 878-3459

Objective: Develop probabilistic-based certification methods through experimental and probabilistic modeling to insure the strength and life of critical composite structure.

CONTRACTS

FATIGUE LIFE AND RESIDUAL STRENGTH OF COMPOSITE STRUCTURES
September 83 - September 85

Project Engineer: Dr. D. R. Mulville
Naval Air Systems Command
Washington, D.C. 20361
(202) 692-7443 Autovon 222-7443

Principal Investigators: Dr. J. Yang and
Dr. D. Jones
The George Washington University
Washington, D.C. 20052
(202) 676-6929

Objective: Develop statistical models to describe fatigue life and residual strength of composite structures including bolted and bonded composite joints.

STRENGTH AND IMPACT RESISTANCE OF ADVANCED COMPOSITE
SANDWICH STRUCTURES
N00019-85-C-0090
December 84 - December 87

Project Engineer: Dr. D. R. Mulville
Naval Air Systems Command
Washington, D.C. 20361
(202) 692-7443

Principal Investigators: Prof. E. A. Witmer and
Prof. P. A. Lagace
Massachusetts Institute of Technology
Department of Aeronautics and Astronautics
Cambridge, MA 02139
(617) 253-3628

Objective: Further develop the technology for advanced composite structures with sandwich or honeycomb cores.

NAVAL RESEARCH LABORATORY
WASHINGTON, D.C. 20375

INHOUSE

STRUCTURAL RESPONSE OF DAMAGED COMPOSITES
October 79 - September 86

Project Engineer: Dr. P. W. Mast
Naval Research Laboratory
Washington, D.C. 20375
(202) 767-2165 Autovon 297-2165

Objective: Develop a capability for predicting the structural response of composite structures containing a defect or damage.

NAVAL AIR DEVELOPMENT CENTER
AIRCRAFT AND CREW SYSTEMS TECHNOLOGY DIRECTORATE
WARMINSTER, PA 18974

INHOUSE

IMPROVED MATRIX DOMINATE PROPERTIES
October 82 - September 86

Project Engineer: Ramon Garcia
Naval Air Development Center
ACSTD/6043
Warminster, PA 18974
(215) 441-1321 Autovon 441-1321

Objective: Investigate methods to improve composite performance by reinforcing the matrix with silicon carbide whiskers.

HYBRID COMPOSITE FRACTURE CHARACTERIZATION
September 85 - October 87

Project Engineer: Lee W. Gause
Naval Air Development Center
ACSTD/6043
Warminster, PA 18974
(215) 441-1330 Autovon 441-1330

Objective: Characterize the strength, mechanical properties, and damage tolerance of woven and hybrid composite structures.

METAL MATRIX CRACK INITIATION/PROPAGATION
September 85 - October 87

Project Engineer: Dr. H. C. Tsai
Naval Air Development Center
ACSTD/6043
Warminster, PA 18974
(215) 441-2871 Autovon 441-2871

Objective: Characterize the crack initiation/propagation mechanics of silicon carbide/titanium metal matrix composites as applied to landing gear and arrester hooks in the Naval shipboard environment.

CONTRACTS

DESIGN OF HIGHLY LOADED COMPOSITE JOINTS AND
ATTACHMENTS FOR TAIL STRUCTURES
N62269-82-C-0239
February 82 - January 86

Project Engineer: Ramon Garcia
Naval Air Development Center
ACSTD/6043
Warminster, PA 18974
(215) 441-1321 Autovon 441-1321

Principal Investigator: S. W. Averill
Northrop Corporation
Aircraft Group
Hawthorne, CA 90250
(213) 970-3442

Objective: To develop composite designs which will permit the use of metal to composite bolted root attachments in aircraft tail structures as an alternative to high-load transfer adhesive bonded titanium step joints. To improve damage tolerance, survivability and repairability over current composite designs. Structural efficiency, manufacturing feasibility and quality assurance requirements will be determined.

DESIGN OF HIGHLY LOADED COMPOSITE JOINTS

AND ATTACHMENTS FOR WING STRUCTURES

N62269-82-C-0238

February 82 - December 85

Project Engineer: Ramon Garcia
Naval Air Development Center
ACSTD/6043
Warminster, PA 18974
(215) 441-1321 Autovon 441-1321

Principal Investigator: M. J. Ogonowski
McDonnell Aircraft Co.
P.O. Box 516
St. Louis, MO 63166
(314) 233-8630

Objective: To develop composite designs which will permit the use of metal to composite bolted root attachments in aircraft wing structures as an alternative to high-load transfer adhesive bonded titanium step joints. Strain concentration around fastener holes, fatigue and environmental affects, damage tolerance and repairability for each concept will be determined.

IMPACT RESPONSE OF COMPOSITE STRUCTURES

N62269-85-M-3131

March 85 - September 85

Project Engineer: Lee W. Gause
Naval Air Development Center
ACSTD/6043
Warminster, PA 18974
(215) 441-1330 Autovon 441-1330

Principal Investigator: Prof. P. V. McLaughlin
Villanova University
Department of Mechanical Engineering
Villanova, PA 19085
(215) 645-4991

Objective: Analytically describe the effects of viscoelasticity, contact deformation, and shear deformation to the impact response of composite material and correlate these results to observed experimental behavior.

INFLUENCE OF LOAD FACTORS AND TEST METHODS ON
IN-SERVICE RESPONSE OF COMPOSITE MATERIALS AND
STRUCTURES

N62269-85-C-0234

June 85 - June 88

Project Engineer: Lee W. Gause
Naval Air Development Center
ACSTD/6043
Warminster, PA 18974
(215) 441-1330 Autovon 441-1330

Principal Investigator: Prof. K. L. Reifsnider
Virginia Polytechnic and State University
Dept. of Engineering Science & Mechanics
Blacksburg, VA 24061
(703) 961-5316

Objective: Develop an understanding of the relationship between composite laminate response to high load levels for short time periods and response to low load levels for long time periods. Develop an understanding of the relationship between test methods and laminate response. Establish the manner in which these relationships are associated with strength and life. Formulate a mechanistic model which can be used to anticipate long-term behavior.

LAMINATED COMPOSITE MIXED-MODE PLANE CRACK GROWTH CRITERIA
N62269-85-C-0246
June 85 - June 86

Project Engineer: Lee W. Gause
Naval Air Development Center
ACSTD/6043
Warminster, PA 18974
(215) 441-1330 Autovon 441-1330

Principal Investigator: Prof. A. S. D. Wang
Drexel University
Department of Mechanical Engineering & Mechanics
Philadelphia, PA 19104
(215) 895-2297

Objective: Define the critical conditions necessary to propagate a mixed-mode plane crack in composite laminates for use in the automated crack-growth simulation program.

Eleventh Annual Mechanics of Composites Review
October 22-24, 1985

FORMULATION OF LAMINATED BEAM AND PLATE
FINITE ELEMENTS FOR A MICROCOMPUTER

A. T. Chen and T. Y. Yang

School of Aeronautics and Astronautics
Purdue University
West Lafayette, Indiana 47906

ABSTRACT

The purpose of this paper is to develop simple yet efficient formulation for laminated composite finite elements and also to develop highly efficient numerical algorithms for structural analysis and design using stand alone desktop microcomputers.

In the finite element formulations, an 8 degree of freedom beam element and an 18 d.o.f triangular plate element in bending with anisotropic symmetrically laminated composite materials are formulated. In the development of numerical procedures, emphasis has been placed upon minimization and condensation of memory storage and efficiency of computation so that the present development is suitable for implementation on desktop microcomputers. The present development is not only limited to linear static stress analysis, it also includes eigenvalue analysis for free vibration and buckling problems. For the special case of lumped mass matrices, a special condensation technique making use of zero terms along the diagonal of the mass matrix is used.

To demonstrate and evaluate the present development, numerical analyses on the static, free vibration, and buckling analysis of anisotropic symmetrically laminated beam and plate problems have been analyzed using a microcomputer.

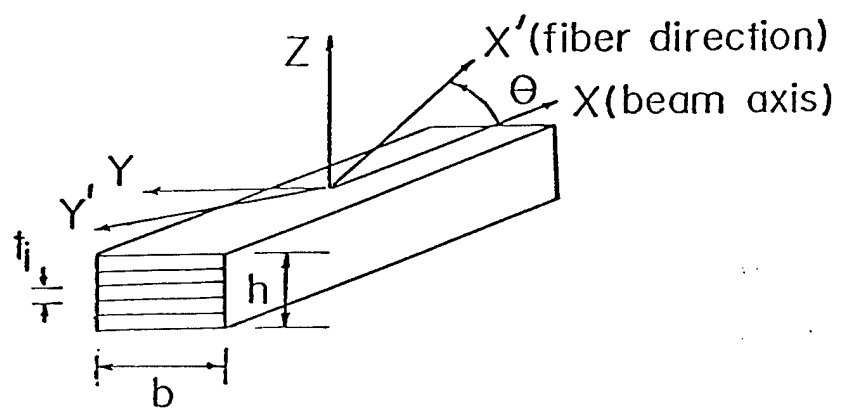


FIG. 1. LAMINATED BEAM CONVENTIONS

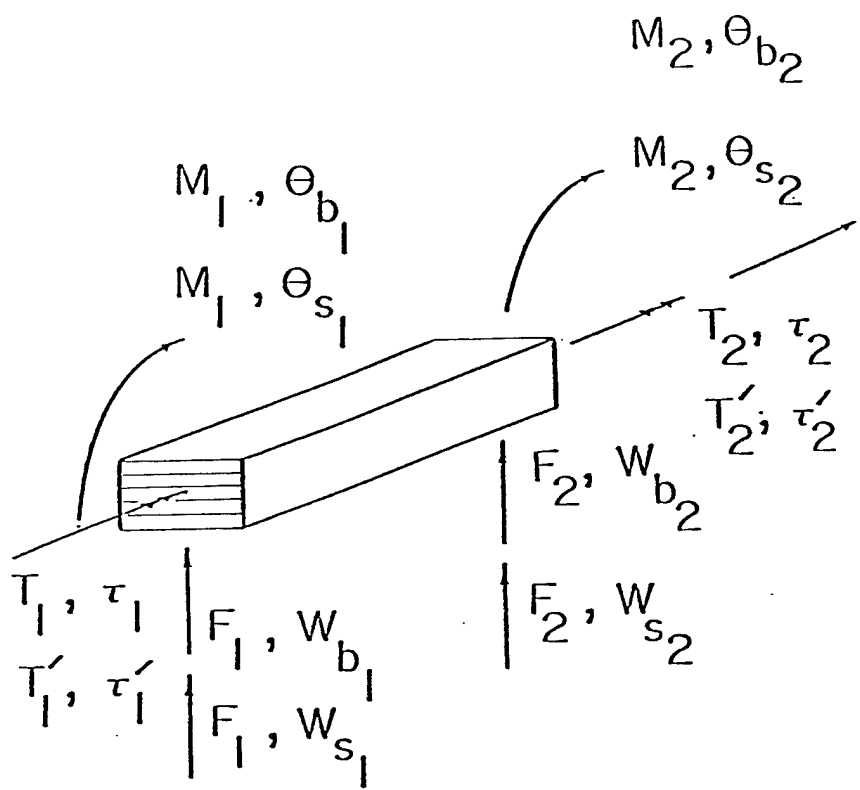


FIG. 2a. 12 D.O.F. BEAM FINITE ELEMENT

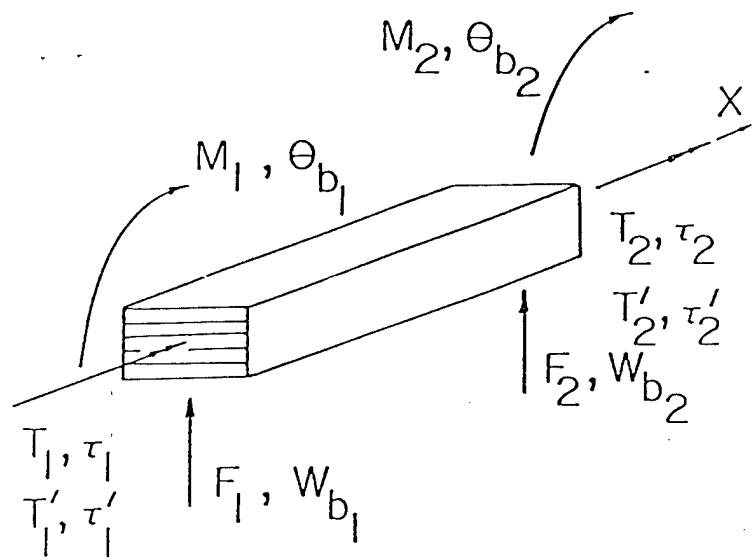


FIG. 2b. 8 D.O.F. BEAM FINITE ELEMENT

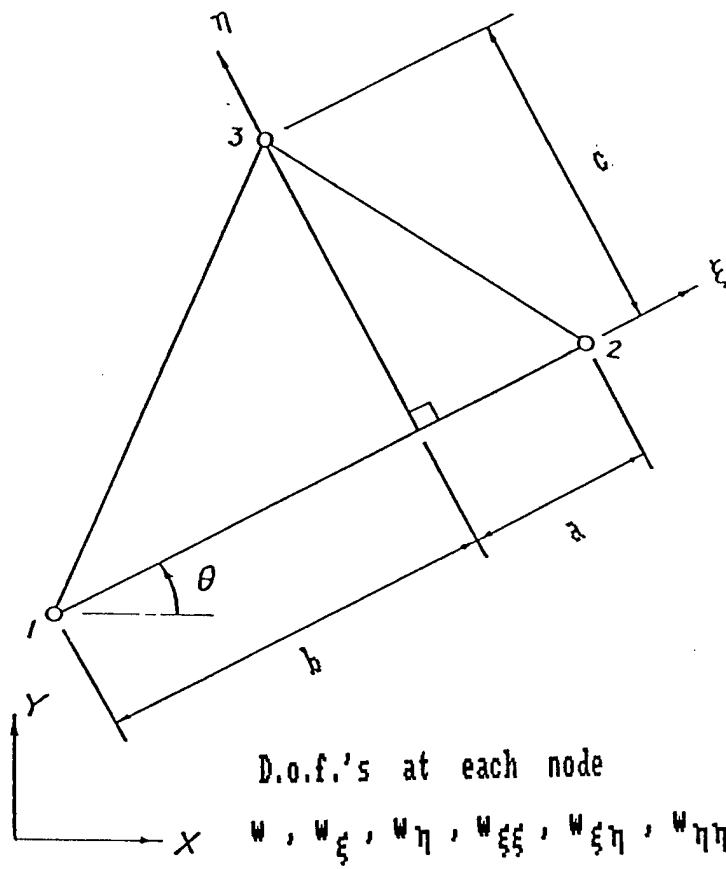
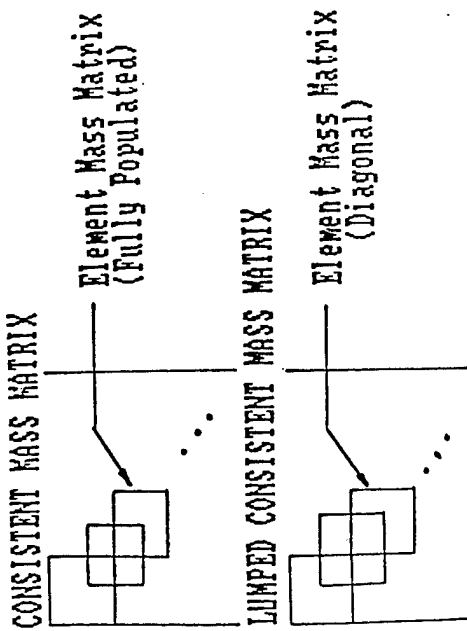


FIG. 3. 18 D.O.F. PLATE FINITE ELEMENT



1.11, 1.22, diagonal element matrix

let $M_{tt} = M_{11} + M_{22} + M_{33} + \dots + M_{nn}$

$M_{tt}(M_{11}/M_{tt}, M_{22}/M_{tt}, \dots, M_{nn}/M_{tt})$

M_e = MASS of element

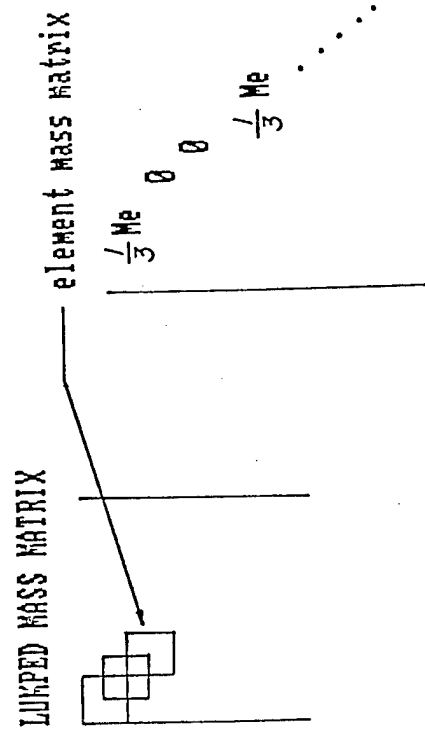


FIG. 4. TWO WAYS OF LUMPING THE ELEMENT MASSES

CONSISTENT MASS MATRIX

Element Mass Matrix
(Fully Populated)

$$-\lambda [M]\{x\} + [K]\{x\} = 0$$

$$-\lambda \begin{bmatrix} M & 0 \\ 0 & 0 \end{bmatrix} \begin{bmatrix} y \\ z \end{bmatrix} + \begin{bmatrix} K_{PP} & K_{PQ} \\ K_{PQ}^T & K_{QQ} \end{bmatrix} \begin{bmatrix} y \\ z \end{bmatrix} = \begin{bmatrix} 0 \\ 0 \end{bmatrix}$$

where $\{y\}$ denote degree of freedom associated with mass
 $\{z\}$ denote massless d.o.f.

$$\begin{aligned} [K_{PQ}]^T \{y\} &= -[K_{QQ}] \{z\} \\ \{z\} &= -[K_{QQ}]^{-1} [K_{PQ}]^T \{y\} \\ &- \lambda [M] \{y\} + \{ [K_{PP}] - [K_{PQ}] [K_{QQ}]^{-1} [K_{PQ}]^T \} \{y\} \\ &- \lambda [M] \{y\} + [K_{TT}] \{y\} = 0 \end{aligned}$$

where $[M]$ is a diagonal matrix
 $[K_{TT}]$ is the symmetric reduced matrix

FIG. 5. STATIC CONDENSATION FOR LUMPED MASSES

$$\begin{aligned}
 & \text{[M]}^{-\frac{1}{2}} \text{ MATRIX} \\
 & \text{[M]} = \begin{bmatrix} a & b & & & \\ c & d & e & & \\ & & \ddots & & \\ & & & \ddots & \\ & & & & \ddots \end{bmatrix} \\
 & \text{[M]}^{-\frac{1}{2}} = \begin{bmatrix} 1/\sqrt{a} & & & & \\ & 1/\sqrt{b} & & & \\ & & 1/\sqrt{d} & & \\ & & & 1/\sqrt{e} & \\ & & & & \ddots \end{bmatrix} \\
 & \text{[M]}^{-\frac{1}{2}} \text{[M]} \text{ [M]}^{-\frac{1}{2}} = \text{[I]}, \text{ identity matrix} \\
 & -\lambda \text{[I]} \{y\} + \text{[M]}^{-\frac{1}{2}} \text{[KTT]} \text{ [M]}^{-\frac{1}{2}} \{y\} = 0
 \end{aligned}$$

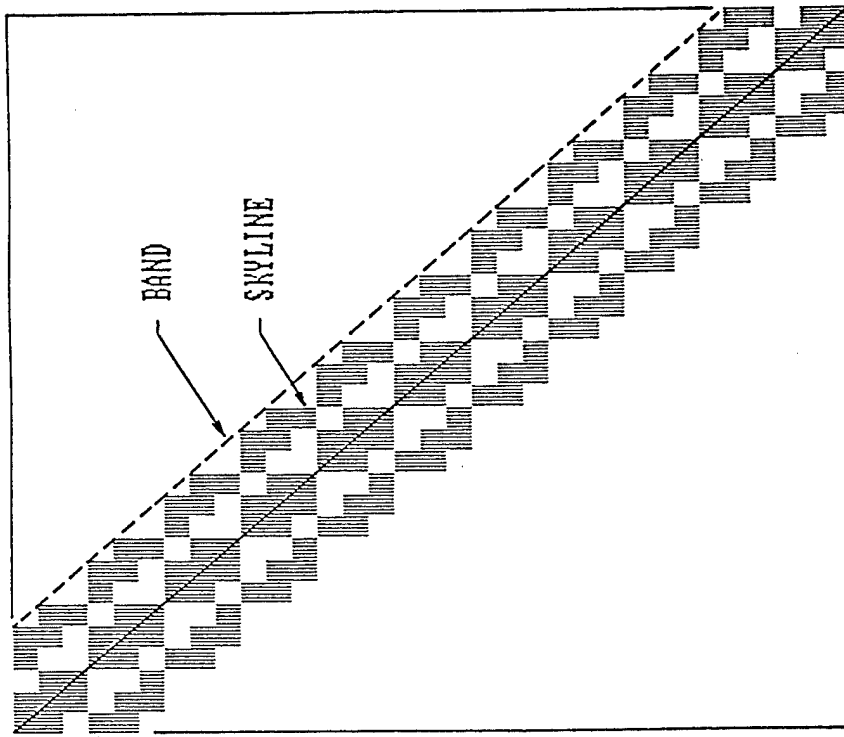


FIG. 6. TECHNIQUE TO MAKE EIGENVALUE MATRIX SYMMETRIC

FIG. 7. VARIOUS STORAGE SCHEMES

Table 1. Various Schemes for Memory Storage for [K] for a Simply Supported Square Isotropic Plate Under Uniform Load

Mesh Pattern

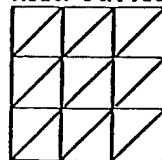
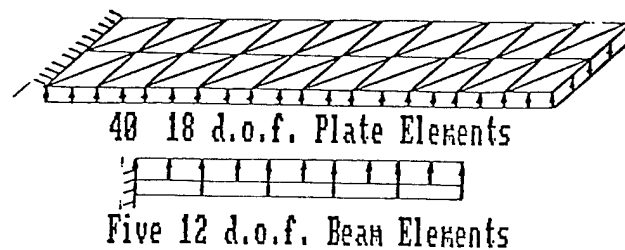


Plate Element (18 d.o.f. triangular)

Mesh for a Quadrant	Degrees of Freedom	Storage Modes			
		Full Matrix	Symmetric	Band	Skyline
3x3	60	3600	1830	1395	1001
4x4	104	10816	5460	3569	2737
5x5	160	25600	12880	6664	5257

Table 2. Comparison of Centerline Deflections of Two Modellings for a Uniformly Loaded Cantilever Beam

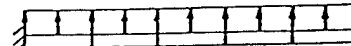


Fiber Angle	Beam Deflection				Plate Deflection		
	Tip ($x=L$) (1)	$x=0.6L$ (2)	$x=0.6L/x=L$ (2)/(1)	Tip ($x=L$) (3)	$x=0.6L$ (4)	$x=0.6L/x=L$ (3)/(4)	
0	5.45	2.57	0.4722	5.299	2.518	0.4752	
30	34.24	16.17	0.4723	29.108	13.351	0.4587	
45	58.89	27.81	0.4722	52.788	24.550	0.4651	
60	79.37	37.48	0.4722	74.578	35.113	0.4708	
90	95.69	45.19	0.4723	93.160	44.262	0.4751	

Table 3. Comparison of Centerline Twist
of Two Modellings for a Uniformly
Loaded Cantilever Beam



40 18 d.o.f. Plate Elements



Five 12 d.o.f. Beam Elements

Fiber Angle	Beam Twist			Plate Twist		
	Tip (x=L) (1)	x=0.6L (2)	x=0.6L/x=L (2)/(1)	Tip(x=L) (3)	x=0.6L (4)	x=0.6L/x=L (3)/(4)
0	0.0	0.0	---	0.0	0.0	---
30	-3.126	-2.885	0.9231	-2.687	-2.483	0.9240
45	-3.047	-2.813	0.9232	-2.787	-2.597	0.9317
60	-2.153	-1.987	0.9231	-2.046	-1.912	0.9347
90	0.0	0.0	---	0.0	0.0	---

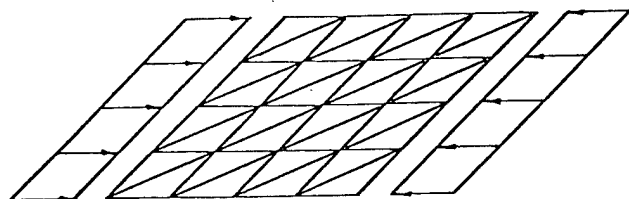
Table 4. Natural Frequencies (Hz) for a Thin Anisotropic
6 layer $[0_2/90_2]_s$ Cantilever Plate

Layup Sequence	Lumped Mass				Consistent Mass		REF [1] Exp 365 dof
	(1)		(2)		50 dof	147 dof	
	8 el 50 dof	32 el 147 dof	8 el 8 dof	32 el 24 dof			
$[0_2/90_2]_s$	10.7	10.9	10.7	11.0	11.0	11.0	11.2 11.1
	21.0	31.0	22.9	32.2	39.5	39.5	42.4 39.5
	56.9	66.4	59.2	67.0	69.2	69.2	70.5 69.5
	8.6	8.8	8.8	8.9	8.9	8.9	9.4 8.9
$[15_2/0]_s$	24.7	35.2	26.7	36.7	42.9	42.8	45.8 42.9
	47.4	56.8	50.3	57.6	62.9	62.6	66.2 62.7
	6.1	6.2	6.2	6.3	6.3	6.3	6.6 6.3
$[30_2/0]_s$	27.2	34.5	28.9	35.6	37.3	37.2	40.0 37.3
	35.4	45.9	36.9	47.1	58.0	57.0	59.1 56.9
	4.7	4.8	4.8	4.8	4.9	4.9	4.8 4.9
$[45_2/0]_s$	25.3	28.8	27.4	29.4	30.1	30.0	29.8 30.1
	27.6	39.0	29.0	40.4	50.8	49.7	51.3 49.4
	4.1	4.1	4.1	4.2	4.2	4.2	4.3 4.2
$[60_2/0]_s$	22.7	25.1	23.5	25.5	26.1	26.0	27.1 26.1
	22.9	32.8	24.9	24.1	42.8	41.9	47.7 41.7
	3.8	3.8	3.8	3.9	3.9	3.9	3.8 3.9
$[75_2/0]_s$	19.8	23.5	20.9	23.7	24.3	24.3	25.1 24.3
	21.5	28.9	22.9	30.1	37.3	36.8	38.9 36.7
	3.7	3.8	3.7	3.8	3.8	3.8	3.7 3.8
$[90_2/0]_s$	18.7	23.0	19.9	23.2	23.8	23.8	24.3 23.9
	21.1	27.6	22.3	28.7	35.2	35.1	38.2 35.1

Table 5. Comparison of Natural Frequencies (Hz) of Two Modellings for a Cantilever Beam

Layup Sequence	Beam Element		Plate Element			
	Consistent Mass		Lumped Mass		Consistent Mass	
	4 el 17 dof	10 el 52 dof	20 el 20 dof	40 el 30 dof	20 el 122 dof	40 el 183 dof
[0 ₂ /90] ₅	0.01026	0.01026	0.01022	0.01022	0.01026	0.01026
	0.06436	0.06429	0.04751	0.06301	0.06432	0.06432
[30 ₂ /0] ₅	0.07716	0.07716	0.06322	0.06755	0.08235	0.08234
	0.00525	0.00525	0.00549	0.00549	0.00551	0.00551
[45 ₂ /0] ₅	0.03278	0.03274	0.03374	0.03390	0.03440	0.03439
	0.09172	0.09092	0.06970	0.09393	0.09651	0.09646
[60 ₂ /0] ₅	0.00424	0.00424	0.00435	0.00435	0.00436	0.00436
	0.02655	0.02651	0.02688	0.02690	0.02730	0.02730
[90 ₂ /0] ₅	0.07456	0.07404	0.06260	0.07455	0.07645	0.07645
	0.00378	0.00378	0.00382	0.00382	0.00383	0.00383
[60 ₂ /0] ₅	0.02374	0.02371	0.02363	0.02364	0.02399	0.02400
	0.06685	0.06634	0.05351	0.06548	0.06715	0.06717
[90 ₂ /0] ₅	0.00353	0.00353	0.00352	0.00352	0.00354	0.00354
	0.02218	0.02215	0.02180	0.02181	0.02216	0.02216
[90 ₂ /0] ₅	0.06250	0.06204	0.04560	0.06023	0.06204	0.06204

Table 6. Critical Buckling Loads for a Simply Supported Anisotropic Square Plate Under Uniform Compressive Axial Load



Fiber Angle	Present 32 el 94 dof	Ref. [2]	Exp. [3]	Exact [4]
0	318.86	285	271	318.91
30	387.90	425	399	--
45	354.67	406	364	--
60	355.40	381	433	--
90	203.88	210	251	203.75

REFERENCES

1. Jensen, D.W. and Crawley, E.F., "Frequency Determination techniques for Cantilevered Plates with Bending-Torsion Coupling", AIAA Journal, vol 22, No 3, P.415 (March, 1985)
2. Chamis, C.C., Buckling of Anisotropic Composite Plates, Journal of the Structural Division, Proceedings of the American Society of Civil Engineers, Oct., 1969, ST 10, PP 2119-2139.
3. Mandell, J.F., An Experimental Investigation of the Buckling of Anisotropic Plates, thesis, presented to Case Western Reserve University, in Cleveland, Ohio, in June, 1968, in partial fulfillment of the requirements for the degree of Master of Science.
4. Aston, J.E., Whitney, J.M., Theory of Laminated Plates, Progress in Material Science Series vol IV, Technomic Publishing Co., Inc., Stamford, Conn., 1970.

8-9

STRENGTH, DEFLECTIONS AND IMPACT DAMAGE IN ADVANCED COMPOSITE STRUCTURES

PAUL A. LAGACE

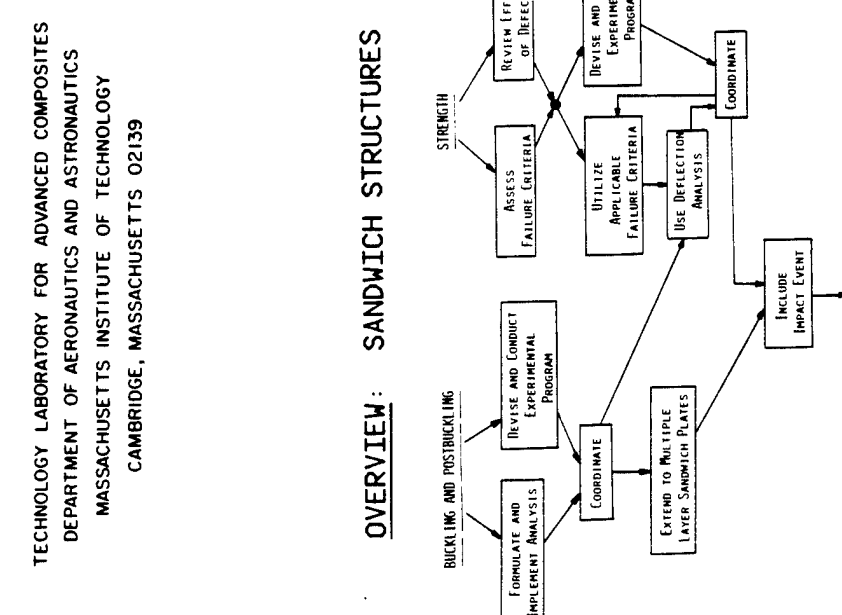


TECHNOLOGY LABORATORY FOR ADVANCED COMPOSITES
DEPARTMENT OF AERONAUTICS AND ASTRONAUTICS
MASSACHUSETTS INSTITUTE OF TECHNOLOGY
CAMBRIDGE, MASSACHUSETTS 02139

JOINT NAVY / FAA EFFORT

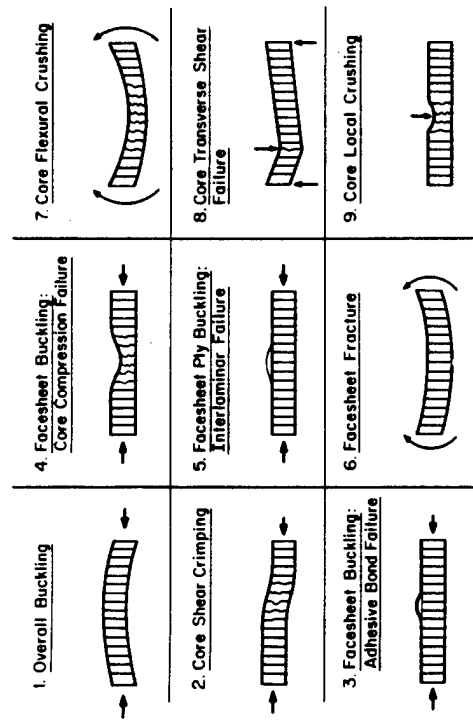
NAVAIR, : STRENGTH AND DEFLECTIONS OF ADVANCED
NADC : COMPOSITE SANDWICH STRUCTURES

OVERVIEW : SANDWICH STRUCTURES

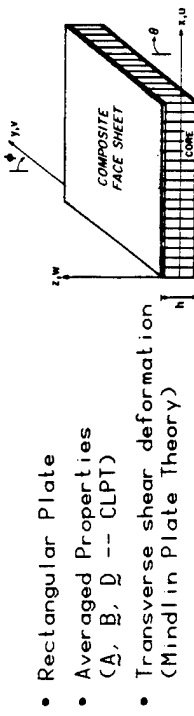


FAA: THE SENSITIVITY OF KEVLAR/EPOXY AND
GRAPHITE/EPOXY STRUCTURES DAMAGE
FROM FRAGMENT IMPACT

SANDWICH STRUCTURES: MODES OF FAILURE



ANALYSIS OVERVIEW



- Rectangular Plate
- Averaged Properties (A, B, D -- CLPT)
- Transverse shear deformation (Mindlin Plate Theory)
- Non linear (geometric) strains used for postbuckling (similar to von Karman, equations)
- Effect of initial out-of-plane imperfections (Marguerre equations)
- Linear stress-strain behavior assumed
- Core has only transverse shear stiffness

SOLUTION PROCEDURE

- Use Rayleigh-Ritz method

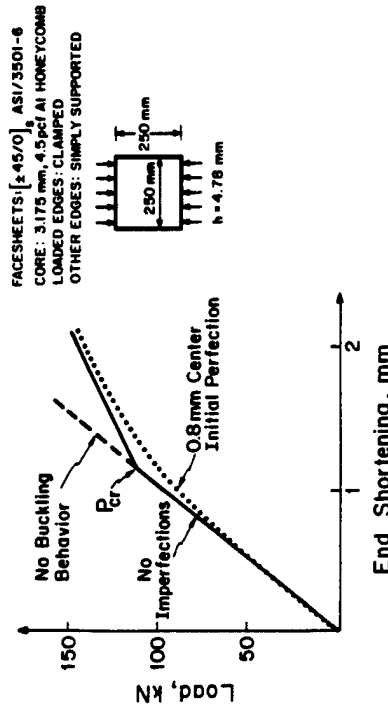
$$u, v, w, \phi, \theta = \sum_j \psi_j f_j(k) g_j(y)$$
- Use Potential Energy approach

$$\Pi_p = \frac{1}{2} \iint \{f\}^T [E] \{f\} dV - \int p \{u\} d\ell$$
- Use direct energy minimization to find plate response for a given loading

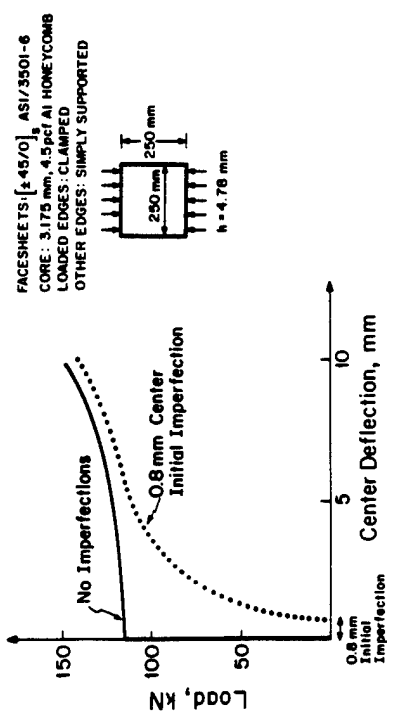
SOFTWARE OPERATION

- INPUTS
 - Facesheet layup, material properties
 - Core properties, thickness
 - Boundary conditions
 - Initial imperfections
 - Loading
- OUTPUTS
 - Displacements
 - Stresses and strains in core and facesheets (ply-by-ply)
- 2000 FORTRAN instructions
- VAX 11/782
- 20 seconds CPU time for one complete loading

TYPICAL RESULTS: LOAD VS. END SHORTENING



TYPICAL RESULTS: LOAD VS. CENTER DEFLECTION



TEST MATRIX FOR BUCKLING/POSTBUCKLING CHARACTERISTICS OF SANDWICH PLATES

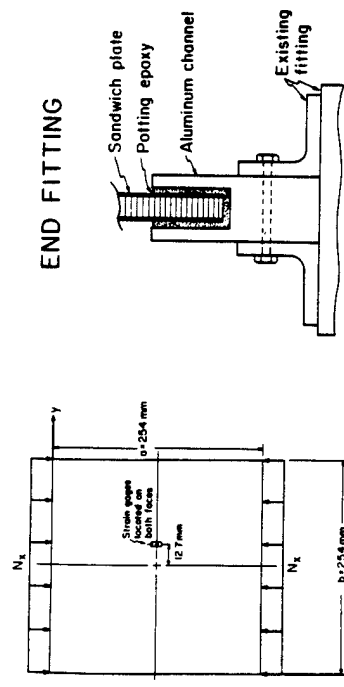
Core Material		Aluminum Honeycomb (4.5 pcf)	Honey comb (4.5 pcf)	Synthetic Foam (6.8 pcf)	Rubber Cell (4.4 pcf)
Core Thickness (mm)	Thickness-Width Ratio (N/Faces)				
5.18	.019	-	3 ^a	3	5
6.35	.031	-	3 ^a	3	3
9.53	.043	-	3 ^a	3	3
		400	80	40 ^b	30
Core Shear Modulus (MPa)					

A INDICATES NUMBER OF SPECIMENS
TOTAL: 30 SPECIMENS

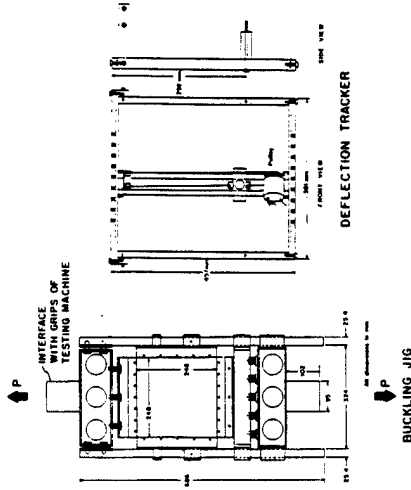
BIBLIOGRAPHIC REFERENCES

NOTES: ALL FACE SHEETS ARE {45/0}, AS4/3501-6 GRAPHITE/EPOXY
CLAMPED: SLICE EDGES SIMPLY-SUPPORTED

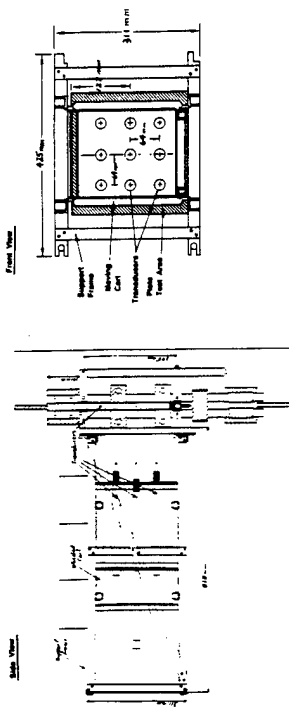
TEST SPECIMEN GEOMETRY



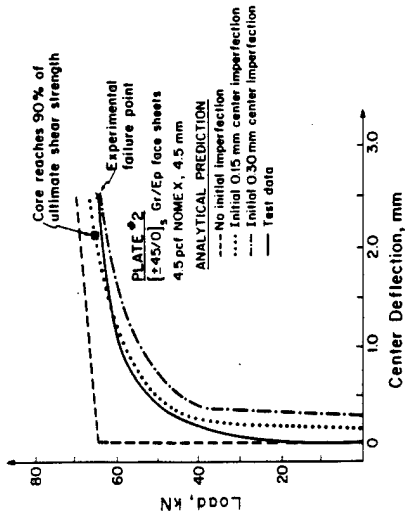
EXPERIMENTAL APPARATUS



EXPERIMENTAL APPARATUS: 9-TRANSDUCER RACK

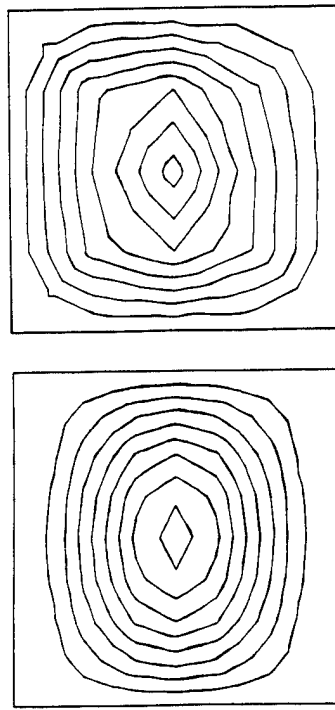


LOAD VS. CENTER DEFLECTION

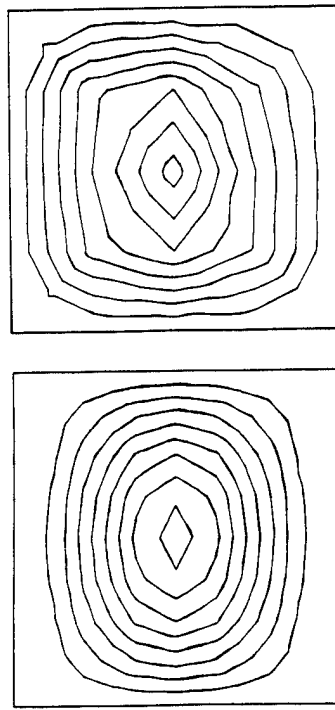


PREDICTED VS. EXPERIMENTAL CONTOUR PLOTS

PREDICTED CONTOUR



MEASURED CONTOUR

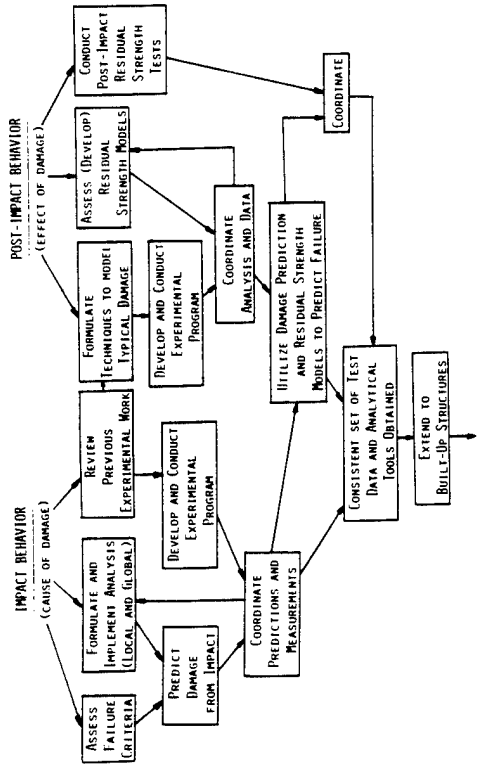


LOAD = 62 kN
EACH LINE REPRESENTS 0.25 MM DEFLECTION

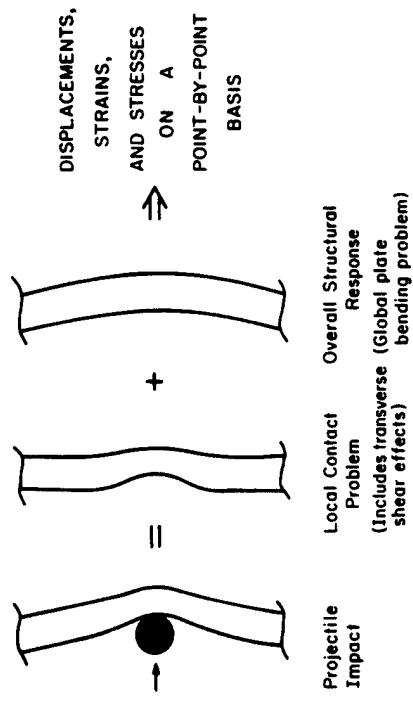
STATUS OF WORK ON SANDWICH STRUCTURES

- Buckling and postbuckling analysis operational
- Experimental program for buckling/postbuckling well underway
- Effort on failure, effects of defects commencing

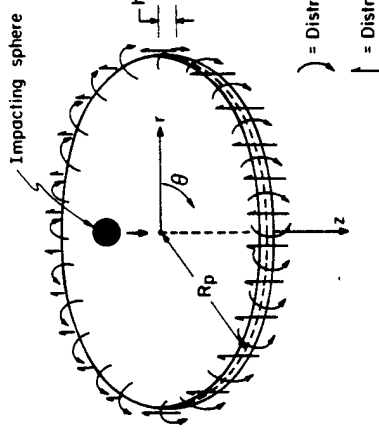
OVERVIEW: IMPACT RESPONSE



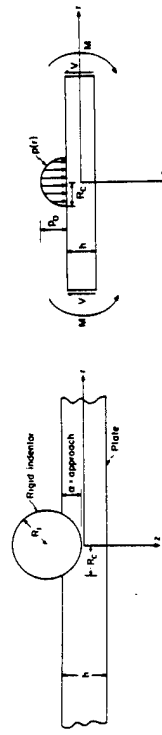
DEFORMATION RESPONSE OF LAMINATE TO LOW VELOCITY IMPACT



LOCAL CONTACT PROBLEM



INDENTOR AND LOAD MODEL



LOCAL CONTACT PROBLEM SOLUTION OVERVIEW

- **INPUTS**
 - Constitutive properties $E_0, E_1, \nu_0, \nu_1, G_{12}$ (transverse isotropy assumed in $r-\theta$ plane)
 - Indentor radius and penetration (approach)
 - Edge moment (from plate or FEM solution of impact event)

- **PROCEDURE**
 - Stress potential approach: $\phi(r, z)$
 - Loading and solution in form of Fourier-Bessel Series
 - Implemented on DEC Pro 350 personal computer

- **OUTPUTS**
 - Load vs. approach
 - Axisymmetric strain distribution throughout entire plate

LOAD VS. APPROACH

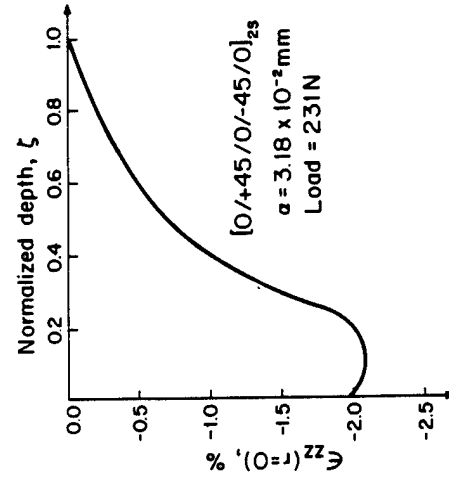
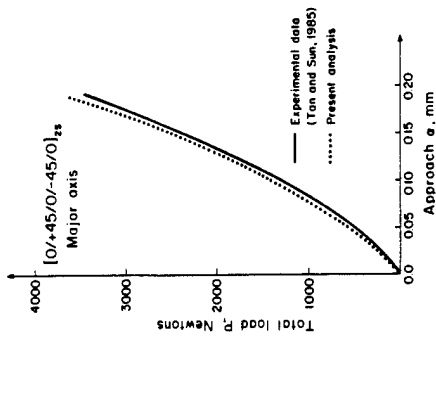
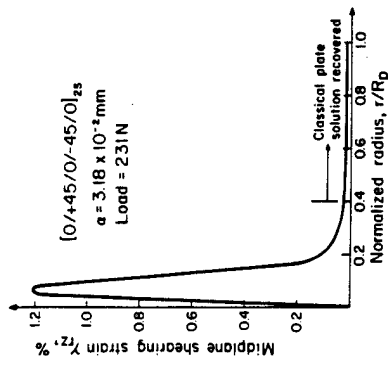
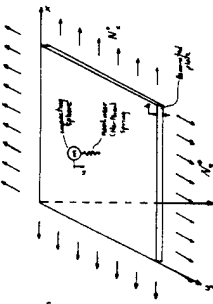


Fig. 6



GLOBAL PLATE BENDING SOLUTION OVERVIEW

- ASSUMPTIONS
 - Transversely loaded anisotropic plate (include D_{16} , D_{28})
 - Forcing function is impacting mass (ball) with nonlinear spring
- INPUTS
 - Mass, velocity of ball
 - Density and mechanical properties of plate
 - Support conditions, geometric parameters
 - Initial loads: N_x , N_y
- OUTPUTS
 - Force on plate due to ball
 - Center deflection



STATUS OF GLOBAL PLATE BENDING SOLUTION

- Solution implemented on computer and nearly completely debugged
- Newmark Implicit Integration Scheme employed
- Software runs and initial results obtained. (Results will be compared with previous work.)

CAPABILITIES OF IMPACT GUN SETUP

- Launch any 12.7 mm diameter ball
- Velocity measurement device designed, built, and installed
- Maximum recorded velocity of 106 m/s for steel ball
- Frame constructed to handle various sized test specimens with various edge boundary conditions

PHASE I TEST PROGRAM FOR IMPACT RESPONSE

LAMINATE	IMPACT INSPECTION INSPECTION		
	SECTIONING AND MICROSCOPY	L-SCAN	X-RAY
$[+45/-12.5]_S$ AS4/3501-6	5A	5	5
$[+45/-12.5]_S$ Kevlar/Epoxy	5A	5	5

^aWill not be tested to failure after impact

NOTES: TEST OTHER IMPACTED SPECIMENS TO FAILURE
IMPACT AT VARIOUS VELOCITY LEVELS
ONLY STEEL BALLS USED

PHASE II TEST PROGRAM FOR IMPACT RESPONSE

SPECIMEN CONFIGURATION FOR IMPLANTED DELAMINATION TESTS

Number of Specimens	Energy Level	Velocity Level	In-Plane TENSILE LOAD		Boundary Conditions	
			LHD	RHD	C	F
5 ^a	L ₁	V ₁	0	0	C	F
S	L ₂	V ₁	0	0	C	F
S	E ₃	V ₁	0	0	C	F
S	L ₁	V ₂	0	0	C	F
S	L ₁	V ₃	0	0	C	F
S	L ₁	V ₄	0	0	C	F
S	L ₁	V ₁	L ₁	L ₂	C	F
S	E ₁	V ₁	L ₁	L ₁	C	F
S	E ₁	V ₁	V ₁	0	C	C
S	E ₁	V ₁	V ₁	0	C	S
S	E ₁	V ₁	V ₁	0	S	F
S	E ₁	V ₁	V ₁	0	S	F

^a ALL TESTS CONDUCTED ON [45/0/0]S SPECIMENS OF BOTH

GRAPHITE/EPoxy AND KEVLAR/EPoxy

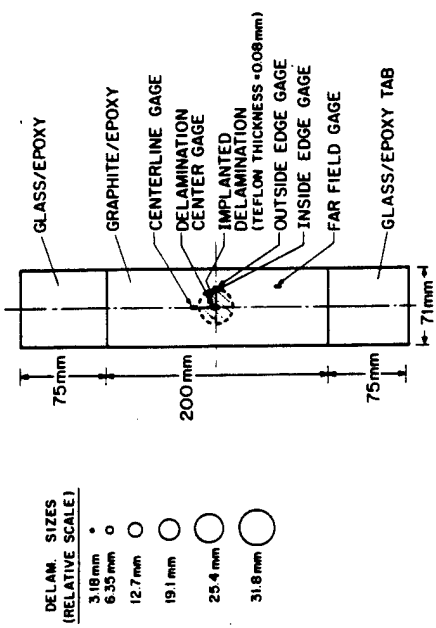
C = CLAMPED

S = SIMPLY SUPPORTED

F = FREE

NOTE: ALL SPECIMENS INSPECTED VIA MIC. AFTER IMPACT AND

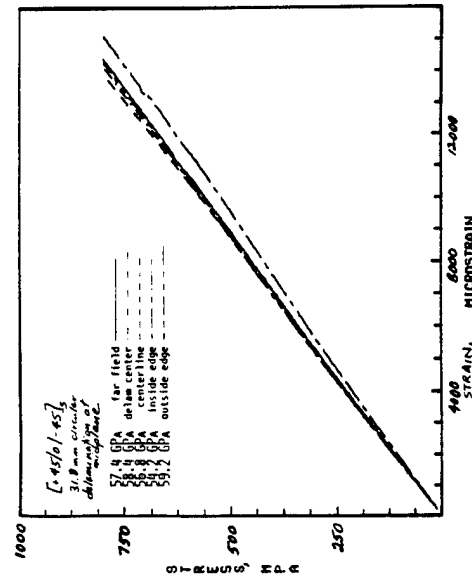
BEFORE RESIDUAL STRENGTH TESTING



CHARACTERISTICS OF TESTING

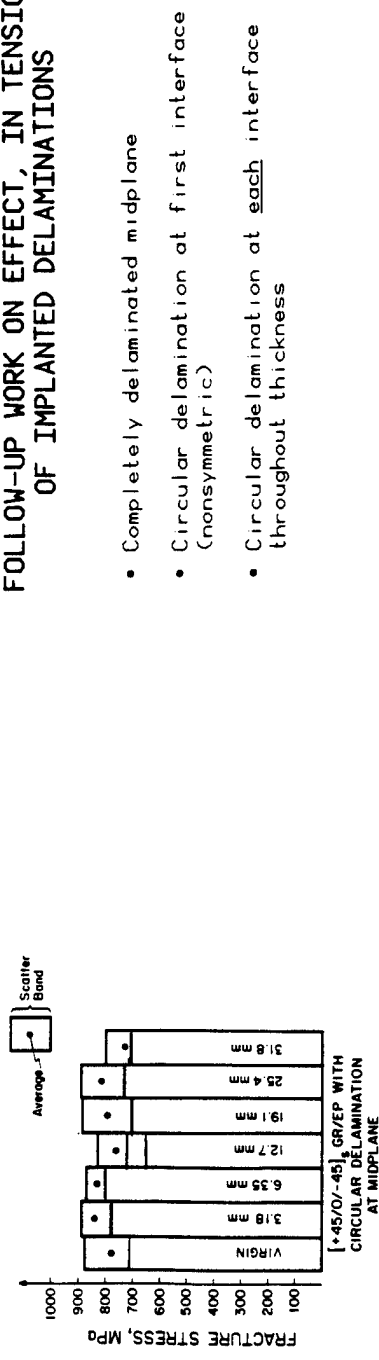
- MTS 810 MATERIAL TEST SYSTEM
- HYDRAULIC GRIPS
- CONSTANT STROKE RATE (~ 1 mm/minute) GIVES STRAIN RATE OF ~ 5000 MICROSTRAIN/MINUTE
- DATA TAKEN AUTOMATICALLY THROUGH PROPER CONDITIONERS TO PDP/1134 COMPUTER
- TESTED TO FRACTURE
- EACH SPECIMEN PHOTOGRAPHED AFTER FRACTURE

LOCAL STRESS VERSUS STRAIN FOR SPECIMEN WITH CIRCULAR DELAMINATION AT MIDPLANE



FRACTURE STRESSES FOR VARIOUS DELAMINATION CONFIGURATIONS

FOLLOW-UP WORK ON EFFECT, IN TENSION, OF IMPLANTED DELAMINATIONS



STATUS OF IMPACT WORK

- Analysis for local contact problem operational.
- Analysis for dynamic plate response formulated and implemented and is being checked
- Experimental facility established.
 - Impact, sectioning, and microscopic examination underway
- Delaminations modelled with teflon inserts and experiments conducted in tension
- Residual strength tests on impacted specimens commencing
- Failure criteria being assessed